Nitric oxide in acute and chronic inflammation.

Paul-Clark, Mark John

NITRIC OXIDE IN ACUTE AND CHRONIC INFLAMMATION

Mark John Paul-Clark
2002

A thesis submitted to the University of London (Faculty of Science) for the degree of Doctor of Philosophy

Department of Experimental Pathology
William Harvey Research Institute
Barts and the London School of Medicine and Dentistry
Queen Mary University of London
Charterhouse Square
London

This thesis is dedicated to Gaynor, Ronald, Reneè and my close friends, whose love, interest and encouragement has made this possible.

ABSTRACT

Nitric oxide (NO) is a signalling molecule formed when L-arginine is converted to L-citrulline by the enzyme NO synthase (NOS). NOS exists as three isoforms, ecNOS is constitutively expressed in endothelial cells and nNOS in neuronal cells, while a third isoform (iNOS) is induced in response to inflammatory stimuli and is capable of sustained production of high levels of NO. NO produced in response to an inflammatory insult, has been shown by use of NOS inhibitors to be detrimental during inflammation by producing the potent oxidising agent peroxynitrite. However, iNOS knockout animals generally produce a similar inflammatory profile to wild type controls. Hence, there is a discrepancy between the effects of phamacological inhibition and gene deletion of iNOS *in vivo*. Therefore, the aim of this thesis is to use a number of approaches to modulate NO production in acute and chronic inflammatory models and to assess the effects on the NOS pathway and other markers of the inflammatory response.

In this thesis, it was established that iNOS protein expression and nitrite formation was significantly elevated after injection of the inflammatory stimulus in the carrageenin-induced pleurisy (RCIP), bovine serum albumin (BSA)-induced pleurisy and methylated BSA-induced pleurisy in the rat, and a murine models of croton oil-induced chronic granulomatous tissue of the air pouch (MCGTAP). The majority of immunostaining was associated with migrating inflammatory cells. NO production was modulated in acute and chronic models of inflammation using NOS inhibitors and NSAIDs. Local injection of NOS inhibitors in the RCIP model caused an increase in pro-inflammatory mediators, including superoxide, histamine and PMN chemoattractants that resulted in an exacerbation of inflammation. This was a result of inhibition of both eNOS and iNOS at the inflammatory site. In contrast, systemic inhibition of NOS reduced both inflammatory cell influx and exudation into the pleural cavity. A similar inhibitory

result was obtained after NOS inhibition in the MCGTAP model. This anti-inflammatory effect was supported by experiments in mice whose iNOS gene had been genetically deleted. Interestingly, oral aspirin administration significantly elevated nitrite formation in both the RCIP and MCGTAP with a concomitant decrease in inflammation. Further analysis demonstrated that aspirin was able to elevate NO production in lipopolysaccharide induced J774 macrophages and A23187 stimulated EA.hy926 endothelial cells, suggesting that both cell types may be involved in the pharmacological actions of aspirin.

In conclusion, NO is a multi-functional free-radical which had advantageous effects in the acute resolving model and detrimental effects in chronic inflammation. Therefore, depending on the levels and micro-environment in which it is produced NO can be either good or bad.

TABLE OF CONTENTS

LIST OF FIGURES

LIST OF TABLES

Abbreviations	Full Name
1400W	N-(3-(aminomethyl)-benzyl)acetamide
5-HT	5 Hydroxytryptomine
12-HETE	12(R)-Hyroxyeicosatetetraenoic acid
A-I	Hepatic arginase
A-II	Extra-hepatic arginase
AE-ITU	Aminoethyl-isothiourea
AP-1	Activator protein 1
BSA	Bovine serum albumin
CINC	Cytokine neutrophil chemoattractant
cGMP	Cyclic guanidine monophosphate
CO	Carbon monoxide
COX	Cyclooxygenase
CMP 48/80	Compound 48/80
DAB	diaminobezidinetetrahydrochloride
DIG	Deoxygenin
DNA	Deoxyribonucleotide
D-NAME	N^G-nitro-D-arginine methyl ester
ecNOS/eNOS	Endothelial nitric oxide synthase
ECL	Electrochemiluminescence
EDRF	Endothelium-derived relaxing factor
ELISA	Enzyme-linked immunosorbant assay
GAS	Y activated site
HRP	Horse radish peroxidase
HO	Hemeoxygenase
HSP	Heat shock proteins
γINF	Gamma interferon
iNOS	Inducible nitric oxide synthase
IRF-E	Interferon regulatory factor element
ISRE	Interferon stimulated response element

IL-2	Interleukin-2
IL-5	Interleukin-5
L-NAME	N^G-nitro-L-arginine methyl ester
L-NIO	N^G-iminoethyl-L-ornithine
L-NMMA	N^G-monomethyl-L-arginine
L-NA	N^G-nitro-L-arginine
L-NMA	N^G-methyl-L-arginine
LPS	Lipopolysaccharide
LTB_4	Leukotriene B_4
MCGTAP	Murine chronic granulomatous tissue air pouch
MHC	Major histocompatability complex
MN	Mononuclear cells
MWM	Molecular weight markers
NADPH	Nicotinamide adenine dinucleotide phosphate dehydrogenase
NFκB	Nuclear factor kappa beta
NF-IL6	Nuclear factor for interleukin-6
NO	Nitric oxide
NOS	Nitric oxide synthase
nNOS	Neuronal nitric oxide synthase
NSAIDs	Non-steroidal anti-inflammatory drugs
PAF	Platelet activating factor
PBS	Phosphate buffered saline
PBST	Phosphate buffered saline with 0.1% Triton-x100
PGE_2	Prostaglandin E_2
PGI_2	Prostaglandin I_2
RA	Rheumatoid arthritis
RCIP	Rat carrageenin-induced pleurisy
PMNs	Poly morphonuclear neutrophils
SSA	Superoxide scavenging activity

TBS	Tris buffered saline
TTBS	Tris buffered saline with 0.1% Triton-x100
T_0	Theiler's original
TAOS	Total anti-oxidant status
Tc	Cytotoxic T-lymphocytes
TdT	Terminal deoxynuceotide transferase
Th	T-helper lymphocytes
TNF-α	Tumour necrosis factor alpha
TNF-RE	Tumour necrosis factor response element
Tnk	Natural killer lymphocytes
TUNEL	Terminal deoxynuceotide transfer mediated dUTP biotin nick end labelling
v/v	Volume by volume
w/v	Weight by volume

ACKNOWLEDGEMENTS

I would like to thank Prof. D. A. Willoughby and Dr A. Tomlinson for their supervision and invaluable guidance throughout this project and for the opportunity of working within this department. The knowledge and experience that they have imparted to me has permitted me a better understanding of how to organise a scientific project with clarity of mind and scientific acumen.

I would also like to extend my sincere gratitude to Dr D. W. Gilroy, Dr P. Colville-Nash and Dr M. Perretti for their scientific and technical guidance which has been unfailing throughout. This, together with their moral support, encouragement and patience, has made writing this thesis possible.

CHAPTER 1

1.1 The Inflammatory reaction: a historical perspective (Reviewed by Spector and Willoughby, 1968; Florey, 1970).

The word inflammation originates from the Latin verb *inflammare,* meaning to burn and was first described nearly 2000 years ago by Celsus (30 BC - 38 AD) who outlined some of the characteristics of this reaction. In his classical text *De Re Medicina* he described four cardinal signs of inflammation; *rubor* (redness), *calor* (heat), *tumor* (swelling) and *dolor* (pain). A fifth cardinal sign, *functio leasa* (loss of function), was added over 1800 years later by Rudolf Virchow.(1858; Figure 1.1). The process of inflammation is dependent on the surrounding microvascular system which allows the movement of serum proteins and phagocytic cells from the blood into the affected extravascular tissue.

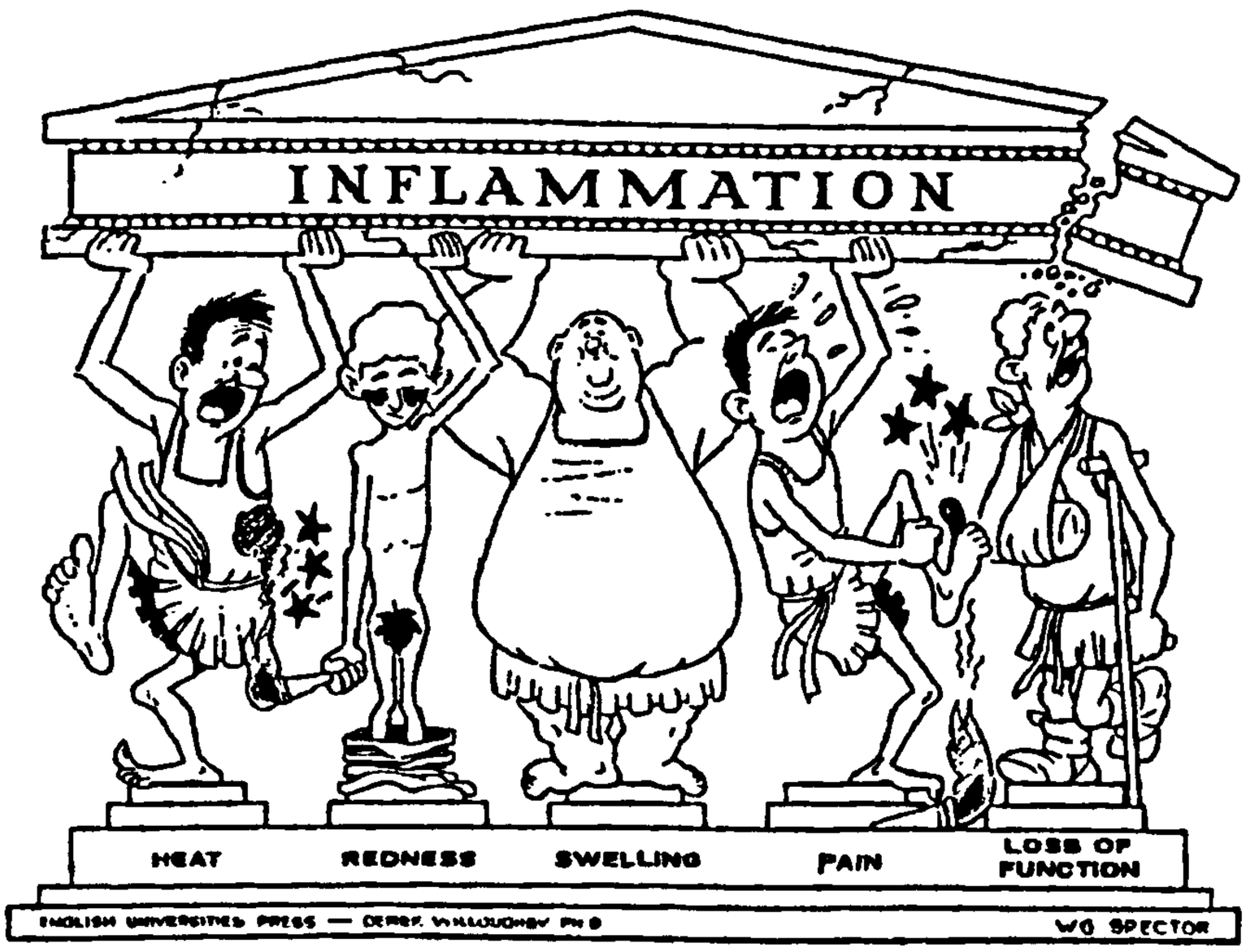

Figure 1.1 Depiction of the cardinal signs of inflammation. *This was taken from "Inflammation and inflammatory desease" written and edited by Spector and Willoughby 1970.*

Early studies in inflammation centered around accurate observations of a wide variety of inflammatory lesions. The reactive nature of inflammations was first described by John Hunter (1794), who concluded "inflammation is itself not to be considered as a disease, but as a salutary operation consequent either to violence or some disease". The basis of the cardinal signs were not further

eluded to until the early 19th century, when Thomson (1813) working with frog transparent foot web, observed that no matter what the stimuli, acid, alkali or saturated salt solutions, there was an increase in blood circulation in capillaries which was normally accompanied by a reduced flow rate in vessels. This suggested that the primary process in inflammation was exudation from small blood vessels. An alternative hypothesis was composed by Virchow (1871) who believed that inflammation was induced by the metabolism of diseased or damaged cells. He suggested the primary changes occured in tissue cells, causing them to swell and divide to produce "pus cells" which later extruded into the surrounding tissue, with the vascular changes only being secondary. This theorem was heavily criticised by Cohnheim (1873) who advocated that the initial inflammatory events were bought about by adaption in the vessel wall. This theory of vascular permeability was added to later by Starling (1896) who demonstrated the importance of osmotic pressure. Our understanding of inflammation today was further added to by Elie Metchnikoff (1892), who was the first to observe and study cellular immunity. His experiments led him to believe that leukocytes were essential to the inflammatory response. The idea that proteins secreted by cell played an integral role in the inflammatory response was developed by Paul Ehrlich who championed the theory of humoral immunity (antibodies) for which he received the Nobel prize. Neuronal involvement in inflammation was shown by Thomas Lewis who found that severance of the autonomic nerve could eliminate the flare but not the wheal or redness caused by experimental inflammation.

Therefore, by the start of the 20th century there was a sound theoretical basis for the inflammatory response, which required further analysis. The description of the inflammatory reaction described below is by no means comprehensive, but includes most of the basic principles involved.

1.2 Cells involved in the inflammatory process

Polymorphonuclear neutrophils (PMNs) are multi-nucleated granulocytes that

are the predominant cell in the early phase of an inflammatory reaction. They release numerous enzymes including collagenase and alkaline phosphatase which are packaged in specific granules. In addition, PMNs release other enzymes such as elastase, myloperoxidase and acid hydrolases from azurophilic granules. Both types of granules are able to release lysozymes (Boxer and Smolen, 1988). PMNs also produce and release the free radical nitric oxide (NO) from both constitutive and inducible forms of nitric oxide synthase (Wright *et al.*, 1989; McCall *et al.*, 1989). This free radical has a number of roles, firstly to act as an anti pathogenic agent (Liew, 1993; Croen, 1993) and secondly plus it may influence the programmed cell death in PMNs. Other free radicals are produced including superoxide that cause tissue destruction by contributing to the degradation of hyaluronic acid, proteoglycans and collagen (Greenwald, 1991). PMNs also release prostaglandins and leukotrienes. Leukotriene B_4 acts as a potent chemoattractant for PMNs promoting the influx of new PMNs to the inflammatory site.

Monocytes are recruited to the inflammatory site by chemotactic stimuli. Once they have migrated out of the circulation they differentiate into macrophages and accumulate at the inflammatory site (Musson *et al.*, 1983; Ridley *et al.*, 1990). In the latter stages of inflammation the macrophage predominates, releasing acid hydrolases (Riches and Stanworth, 1982), collagenases (Wahl *et al.*, 1975) and elastase (Werb and Gordon, 1975). The macrophage is an important cell in the regulation of the inflammatory process releasing free radicals, eicosanoids and a wide range of pro- and anti-inflammatory cytokines (for review see Warrens and Lechler, 1992).

Mast cells are large granulocytes which are widely distributed in most tissues and are particularly numerous adjacent to small blood vessels (Tucker *et al.*, 1977). These cells are important in the initiation of the inflammatory response, rapidly releasing mediators from large basophilic cytoplasmic vesicles that promote vasodilatation and oedema formation at the inflammatory site. They release mediators such as histamine, 5-hydroxytryptamine (5-HT), platelet-

activating factor (PAF), free-radicals, cysteinyl leukotrienes and tumor necrosis factor α (TNF-α) by components of the complement cascade stimulated by IgE (Musch *et al.*, 1987; Jakschik and Lee, 1980: Amon *et al.*, 1994).

Basophil leukocytes constitute less than 1% of circulating leukocytes and bear a close resemblance to mast cells at the electron microscope level. Like other leukocytes they can migrate from the blood to the tissue in response to chemotaxins (Shute, 1992). They can release similar products to mast cells and are particularly prevalent in tissues responding to an allergic stimuli e.g. lung tissue in asthma.

Eosinophils are associated with allergic inflammatory reactions such as asthma (Corrigan and Kay, 1996) where in the lung they are present in large numbers (Makino and Fukada, 1995). They migrate from the bone marrow into the blood stream and from the circulation into the affected tissue in response to an Interleukin-5 (IL-5) gradient (Fernvik et al., 2000). They exert their actions by the release of lipid mediators, cytokines and cytotoxic cationic granule proteins. Like most cells involved in the inflammatory reaction they are able to modulate the immune response by the type and concentration of cytokines released.

T-Lymphocytes are a rich source of cytokines which have potent regulatory effects on the inflammatory reaction (O'Gara and Murphy, 1994, Fitch et al., 1995). During maturation T lymphocytes migrate from the cortex to the medulla of the thymus, where they acquire different cell surface markers that distinguish their function once mature. Two different cell populations exist in the medulla, helper cells containing CD4 cell surface marker and suppressor/cytotoxic T cells with CD8 cell surface marker. Effector functions of lymphocytes include the secretion of pro-inflammatory cytokines and cytotoxic responses to cells containing non-self material or altered membrane antigens. Their regulatory functions include increasing or decreasing the immune response. In general, $CD4^+$ cells secrete pro-inflammatory cytokines that include gamma interfron (γINF), whilst $CD8^+$ cells secrete anti-inflammatory cytokines and perform

cytotoxic functions.

B lymphocytes are important for the secretion of antibodies to invading pathogens and play a key role in antigen mediated immune reactions. B cells are initially stimulated in lymph nodes then migrate to inflammatory sites, where they differentiate terminally to immunoglobulin-producing plasma cells. Activated B cells and plasma cells secrete antibodies that give rise to immune complex formation and activation of the inflammatory cascade.

1.3 Mechanisms of inflammation

Inflammation is normally a localised protective reaction to irritants and trauma. Its function is to destroy and remove noxious and infectious stimuli and limit injury to the host tissue. Microscopically it involves a complex series of responses which include: dilation of arterioles and venules to increase vascular permeability and blood flow to the affected site, exudation of fluid which contains plasma factors and the migration of leukocytes into the inflammatory lesion. These events are controlled by an ever increasing list of inflammatory mediators. Inflammation can be divided into two main areas acute and chronic responses.

1.3.1 Acute inflammation

Acute Inflammation can be divided into two major categories an innate or immunologically non-specific reaction and an adaptive or specific immunological response.

The innate reaction is associated with acute inflammation and can be divided into vascular and cellular changes. This process is dependent on the generation of vasoactive and chemotactic agents, which diffuse from the site of the inflammatory stimulus to the blood vessels (Sorkin *et al.*, 1970; Ryan and Majino, 1977). The initial steps involved in inflammation are increased local vasodilatation which elevates regional blood flow to the affected area and an

increase in microvascular permeability in response to the release of locally formed mediators such as histamine (Movat, 1987). This results in an accumulation of fluid and plasma proteins into the inflamed tissue though large venular junction gaps (Grega *et al.*, 1985). Chemotactic mediators such as IL-8 and are produced by the affected area and stimulate the adherence of circulating granulocytes and mononuclear cells to the vascular endothelium. These cells then migrate under the influence of a chemotactic gradient to the inflammatory site (Lee, 1987). At the focal point of the stimulus, recruited cells accumulate and become activated. The principal cell types involved in this reaction are PMNs and monocytes/macrophages. These phagocytic cells ingest foreign material and cellular debris into an infolding of the cytoplasmic membrane called a phagosome by a process known as endocytosis. The phagosomes containing ingested particles fuse with lysosomes produced by the Golgi which release by endocytosis an extensive array of hydrolytic enzymes (e.g. nucleases, proteinases, lipases etc) capable of breaking down most classes of biological macromolecules (Chayen and Bitensky, 1971). This process is a method of limiting tissue damage, however paradoxically the release of lysosomal enzymes and reactive oxidants into the cellular environment may also contribute to cellular injury.

The adaptive response is mediated by specific immune reactions to antigens which is superimposed over and potentiates the basic innate response. This results in a more prolonged and efficient reaction. The immune response to antigens can be divided into two components, humoral or antibody-mediated reaction and the cell-mediated response. Since the adaptive response does not form the major part of this thesis, it is described only briefly. In cell-mediated immunity, antigens are presented on major histocompatibility complex (MHC) to T helper (Th) lymphocytes in the lymph nodes by antigen presenting cells like macrophages and dendritic cells (Rosenthal and Shevach, 1973). Antigen presentation to Th0 lymphocytes stimulates the release of IL-2, a T lymphocyte differentiation factor. This event results in the production of cytotoxic T lymphocytes (Tc) or natural killer lymphocytes (Tnk) and together with cytokines

released by Th cells elicit the effector system of cell mediated immunity (Young *et al.*, 1990). Recent evidence suggests that Th and Tc cells can be separated into two distinct subtypes, classed on their cytokine production profiles. These are Th1 (or Tc1) type lymphocytes or Th2 (or Tc2) type lymphocytes. The derivation of these two subsets is not fully understood but seems to be reliant on antigen dose, route of administration, APC phenotype, co-receptors present on APC and biological mediators prevalent during antigen presentation (for review see Mosmann and Sad, 1996; Kane *et al.*, 2001). These subsets of T cells have been implicated in different pathologies. Th1 type reactions are associated with cell mediated immune responses and Th2 antibody mediated allergic immune responses. However it must be noted that although these reactions seem to be mutually exclusive, both can occur within any one pathological reaction. Indeed it is the cytokines released by either Th 1 or Th 2 lymphocytes that mediate the relevant immune response. Due to the specific nature of these responses it is believed that the immune reaction is polarised in various diseases and this then contributes to the ongoing pathology. The majority of the work on Th1 and Th2 subsets has been carried out *in vitro* with recently some new evidence coming from *in vivo* studies for subsets in inflammation (Dong and Flavell, 2001).

1.3.2 Chronic inflammation

Post acute injury, PMNs undergo a process known as apoptosis which facilitates their removal by macrophages in the inflammatory site. This 'subacute' inflammatory response represents the early stages of resolution leading to the formation of granulation tissue.

In chronic inflammation both the innate and adaptive response contribute to the formation of the chronic lesion, which is synonymous with formation of granulomatous tissue. This type of inflammatory tissue is characterised by the proliferation of endothelial cells resulting in the formation of new capillaries (angiogenesis) within the granuloma leading to a restoration of the vascular supply (Risau, 1990; Diaz-Flores *et al.*, 1994). In addition, proliferation of

fibroblasts restore the connective tissue matrix in the injured area by increasing the synthesis of glycosaminoglycans and collagen type I and type III (Ross, 1975; Duncan and Berman, 1989a; Duncan and Berman, 1989b). Proliferation of endothelial cells and fibroblasts is orchestrated by specific mediators secreted by activated macrophages, T-lymphocytes (Lowry, 1993), plasma and platelet derived factors (Deuel *et al.*, 1991). These processes result in increased connective tissue synthesis, deposition and perfusion of the granuloma. In circumstances where the inflammatory response is unable to eliminate the injurious agent or restore involved tissue to its normal physiological state, there is a progression of inflammation and of the chronic lesion. Acute and chronic inflammation represents a complex series of events which are frequently overlaid. However, our understanding of the involvement of specific mediators present in this complex reaction is still limited. Further investigation is still required to elucidate their role and potential as therapeutic targets.

1.4 Nitric oxide (NO) synthase pathway, its products and function in inflammation

NO is one of the most recently described mediators that has been implicated in the pathophysiological changes seen in acute and chronic inflammation. In fact, within the last 10 years considerable advances have been made in the understanding of NO as an inter- and intra- cellular messenger and its function within the inflammatory reaction. The involvement of NO in mammalian and rodent cell biology is enormous (for detailed reviews see Nathan, 1992; Bredt and Snyder, 1994), but since this thesis focuses on inflammation, the involvement of the NOS pathway will be discussed within this realm.

1.4.1 Brief History

The history of the discovery of the L-arginine-NO pathway is discussed only briefly, as excellent reviews are available (Hibbs *et al.*, 1990; Moncada *et al.*, 1991; Nathan, 1992). The possibility that NO could have a biological role was first suggested by Murad and colleagues (1977), who demonstrated that

exogenous NO and NO releasing compounds could activate guanylate cyclase in various tissue preparations. However, it wasn't until the early 1980s, in studies inspired by analysis of carcinogenesis that mammalian cells were first demonstrated to synthesise inorganic oxides of nitrogen. In 1981 Green and colleagues (1981a, b) reported that germ-free rats and humans were able to excrete more nitrate than they consumed, suggesting that mammals can synthesise nitrogen oxides endogenously. The excretion of nitrite was found to be further elevated during inflammatory episodes induced by inflammatory and infectious agents, and could in part be explained by the ability of influxing macrophages to excrete nitrite and nitrate (Stuehr and Marletta, 1985). These macrophages were able to metabolise L-arginine to form L-citrulline and a substance that causes nitrosation of amines.

Independently, researchers working on the biochemistry of the cytostatic/cytocidal effects that activated macrophages have on tumour cells and fungi showed a degree of oxidative damage and iron loss associated with this phenomenon (Hibbs *et al.*, 1990). These same investigators demonstrated that substituting one or both of the terminal guanidino nitrogens of L-arginine inhibited this cytotoxic activity. This oxidising activity observed in macrophages could not be mimicked by the addition of exogenous nitrite or nitrate (Hibbs *et al.*, 1987) except at lower than physiological pH, where nitrite was reduced to nitrite and NO (Stuehr and Nathan, 1989). This suggested once again that the biologically active component was a highly reactive oxide of nitrogen which could be oxidised rapidly to nitrite and nitrate.

A third line of investigation also centred upon a nitrogen oxide being a potent signalling molecule. Arnold and co-workers (1977) showed that a diverse range of compounds that release NO could activate soluble guanylate cyclase, and in some circumstances this occurred through *S*-nitrosothiol intermediates (Ignarro *et al.*, 1981). These compounds had profound physiological effects *in vitro* which included inhibition of platelet aggregation (Mellion *et al.*, 1981) and the induction of vasorelaxation (Gruetter *et al.*, 1979). *In vivo* data generated by Furchgott and

Zawadzki (1980) showed that compounds which did not release NO themselves were able to evoke vasorelaxation. They demonstrated that these substances exerted their actions by stimulating endothelial cells to release a short lived vasodilator mediator termed endothelium-derived relaxing factor (EDRF), whose properties were remarkably similar to that of NO.

The identity of EDRF was confirmed by two independent groups (Ignarro *et al.*, 1987; Palmer *et al.*, 1987) who showed that the vasodilator activity attributed to EDRF could be accounted for by NO. The verification that macrophages also released an EDRF-like substance indistinguishable from NO (Stuehr et al., 1989) confirmed the importance of this free radical as a biological signalling molecule. Therefore, NO could account for two fundamental mechanisms observed *in vivo*, one being physiological (vasodilation) and the second pathophysiological (inhibition of pathogen metabolism). These discoveries opened the flood gates to thousands of investigations which implicated NO in neurotransmission, reproduction, host defence mechanisms and several pathological events (for review see Moncada et al., 1989). This led to NO being named as "molecule of the year" (Koshland, 1992), with to date numerous reviews available on all aspects of its biology and chemistry.

The enzyme responsible for the production of NO was named nitric oxide synthase (NOS; EC 1.14.13.39). Although there is no argument about the fact that NO is the primary product released by NOS, it remains unclear which reactive oxides of nitrogen are responsible for individual nitrosation products and the eventual effects ascribed. Therefore, throughout this thesis effects that are assigned to NO are done so for simplicity. The real cellular protagonists formed by NOS producing cells are probably a combination of NO, NO_2, NO_3, N_2O_3, NO_2^-, NO_3^-, $ONOO^-$, nitrosoamines, non-protein and low molecular weight protein *S*-nitrosothiols and *S*-nitrosylated proteins.

1.4.2 NO in inflammation

When considering the role played by NO in inflammation, the cells and

mediators present during various stages of the inflammatory response must be considered. In the acute phase of inflammation PMNs are dominant at the initial stage, which usually spans 4-6 h. Continued insult results in a chronic inflammatory response which is characterised by the activation of mononuclear cells and the expression of iNOS in a wide variety of cells.

Acute inflammation: Acute inflammation is a short-lived resolving event. Mechanical and thermal trauma or the invasion of pathogens results in the release of acute phase mediators, of these histamine, 5-hydroxytryptamine, bradykinin, platelet activating factor (PAF) and substance P, evoke release of endothelial NO, causing vasodilatation and vascular permeability, thus facilitating oedema formation and trafficking of inflammatory cells (Fujii *et al.*, 1994). In a series of experiments endothelial-derived NO was demonstrated to inhibit platelet aggregation and adhesion to the vessel wall and with PGI_2 to regulate platelet-endothelial cell interactions (Radomski *et al.*, 1987a-d). Carrageenin-induced rat skin permeability and carrageenin and dextran-induced models of paw oedema show a dose-dependent inhibition of vascular permeability and oedema formation with L-arginine analogues, which inhibit NOS, suggesting that NO released at the inflammatory site was involved (Ialenti *et al.*, 1992).

The majority of the literature available up to 1996, looking at the impact of NOS inhibition in acute models of inflammation, concluded that inhibition of NO at the inflammatory site was beneficial (Iuvone *et al.*, 1994; Salvemini *et al.*, 1995, Tracey *et al.*, 1995; Medeiros *et al.*, 1995; Sautebin *et al.*, 1995; Salvemini *et al.*, 1996). These studies performed in acute inflammatory models in the rat, demonstrated that systemic inhibition of NO with a number of different NOS inhibitors (ranging from non-specific NG-nitro-L-arginine methyl ester (L-NAME) to selective iNOS inhibitors L-NIL) significantly reduced the number of inflammatory cells and exudate present at the inflammatory site compared with vehicle treated animals. In the majority of these studies the anti-inflammatory effects were accompanied by an inhibition of iNOS protein and/or nitrite, with

some showing no effect on systemic arterial blood pressure. Therefore, the conclusion was drawn that inhibition of NO was beneficial in acute inflammation. However, the NOS inhibitors used were at best only 20% more selective for iNOS, and at worst had no selectivity between all three isoforms. Given their lack of selectivity, it is conceivable that systemic administration may also inhibit ecNOS remote from the inflammatory locus resulting in vasoconstriction, reduced blood delivery to the inflamed site and leucocyte margination: hence, a reduction in inflammation. Greenblatt and colleagues (1993) suggested that the control of leukocyte-endothelial cell interaction may be more complex and involve local regulation of the cardiovascular system, since there was a great variability in the magnitude of basal NO-dependent tone depending on the microvascular bed. Therefore, in summary it appears that in models of shock and inflammation, NO derived from iNOS may be responsible for most of the pathophysiological actions, whereas, eNOS has beneficial and protective roles by virtue of its ability to maintain vascular perfusion of the affected area and so its inhibition is not advantageous (for review see Kubes, 2000). Excessive inhibition of eNOS may mask the beneficial effects of inhibiting iNOS, therefore care must be taken in interpreting data obtained from pharmacological studies.

Leukocyte endothelial interactions: The recruitment of leukocytes at the inflammatory site is one of the main host responses that occur in inflammation and is largely determined by events that take place in the specific region of the microvasculature (postcapillary venules). When the leukocytes move out from the capillaries, the hemodynamic forces in the venules favour the outward movement of these cells to the blood vessel wall. The sequential series of events that ensue result in the transmigration of PMNs into the perivenular interstitium and then to the inflammatory site under the influence of various chemotactic agents. NO has been shown to be involved in this process (Granger and Kubes, 1994). More specifically, inhibition of NO synthesis promotes P-selectin-dependent leukocyte rolling (Terada, 1996), suggesting that NO may be a hemostatic factor in the downregulation of PMN rolling under normal conditions. In support of this finding, the addition of exogenous NO decreases

PMN rolling under normal conditions (Gaboury *et al.*, 1993; Gauthier *et al.*, 1994). Under inflammatory conditions the same effects ascribed to NO were also demonstrated (Kubes *et al.*, 1997; Hickey *et al.*, 1997).

NO has been proposed to be involved in adhesion since in a model of ischemic reperfusion, NO significantly reduces leukocyte adhesion to endothelium (Ma *et al.*, 1993) and its associated injury (Lefer *et al.*, 1993). The anti-adhesive properties of NO is suggested to be related to its ability to inactivate superoxide by a mutual scavenging pathway, therefore nullifying the effects of both free-radicals. Since superoxide produced by the neutrophil is believed to be important in activating the endothelium, promoting firm adhesion of the PMN (Kubes *et al.*, 1994). The role of NO in migration has been demonstrated using NOS inhibitors, which elicit leukocyte migration, a phenomenon that was reversed by L-arginine (Kurose *et al.*, 1994). In conclusion, NO seems to be an important regulator of PMN function in both physiological and pathophysiological conditions and therefore would be of interest as therapeutic target in inflammation. However, there are many contradictory reports for the effect of NO in inflammatory process, therefore this area requires further investigation.

Chronic inflammation: iNOS has also been shown to be present during chronic inflammatory tissue formation (Vane *et al.*, 1994) with iNOS activity associated with the peak of granulomatous tissue formation in mice. In another model of chronic granulomatous tissue formation in rats, L-NAME dose-dependently reduced the lesion size, cell infiltration and nitrite production (Iuvone *et al.*, 1994). In other studies in rodents, it was suggested that iNOS expression in the chronic state may be part of a maladaptive process, with NO production being associated with synovial tissue in a streptococcal wall-induced arthritis. NO was involved in the development of destructive inflammation, which could be inhibited using NOS inhibitors (McCartney-Francis *et al.*, 1993). In MRL-lpr/lpr mice, animals that spontaneously develop a systemic autoimmune disorder, that the development of inflammatory nephritis and arthritis coincide with the appearance of nitrate and nitrite in the urine. The chronic inflammatory changes

that occurred in these mice were significantly reduced by the administration of a NOS inhibitor (Weinberg *et al.*, 1994). However, still little is known about NO's involvement in chronic inflammation, therefore further work is required. A summary of the role of NO in inflammation can be seen in Figure 1.2

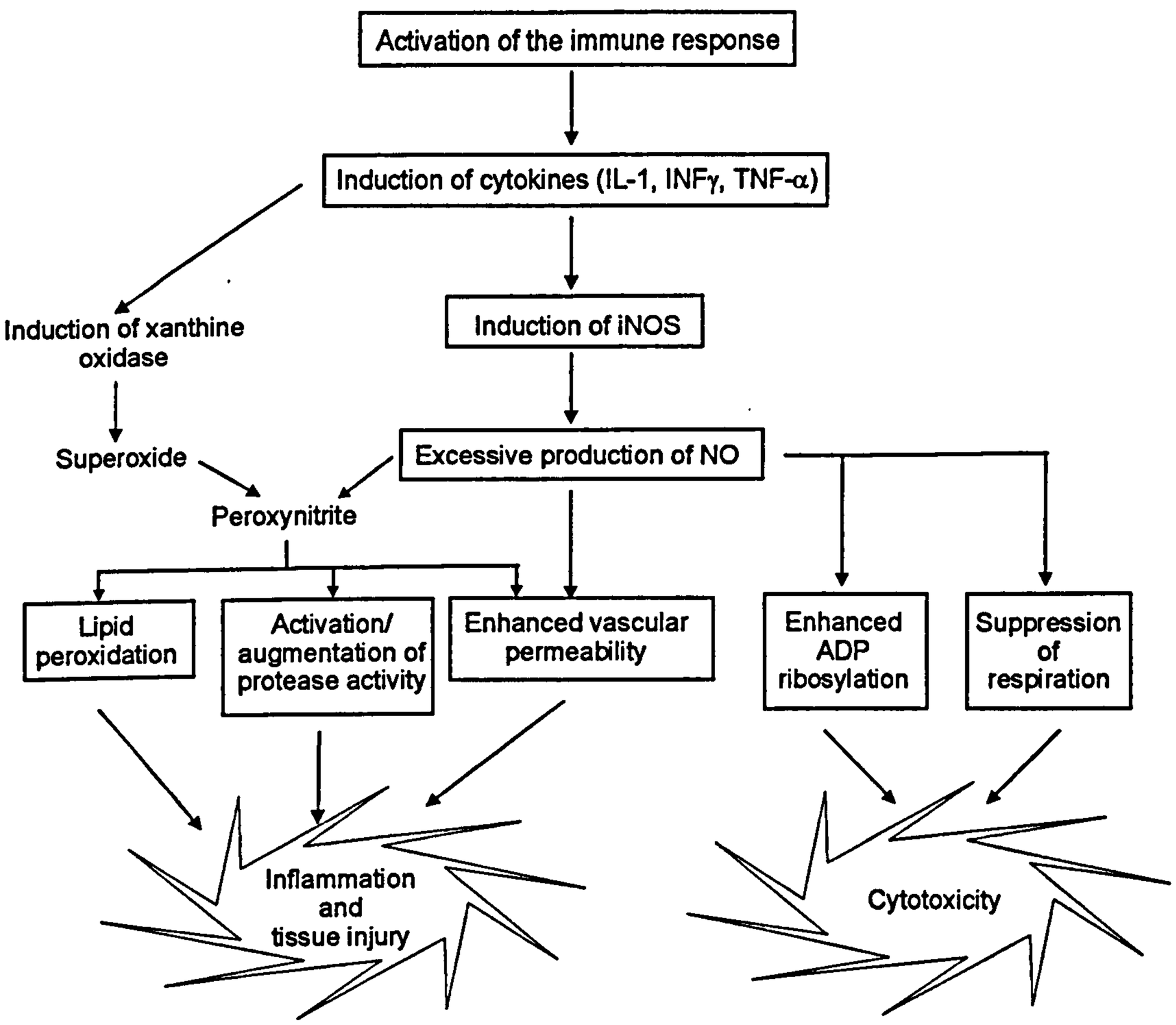

Figure 1.2 Summary of the role of NO in inflammation and immunity (modified from Maeda et al., 1994).

1.4.3 NO in inflammatory diseases

Rheumatoid arthritis: Rheumatoid arthritis (RA) is a chronic inflammatory autoimmune disease, characterised by proliferation of the synovial lining of the joint cavity forming an invasive inflammatory tissue termed pannus. RA is a relapsing and remitting disease with reoccurrences accompanied by PMN influx into the synovium. The evidence for NO's involvement in RA is accumulating. Elevated levels of nitrite have been reported in serum and synovial fluids taken

from patients with active rheumatoid arthritis (Farrel *et al.*, 1992). NO production and iNOS expression in RA patients was localised to the inflamed synovium and cartilage by immunohistochemisty and RT-PCR (Sakurai *et al.*, 1995; McInnes *et al.*, 1996). Stimulation of human articular chondrocytes with inflammatory cytokines and LPS in culture causes a sizable induction of nitrite levels accompanied by an inhibition of proteoglycan synthesis (Hauselmann *et al.*, 1994). Ueki and colleagues (1996) demonstrated a close correlation between serum nitrite and disease activity, which included joint swelling, C-reactive protein, TNF-α and IL-6 levels. Similar findings concerning the relationship of NO and severity of inflammation were also found in rodent models of the disease (Ialenti *et al.*, 1992) with a suppression of the development of arthritis after the administration of NOS inhibitors (McCartney-Francis et al., 1993; Stefanovic-Racic *et al.*, 1995; Conner *et al.*, 1995). Thus, the involvement of NO in the pathogenesis of autoimmune and inflammatory arthritis is particularly strong.

Gastrointestinal inflammation (GI): Inflammation of the GI tract is characterised by inflammatory cell infiltration and often involves motility disorders associated with toxic dilatation. Ulcerative colitis and Crohn's disease are inflammatory disorders of the GI tract in man. The colonic mucosa of patients with ulcerative colitis has a considerable elevation of iNOS activity compared with non-inflamed tissue, with similar levels in the surrounding musculature. In contrast, iNOS activity in the mucosa of patients with Crohn's disease was no different from controls (Boughton-Smith *et al.*, 1993a). Modulation of NO production in animal models of GI tract inflammation have produced conflicting results. Exogenous administered NO appears to afford protection against tissue damage by inhibiting capillary leakage, PMN infiltration and to a greater or lesser extent depending on the model used and parameters measured (Hutcheson *et al.*, 1990; Boughton-Smith *et al.*, 1992; Miller *et al.*, 1993). In comparison, iNOS activity in the intestines of LPS-treated rats was accompanied by increased vascular permeability which could be inhibited by L-arginine analogue (Boughton-Smith *et al.*, 1993b).

1.4.4 Biochemistry of NO synthesis from L-arginine

Molecular characterisation of the various isoforms of NOS has given rise to considerable information concerning its regulation, physiological and pathophysiological roles. The L-arginine-NO pathway has been identified in many species including fish, birds, plants and bacteria, but has been most extensively studied in mammals (Nathan, 1992; Knowles et al., 1994). The expanding family of NOS enzymes falls into two categories, the first are constitutive isoenzymes regulated by Ca^{2+} and calmodulin of which there are two distinct isoforms; neuronal NOS (nNOS) also described as Type I NOS or NOS-1 or bNOS and endothelial NOS (eNOS) also known as ecNOS Type III NOS or NOS-3. The second is a cytokine-inducible form that has calmodulin tightly bound within the dimer, therefore is permanently active and reasonably unaffected by post-transciptional control (for review see Marletta *et al.*, 1994). The three NOS isoforms are encoded by distinct genes and consist of either 26 exons (iNOS and eNOS) or 29 exons (nNOS; Nathan, 1992; Knowles et al., 1994). The isoforms share 50-60% homology between species and isoforms and ~90% between isoforms of a specific species (Figure 1.3), and display many similarities to the cytochrome P_{450} family of enzymes. eNOS and nNOS consist of an inactive dimer (subunits ~130 kDa in size) held together with a heme prosthetic group. This dimer is activated by Ca^{2+} and calmodulin. Both iNOS and nNOS are cytosolic, but eNOS is more then 90% particulate (Forstermann et al., 1991) with myristylation at the N-terminal glycine as well as palmitylation which associates the enzyme with membrane caveolae (Pollock et al., 1991; Garcia-Gardena et al., 1997).

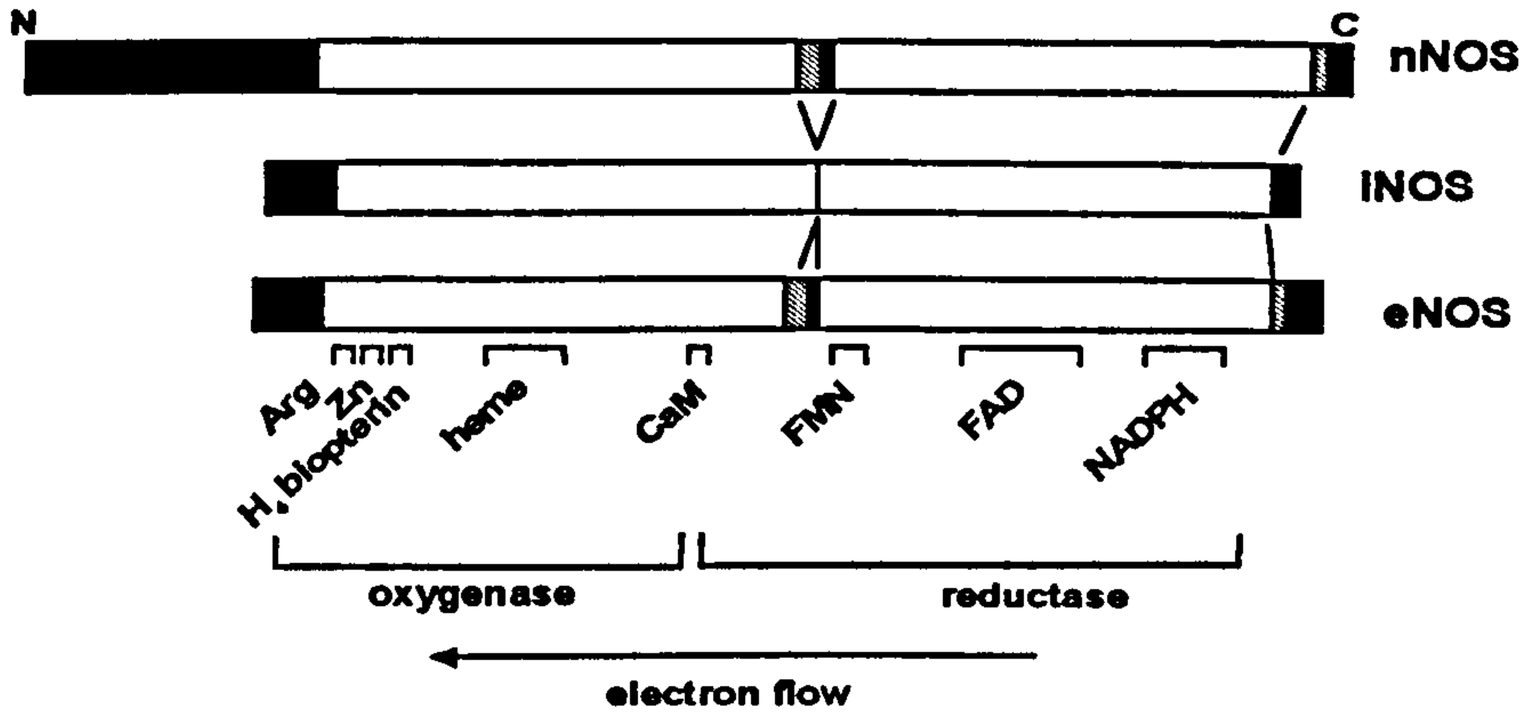

Figure 1.3 Structure of NOS isoforms. *NH_2 (N) and COOH (C) termini are indicated. Homology in amino acid sequence is depicted: open boxes, homologous regions; hatched boxes in nNOS and eNOS; solid boxes, isoform specific sequences. Regions involved in the binding of co-factors are indicated as well as the oxygenase and reductase domain and the direction of intramolecular electron flow. Arg, arginine; H4 biopterin, tetrahydrobiopterin; CaM, calmodulin; FMN, flavin mononucleotide; FAD, flavin adenine dinucleotide.*

The proposed biochemical scheme for the formation of NO was eluded to by a series of isotope studies (Kwon *et al.*, 1990; Leone *et al.*, 1991). In summary, these experiments showed that L-arginine is hydroxylated at the terminal amidine nitrogen followed by the specific further oxidation of that nitrogen. This reaction requires a 5 electron oxidation and ultimately leads to the formation of citrulline and NO (summarised in Figure 1.4), which decomposes to nitrite and nitrate.

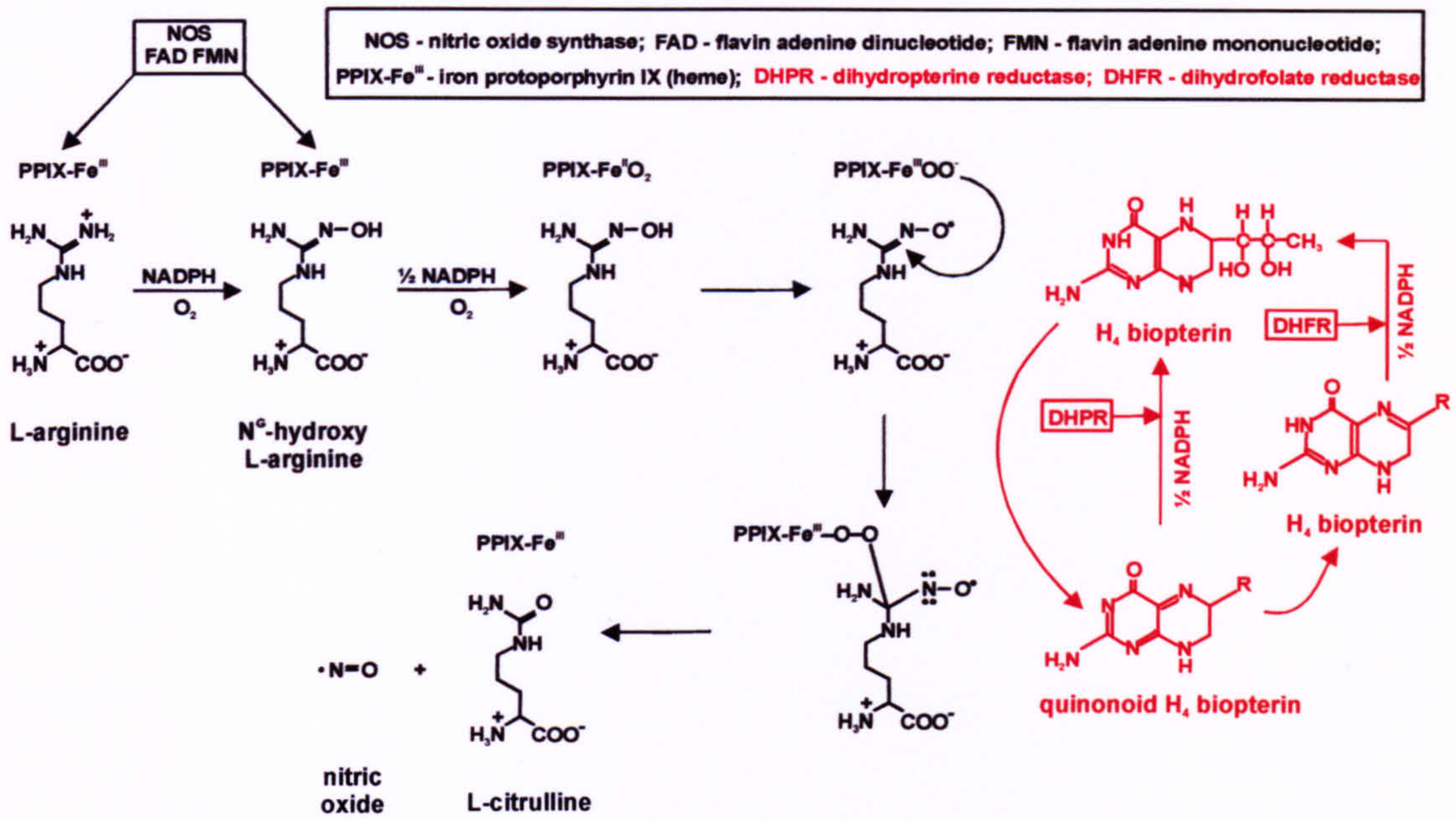

Figure 1.4 Proposed reaction mechanism for NO synthesis. *Molecular oxygen is incorporated into both NO and L-citrulline in at least two phases. The first step consist of the N-hydroxylation of L-arginine to the stable intermediate N^G-hydroxy-L-arginine which requires 1 mol of the electron donor NADPH and the second its subsequent oxidation to L-citrulline and NO which needs 0.5 mol NADPH and is dependent on H$_4$ biopterin. The flavin cofactors FAD and FMN, and the cytochrome P$_{450}$ domain of NOS may mediate electron transfer from 1.5 mol NADPH to molecular oxygen in one or both phases. Terahydrobiopterin (H$_4$ biopterin) may also be involved in electron transfer and both flavins and H$_4$ biopterin may then recycle in an NADPH-dependent manner (modified from Nathan, 1992; Marletta, 1993).*

The process involves two successive monooxygenation reactions, the first yielding N^G-hydroxy-L-arginine as an intermediate (Stuehr *et al.*, 1991b). The second step involves an oxygenation reaction which forms the final products NO and L-citrulline (Stuehr and Griffiths, 1992), however the exact process remains unclear, but is predicted in Figure 1.4, based upon cytochrome P$_{450}$ enzymology. Recent studies have shed light on this one electron anomaly for the production of NO from N^G-hydroxy-L-arginine. They suggest that nitroxyl (HNO), and not NO, is the preferred nitrogen product (Fukuto *et al.*, 1992, Fukuto et al., 1993) and HNO is converted to NO by a variety of physiological oxidants including superoxide dismutase (SOD), oxygen and hemeproteins. This is supported by the fact that HNO has been shown to have biological activity indistinguishable from NO and that SOD enhances directly the formation of free NO from L-

arginine by NOS (Hobbs *et al.*, 1994). The mechanism for this potentiation was independent of superoxide dismutation and NOS activation. Production of NO by NOS requires the presence of the co-substrates L-arginine, nicotinamide adenine dinulceotide phosphate (NADPH) and molecular oxygen (O_2). Sequence analysis of the NOS isoforms primary structure has distinguished important functional motifs. These manifest themselves as 4 prosthetic groups which are required for NO formation: flavin adenine dinucleotide (FAD; Stuehr *et al.*, 1991a; Stuehr *et al.*, 1995), flavin adenine mononucleotide (FMN; Stuehr *et al.*, 1991a; Stuehr *et al.*, 1995), iron protopophyrin IX (heme; White and Marletta, 1992), calmodulin and tetrahydrobiopterin (H_4 biopterin; Tayeh and Marletta, 1989; Kwon *et al.*, 1989). FAD and FMN are involved in the transfer of electrons from NADPH to the catalytic centre (Bredt *et al.*, 1991), whereas heme functions as a redox-active co-factor in NOS catalysis (Klatt *et al.*, 1992; McMillan *et al.*, 1992). Finally, H_4 biopterin is necessary for the monooxygenation steps performed by NOS (Stuehr and Griffiths, 1992). For a detailed review see Marletta (1994a).

1.4.5 Promoter sequences and control of iNOS expression

The 5'-flanking region of human iNOS has approximately 66% homology with its murine counterpart, and this 37kb, 26 exon gene is located on chromosome 17 at position 17cen-q11.2 (Chartrain *et al.*, 1994). The control of expression of iNOS, which is complex, is for the most part at the transcriptional level. Cytokines upregulate human iNOS mRNA transcripts with different transcription initiation sites as well as both regularly spliced and alternatively spliced human iNOS mRNA in which various coding and/or non-coding regions are absent (Chu *et al.*, 1995; Eissa *et al.*, 1996). Mechanisms for the expression of human and murine genes are very different and reflect the tighter regulation that human iNOS is under (De Vera et al., 1996). All or most of the cis-regulatory elements that control the transcription of the murine iNOS gene are in a 1.6 kb 5'-flanking region (Xie and Nathan, 1993; Lowenstein *et al.*, 1993; Weisz *et al.*, 1996; Kim *et al.*, 1997). In contrast, up to 3.7 kb of the 5'-flanking region of the human iNOS gene does not contain all the cis-regulatory elements required for the

transcriptional induction by cytokines. In addition, the human iNOS gene contains three human specific *Alu* regulatory sequences (dimeric sequences of approximately 300bp in length) which modulate processes that include recombination, transcription and translation (De Vera *et al.*, 1996; Laubach *et al.*, 1997).

The region that contains many cis-regulatory elements for binding of transcription factors involved in the cytokine induction of iNOS, include sites for activator protein 1 (AP-1), nuclear factor-κB (NF-κB), γ interferon (γ-IRE), nuclear factor for IL-6 (NF-IL6), γ-activated site (GAS), IFN regulatory factor element (IRF-E), IFN -stimulated response element (ISRE), TNF response element (TNF-RE) and an X box (Kaling *et al.*, 1991; Chu *et al.*, 1998). The majority of work on the promoter sequence of iNOS has centred upon the transcription factors NF-κB and interferon response factor. The latter appears to function as an enhancer and is not able to initiate gene expression independently (Lowenstein *et al.*, 1993). This is supported by the observation that γINF enhances the production of NO after stimulation with LPS in a murine macrophage cell line through the stabilisation of iNOS mRNA (Martin *et al.*, 1994).

NF-κB exists as an inactive heterodimer in the cytoplasm consisting of the DNA binding proteins p50 and p65 and an inhibitory protein termed IκB (Baeuerle, 1991; Baeuerle and Baltimore, 1988). Once activated, IκB is phosphorylated and the active dimer translocates to the nucleus, where it can bind to its consensus sequence on the promoter regions of genes (Urban *et al.*, 1991). The murine iNOS promoter sequence is described as being exquisitively sensitive to regulation by NF-κB. Therefore, it is not surprising that agents which suppress NF-κB activity inhibit the induction of iNOS in cultured cells. These include many antioxidants such as pyrolidinedithiocarbamate and diethyldithiocarbamate (Sherman *et al.*, 1993; Mulsch *et al.*, 1993). In addition, protease inhibitors such as Nα-p-tosyl-L-phenylalanine, Nα-p-tosyl-L-lysine-cholomethylketone, calpain and the proteosome inhibitors, Z-IE(O-t-Bu)A-

Leucinal, are able to inhibit iNOS induction through suppression of IκB degradation (Griscavage *et al.*, 1995; Griscavage *et al.*, 1996). In fact, the iNOS inhibitory actions of the anti-inflammatory drugs dexamethasone and aspirin have been suggested to occur through interference with NF-κB activity (Auphan *et al.*, 1995; Kopp and Gosh, 1994).

1.4.6 Substrate and co-factor availability as regulators of iNOS activity

Full iNOS and cNOS activity has been shown to be dependent on H_4 biopterin synthesis, which is reliant on the rate-limiting enzyme GTP cyclohydrolase I (Gross and Levi, 1992). This enzyme converts GTP to dihydroneopterin and is co-induced with iNOS in many different cell types (Di-Silvo *et al.*, 1993; Gross and Levy, 1993). Therefore inhibitors of GTP cyclohydrolase (2,4-diamino-6-hydroxypyrimidine, methothrexate and N-acetylseritonin) may be of therapeutic use for limiting iNOS overexpression in certain pathologies like septic shock.

eNOS and nNOS are very sensitive to intracellular Ca^{2+} concentrations for activation and represents the main translational switch for NO production from these isoforms. Cytosolic Ca^{2+} is required for the binding of calmodulin to the NOS homodimer and it has been demonstrated that addition of the calcium chelator EGTA renders these isoforms inactive (Nathan and Xie, 1994).

Substrate availability may also represent a mechanism by which NO production by iNOS may be governed. In various cell types, including macrophages and endothelial cells, L-arginine transport is up-regulated in response to inflammatory stimuli which induce the expression of iNOS (Bogle *et al.*, 1992; Durante *et al.*, 1996). In macrophages this process is regulated by the cationic amino acid transporter MCAT-2B (Closs *et al.*, 1993). It is worth noting that L-lysine and L-ornithine (product of the arginase pathway) are also substrates for this transporter and therefore would act as competitive inhibitors for L-arginine transport (Bogle *et al.*, 1992). Since NO production by iNOS in immune cells is solely dependent on the transport of extracellular L-arginine, inhibition of this pathway would blunt NO production in these cells and inhibit NO-mediated

effects (Bianchi *et al.*, 1995). Interestingly, low levels of L-arginine in the presence of NADPH can lead to the production of superoxide and hydrogen peroxide by nNOS and eNOS, possibly leading to increased tissue damage (Mayer et al., 1990; Vasquez-Vivar *et al.*, 1998).

Phosphorylation is the acceptance of a phosphate group onto an amino acid residue. Accessible serine and tyrosine residues present in the tertiary structures of the NOS enzymes are sensitive to phosphorylation and may provide another target for post-translational regulation. In fact, phosphorylation modulates the activity of all three NOS isoforms. Recently, in LPS induced RAW 246.7 macrophages, iNOS protein was demonstrated to undergo tyrosine phosphorylation resulting in an abatement of protein production and NO formation. This inhibitory event was reversed by brief exposure of the cells to the tyrosine phosphatase inhibitor vanadate (Pan *et al.*, 1996). In contrast, the protein tyrosine inhibitor, phenylarsine oxide, has been shown to activate eNOS in the presence or absence of extracellular Ca^{2+} and the calmodulin inhibitor calmidazolium. This suggests that tyrosine phosphorylation is essential for Ca^{2+}-independent eNOS activation (Fleming *et al.*, 1998). Serine phosphorylation of eNOS occurs rapidly when endothelial cells are exposed to sheer stress and calcium-mobilising agents (Michel *et al.*, 1993; Corson *et al.*, 1996). Phosphorylation of threonine-495 and serine-1177 of human eNOS by protein kinase A results in eNOS activation (Michell *et al.*, 1999). However, inhibitory actions of serine phosphorylation have also been reported (Hirata *et al.*, 1995). Similarly to eNOS, nNOS is also regulated by phosphorylation in a positive and negative manner (Watanabe *et al.*, 1996; Hayashi *et al.*, 1999).

1.4.7 Cellular production and activity of NO at inflammatory sites

The major cell types present at the site of both acute and chronic inflammation are PMNs and macrophages. PMNs have been shown to synthesise NO (Wright *et al.*, 1989; McCall *et al.*, 1989), with levels sufficient to cause vasodilation *in vitro* (Schmidt *et al.*, 1989) and inhibit thrombin induced platelet aggregation (Salvemini *et al.*, 1989). It was hypothesised that PMN-derived NO produced in

the early stages of a wound model mediates vasodilatation, inhibition of platelet aggregation and acts as an antimicrobial effector molecule (Albina *et al.*, 1990). In fact, cytoplasts produced from human PMNs have been demonstrated to kill staphylococcus bacteria (Malawista *et al.*, 1992). PMNs isolated from rat, human and mouse origins are all able to produce reactive nitrogen intermediates, however nitrite levels are lower than that obtained in rodent macrophages (Padgett and Pruett, 1995). Recently, human platelets have been shown to contain nNOS as well as iNOS protein (Wallerath *et al.*, 1997). These same investigators showed that eosinophils also contain iNOS protein. However, although these levels of NO are sufficient for vasodilation and neurotransmission it still remains to be determined whether NO produced by PMNs has a role in non-specific host defence reactions, as an antimicrobial or tumour suppressor agent.

Rodent macrophage cell lines can produce substantial levels of NO in response to bacterial cell wall products and pro-inflammatory cytokines, such as γINF, TNF-α and IL-1β. Macrophages secrete large amounts of IL-1 and TNF-α in both an autocrine and paracrine fashion. NOS activation in macrophages by these pro-inflammatory cytokines can be inhibited by the presence of TGF-β (Tsunawaki *et al.*, 1988; Ding *et al.*, 1990), probably through destabilisation of iNOS mRNA (Vodovortz *et al.*, 1993). This is supported by data obtained from a model of chronic granulomatous tissue formation, in which iNOS activity declined as TGF-β protein increased (Vane *et al.*, 1994). This negative regulatory role of TGF-β was confirmed in a model of carrageenin-induced acute inflammation (Ianaro *et al.*, 1995). Many inflammatory models and diseases require the involvement of T helper lymphocytes, with a Th1 type response being associated with cell-mediated inflammation and Th2 with hypersensitivity reactions. Th2 derived cytokines, in particular, IL-4 and IL-10 suppress macrophage production of NO which can lead to an inhibition of macrophage function.

In addition to recruited inflammatory cells, it can be predicted that NO produced by host tissue may add to NO production at the site of inflammation. This is

supported by the fact that an ever increasing list of cells and tissues can produce NO upon stimulation, including keratinocytes, retinal cells, renal tubular epithelium, mysoepithelium, mesothelium, hepatocytes, vascular endothelium, fibroblast, chondrocytes, T lymphocytes, synoviocytes, osteoclasts and astrocytes (Moncada *et al.*, 1991; Schmidt and Walter, 1994).

The induction of NOS in monocytes or tissue macrophages *in vivo* has been demonstrated or suggested by indirect measurements in several animal models, including septic shock (Knowles *et al.*, 1990), IgA immune-complex vasculitis of the lung (Mulligan *et al.*, 1992) and diabetes (Andrade *et al.*, 1993). NOS inhibition increased leukocyte adhesion to endothelial cells with the up-regulation of CD11/CD18 intergrin on the neutrophil (Kubes *et al.*, 1991). In contrast the same inhibitor attenuated neutrophil-dependent injury of the pulmonary vasculature (Mulligan *et al.*, 1992). In the expanding literature on NO both pro- and anti-inflammatory effects have been ascribed to this free radical in inflammation. These discrepancies seem to depend on the model used, inhibitors chosen, concentrations and the route of administration of these drugs. In addition, most of the cellular effects attributed to NO have been demonstrated *in vitro*, again with conflicting results reported for individual processes. Therefore, further work is required to dissect out mechanisms for NO in models of inflammation and possible reasons for the contradictions that appear in the literature.

1.4.8 Molecular and cellular targets for NO

Analysis of the molecular targets of NO has increased our understanding of the mechanism of action of NO in homeostasis and host defence. The targets that NO has within biology are diverse and include low molecular weight species as well as macromolecules which it either activates or inhibits. However, when considering targets for NO it has to be taken into account how NO is transported out of the effector cell to its target without causing damage, since the NO produced by iNOS is cytosolic and can react with many intracellular species. There may be mechanisms that exist to prevent unintentional reactions.

Therefore, do special intracellular transport routes exist for NO itself or is there a carrier molecule complex formed? Although there is this distinct potential, none of the aforementioned have been proven. However, putative transport forms of NO have been documented and include, dinitrosyl-iron(III) complexes (Mulsch *et al.*, 1991), N^G-hydroxy-L-arginine-NO adduct (Hecker *et al.*, 1995) and glutathione-NO complex (Hogg *et al.*, 1996). The formation of these compounds would limit the toxicity of this free radical to the effector cell.

Haem proteins: At low concentrations NO can react with Fe^{2+}-haem proteins. The classical example of activation is guanyl cyclase (Ignarro *et al.*, 1982), with more recently, its reactions with cyclooxygense being of interest (Salvemini *et al.*, 1993). NO also has been shown to have inhibitory effects on a variety of heamproteins which include cytochrome P_{450} aromatase (Snyder *et al.*, 1996), thromboxane synthase, catalase (Gross and Wolin, 1995), glutathione peroxidase (Asahi *et al.*, 1995). These enzymes are involved in the synthesis of biological mediators and redox based signalling events. Additionally the interaction of NO with haemoglobin and myoglobin decreases the bioavailability of the active molecule (Furchgott and Vanhoutte, 1989).

Enzymes: Native NO is a potential inhibitor of mitochondrial respiration and energy metabolism (Stuehr and Nathan, 1989; Hibbs *et al.*, 1990). Moreover, the ability of NO to react with Fe-S clusters in complex I and II in mitochondrial respiration and aconitase in the citric acid cycle has been linked to the cytostatic/cytotoxic properties of NO (Drapier and Hibbs, 1988; Stadler *et al.*, 1991). Importantly NO can also inhibit the glycolytic enzyme glyceraldehyde-3-phosphate dehydrogenase, which results in the suppression of ATP generation (Molina y Vedia *et al.*, 1992). Inhibition of these two important cellular processes may be fatal to the affected cell. In fact NO has been shown to cause apoptosis in a number of cell types *in vitro* (Albina *et al.*, 1993; Fehsel *et al.*, 1995; Palluy and Rigaud, 1996).

DNA: NO can inhibit DNA synthesis, in part by inhibiting the DNA biosynthesis

enzyme ribonucleotide reductase (Kwon *et al.*, 1991; Lepoivre *et al.*, 1991). Exogenous NO can also cause mutagenicity by deaminating DNA when present at high concentrations (Wink *et al.*, 1991). However, intracellular production has yet to be shown to facilitate this event. NO has also been shown to inhibit the zinc finger DNA repair enzyme Fpg (Wink and Laval, 1994), which may further increase mutagenic changes within the target cell.

Thiols: The interaction of NO with sulphydryls has been extensively examined (Ignarro, 1990), with NO being able to react with free thiols under aerobic conditions to form S-nitrosothiol compounds (Myers *et al.*, 1990; Clancy and Abramson, 1992). As already mentioned these compounds may provide a means by which NO can be stored in a bioaccessible form for signal transduction processes (Stamler *et al.*, 1992a). Molecules that can be regulated by thiol-nitrosation include receptor proteins (Lei *et al.*, 1992), ion channel proteins (Bolotina *et al.*, 1994), G proteins (Lander *et al.*, 1993), protein kinase C (Gopalakrishna *et al.*, 1993), transcription activating factors (Peunova and Enikolopov, 1993) and proteases (Devi *et al.*, 1994).

Superoxide anion: The outcome of the reaction of NO with superoxide is hypothesised to be both advantageous, representing a detoxification pathway for both molecules (Gryglewski *et al.*, 1986) or detrimental with the formation of the highly reactive and potent oxidising agent peroxynitrite (Beckman *et al.*, 1990). Therefore, depending on the circumstances in which it is produced, the interaction of NO with superoxide may be cytoprotective or cytotoxic (Darley-Usmar *et al.*, 1995).

1.4.9 Pharmacological inhibitors of NOS

The are a number of classes of inhibitors of NOS which vary greatly in their specificity and selectivity between the three isoforms. As described earlier, several important differences exist among the isoforms suggesting, that at least in theory isoform selective inhibition is possible. Strategies include interaction at the L-arginine binding site, ligands directed towards the haem and interaction

with the H_4 biopterin binding site.

L-arginine analogues: All three NOS isoforms have shown narrow specificity at the L-arginine binding site with stereochemical rigidity associated with at the α-carbon. L-arginine analogues were first described by Hibbs and colleagues (1987a), who used N^G-methyl-L-arginine (L-NMA) to inhibit NO formation in macrophage pathogenicity studies. The reported studies using this type of NOS inhibitor have been carried out with crude, partially purified NOS or cells in culture (Marletta, 1994b) and therefore must be interpreted with caution. Examples of L-arginine analogues are shown in Figure 1.5.

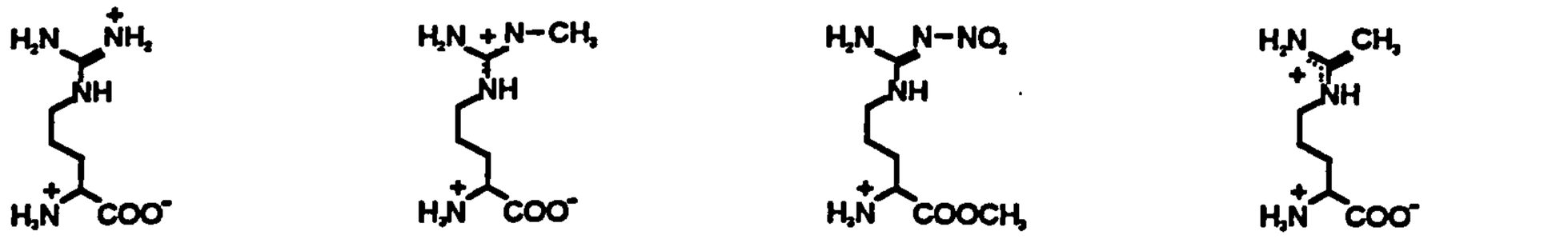

Figure 1.5 The structures of L-arginine and the L-arginine based NOS inhibitors, N^G-methyl-L-arginine, N^G-nitro-L-arginine methyl ester and N-(iminoethyl)-L-ornithine.

All three isoforms can be inhibited to a variable degree with N^G substituted L-arginine analogues. However, some do exhibit some isoform selectivity, mostly towards the constitutive isoforms. N^G-cyclopropyl-L-arginine shows a preference for nNOS over iNOS *in vitro* (Lambert *et al.*, 1992), whereas N^G-nitro-L-arginine (L-NA) and L-NAME after hydrolysis. N^G-methyl-L-arginine (L-NMA) and N^G-amino-L-arginine show no marked preference for either isoform (Gross *et al.*, 1990; Lambert *et al.*, 1991; Furfine *et al.*, 1993). Most of this group of inhibitors are competitive inhibitors of NO and exclude the substrate L-arginine from entering the active site, with their effects being reversible by L-arginine. Compounds such as N-iminoethyl-L-ornithine (L-NIO), show inhibition that cannot be reversed by L-arginine or other factors (McCall et al., 1991). The non-specific properties of L-arginine analogues include the inhibition of the activity of iron-containing enzymes such as catalase (Rotzinger *et al.*, 1995) and the reduction of cytochrome c (Peterson *et al.*, 1992). In addition to these non-

specific effects of these L-arginine based inhibitors *in vitro*, unexpected side effects have also been reported *in vivo*. High concentrations of N^G-amino-L-arginine is reported to cause epileptic seizures in dogs (Cobb *et al.*, 1992), which may be related to its ability to block NO in the central nervous system or alternatively to a non-specific effect of the drug itself.

Non amino acid based inhibitors of NOS: Non amino based inhibitors of NOS represent probes to determine the structure of the L-arginine binding site without constraints imposed by specific stereochemistry of the binding of the amino acid group. Hence, they may prove to be a useful tool in the design of isoform specific inhibitors. Despite a requirement for the conserved stereochemistry of L-arginine analogues, a variety of compounds that are not amino acid based are inhibitors of NOS. Examples include imidazoles (Wolff *et al.*, 1994), 7-nitroindazole (Moore *et al.*, 1993), guanidines (Hasan *et al.*, 1993), tannin (Chiesi *et al.*, 1995), plencyclidine (Osawa *et al.*, 1993) and methylene blue (Mayer *et al.*, 1993). Among this large and increasing list of inhibitors only a few groups of compounds show selectivity, namely, aminoguanidine, isothioureas and certain imidazoles. The guanidines (Figure 1.6) are structurally similar to L-arginine therefore were investigated as potential inhibitors of NOS.

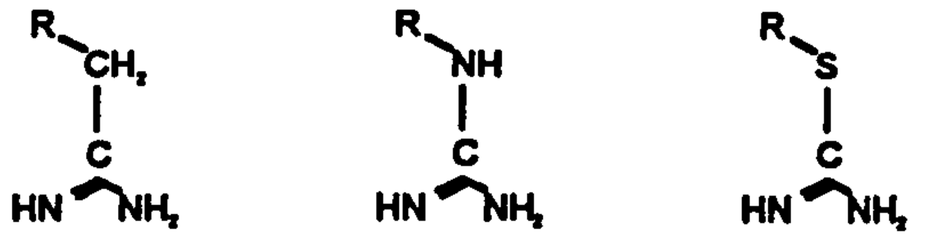

Figure 1.6 General structures of the amidine derivatives

Aminoguanidine is probable the most commonly used of all these drugs, since its recognition that it has selectivity towards iNOS (Corbett *et al.*, 1992). In most *in vitro* systems aminoguanidine displays a similar potency to L-NMA in its ability to inhibit NO production by immunostimulated macrophages, with less of an effect then L-NMA on nNOS and eNOS (Szabo *et al.*, 1994; Wu, 1995). However, it has to be noted that aminoguanidin's ability to inhibit NO production

varies depending on the length of incubation, with short incubation times resulting in a reduced inhibitor action (Wu, 1995; Joly *et al.*, 1994). Like some of the L-arginine analogues, aminoguanidine can have NO-independent effects like inhibition of histamine metabolism (Bieganski *et al.*, 1983), inhibition of polyamine catabolism (Seiler *et al.*, 1985) and inhibition on catalase (Ou *et al.*, 1993). Other guanidino inhibitors of iNOS include mercaptoalkyl-guanidine (Southan *et al.*, 1995), 1400W (Garvey *et al.*, 1997) and amino ethyl-isothiourea (Garvey *et al.*, 1994), which have beneficial effects in iNOS mediated pathologies (Thiemermann *et al.*, 1995), again these compound have NO-independent effects that include inhibition of membrane sodium/potassium ATPase (David *et al.*, 1992). However, taking this into consideration amino ethyl-isothiourea was used in this thesis as an iNOS selective inhibitor, due to its reported selectivity to this isoform *in vivo.*

1.5 Arginase

Arginine is a semi-essential amino acid that can be metabolised by two major enzyme pathways, NOS (substantially reviewed in Section 1.4) and arginase. As there is a possibility that during inflammation one enzyme system could effect the other, both NOS and arginase were investigated in the models used in this thesis. Arginase has two isoforms, hepatic arginase (A-I) and liver or extra-hepatic arginase (A-II), which are highly conserved proteins that appear to be present in most fungi and all higher organisms (Grody *et al.*, 1987; Takiguchi *et al.*, 1989). A-I and A-II are binuclear manganese metalloenzymes that catalyse the hydrolysis of L-arginine to urea and ornithine (Jenkinson *et al.*, 1996; Kanyo *et al.*, 1996). In rats, mice and humans the majority of arginase islolated from individual tissues seem to be either trimers or tetramers with molecular weights ranging from 94 to 127 kDa with subunits sizes estimated between 34 and 40 KDa (For review see Jenkinson *et al.*, 1996). This great variation between tissue suggests that expression and regulation of arginase is highly tissue specific. In fact, cellular localisation of the two isoforms differs with A-I being localised to the cytoplasm whereas A-II is mainly mitochondrial and has a wider tissue

distribution (Grody *et al.*, 1987). All arginases are heat stable and are protected by the presence of divalent cations (eg Mn^{2+}), which are essential for enzyme activity. In the presence of Mn^{2+}, little to no loss of activity was observed over several hours at 68-70^{0}C, days at 4^{0}C and freezing/thawing cycles (Grody *et al.*, 1987).

Arginases A-I and A-II appear to be expressed constitutively in murine macrophages although more recently different stimuli may modulate the expression of these isoforms (Boucher *et al.*, 1999). A-I and A-II contribute to the immune system function since, L-ornithine is a key precursor for polyamines involved in cell replication. In fact ornithine/urea production markedly increased during tumour growth, with arginase activity being blunted during tumour rejection (Mills *et al.*, 1992). Recently, it has become apparent that both isoenzymes can be involved in the regulation of the numerous cytostatic/cytotoxic action mediated by NO in macrophages. In these cases modulation of local L-arginine concentrations by arginases could regulate NO production by iNOS (Feldman *et al.*, 1993; Kerwin *et al.*, 1995; Hrabak *et al.*, 1994; Chang *et al.*, 1998). More detailed comparisons between NOS and arginase are made and discussed throughout this thesis where appropriate.

1.6 Cyclooxygenase

The COX and NOS pathways have been demonstrated in the literature to regulate each others protein expression and enzyme activity *in vitro* and *in vivo* (Di Rosa et al., 1996), but investigations have produced conflicting and controversial data. It has been demonstrated in rat Kuppfer cells that endogenously-formed prostaglandin E_2 (PGE_2) increases NO synthesis after stimulation with LPS (Gaillard *et al.*, 1992). However, in J774 macrophages both exogenous PGI_2 and PGE_2 were able to inhibit NO production (Marotta *et al.*, 1992). However, individual effects seem to be cell and stimulus specific. Therefore, the results and hypotheses are further elucidated to within the results and general discussion sections of this thesis.

Two isoforms of cyclooxygenase (COX) have been identified, COX-1 and COX-2 (for extensive reviews see Appleton *et al.*, 1997 and Gilroy *et al.*, 2000). The non-inducible or constitutive isoenzyme is known as COX-1, whilst the inducible isoenzyme was designated COX-2. The COX enzymes both metabolise membrane-bound, essential 20-carbon fatty acid known as arachidonic acid (5,8,11,14-eicosatetraenoic acid). Metabolites of the arachidonic acid cascade include products of COX, lipoxygenase and cytochrome P_{450} pathways. These metabolites are collectively known as eicosanoids. COX protein has a molecular weight of 72kDa and contains 600 to 602 amino acids produced from mRNA 2.8kb in size. COX is made up of a dimeric complex of two polypeptides each of which requires one molecule of heme for maximal catalytic activity (for extensive reviews on COX gene and protein structures see Xie, 1992; Smith and Marnett, 1991, respectively). The two isoforms of COX differ in their protein sequence, regulation and sensitivity to non-steroidal anti-inflammatory drugs (NSAIDs). At the protein level, the major difference between the two isoenzymes is that COX-1 contains a 17 amino acid sequence at its amino terminus that is absent in COX-2, whilst COX-2 has an additional 18 amino acid sequence at its carboxy terminus (Kurumbail *et al.*, 1996). This difference has enabled the generation of specific antibodies which are raised against the unique 18 amino acid terminus to distinguish COX-2 from COX-1 (Habib *et al.*, 1993).

The COX enzymes are inhibited by a series of chemically unrelated compounds which share a common therapeutic action and are collectively known as NSAIDs. The best known of these are aspirin, ibuprofen, indomethacin and diclofenac. However, in relation to the NOS pathway aspirin is the most interesting since it has been reported to both inhibit and exacerbate NO production both *in vitro* and *in vivo* (Amin *et al.*, 1995; Kepka-Lenhart *et al.*, 1996; Lopez-Farre *et al.*, 1996). Aspirin is a class III NSAID and therefore is a competitive, irreversible inhibitor of COX activity. It covalently modifies COX protein by acetylating a single serine residue (Ser^{530} or Ser^{516}) in the substrate binding channel that causes stearic inhibition of arachidonic acid entry into COX's catabolic site (for extensive

reviews on aspirin see Moncada and Vane, 1979; Vane and Botting., 1997).

1.7 Heat shock proteins

At the start of this thesis there were a few papers suggesting an interaction between the NO and the induction of heat shock proteins (HSP; Willis *et al.*, 1995) however little was known about their interactions. HSP can be induced by a number of stressful stimuli which include heat, inflammation, oxidative injury, transition heavy metals and damaged proteins (for review see Morimoto *et al.*, 1992). Although, the exact mechanism that induces this family of proteins is not well understood, the heat shock proteins with the exception of heme oxygenase (HO or HSP32) share a common function, which is that they act as protein chaperones ie are able to refold damaged proteins or prevent protein damage from occurring (Hightower *et al.*, 1980). Since this thesis' main focus is inflammation, the roles that HSPs may play are discussed in this context. The majority of published work on HSP's in inflammation has been concentrated on two members of this family of proteins, HSP72 (inducible isoform of the HSP70 family of isoenzymes) and HO-1 (inducible HO).

1.7.1 HSP72

Several *in vitro* studies have shown that HSPs are induced by mediators that are present in the inflammatory lesion, and that this induction affords these cells a degree of cytoprotection. Konig and colleagues (1992) demonstrated that TNF-α and 12(*R*)-hydroxyeicosatetraenoic acid (12-HETE) induced HSP72 expression in neutrophils and protected these cells against lytic attack. In addition, IL-6 and LPS treatment are also able to upregulate HSP72 in PMNs (Koller et al., 1993). Similarly, in macrophages elevated expression of HSP72 affords protection against hydrogen peroxide induced cytotoxicity (Polla *et al.*, 1987) and apoptosis (Samali and Cotter, 1996). Conversely, inhibition of HSP72 in mouse J774A.1 macrophages increased their susceptibility to TNF-α induced cell death (Nishimura *et al.*, 1997). In *vivo* evidence also suggests an anti-inflammatory role for HSP72, with over expression in rat lungs protecting this tissue from sepsis-induced injury (Ribeiro *et al.*, 1994). Finally, a number of recent studies have

demonstrated that HSP72 can be induced in a variety of cell types by NO, thus affording protection against further inflammation-induced injury (Bellmann *et al.*, 1996; Kim *et al.*, 1997; Xu *et al.*, 1997; Calabrese *et al.*, 2000) . These examples presented above support the view that HSP72 is in fact important for cell survival (for an extensive review on HSP70 see Kiang and Tsokos, 1998).

1.7.2 Heme oxygenase (HO-1 or HSP32)

The other major HSP that is associated with inflammation is HO-1 or inducible HSP32. Unlike the other HSPs this protein is an enzyme, that metabolises the conversion of free heme to the bile salts biliverdin and bilirubin and carbon monoxide (CO) (for an extensive review on HO-1 see Willis et al., 1999). HO-1 is induced by a plethora of mediators involved in the inflammatory cascade that include LPS, IL-1, TNF-α, LPS, phorbol esters, cyclopentanone prostaglandins and a number of NO donors. Once again the exact mechanism by which HO-1 protects cells from the adverse effects of inflammatory associated damage is not well understood, but seems to centre upon this enzymes ability to scavenge free radicals through the production of the anti-oxidant bile pigments. HO-1 metabolises free heme which is a potent generator of reactive oxygen species (Balla *et al.*, 1993). Bilirubin, a product of HO-1 catabolism, has been demonstrated in a number of circumstances to be a potent anti-oxidant (Stocker *et al.*, 1987; Neuzil *et al.*, 1993; Wu *et al.*, 1996). CO may also be cyto-protective by modulating other inflammatory enzyme cascades in a similar manner to NO. These effects include the prevention of platelet aggregation and increasing levels of the second messenger cyclic guanidine monophosphate (cGMP; Kharitonov et al., 1995). Finally, HO-1 gene deleted mice develop spontaneous chronic inflammatory disease thereby demonstrating an auto-regulatory effect on inflammation.

It is clear from the evidence presented above that both HSP72 and HO-1 have important cyto-protective/anti-inflammatory mechanisms. It is also well documented that NO can induce both of these proteins and once up-regulated these HSPs are able to inhibit NO production from inducible NOS (iNOS).

Therefore it can be envisaged that NO may be an important mediator/inducer of the anti-inflammatory cascade via regulation of HSPs.

1.8 Aims.

The aim of this thesis are to examine the pro- or anti-inflammatory role of NO in acute and chronic inflammation. The individual aims are as follows:

1. To examine the temporal and spatial expression of NOS in: (a) three models of acute inflammation, carrageenin-induced pleurisy in the rat, bovine serum albumin-induced pleurisy in the rat and the methylated bovine serum albumin-induced pleurisy in the rat and (b) chronic croton oil-induced granulomatous tissue air pouch in the mouse.

2. To assess the effects of NOS inhibition in the carrageenin-induced pleurisy in the rat using NOS inhibitors.

3. To assess the effects of NOS inhibition in the chronic croton oil-induced granulomatous tissue air pouch in the mouse using NOS inhibitors.

4. To assess the effect of iNOS gene deletion in the chronic croton oil-induced granulomatous tissue air pouch in the mouse .

5. To assess the effects of the a classical anti-inflammatory, the NSAID aspirin on the production of NO in (a) carrageenin-induced pleurisy in the rat and (b) chronic croton oil-induced granulomatous tissue air pouch in the mouse.

CHAPTER 2

2.1 Chemicals and suppliers.

2.1.1 Chemicals, biochemicals, antibodies and kits.

All inorganic and general use chemicals were of Analar™ grade and purchased from Merck Ltd. Gases and liquid nitrogen were supplied from BOC Ltd. All Laboratory plastics were obtained from L.I.P. and tissue cultureware was from Becton Dickinson. All biochemicals, antibodies, normal animal serum and detection kits were from Sigma Chemical Co. with the exception of the following:

Chemicals and Biochemicals	*Source*
Polyclonal rabbit anti murine-iNOS	Santa Cruz Biotechnology
Polyclonal rabbit anti murine-COX 2	Santa Cruz Biotechnology
Polyclonal rabbit anti murine-HO-1	StressGen Biotechnology
Polyclonal rabbit anti murine-HSP 70	StressGen Biotechnology
Polyclonal rabbit anti bovine-arginase I	Biogenesis
High range biotinylated molecular weight markers	Santa Cruz Biotechnology
Polyclonal biotinylated goat anti-rabbit IgG	Santa Cruz Biotechnology
Polyclonal HRP donkey anti-rabbit IgG	Santa Cruz Biotechnology
Tetrahydrobiopterin	Alexis Corporation
1400W	Alexis Corporation
2(Aminoethyl)-isothiourea	Alexis Corporation
N^G-Monomethyl-L-arginine	Alexis Corporation
Radiolabelled L-arginine	Amersham
Radiolabelled PGE_2	Amersham
Radiolabelled $PGF_{1\alpha}$	Amersham
PGE_2 quantification kit	Amersham
LTB_4 quantification kit	Amersham
Rainbow™ molecular weight markers	Amersham
Hybond™-C super, 0.45 Micron membrane	Amersham
ECL biotinylated molecular weight markers	Amersham
Western blot grade dry milk block	Bio-Rad Laboratories Ltd
Blotting paper	Bio-Rad Laboratories Ltd
Bradford reagent	Bio-Rad Laboratories Ltd

Acrylamide/Bisacrylamide	Bio-Rad Laboratories Ltd
Dowex columns	Bio-Rad Laboratories Ltd
KC ELISA	R&D systems
IL-1α ELISA	R&D systems
LIP Freeze	LIP Ltd
20ml screw capped scintillation vials	LIP Ltd
Apoptag® *In situ* apoptosis detection kit	Oncor Co.
J774.2 macrophages	ECACC
EA.hy926 endothelial cells	(Gift)
Pico-Fluor 40 scintillation fluid	Canberra Packard Co.
Flat bottom 96 well plates	Greiner Laboratechnik
Slides, 4 spot PTFE (1cm diameter)	C. A. Hendley (Essex) Ltd.
Cryo-M-Bed	Brights Ltd.
Michel clips	Harvard Apparatus Ltd.
Carrageenin	Marine Colloids Co.
Mycobacterium turberculosis (strains C, DT & PN; Nº PPD298)	Ministry of Agriculture, Fisheries and Food
Hypnorm	Southern Veterinary Supplies
Hypnovel	Southern Veterinary Supplies

2.2 Drug Preparation.

2.2.1 For in vitro studies.

Acetylsalicylic acid was prepared in dimethyl sulphoxide at a concentration of 100mM, followed by dilution in culture medium to give the final concentrations stated in the individual experiments. In all the *in vitro* experiments where dimethyl sulphoxide was used, the final concentration of this solvent was never higher than 0.1% v/v. However, to ensure that any possible solvent effects were controlled for, dimethyl sulphoxide (0.1% v/v) was always added to the medium

in which control cells were incubated.

2.2.2 For in vivo studies.

The NOS inhibitors; S(2-aminoethyl)-isothiourea (AE-ITU), N-(3-(aminomethyl)-benzyl) acetamide (1400W), N^G-monomethyl-L-arginine (L-NMMA), L-N^5(1-iminoethyl)-ornithine (L-NIO) were dissolved at the desired concentrations in sterile saline. Similarly, the inactive enantiomer of L-NAME, D-NAME was also dissolved in sterile saline. The NO donor DPTA NoNoate was also dissolved in sterile saline for injection. The injection sites varied depending on the experiment performed, but included the pleural cavity, peritoneal cavity and pre-formed air pouch. The iNOS inhibitor aminoguanidine (hemisulphate preparation) was dissolved in the drinking water. The dose was computed by measuring water consumption of the mice over a period of 1 week, which was calculated as 5ml/mouse/day.

The COX inhibitor aspirin was prepared by grinding to a fine powder using a mortar and pestle. Small aliquots were added to make into a paste followed by increasing amounts of vehicle to achieve the desired concentration. Aspirin at 200mg/kg and above was sonicated for 30s using a Merck Sharp Equipment sonicator (serial N° 30363) at 1.5 amperes. All COX inhibitors were dosed orally.

2.3 Animals and their Maintenance.

For pharmacological studies outbred strains of mice and rats were used. Male Wistar rats and female Theiler's original (T_0) mice were purchased from Tuck and Sons, U.K. iNOS knockout transgenic mice were from B&K Universal Ltd. All rats (150-250g) and mice (25-30g) were housed in plastic cages (rats, 5 per cage; mice 10 per cage) lined with sawdust and maintained in a light, humidity and temperature-controlled environment. Food (RM1E; Special Diet Sevices, U.K.) and water were allowed *ad libitum*.

2.4 Acute inflammatory models.

2.4.1 Carrageenin-induced pleurisy (complement-mediated reaction).

Male Wistar rats were anaesthetised with halothane and 0.15ml carrageenin (1% w/v in 0.9% w/v sterile NaCl) was injected into the pleural cavity between the 5th and 6th intercostal space using a 1.0ml syringe fitted with a 21 gauge needle blunted to 5mm in length. The cut was closed using Michel clips and animals were allowed to recover from the anaesthetic. Rats were killed at several time points after carrageenin injection and inflammatory exudates collected after addition of a 1ml pleural lavage (50mM Tris buffered saline pH 7.4, 3.15% w/v trisodium citrate, 1mM phenylmethylsulphonylfluoride, 1.5mM pepstatin A and 0.2mM leupeptin).

2.4.2 BSA induced pleurisy (Arthus, antigen/antibody complex-mediated, immediate type III hypersensitivity reaction).

Male Wistar rats were sensitised at the base of the tail by intradermal injection of 0.1ml incomplete Freund's adjuvant and saline (ratio 1:1) containing bovine serum albumin (BSA, 10mg/ml). Twelve days after sensitisation, the animals were challenged intrapleurally with 0.1ml saline containing 10mg/ml BSA (Section 2.4.1). Rats were killed at various time points after challenge and exudates were collected after addition of a 1ml pleural lavage.

2.4.3 Methylated BSA-induced pleurisy (cell-mediated, type IV, delayed hypersensitivity reaction).

Male Wistar rats were sensitised at the base of the tail by intradermal injection of 0.1ml incomplete Freund's adjuvant and saline (ratio 1:1) containing methylated bovine serum albumin (methylated BSA, 10mg/ml). Twelve days after sensitisation, the animals were challenged intrapleurally with 0.1ml saline containing 10mg/ml methylated BSA (Section 2.4.1). Rats were killed at various time points after challenge and exudates were collected after addition of a 1ml pleural lavage.

2.4.4 Preparation of pleural inflammatory exudates.

Inflammatory exudates were harvested on ice from the pleural cavity of animals terminated at various time points after injection of inflammatory irritants. Inflammatory exudates were measured by weight and inflammatory cells counted (Coulter electronics, Luton, U.K.). A 5µl aliquot of the exudate was smeared onto 4 spot glass slides coated with poly-L-lysine (0.01% v/v in deionised H_2O) and allowed to air dry over night. Slides were transferred to an air tight box for storage at room temperature until required. Inflammatory exudates were centrifuged (Beckman, U.S.A.; 800xg) for 10min at 4°C. Exudates and cells were separated by decanting and immediately snap frozen in liquid N_2 and stored at -80°C for further analysis. Cell-free exudates were used for the measurement of nitrite (Section 2.6), a stable breakdown product of NO, quantification of eicosanoid (Sections 2.11, 2.12), evaluation of histamine content (Section 2.15) and the assessment of chemokines (Section 2.16).

Cell pellets were sonicated at 4°C using a micro-probe (Sonics and Materials Inc. U.S.A.) in protease inhibitory buffer which contained pepstatin A (1.5mM), phenylmethylsulphonylfluoride (1mM) and leupeptin (0.2mM) in 50mM Tris buffer, pH 7.4. The lysate was centrifuged (800xg) for 10min at 4°C and the pellet discarded. The protein concentration of the supernatants was measured by the Bradford assay (Bradford *et al.*, 1976; Section 2.8) then used for the determination of iNOS activity (Section 2.7), arginase activity (Section 2.10), COX activity (Section 2.11) and Western blotting (Section 2.9).

2.5 Chronic inflammatory models.

2.5.1 The croton oil-induced murine chronic granulomatous tissue air pouch.

2.5.2 Induction of air pouch.

Female T_0 mice were injected with 3ml of air into the dorsal subcutaneous tissue. 24h later, 0.5ml of Freund's incomplete adjuvant containing 0.1%v/v croton oil and a 5mg/ml suspension of heat inactivated *Mycobacterium*

turberculosis was injected into the air pouch.

2.5.3 Preparation of granulomatous tissue.

The resultant granuloma was dissected in its entirety at various time points and dried at 56°C (3 days) for the determination of dry weight. Exudates were removed from the air pouch using a 16 gauge needle and then were centrifuged at 1000 *xg* and the aqueous phase removed and snap frozen. Granulomatous tissue was also prepared for biochemical and immunohistochemistry analysis. Granuloma from the ventral region of the pouch was removed and homogenised (Kinematic, Switzerland) at 4°C in protease inhibitory buffer in a ratio of 5:1 (vol/wt). The homogenate was centrifuged at 10,000 xg for 20min at 4°C and the pellet discarded. The protein concentration of the supernatant was measured by the Bradford assay (Section 2.8) then used for the determination of iNOS activity (Section 2.7), arginase activity (Section 2.10), COX activity (Section 2.11) and Western blotting (Section 2.9).

For immunohistochemical analysis, the dorsal region of the granulomatous tissue was immediately snap-frozen in n-hexane at -68°C, to preserve the epitopes of interest. Frozen tissue was mounted on brass chucks in O.C.T. compound and allowed to equilibrate to -30°C. 10µm sections were cut in a cryostat (Bright, UK) and allowed to air dry overnight. Sections were then fixed prior to immunolabelling in either acetone (10min, room temperature) or freshly made 4%w/v paraformaldehyde in 0.1M phosphate buffered saline (PBS; pH 7.3; 30min) and allowed to air dry.

2.6 Measurement of nitrite by the Greiss reaction.

The Greiss reaction detects nitrite by the formation of a coloured NO-formazan dye adduct in a linear manner between 1-100µM. *In vivo* nitrite is rapidly converted to its end oxidation product nitrate, thereby making it necessary to reduce nitrate to nitrite prior to its estimation with the Greiss reagents. Therefore, a modification of the Greiss reaction (Verdon *et al.*, 1995), that converts nitrate

to nitrite was used to measure this product in cell-free inflammatory exudates. A nitrite standard curve was constructed (1, 5 10, 20, 50, 80, 100µM) using sodium nitrite. Cell-free exudates were defrosted and 50µl of standards and samples were pipetted into a 96 well plate. Nitrate in the samples was converted to nitrite by the addition of 10µl of reduced β-nicotinamide adenine dinucleotide phosphate (NADPH; 10µM), 10µl glucose-6-phosphate (5mM), glucose-6-phosphate dehydrogenase (0.16units), phosphate buffered saline (10mM) and 10µl nitrate reductase (0.08units). The reaction was allowed to proceed for 45min at room temperature. Nitrite in the samples and standards was visualised by the addition of 100µl sulfanilamide (1% w/v in 5% v/v phosphoric acid) and 100µl N(1-naphthyl)ethylenediamine (0.1% w/v). After 10min nitrite concentrations were measured spectrophotometrically at λ_{max}=570nm with a reference filter at 620nm. Nitrite concentrations were calculated from the standard curve and results expressed as µM nitrite.

2.7 NOS activity.

NOS activity was measured as the ability of inflammatory cell and tissue homogenates to catalytically convert [^{3}H]-L-arginine to [^{3}H]-l-citrulline in the presence of excess concentrations of co-factors. For each sample, total NOS, calcium-independent NOS and non-NOS-dependent arginine breakdown was measured in duplicate. The reaction buffer for total NOS activity consisted of: NADPH (1mM), tetrahydrobiopterin (5µM), calmodulin (300 units/ml), calcium chloride (2mM) and valine (1mM); for iNOS activity, NADPH (1mM), tetrahydrobiopterin (5µM), calmodulin (300 units/ml), EGTA (1mM) and valine (1mM); for NOS-independent activity conversion assay medium included tetrahydrobiopterin (5µM), calmodulin (300 units/ml), calcium chloride (2mM) and valine (1mM). Samples were homogenised as described (Sections 2.4.4 and 2.5.3) and 30µl added to each reaction tube and allowed to equilibrate in a water bath at 37^{0}C for 10min. The reaction was started by the addition of 10µl of L-arginine/[^{3}H]-L-arginine (10µM; ratio of 1000:3 pmol of L-arginine:[^{3}H]-L-arginine) and samples incubated for 30 min at 37^{0}C. The reaction was terminated by the

addition of 1ml ice-cold stop buffer (2mM EGTA, 2mM EDTA in 20mM HEPES, pH 5.5). L-arginine/[^{3}H]-L-arginine was removed from samples by eluting them through Dowex cationic exchange resin columns with 1ml stop buffer. The amount of radioactive L-citrulline was determined in a liquid scintillation counter after the addition of 9ml Pico-Flour 40 scintillation fluid. The protein concentration of samples was measured by the Bradford assay and NOS activity expressed as pmol L-citrulline/mg protein/30min.

2.8 Bradford protein assay.

The binding of Coomassie brilliant blue (R250) to protein causes a shift in λ_{max} of the dye from 465 to 595nm and it is the increase in absorption at 595nm which is monitored. The reaction is rapid, usually complete within 2min and with good colour stability for 1h. Bradford reagent was diluted 1:4 with deionised H_2O and filtered through Whatman N°1 filter paper before use. A standard curve ranging from 0.05-0.5 mg/ml BSA in Tris (50mM, pH 7.4) or phosphate buffered saline (PBS, 10mM, pH 7.4) was prepared. Samples were diluted in Tris or PBS to fall within the range of the standard curve. 10µL of sample or standard was placed into a 96-well microtitre plate followed by 200µl of diluted Bradford reagent. The plate was placed on a shaker for 10 min and read on a microtitre plate reader at λ_{max}=595nm.

2.9 Western Blotting.

Lysates from cell pellets and tissue homogenates were further processed for Western blotting. The protein concentration of sonicated cell preparations or tissue homogenates was determined as described in Section 2.8. All samples were diluted to give a final concentration of 1mg/ml, then heated up to 95^{0}C for 5min with 2x gel loading buffer (50mM Tris, 10% w/v SDS, 10% v/v glycerol, 10% v/v 2-mecaptoethanol, 2mg/ml bromophenol blue) in a ratio of 1:1 and centrifuged (10,000xg) for 10min. Samples were used immediately or stored at

-80^{0}C. Equivalent protein concentrations were loaded on to an 8 or 10% SDS-polyacrylamide mini-gels (Table 3.1).

Chemicals	Resolving Gel		Stacking gel
	8%	10%	3%
29:1 Acrylamide/Bis solution	2.65ml	3.35ml	1.6ml
1.5M Tris pH 8.8	2.5ml	2.5ml	
1.5M Tris pH6.8			820µl
20% w/v SDS	50µl	50µl	100µl
Distilled water	4.3ml	3.6ml	7.48ml
50% v/v glycerol	0.5ml	0.5ml	
TEMED	30µl	30µl	10µl
10% w/v ammonium persulphate	72µl	72µl	100µl

Table 2.1 Constituents of SDS-polyacrylamide gels used for Western blot analysis. Volumes represent sufficient reagents for two 1.5mm gels.

Two types of molecular weight marker (MWM) were used depending on the method used for end detection, 5-bromo-4-chloro-3-indolyl phosphate/nitro blue tetrazolium precipitation (BCIP/NBT) or 3-aminophthalate elecro-chemiluminescence (ECL). For BCIP/NBT detection, high molecular weight rainbow markers were used and for ECL biotinylated protein molecular weight markers (MWM) were used. Gels were run at 100 volts using Biorad Mini Protean II gel electrophoresis system until the Coomassie blue dye front was at the bottom of the gel. Separated proteins were transferred electrophoretically (1h at 100 volts) to a nitrocellulose membrane in transfer buffer. Post-transfer of the nitrocellulose membrane was blocked overnight in 50mM Tris buffered saline, pH 7.4 containing 0.1% v/v Triton X100, 5% w/v non-fat dried milk and 1mg/ml essentially globulin free BSA). The nitrocellulose membrane was washed with Tris buffered saline (TBS) containing 0.1% v/v Triton X100(TTBS) and incubated

overnight with primary antibody (polyclonal rabbit anti-mouse iNOS, 1:5000; polyclonal rabbit anti-mouse COX 2, 1:3000; polyclonal rabbit anti-mouse HO-1, 1:2000; polyclonal rabbit anti mouse HSP70, 1:20,000). Blots were washed 3 times with TTBS to remove any unbound antibody.

When using the precipitation detection system, blots were incubated with a biotinylated goat anti-rabbit secondary antibody (TTBS containing 5% milk) at room temperature for 2h, after which the membrane was washed 3 times with TTBS. The final step prior to visualisation required incubating the blots with stepavidin linked alkaline phosphatase complex (TTBS, 1:1000) for 2h. Blots were then washed 3 times in TTBS and 2 times in TBS. The protein bands were detected by developing the nitrocellulose with BCIP/NBT, which visualised the target antigens as purple bands.

When using the electrochemiluminescence (ECL) system, blots were incubated with a HRP-linked donkey anti-rabbit secondary antibody (TTBS containing 2% v/v normal donkey serum, 1:10,000) at room temperature for 2h, after which membranes were washed 3 times with TTBS. The bands were visualised using ECL detection reagents (Amersham Pharmacia Biotech, Buckinghamshire) onto Kodak X-OMAT film in X-ray cassettes for between 1 and 15 min depending on the time required to visualise the specific bands, then developed using an RGII X-ray film processor (Fuji).

Some of the Western blots were quantified by densitometry (SeeScan Imaging Ltd.) Band density was calibrated against a known concentration of antigen standard on the same membrane. As the exact ratio of antibody to antigen is not known results were expressed as a proportion of the antigen standards density.

2.10 Arginase activity.

Urea formation was determined colorimetrically by its reaction with 1, 2-propanedione-2-oxime (IPSF; Schimke, 1970). The sensitivity of the assay

developed by Schimke was increased by reducing sample volume, reaction volume and the elimination of perchloric acid as reaction terminator (Corraliza *et al.*, 1994).

Arginase activity was measured as the ability of inflammatory cell and tissue homogenates to catalytically convert L-arginine to urea in the presence of excess $MnCl_2$ and L-arginine. Samples were homogenised as described (Sections 2.4.4 and 2.5.3) and 250µl added to each reaction tube containing 250µl 50mM Tris HCl and 20mM $MnCl_2$. The reaction mixture was then vortexed for 5min at room temperature, followed by activation of the arginase enzyme by incubation of the reaction mixture at 55°C for 10 min. 25µl aliquots of the activated samples, in duplicate, were transferred to fresh reaction tubes and the hydrolysis reaction initiated by the addition of 25µl L-arginine (0.5M) in Delroy and King's carbonate-bicarbonate buffer (0.2M anhydrous sodium carbonate, 0.2M sodium bicarbonate, pH 9.7) and incubated at 37°C for 60 min. The reaction was terminated by the addition of 400µl acid mixture (1:3:7 v/v, concentrated sulfuric acid: concentrated orthophosphoric acid: deionised H_2O). A standard curve was constructed using urea to give concentrations of 300, 100, 75, 37.5, 18.75 and 9.38 µg/ml. 400µl of acid mixture was added to the standards to keep reaction conditions consistent. Urea content of the samples and standards were evaluated by the addition 25µl IPSF (9% w/v in ethanol) and incubated at 100°C for 60 min. After a further 30 min incubation in the dark, 200µl of standards and samples were transferred to a 96 well plate and the resulting colour formation read at λ_{max} = 540nm. The results were expressed as specific activity, where 1mU = 1nM urea/mg protein/min, using the following calculation where X designates arginase activity of the sample (µg/ml) and Y is the protein concentration;

$$\frac{\left(\frac{X}{60 \times 120}\right)}{Y \times 1000}$$

All samples were measured at least in duplicate and expressed as specific

activity (mU/mg protein/min).

2.11 COX activity.

In this assay, inflammatory cell or granulomatous tissue COX activity is measured by the incubation of sample with excess arachidonic acid and cofactors. It is a measure of total COX activity and does not discriminate between COX 1 or COX 2 enzymic activity. Samples were homogenised as described (Sections 2.4.4 and 2.5.3) and 30µl added to each reaction tube containing 5mM glutathione and 5mM adrenalin. COX activity was determined in each sample in the presence and absence of 30µM indomethacin. Samples were incubated with this mixture for 10 min. Enzymic catalysis was initiated by the addition of 30µM arachidonic acid to the reaction mixture and incubated at 37^0C for 30 min. The reaction was halted by boiling the samples for 5 min followed by centrifugation for 30 min at 10,000xg. The concentration of Prostaglandin E_2 (PGE_2) was determined by radioimmunoassay (Section 2.12) and the results expressed as ng PGE_2/mg protein/30 min.

2.12 Measurement of PGE_2 and PGI_2 levels by radioimmunoassay.

PGE_2 and PGI_2 (measured as the stable breakdown product 6 keto-$PGF_{1\alpha}$) from cell-free inflammatory exudates were measured by radioimmunoassay. This is based on competition between PGE_2 or PGI_2 in the sample and a known amount of ^{3}H-labelled PGE_2 or PGI_2 added exogenously for a limited number of binding sites on an antibody raised against PGE_2 or PGI_2. After incubation, unbound prostaglandins were removed by activated charcoal and dextran, with the quantity of labelled eicosanoid remaining being inversely proportional to the concentration of unlabelled PGE_2 or PGI_2 in the test sample.

Antisera to PGE_2 or PGI_2 were diluted in Tris-HCl (50mM, pH 7.5) containing 0.1% w/v gelatin (mixed Tris buffer). ^{3}H-labelled PGE_2 or PGI_2 was added to

mixed Tris buffer to give a reading of 3500 counts per minute in a total volume of 600µl. 100µl of tracer and antibody was added to 50µl of either standard or sample. The reaction mixture was incubated at 4°C for 24h. Unbound eicosanoid was removed by the addition of 200µl Tris buffer (50mM, pH 7.5) containing 4mg of activated charcoal and 800µg of dextran 70 and vortexed. Samples were placed on ice for 10 min, then centrifuged at 200xg. The supernatant (containing antigen-antibody complex) was removed and placed in scintillation tubes to which 5ml scintillant was added. Radioactive content of samples was measured by liquid scintillation (LS 3801, Beckman, USA) and unknown sample concentrations of PGE_2 or PGI_2 were calculated from a standard curve ranging from 70 pg/ml to 80 ng/ml. Results are expressed as ng of eicosanoid per cavity.

2.13 Measurement of LTB_4 and PGE_2 using enzyme immunoassay.

This enzyme immunoassay system for leukotriene B_4 (LTB_4) and PGE_2 is based on the same principles as the radioimmunoassay for PGE_2 and PGI_2, relying on the competition between unlabelled LTB_4 or PGE_2 and a fixed quantity of HRP-labelled LTB_4 or PGE_2 for a fixed number of binding sites on a LTB_4 or PGE_2 specific antibody. With fixed amounts of antibody and HRP-labelled eicosanoid, the quantity of HRP-labelled ligand bound to the antibody will be inversely proportional to the concentration of unlabelled ligand in the standard and samples.

50µl of standard or cell-free pleural exudate (Section 2.4.4) was pipetted into a 96 well plate followed by the addition of 50µl of antiserum (rabbit anti-LTB_4 or PGE_2) into all wells with the exception of the blank and non-specific binding, followed by the addition of 50µl of LTB_4 or PGE_2-HRP linked conjugate. The plate was then incubated with shaking for 1h at room temperature. All wells were aspirated and washed 4 times with 300µl of wash buffer (0.01M phosphate buffer containing 0.05% v/v Tween-20). 150µl of enzyme substrate, tetramethylbenzidine/hydrogen peroxide, was dispensed into all wells and incubated with shaking at room temperature for 30 min. The reaction was

terminated by the addition of 1M sulphuric acid and the resulting colour formed was read at λ_{max} = 450nm on a microtitre plate reader (Anthos, Labtec instruments). Unknown concentrations were read off a standard curve constructed for PGE_2 or LTB_4. Results are expressed as ng of eicosanoid per cavity.

2.14 Air pouch vascularity.

This technique gives an index of granuloma tissue vascularity in the murine air pouch (Section 2.5.1). Vascularity was determined as follows: animals were terminally anaesthetised with an i.p. injection of 0.5ml hypnorm/hynoval (1:1:2; hypnorm®, hypnoval® and deionised H_2O). Animals were maximally vasodilated at 40°C and 1ml of carmine solution (10% w/v carmine red in 5% w/v gelatin solution) at 40°C was injected i.v into the tail vein of mice while they were still alive. The cadavers were refrigerated overnight to solidify the gelatin, thus forming a vascular cast. The air pouch was dissected and the granulomatous tissue dried in preweighed borosilicate glass tubes for 3 days at 56°C. After the dry weight of the tissue was determined, samples were digested in 9ml of digestion buffer (330mg L^{-1} N-acetyl cysteine, 12 units ml^{-1} papain, 0.001M EDTA in 0.05M phosphate buffer pH7.0) at 56°C for 3 days. The carmine red dye in the resulting solution was solubilised by the addition of 1ml of 5M NaOH. 1ml aliquots of each sample were filtered through a 0.22µm Whatman disposable filter and centrifuged for 15 min 10,000xg. The amount of carmine present was assessed spectrophotometrically by the addition of 200µl of sample to a 96 well microtitre plate. A standard curve was constructed from 1-100µg/ml carmine dye in 0.5M NaOH. Samples and standards were read at λ_{max} = 490nm on a microtitre plate reader (Anthos, Labtec instruments; Figure 3.6). Results were expressed as both carmine content (µg) and as a vascular index (µg carmine per mg of tissue dry weight).

2.15 Histamine.

The histamine radioimmunoassay procedure is also based on the competition between radioactive and non-radioactive ligands for a fixed number of specific antibody binding sites. The amount of ^{3}H labelled histamine bound by the antibody is proportional to the concentration of unlabelled histamine in the samples and standards. The separation of the free from the bound ligand is achieved by using a precipitating second antibody. Measurement of histamine was used as a marker of mast cell activation in the carrageenin-induced pleurisy.

200µl of standards, controls and cell-free pleural exudates (Section 2.4.4) were added to reaction tubes followed by the addition of histamine antisera. The reaction mixture was vortexed then incubated for 1h at room temperature. 100µl of ^{3}H labelled histamine antigen was added and incubated for a further 1h at room temperature. After this incubation, 100µl of histamine secondary antibody was added, vortexed and incubated at 2-8^{0}C for 30 min. Unbound antigen was removed by centrifugation (15min, 4,000xg, 4^{0}C). The supernatant was completely removed and the pellet containing the antibody-antigen complex solubilised in 50µl 0.5M NaOH. 2ml of scintillation fluid was added to all tubes and radioactive content of samples measured by liquid scintillation (LS 3801, Beckman, USA).

2.16 CINC and IL-α.

Commercially available enzyme linked immunosorbant assay (ELISA) kits were used for the quantitative determination of cytokine induced neurophil chemoattractant (CINC) and IL-1α in cell-free pleural exudates (Section 2.4.4). This assay measures directly the amount of protein of interest in samples read off a standard curve. The capture antibodies are affinity purified polyclonal antibody specific for CINC or IL-1α which are supplied pre-coated on a 96 well microtitre plate.

50µl of assay diluent was added to each well followed by 50µl of samples and

antigen, then incubated at room temperature for 2h. After washing the plate 5 times with 300µl wash buffer (0.01M phosphate buffer containing 0.05% v/v Tween-20), 100µl of CINC or IL-1α conjugated antisera was added and incubated for a further 2h at room temperature. The plate was washed 5 times with 300µl wash buffer and 100µl of substrate solution (tetramethylbenzidine/hydrogen peroxide) added to each well and incubated for 30 min. The reaction was terminated by the addition of 1M sulphuric acid and the resulting colour formed was read at λ_{max} = 450nm with a reference wavelength at λ_{max} = 570nm (Anthos, Labtec instruments). Unknown concentrations were read off a standard curve constructed for CINC or IL-1α.

2.17 Total antioxidant status.

Total antioxidant status (TAOS) of exudates and cells were measured as previously described (Laight *et al.*, 1999). The principle of this assay is based on the suppression by antioxidants of 2,2'-azino-bis(3-ethylbenzthiazoline-6-sulfonic acid) radical cation ($ABTS^{\bullet}$) formation catalysed by peroxidase. This assay gives an indirect measure of oxidant stress *in vivo*. Cell homogenates and inflammatory exudates were diluted to a degree where diluting the sample 1:2 caused a two-fold reduction in reaction rate, this dilution of the sample was used throughout the assay. The reaction mixture consisted of (final concentration): 20µl 2,2'-azino-bis(3-ethylbenzthiazoline-6-sulfonic acid) (ABTS; 2mM), 10µl horseradish peroxidase (30mU/ml), 20µl H_2O_2 (0.1mM) and 30-45µl phosphate buffered saline (pH 7.4) and 5-20µl sample to make a total volume of 100µl in a 96 well plate. The reaction was initiated by the addition of H_2O_2 and conducted at 37^{0}C. The increase in absorbance at 405nm, a reflection of accumulation, was determined using an Anthos Labtech type plate reader. Experiments were carried out in triplicate on both cell-free inflammatory exudate as well as inflammatory cells. For the latter determinant, values were adjusted for protein concentration.

2.18 Superoxide scavenging activity.

Superoxide scavenging activity (SSA) was measured in cell-free exudates and inflammatory cells as previously described (Laight *et al.*, 1997). The principle of this assay is based upon the reduction of ferricytochrome c by the superoxide anion and the inhibition of this reaction by intracellular and extracellular antioxidants. The initial rate of reduction of ferricytochrome c by the xanthine oxidase/hypoxanthine system was linearly related to the concentration of xanthine oxidase and could be inhibited by superoxide dismutase

Cell homogenates and inflammatory exudates were diluted to a degree where diluting the sample 1:2 caused a two-fold reduction in reaction rate, this dilution of the sample was used throughout the assay. The reaction mixture consisted of (final concentration): 50µl ferricytochrome c (50µM), 5-10µL xanthine oxidase (20mU/ml), 20µl hypoxanthine (100µM), 5-10µl sample with the volume being made up to 100µl with phosphate buffered saline (pH 7.4). The reaction was initiated by the addition of hypoxanthine and conducted at 37°C. The increase in optical density at 550nm was measured over a 3 min period at 30s intervals using an Anthos Labtech type plate reader. All determinants of initial reaction rates were made with and without sample at least in triplicate. Rates of reaction in the inflammatory cells were corrected for protein concentration. Data was expressed as % inhibition of the initial rate of reaction, however statistics were performed on the raw data.

2.19 *In vitro* culture of J774.2 macrophages and EA.hy926 endothelial cells.

Murine J774.2 macrophages and EA.hy926 endothelial cells were stimulated with LPS and INFγ and the calcium ionophore A23187 respectively, then incubated with acetylsalicylic acid.

J774.2 murine macrophages were resuspended at $2x10^6$ cells/ml in Dulbecco's modified Eagle's medium supplemented with 10% v/v fetal calf serum (low

endotoxin) and gentamycin (100µg/ml). Cells were stimulated by the addition of 0.1µg/ml lipopolysaccharide (LPS; E coli 0111:B4) and 100U/ml murine γINF. This was further supplemented with acetylsalicylic acid as appropriate (Chapter 5). Cells were incubated in an environment of 37^{0}C in a humidified incubator (5% CO_2, 95% air) for 24h prior to harvesting. Media taken from cells after treatment was snap frozen until required for nitrite quantitation (Section 2.6). J774.2 cells were resuspended using a cell scraper and pipette agitation for routine culture and passaging.

EA.hy926 endothelial cells were resuspended at 2x10^6 cells/ml in Dulbecco's modified Eagle's medium supplemented with 10% v/v fetal calf serum (low endotoxin) and gentamycin (100µg/ml). Cell were stimulated by the addition of 1-0.005µM A23187 (calcium ionophore) and further supplemented with acetylsalicylic acid as appropriate. Cells were incubated in an environment of 37^{0}C in a humidified incubator (5% CO_2, 95% air) for 24h prior to harvesting. Media taken from cells after treatment was snap frozen until required for nitrite quantitation (Section 2.6). The metabolic condition of the cells was measured by the MTT assay (Section 2.21). EA.hy926 cells were resuspended using trypsin/EDTA (0.25% w/v trypsin supplemented with 0.1% w/v EDTA in Dulbecco's phosphate buffer modification A) followed by centrifugation at 1000xg and resuspension by pipette aggitation in Dulbecco's modified Eagle's medium supplemented with 10% v/v fetal calf serum for routine culture and passaging.

2.20 Cell viability assay.

Cell viability prior to the experiment was assessed as follows. Equal volumes (50µl) of either J774.2 or EA.hy926 cell suspension and 0.4% w/v trypan blue in Hanks buffered saline solution were mixed gently for 5 min. 10µl of this mixture was introduced into the counting chamber of a haemocytometer (BDH, UK). The number and viability of cells was assessed by determining the ratio of trypan blue-stained (dead) cells to unstained (viable) cells, a viability of 98% being the

lowest acceptable.

2.21 MTT assay

Cell viability of either J774.2, EA.hy926 or inflammatory cells from a 6h carrageenin-induced pleurisy was assessed after termination of the experiment by measuring their dehydrogenase activity. This is quantified as the dehydrogenation of MTT to its formazan dye product. 50µl of MTT (0.5mg/ml) was added to each well and incubated until the control lanes were developed (20 min). The cells were then washed twice in Dulbecco's PBS A, the formazan product was dissolved by adding 100µl DMSO to each well and the plates were read at 570nm. All samples were measured in duplicate.

2.22 Immunohistochemistry

2.22.1 Fixation procedure

Air dried cell smears (Section 2.4.4) and tissue sections (Section 2.5.3) were fixed in either 4% w/v paraformaldehyde (in 0.2M phoshate buffer, pH 7.6) or acetone before staining or immunohistochemical labelling. Cell smears and tissue sections were air dried and stored in an air tight container until required for histological staining and immunohistochemical labelling (Section 2.24.2).

2.22.2 Immunohistochemical labelling

Initially for each antigen under investigation different fixation procedures were used; acetone and paraformaldehyde, to determine the best fixative for antigen preservation and epitope presentation for each antibody. A range of antibody dilutions and incubation times were assessed for optimum labelling. Table 2.2 shows dilutions used for optimum conditions.

Antibody	Dilution	Control	Preabsorption
Rabbit ant-rat/murine iNOS	1:1000	NRS	Recombinant murine iNOS
Rabbit anti-rat/murine COX 2	1:400	NRS	No recombinant protein available at the time
Rat anti-murine PECAM (CD 31)	1:1000	NRS	No recombinant protein available at the time
Rabbit anti-rat/mouse HO-1	1:200	NRS	Recombinant rat HO-1
Rabbit anti-bovine arginase I	1:500	NRS	No recombinant protein available at the time

Table 2.2 Antibody dilutions, serum controls and preabsorption controls used for immunohistochemical analysis of cell smears and tissue sections.

Following fixation (Section 2.24.1) slides were rehydrated for 5 min in 0.01M PBS (pH 7.2). Endogenous peroxidases were quenched with 0.3% v/v hydrogen peroxide in methanol (15 min), then washed in 0.01M PBS (pH 7.2; 15 min) containing 0.1% v/v TritonX-100 (PBST). Non-specific binding of IgGs was blocked using 2% v/v of the appropriate normal serum in PBS containing 0.1% w/v essentially globulin free BSA for 30 min. The normal serum used was the same as the host species used to raise the secondary antibody.

Slides were incubated overnight at $4^{0}C$ with the primary antibody (in PBS containing 0.01% w/v BSA, 0.1% w/v NaN_2 and 0.1% v/v Triton-X100). For negative controls the primary antibody was replaced with normal serum IgG's from the appropriate species. After incubation slides were washed three times (5 min) in 0.01M PBS, pH 7.2, containing 0.1% v/v TritonX-100 (PBST). Slides were incubated for 30 min with the relevant biotinylated secondary antibody (50µl in 10ml PBS containing the appropriate normal serum). After the incubation slides were washed three times in PBST, followed by one wash in PBS (15 min) The Vectastain™ avidin-biotinylated HRP complex was made up 30 min before use in PBS containing 0.5M NaCl. This complex was then incubated with the

sections for 30 min.

Afer incubation with the ABC complex, slides were washed 3 times in PBS, then for 15 min in 0.05M Tris buffer, pH 7.6. Sections were visualised with diaminobezidine tetrahydrochloride (DAB) for 1 to 10 min in the dark. The reaction was halted by washing the sections in distilled water for 5 min. Sections were counterstained and mounted. The nuclei of the cells was stained with Harris's haematoxylin for 1 min, excess stain was removed under tap water (30 seconds) and the haematoxylin differentiated in acid alcohol (70% v/v industrial methylated spirits and 1% v/v concentrated HCl) for 2 min. Sections were blued under tap water, therefore the nuclei of all cells from smears and tissue sections appeared blue and immunopositive cells for the antigen in question were stained brown.

2.22.3 Morphometric analysis of PECAM (CD 31) staining

The effect of drug administration on the vascular component of the granulomatous tissue was assessed by morphometeric analysis after PECAM staining of endothelial cell and compared to the carmine method (Section 2.14). 10µm sections were cut randomly through n=5 granulomas per treatment and per time point. Sections were fixed in acetone and immunolabelled with rat anti-murine PECAM (1:1000). Micrographs were randomly taken from each section cut and analysed using a 1 cm^2 transparent grid that was randomly superimposed upon them. The intersections falling on endothelial cells and blood vessel lumens were counted and calculated as a percentage of total tissue area.

2.22.4 Haematoxylin and eosin staining

Inflammatory cell smears and 10µm tissue sections were fixed in 4% w/v paraformaldehyde solution (Section 2.22.1), rehydrated and stained with haematoxylin and eosin for histological assessment. The nuclei of cells were stained with Harris's haematoxylin for1 min and washed with tap water. Excess stain was removed by differentiation in acid alcohol (70% v/v industrial

methylated spirits and 1% v/v HCl) for 2 min, then blued under tap water. The cytoplasm of the cells was stained with a 1% w/v eosin Y solution (in distilled H_2O) for 10 seconds, followed by 5 min wash in running tap water. Sections were then dehydrated in alcohol, cleared in xylene and mounted with glass cover slips using DPX. Cell phenotypes were identified by nuclear morphology. Cell smears from the acute inflammatory models were differentially counted using the principles described by Gundersen and Osterby (1980) and expressed as percentages of total cell counts.

2.22.5 Toludine blue staining for mast cells

Fixed cell smears and tissue sections (Section 2.22.1) were rehydrated and stained with toludine for histological and mast cell assessment. Slides were stained with a filtered toludine blue solution (50mg toludine blue, 25ml ethanol, 2.5ml formaldehyde (30% w/v), 0.5ml acetic acid and 12ml deionised H_2O) for 2 min and rinsed in tap water until the desired intensity of staining was achieved. Slides were mounted in immersion lens oil for analysis and photography, nuclei stained blue and granules of mast cell had a dichromatic appearance.

2.22.6 Van Gieson staining for collagen and fibrin

Fixed cell smears and tissue sections (Section 2.22.1) were rehydrated and stained with Celestine blue (0.5% w/v Celestine blue in 5% w/v ferric ammonium sulphate and glycerol) for 2 min. Sections were then stained with Mayers haematoxylin for 2 min and blued under tap water for 5 min. Sections were rinsed in distilled water and stained in Van Geison solution (100ml saturated picric acid containing 10ml of 1% v/v acid fuchsin in distilled H_2O) for 5 min, then dehydrated using bottled alcohol, cleared in xylene and mounted in DPX . Nuclei were brown/black to black, collagen deep red and muscle, cytoplasm, red blood cells and fibrin were stained yellow.

2.22.7 NADPH diaphorase staining for iNOS activity

NADPH diaphorase staining was used to detect NOS activity in tissue sections, since NOS is able to catalyse the reaction shown in (Figure 2.1). Nitro-blue

tetrazolium was used as the final substrate which reacts with hydrogen to form a water soluble product. Reactions was carried out on unfixed cryostat sections, using liver as a positive control.

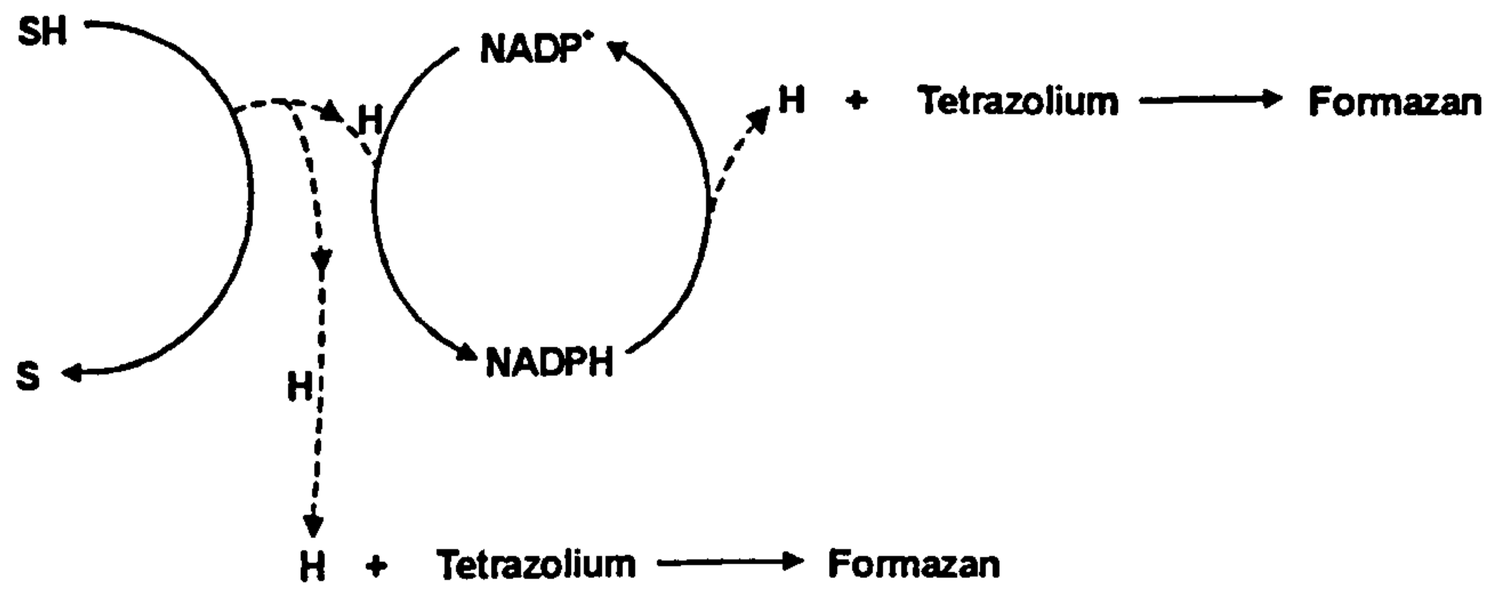

Figure 2.1 SH is substrate and s is oxidised substrate, the H released by the substrate reacts with tetrazolium to form a soluble formazan dye.

Unfixed sections were covered with incubating solution for 1h at 37°C. The NADPH diaphorase incubating medium consisted of 0.9ml of 0.11% w/v nitro-blue tetrazolium solution (in 0.055M phosphate buffer containing 0.006 $MgCl_2$). After the incubation sections were fixed in formol saline for 10-15 min, rinsed in distilled water and counterstained in 1% w/v Neutral red for 20s and washed rapidly in tap water to remove excess stain. Sections were dehydrated in alcohol, cleared in xylene and mounted in DPX.

2.23 Terminal deoxynucleotide transfer-mediated dUTP-biotin nick-end labelling (TUNEL) immunochemical assay for the quantification of apoptosis.

The Apoptag® detection kit was used to label apoptotic cells smears *in situ* by direct immunoperoxide detection of digoxigenin (DIG) labeled DNA. During apoptosis the DNA fragments and these residues of DIG are catalytically added by terminal deoxynucleotidyl transferase (TdT). The incorporated nucleotides from a random heteropolymer of DIG-11-dUTP and dATP, which is recognised by a polyclonal HRP-linked anti-DIG antibody.

Cell smears from the carrageenin-induced pleurisy (Section 2.4.4) were fixed in neutral-buffered formalin (10% v/v) for 10min, then washed twice in PBS (5min). Sections were allowed to air dry for 24h, then rehydrated in PBS and post-fixed in pre-cooled ethanol:acetic acid (2:1 v/v) at -20^{0}C (5 min) to permeabilise the cell membranes. After 3 washes in PBS containig 0.1% v/v Tween-20^{TM} (PBST), endogenous peroxidases were quenched with 2% v/v hydrogen peroxide in PBS for 5 min at room temperature. Slides were washed twice in PBST and then incubated with 13µl/cm^2 Equilibration buffer for 30 min at room temperature, followed by incubation with 11µl/cm^2 of working strength TdT enzyme (specific activity 0.3U/µl; 1h, 37^{0}C). Distilled water was substituted for TdT enzyme and used as a negative control. The reaction was halted by applying pre warmed stop/wash buffer for 10 min at room temperature. After 2 PBS washes, 13µl/cm^2 of anti-DIG-peroxidase antibody was applied to the slides (30 min, room temperature). Finally, slides were rinsed twice in PBS, then in 0.05M Tris buffer (pH 7.6) and the immunolocalisation was visualised with DAB and counterstained with Harris' haematoxylin, differentiated, dehydrated, cleared and mounted. Positive cells were manually counted within a 100µm^2 area using a high power objective (x 40 magnification: 10 x 10µm graticule) and stained cells were expressed as a percentage of total cells. At least 10 fields of view were counted per slide.

2.24 Data and statistics

For *in vitro* experiments, data is reported as mean ± standard error of the mean (sem) of n experiments performed at least in duplicate. Statistical differences were analysed by analysis of variance (ANOVA) for multiple comparisons, using the software package GraphPad Instat™. If the ANOVA analysis predicted a significant difference between groups (F value), post-hoc comparison tests were made using the Bonferroni test for p values. When two groups were compared, statistical differences were measured using a two tailed Student *t* test. In all cases a threshold value of $p \leq 0.05$ was sufficient to reject the null hypothesis and differences were considered significant.

For *in vivo* experiments, data is reported as mean ± standard error of the mean (sem) of individual observations (animals).Statistical differences were analysed by nonparametric Kruskal-Wallis trend test for multiple comparisons, using the software package GraphPad Instat™. The Kruskal-Wallis test is a nonparametric test that compares three or more unpaired groups. To perform the Kruskal-Wallis test, first all the values are ranked from low to high, disregarding which group each value belongs. If two values are the same, then they both get the average of the two ranks for which they tie. The smallest number gets a rank of 1. The largest number gets a rank of N, where N is the total number of values in all the groups. The rank in each group is summed. If the sums of the ranks are very different, the P value will be small. The discrepancies among the rank sums are combined to create a single value called the Kruskal-Wallis statistic (referred to as H). A larger Kruskal-Wallis statistic corresponds to a larger discrepancy among rank sums. The P value answers this question: if the null hypothesis is true then what is the chance of obtaining a Kruskal-Wallis statistic as high (or higher) as observed in this experiment? If the Kruskal-Wallis test predicted a significant difference between groups (H value), pos-thoc comparison tests were made using the nonparametric Mann-Whitney U test, that does not assume Gaussian distribution, for p values. When two groups were compared, statistical differences were measured using a two tailed student *t* test. In all cases a threshold value of $p \leq 0.05$ was sufficient to reject the null hypothesis and differences were considered significant.

CHAPTER 3

3.1 Introduction

The aim of the work presented in this chapter is to map the temporal and spatial expression of NO pathways compared with arginase in three acute and one chronic inflammatory model. Each model has a different initial stimulus, inflammatory mechanism and cellular profile, representing different types of reactions that can occur in man.

Initially, the NOS pathway was investigated in a complement-mediated acute inflammatory model, carrageenin-induced pleurisy in the rat (Section 2.4.1). Inflammatory cell counts, differential cell counts and exudate volume were performed to profile the inflammatory response to carrageenin. The temporal and spatial expression of iNOS was determined from the beginning to the resolution of the reaction by Western blotting (Section 2.9) and immunohistochemistry (Section 2.22). Nitrite (Section 2.6) the stable breakdown product of NO was quantified in cell-free inflammatory exudates, while iNOS activity (Section 2.7) was determined in inflammatory cell pellets. These investigations of iNOS expression and enzyme activity were correlated with exudate volume and inflammatory cell influx. The products of both the arginase and COX pathways are postulated to play an important role in inflammation, however, controversy surrounds the interactions between NO and the arginase and COX pathways. Therefore, the profile of arginase activity and COX activity and its major products PGE_2 and PGI_2 were examined over a time course to investigate the possibility of interactions between these pathways in the rat carrageenin-induced pleurisy.

Similar to the carrageenin-induced pleurisy the NOS pathway was investigated in two other acute pleural inflammatory models, BSA-induced pleurisy (type III hypersensitivity reaction) and metBSA-induced pleurisy (type IV hypersensitivity reaction or delayed hypersensitivity reaction). Again, in these two models the profile of the NOS pathway was compared with both arginase and COX enzyme activity. Increasing evidence indicates that NO may also contribute to chronic

inflammation (Farrel *et al.*, 1992, Middleton *et al.*, 1993, Corbett *et al.*, 1993 and Maeda *et al.*, 1994). Therefore, The NOS pathway was investigated in the murine chronic granulomatous tissue air pouch (MCGAP) as above.

3.2 Carrageenin-induced pleurisy

3.2.1 Exudate volume and inflammatory cell counts

Injection of carrageenin into the pleural cavity of rats resulted in a complement mediated reaction characterised by extravasation and influx of inflammatory cell leucocytes into the pleural cavity, peaking at 18-24h post initiation (Figure 3.1). At 2 h, the pleural cavity contained 0.19 ± 0.04 ml of exudate and 15 ± 6 $x10^6$ inflammatory cell, both cells and exudate were elevated at 6 and 12h, being maximal at 24h with 1.18 ± 0.35 ml of exudate and 101 ± 19 $x10^6$ cells removed from the pleural cavity. By 48h the inflammation had waned to 0.16 ± 0.07 ml of exudate and 26 ± 3 $x10^6$ cells.

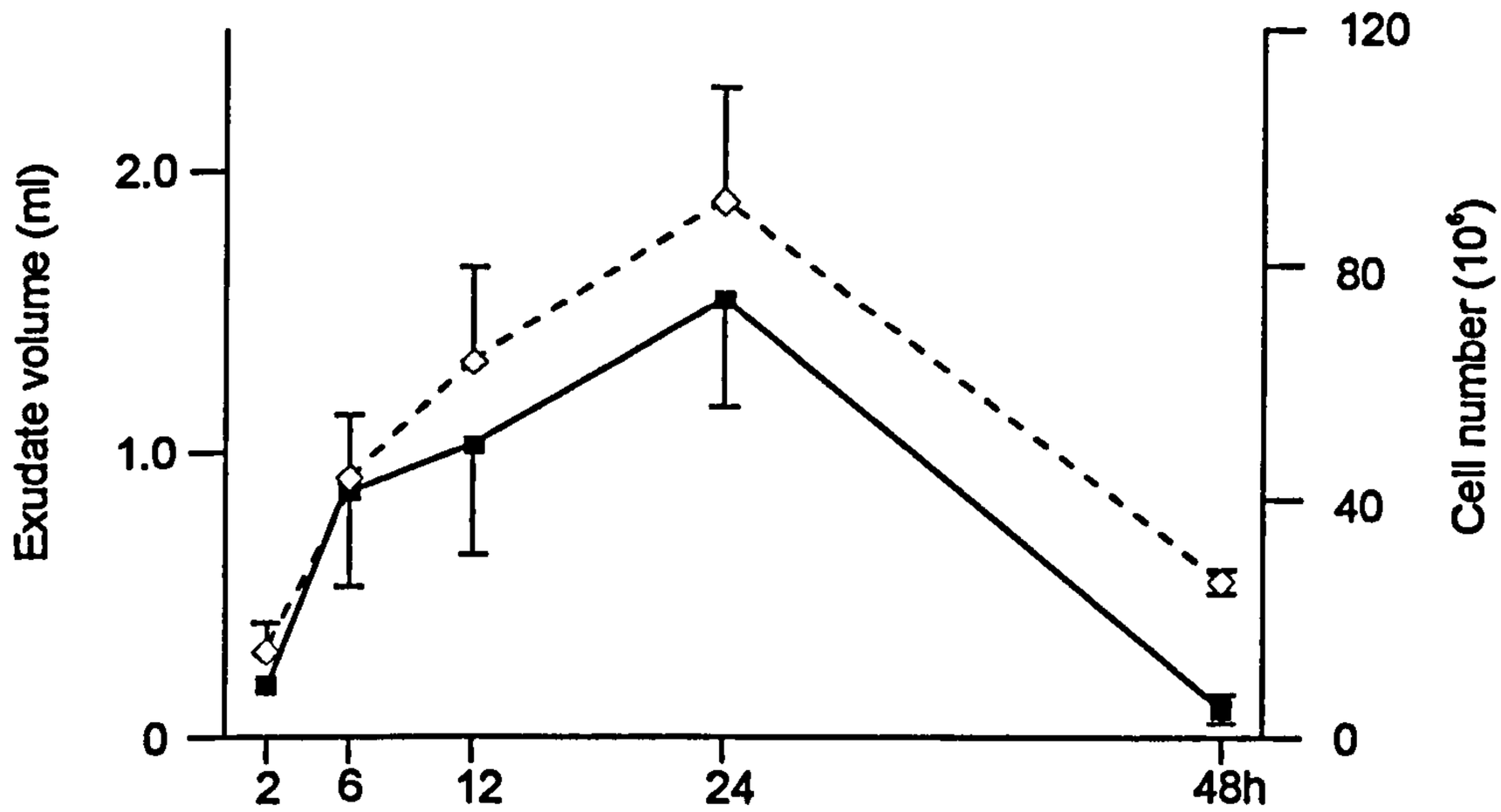

Figure 3.1 Time course of inflammation in the carrageenin-induced pleurisy in wistar rats. *Exudate volume is represented by ■ and inflammatory cell influx by ◊. Data is expressed as mean ± standard error of the mean (n=10 per time point).*

Differential cell counts of inflammatory cell smears stained with hematoxylin and eosin revealed a predominance of PMNs at 2 h (86%) with MN cells being the major cell type at 48 h (70%), specific percentages of cells in this model are

presented in Table 3.1. The cells under the category of "other" contained mast cells, lymphocytes and mesothelial cells.

	Time after carrageenin injection (h)				
	2	**6**	**12**	**24**	**48**
PMNs	86%	92%	99%	61%	28%
MNs	11%	7%	1%	38%	70%
Other	3%	1%	≤1%	1%	1%

Table 3.1 Differential counts of inflammatory cell smears taken from the pleural cavity of rats, injected with carrageenin after staining with haematoxylin and eosin. *n=6 at each time point.*

3.2.2 iNOS protein expression in inflammatory cells

iNOS protein was expressed in inflammatory cell throughout the time course of the carrageenin pleurisy as assessed by Western blotting and quantified by densitometric analysis and expressed as arbitrary units (Section 2.9 as seen in Figure 3.2). iNOS protein was detectable in inflammatory cell pellets at 2h, although the density of the band at this time point was low (154 ± 26). iNOS protein peaked at 6h with a density of 12685 ± 356 , after which levels decreased to baseline by 24h. At 48h there was an increase in density of iNOS protein to 4735 ± 773, however no enzyme activity was measurable at this time point (see Section 3.2.4). cNOS activity was below detection limits in inflammatory cell pellets throughout the time course of this model (data not shown).

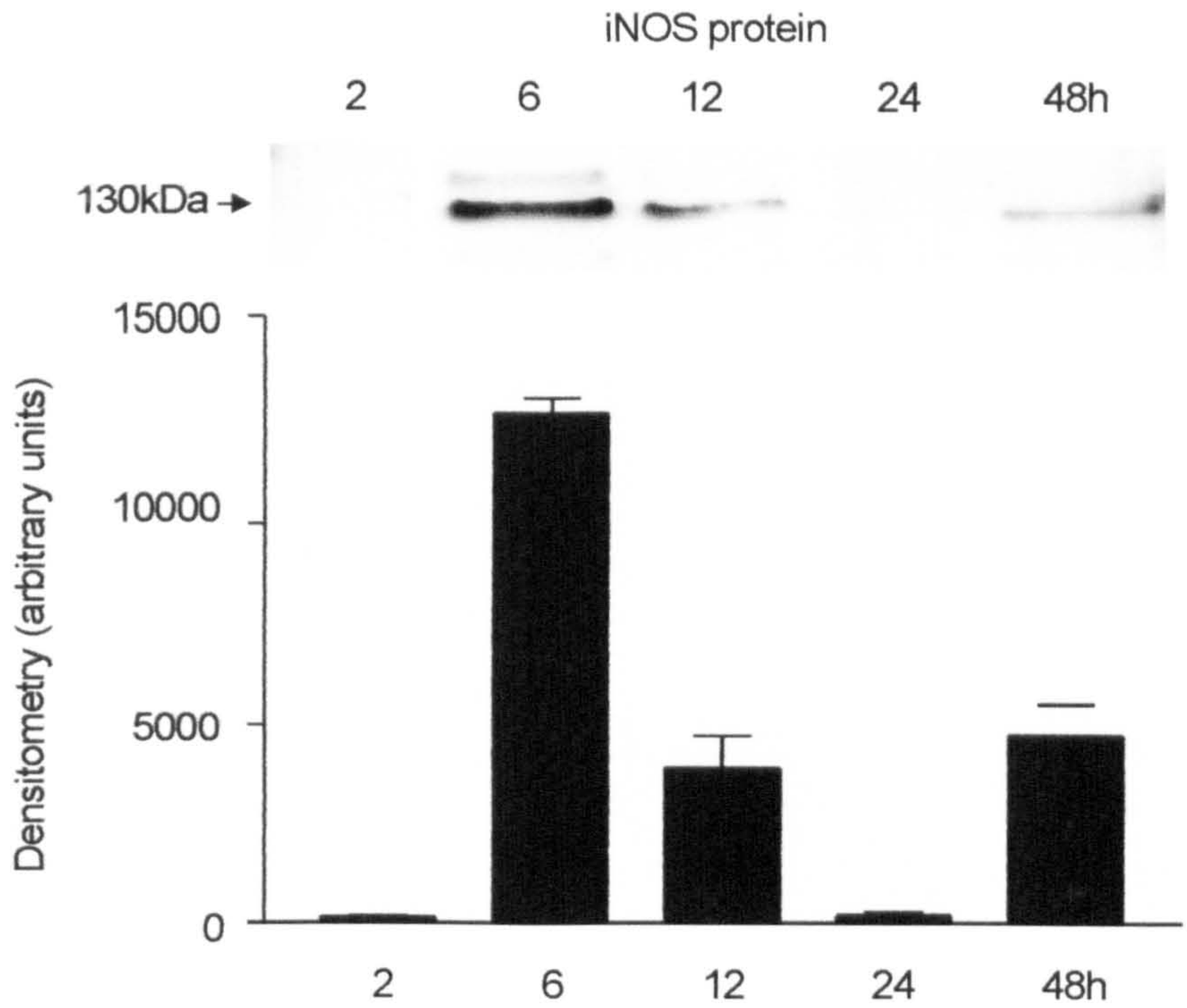

Figure 3.2 Time course of iNOS expression in cell pellets taken from Wistar rats with a carrageenin-induced pleurisy. *Western blot analysis for iNOS protein was performed followed by densitometry. The top panel is a representative Western blot of n=8.*

3.2.3 Levels of nitrite in cell-free inflammatory exudates

Pleural lavage of control animals that did not receive carrageenin contained relatively high levels of nitrite (8.9 ± 0.1 μM), with control plasma levels being low (2.1 ± 0.1 μM). Thirty minutes after carrageenin injection nitrite levels reached a peak of 15.9 ± 1.4 μM, then waned at 1h and 2h (Figure 3.3). iNOS protein was not detectable in inflammatory cells at 0.5h, 1h or in control animals, suggesting that NO at this time point was probably from a cNOS source. A second peak of nitrite was observed at 6 h (8.9 ± 1.6 μM), this correlated with a time at which iNOS protein expression (Figure 3.2) and activity (Figure 3.4) were maximal, hence NO produced at this time point was probably from iNOS. Nitrite levels were very low at 12 and 24h, however, there was a slight increase at 48h (2.4 ± 1.2 μM), which correlated in profile to iNOS protein expression (Figure 3.2).

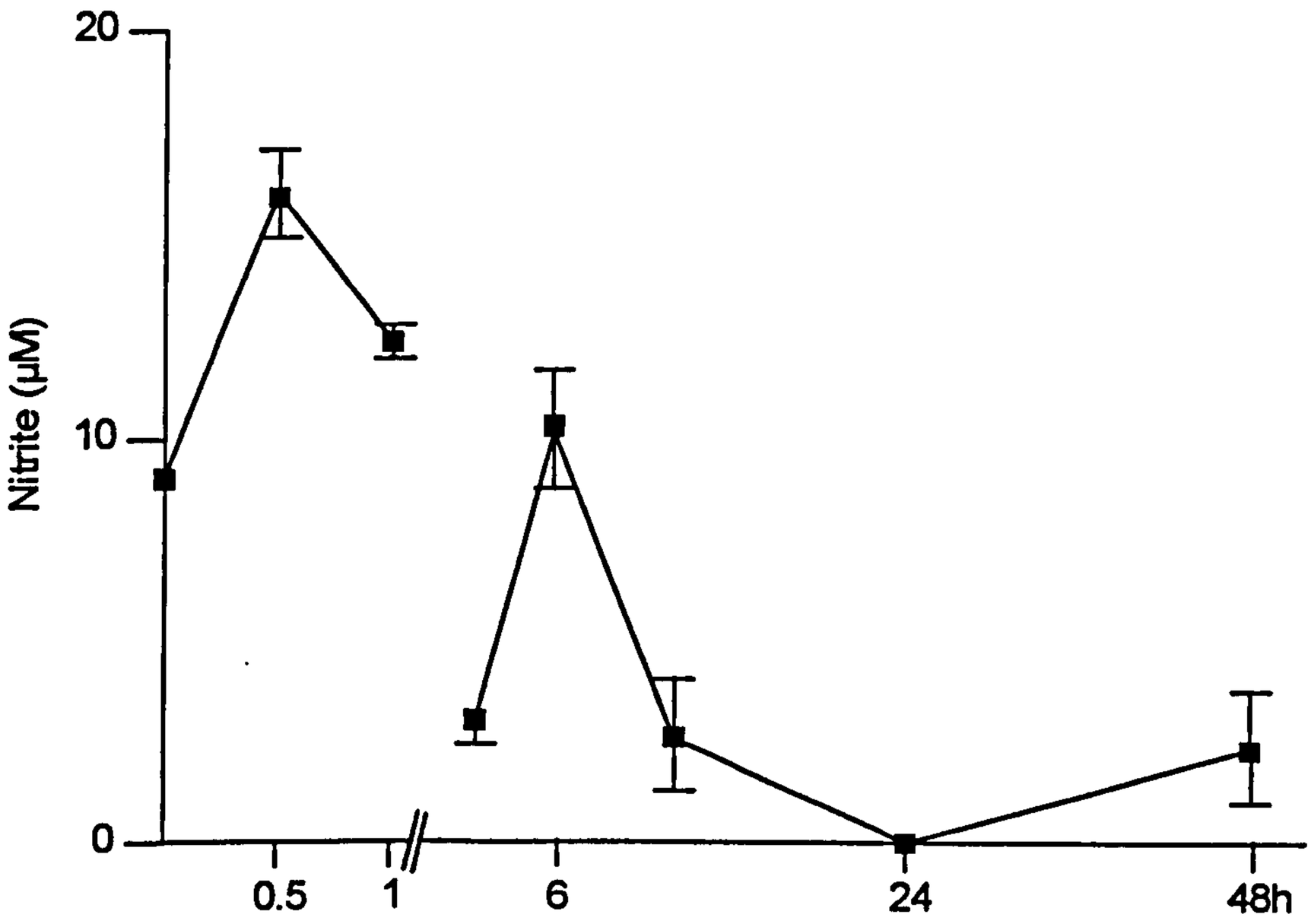

Figure 3.3 Time course of nitrite accumulation in the carrageenin-induced pleurisy. *Nitrite levels in cell-free pleural exudates were measured by the Greiss reaction. Data is expressed as mean ± standard error of the mean (n=10 per time point).*

3.2.4 NOS enzyme activity in inflammatory cell pellets

Pleural lavage of control animals that did not receive carrageenin contained iNOS (21 ± 2 pmol citrulline/mg protein/30 min; Figure 3.4). 30 minutes and 1h post-carrageenin, iNOS activity within inflammatory cells was on the detection limit of the assay (17 ± 10 pmol and 20 ± 9 pmol citrulline/mg protein/30 min respectively). Levels of iNOS activity detected at 2h were 151 ± 21 pmol citrulline/mg protein/30 min, which reached a peak at 6hrs (820 ± 202 pmol citrulline/mg protein/30 min), with decreased levels of iNOS activity at 12h, 24h and 48h. cNOS activity was virtually undetectable at all points measured (2h, 12h, 24h and 48h) except at 6h (124 ± 84 pmol citrulline/mg protein/30 min). Furthermore, depletion of calcium from the enzyme reaction by the addition of the calcium chelator EGTA reduced cNOS enzyme activity to baseline values, whereas iNOS activity was unaffected throughout the time course of this acute inflammatory model.

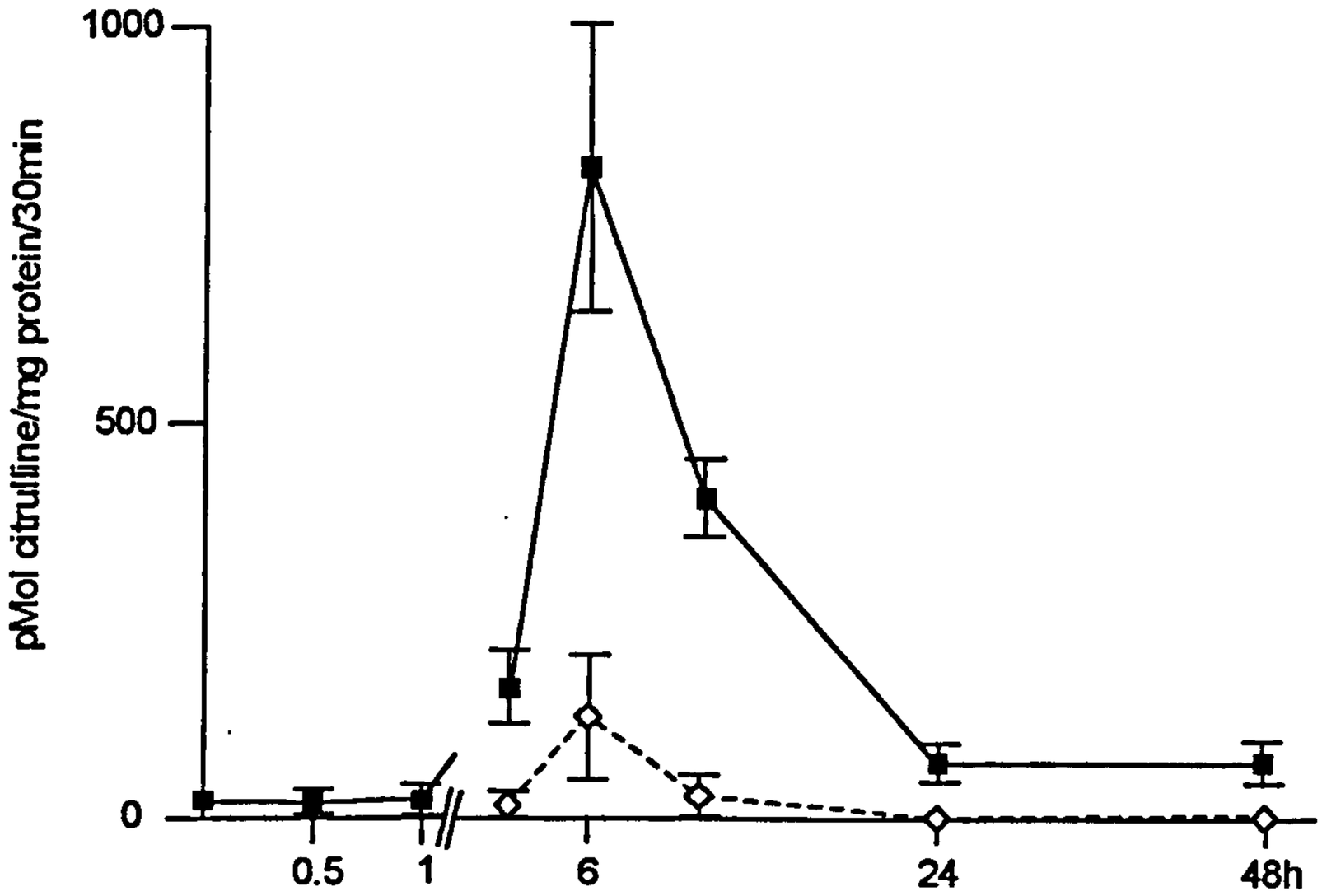

Figure 3.4 Time course of NOS activity in the carrageenin-induced pleurisy. *iNOS activity is represented by ■ and cNOS activity by ◊. Data is expressed as mean ± standard error of the mean (n=6 per time point).*

3.2.5 Spatial expression of iNOS protein in inflammatory cells

Acetone fixed sections of inflammatory cell smears from the pleural cavity were analysed by immunocytochemistry (Section 2.22) for iNOS protein expression (Figure 3.5, panels b-f). The iNOS antibody was deemed specific since pre-absorbed controls showed a considerable reduction in the intensity of staining and a control smear, which received normal rabbit serum had no immunostaining (Figure 3.5 panel a). At 2h nearly all PMNs were negative for iNOS protein, with the occasional positively stained MNs (the percentage of positively stained cells are presented in Table 3.2). By 6h the majority of MNs and PMNs stained for iNOS protein. Post 6h MNs and the diminishing population of PMNs showed some immunoreactivity for iNOS, however this was greatly reduced when compared to 6h.

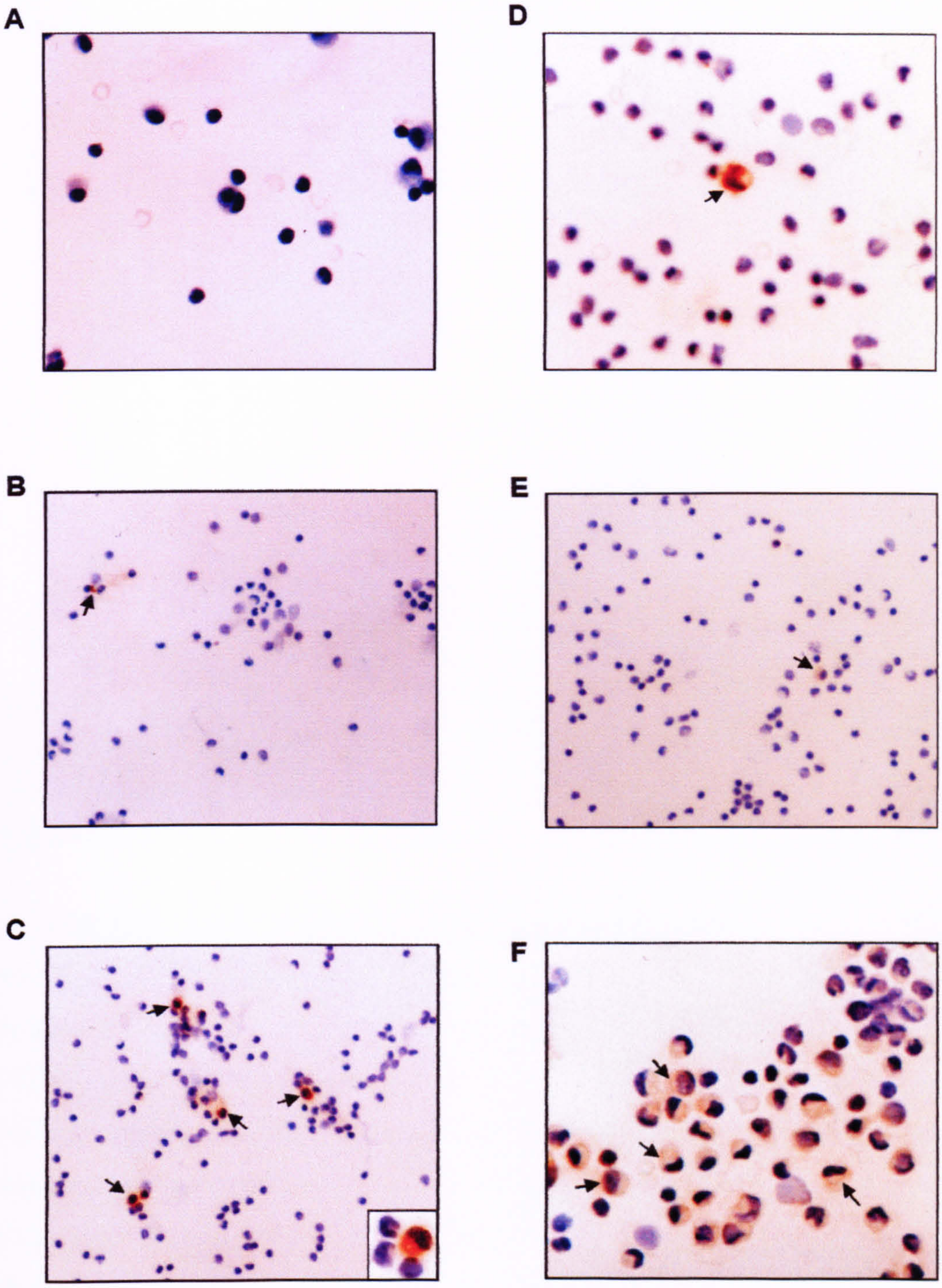

Figure 3.5 Time course of iNOS protein expression within inflammatory cell from the carrageenin-induced pleurisy. *(a) Primary iNOS antiserum was replaced with normal goat serum to act as a negative control and showed no staining for iNOS. Immunolabelling for iNOS protein was observed in both PMNs and MNs in inflammatory cell smears at different time points; (b) 2h, (c) 6h, (d)12h, (e) 24h and (f) 48h. (A), (D), (F) are at magnification x63 and (B), (C), (E) are at magnification x32, arrows indicate cells positive stained for iNOS.*

Time	Cell type	Percentage +ve for iNOS protein
2h	PMNs	0
	MNs	10
6h	PMNs	75
	MNs	92
12h	PMNs	36
	MNs	55
24h	PMNs	0
	MNs	15
48h	PMNs	30
	MNs	41

Table 3.2 Immunocytochemical analysis of iNOS staining in inflammatory cell smears taken from the pleural cavity of rats injected with carrageenin. *Values represent percentage of PMNs and mononuclear cells positive for iNOS protein. Data is expressed as mean of n=5 animals per time point*

3.2.6 Arginase enzyme activity in inflammatory cell pellets

Arginase and nitric oxide synthase share a common substrate L-arginine, which in the case of arginase is metabolised to ornithine and urea. Further, both PMNs and MNs are reported to contain the two isoforms, arginase I and II, upon activation with an inflammatory stimuli. Levels of arginase activity, in the carrageenin-induced pleurisy, were very low at the time points measured. At 2h inflammatory cells produced 0.23 ± 0.09 mU urea/mg protein/min (Figure 3.6), which rose to a peak at 6h (1.05 ± 0.40 mU urea/mg protein/min), then declined thereafter.

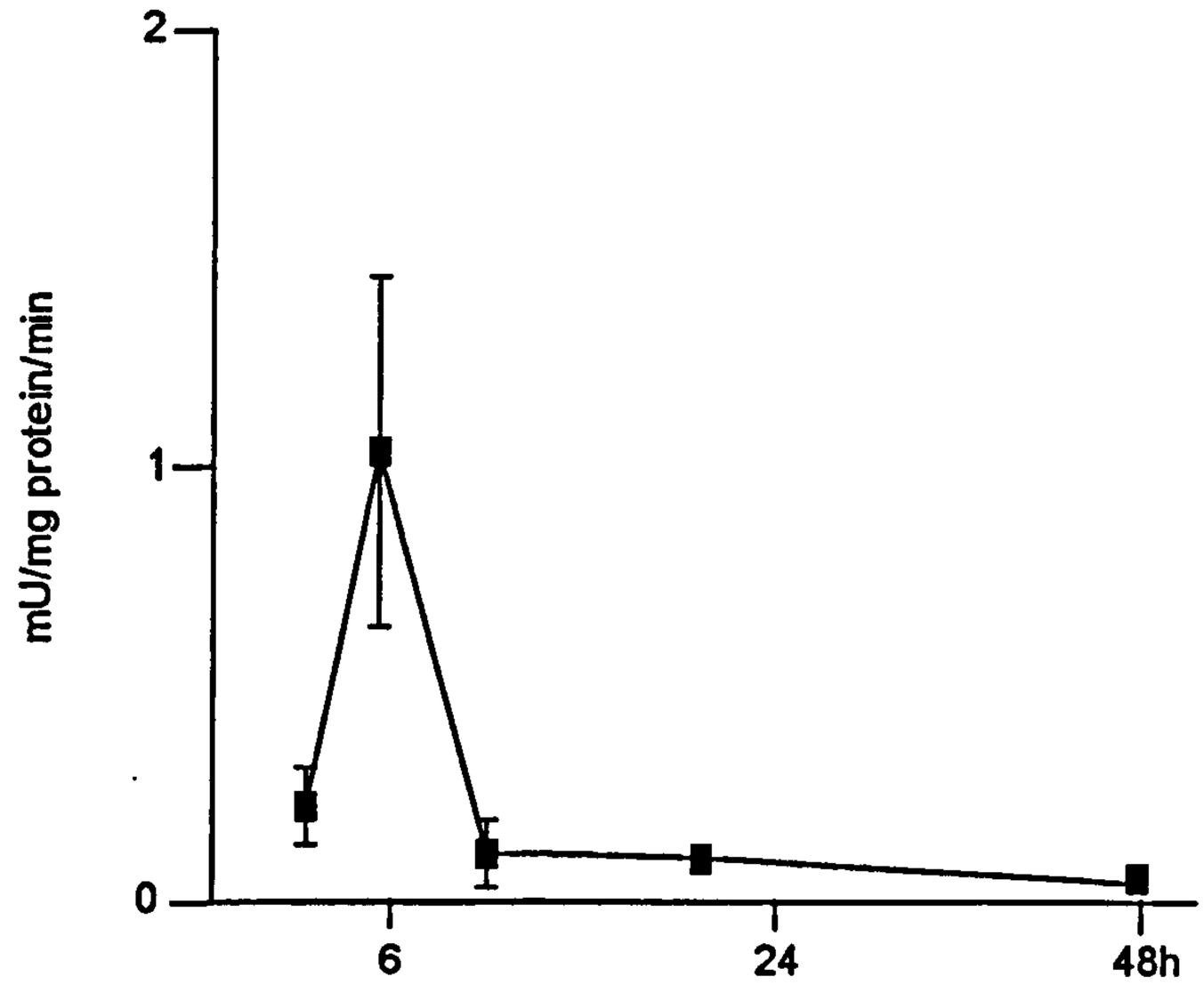

Figure 3.6 Time course of arginase activity in the carrageenin-induced pleurisy. *Data is expressed as mean ± standard error of the mean (n=8 per time point).*

3.2.7 Prostaglandin E_2 and I_2 levels in cell-free inflammatory exudates

PGE_2 levels were not detectable in pleural lavages from animals that did not receive carrageenin. Post carrageenin injection, total exudate PGE_2 levels were maximal at 2h (1028 ± 193 pg) and declined thereafter (Figure 3.7), with levels at 24h and 48h being below the detection limit of the assay.

6-keto PGF1α was measured as a stable breakdown product of PGI_2. PGI_2 levels in exudate peaked at 6h (1631 ± 363 pg) and declined thereafter (Figure 3.7), with levels at 24h and 48h being below the detection limit of the assay.

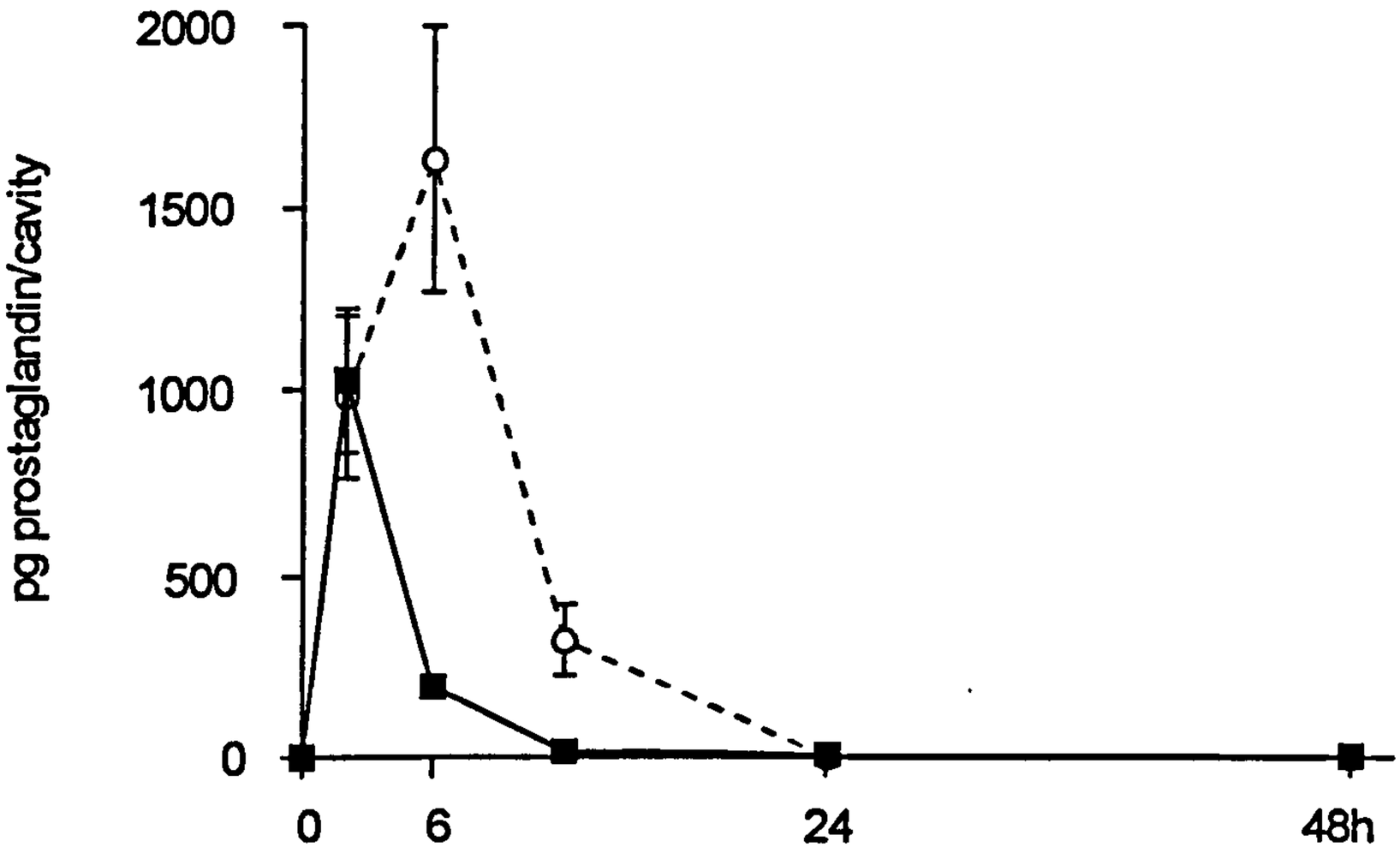

Figure 3.7 Time course of PGE_2 and 6-keto PGF1α levels in the carrageenin-induced pleurisy. *PGE_2 levels are represented by ■ and 6-keto PGF1α levels by ○. Data is expressed as mean ± standard error of the mean (n=6 per time point).*

3.2.8 COX activity in inflammatory cell pellets

COX activity in cell pellet extracts followed a similar profile to PGE_2 in cell-free exudates and was measured as the quantity of PGE_2 produced in the presence of excess substrate and co-factors. At 2h, COX activity was maximal (7.5 ± 2.7 ng/mg protein/30 min, Figure 3.8) after which it declined to baseline from 6h onwards.

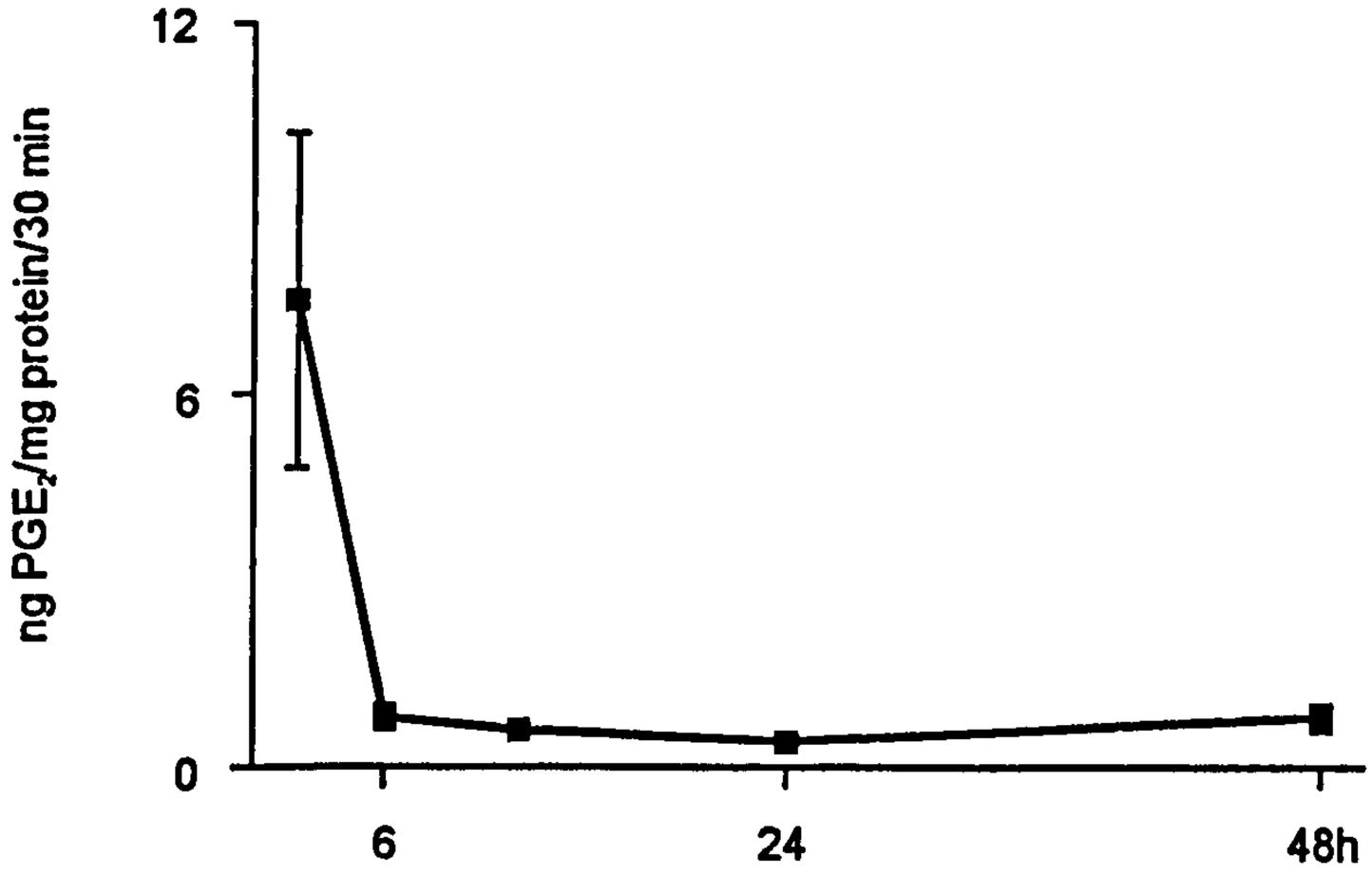

Figure 3.8 Time course of COX activity in inflammatory cell pellets in the carrageenin-induced pleurisy. *Data is expressed as mean ± standard error of the mean (n=5 per time point).*

3.3 Rat BSA-induced pleurisy

3.3.1 Exudate volume and inflammatory cell counts

Challenge with BSA in the pleural cavity of rats pre-treated with BSA resulted in an antibody/antigen reaction which caused the influx of inflammatory cells and exudate into the pleural cavity, both peaked at 6h (Figure 3.9). At 2h, the pleural cavity of rats contained 0.76 ± 0.17ml of exudate and 11.2 ± 1.5 $x10^6$ inflammatory cells. By 6h, both parameters peaked with 1.01 ± 0.19ml of exudate and 15.9 ± 2.1 $x10^6$ cells being recovered. Exudate volume and inflammatory cell number waned thereafter, with 0.30 ± 0.05ml of exudate and 8.6 ± 0.8 cells at 12h and 0.11 ± 0.02ml of exudate and 7.2 ± 0.8 $x10^6$ at 24h.

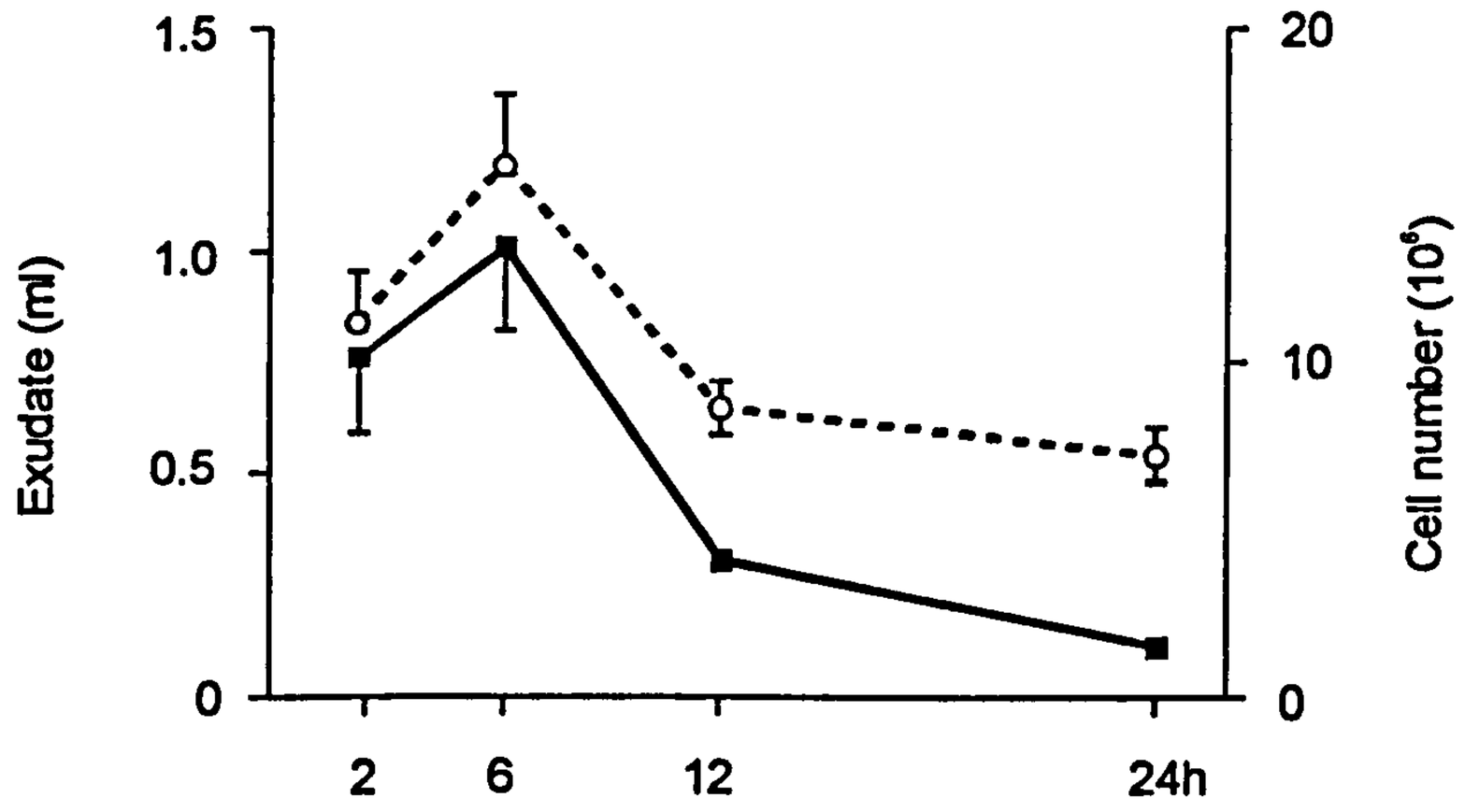

Figure 3.9 Time course of inflammation in the BSA-induced pleurisy. *Exudate volume is represented by ■ and inflammatory cell influx by o in Wistar rats challenged with BSA into the pleural cavity, 12 days after sensitisation with BSA into the tail. Data is expressed as mean ± standard error of the mean (n=6 per time point).*

Differential counts of inflammatory cell smears stained with Harris' hematoxylin and eosin resulted in a predominance of PMNs throughout the inflammatory time course (2-24h). Percentages of cells in this model are presented in Table 3.3.

	Time after intrapleural BSA challenge (h)			
	2	**6**	**12**	**24**
PMNs	81%	95%	75%	57%
MNs	19%	5%	25%	43%

Table 3.3 Differential counts of inflammatory cell smears in the BSA-induced pleurisy. *Rats were sensitised with BSA into the tail, then challenged with BSA in the pleural cavity 12 days later. Cell smears were stained with heamatoxylin and eosin. n=4 per time point.*

3.3.2 iNOS protein expression in inflammatory cells

iNOS protein was expressed throughout the time course of rats challenged intrapleurally with BSA (Figure 3.10). iNOS protein expression was maximal at 2h, after which it declined at 6h and 12h, being almost undetectable at 24h.

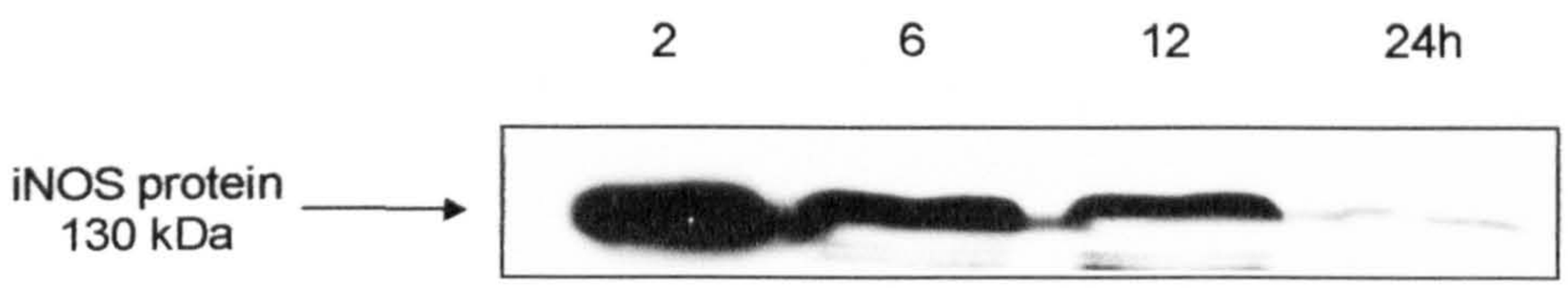

Figure 3.10 iNOS protein expression in the BSA-induced pleurisy*. iNOS expression was determined by Western blotting of cells form inflammatory exudates from rats sensitised into the tail with BSA and challenged 12 days later with BSA intrapleurally. A typical blot.*

3.3.3 Levels of nitrite in cell-free inflammatory exudates

Two hours after intrapleural challenge with BSA nitrite levels were maximal (7.9 ± 0.3μM, Figure 3.11), this correlated with the peak in iNOS protein expression (Figure 3.10) and activity (Figure 3.12). At 6h nitrite levels declined (5.4 ± 0.4μM), being almost undetectable at 12h and 24h.

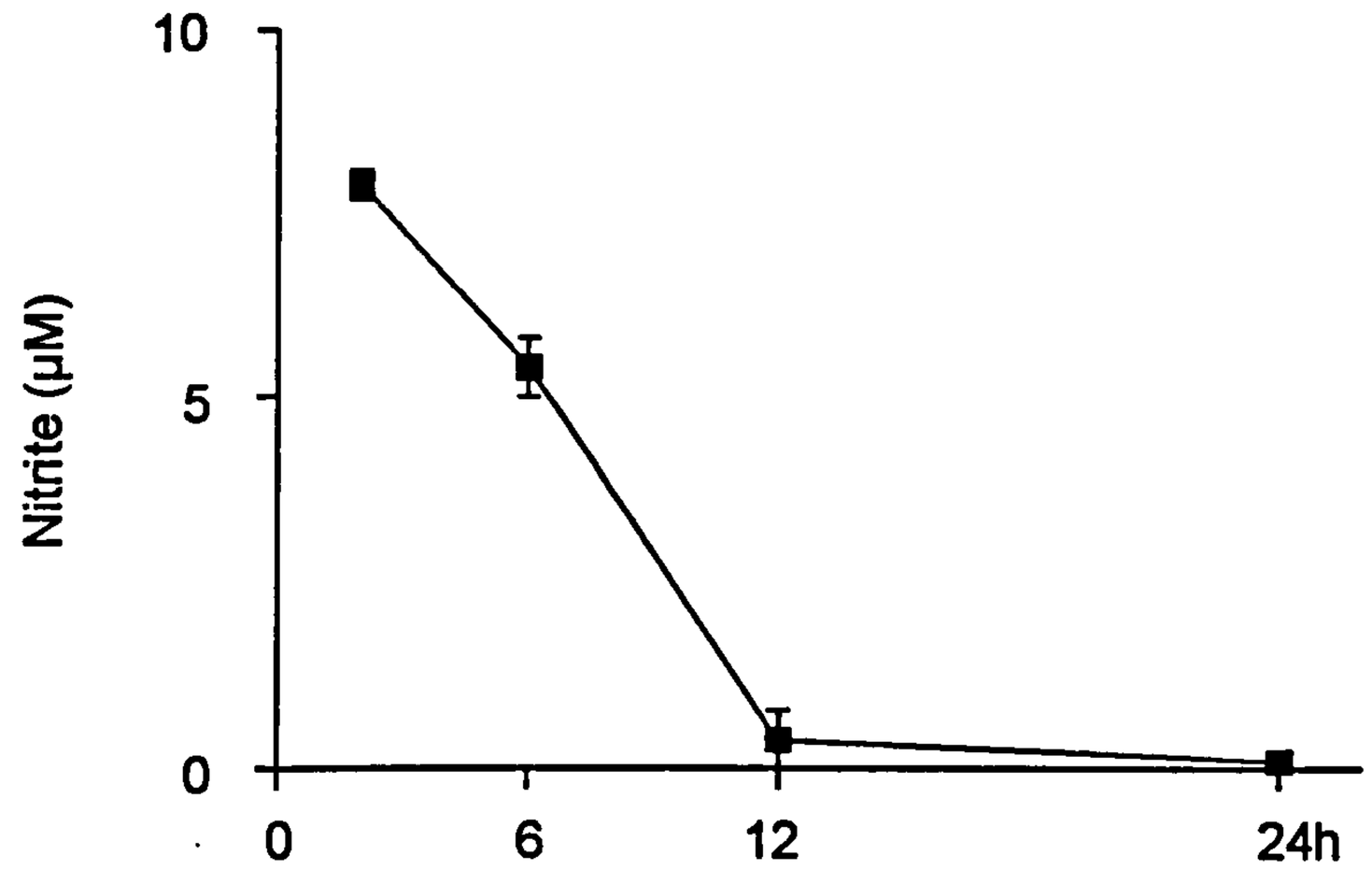

Figure 3.11 Time course of nitrite accumulation in the BSA-induced pleurisy. *Rats were sensitised with BSA into the tail, then challenged with BSA in the pleural cavity 12 days later. Data is expressed as mean ± standard error of the mean (n=6 per time point).*

3.3.4 iNOS enzyme activity in inflammatory cell pellets

Two hours after intrapleural challenge with BSA iNOS activity was maximal (259 ± 45 pMol citrulline/mg protein/30 min, Figure 3.12). At 6h and 12h iNOS activity declined, being much reduced at 24h (62 ± 23 pMol citrulline/mg protein/30 min). cNOS activity was below the detection limit of this assay at all time points measured.

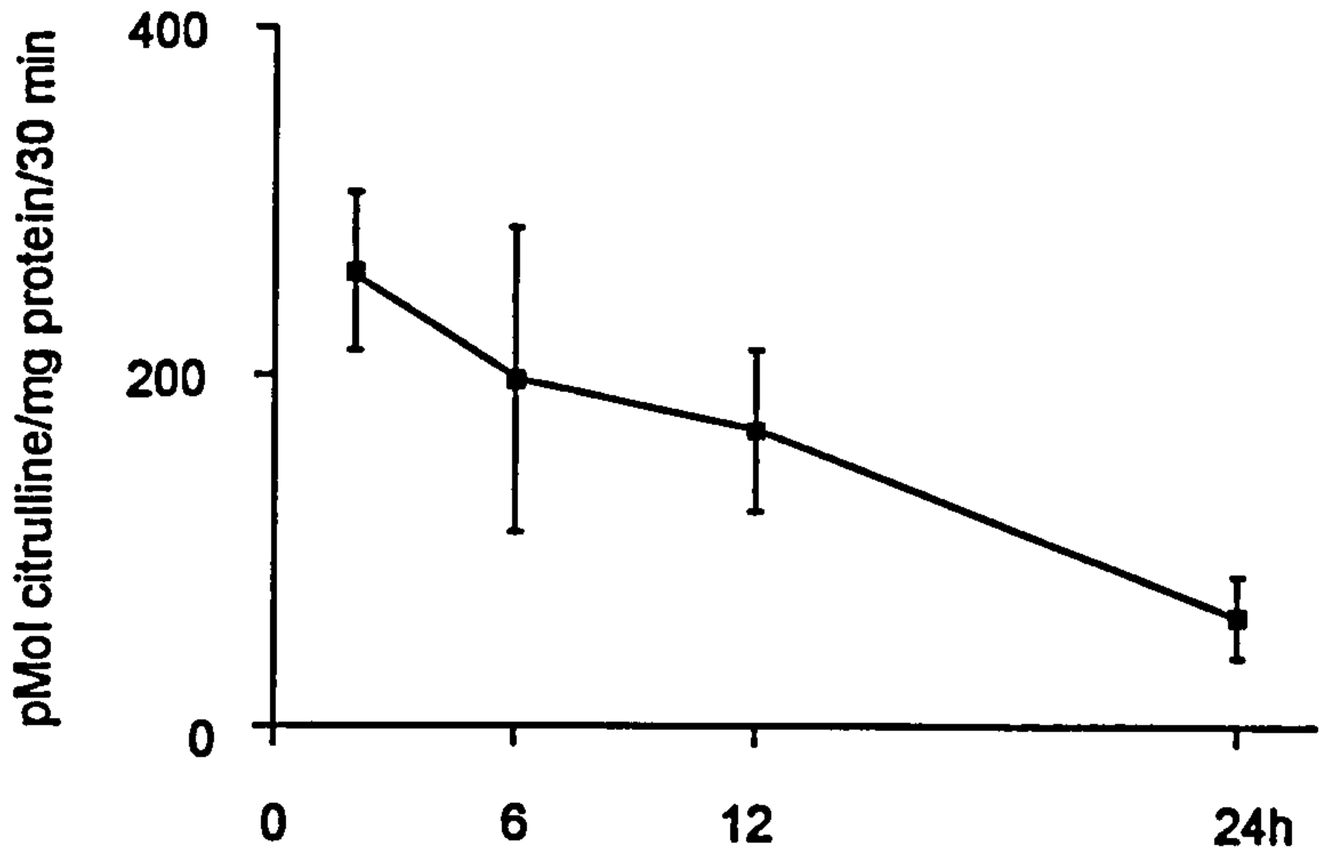

Figure 3.12 Time course of iNOS activity in inflammatory cells in the BSA-induced pleurisy *Rats were sensitised with BSA into the tail, then challenged with BSA in the pleural cavity 12 days later. Data is expressed as mean ± standard error of the mean (n=6 per time point).*

3.3.5 Arginase enzyme activity in inflammatory cell pellets

In the rat BSA-challenged pleurisy, arginase levels were detectable throughout the time course (Figure 3.13). Arginase activity at 2h was 1.179 ± 0.491 mU/mg protein/min, increasing to a peak at 12h (3.099 ± 0.554 mU/mg protein/min), before dropping at 24h to 0.698 ± 0.112 mU/mg protein/min.

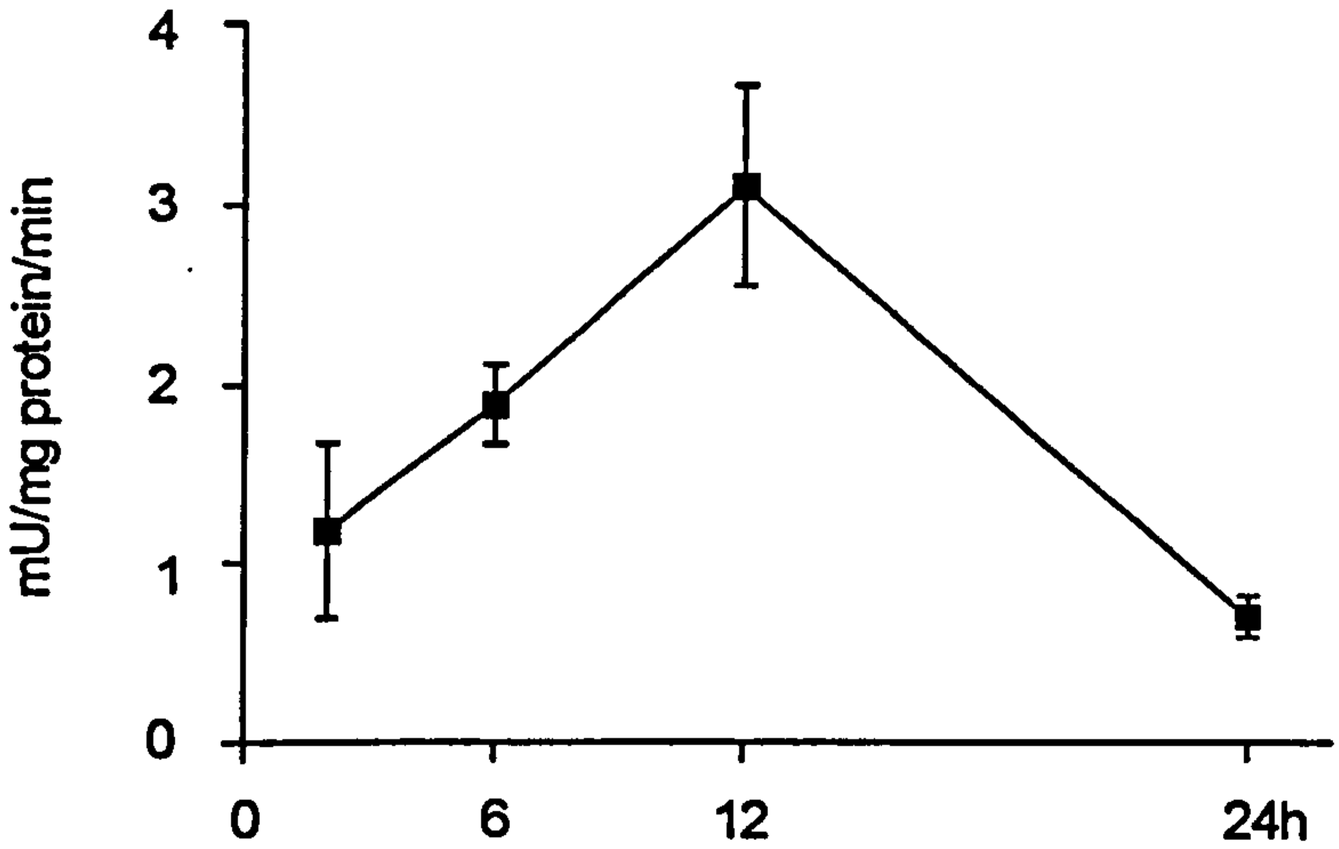

Figure 3.13 Time course of arginase activity in inflammatory cells in the BSA-induced pleurisy. *Rats were sensitised with BSA into the tail, then challenged with BSA in the pleural cavity 12 days later. Data is expressed as mean ± standard error of the mean (n=6 per time point).*

3.3.6 COX activity in inflammatory cell pellets

In this type III, immediate hypersensitivity reaction, COX activity was maximal at 24h (631 ± 146 ng PGE_2/mg protein/30min, Figure 3.14). COX activity prior to this point was 276 ± 65, 399 ± 120, and 500± 88 ng PGE_2/mg protein/30min at 2h, 6h and 12h, respectively.

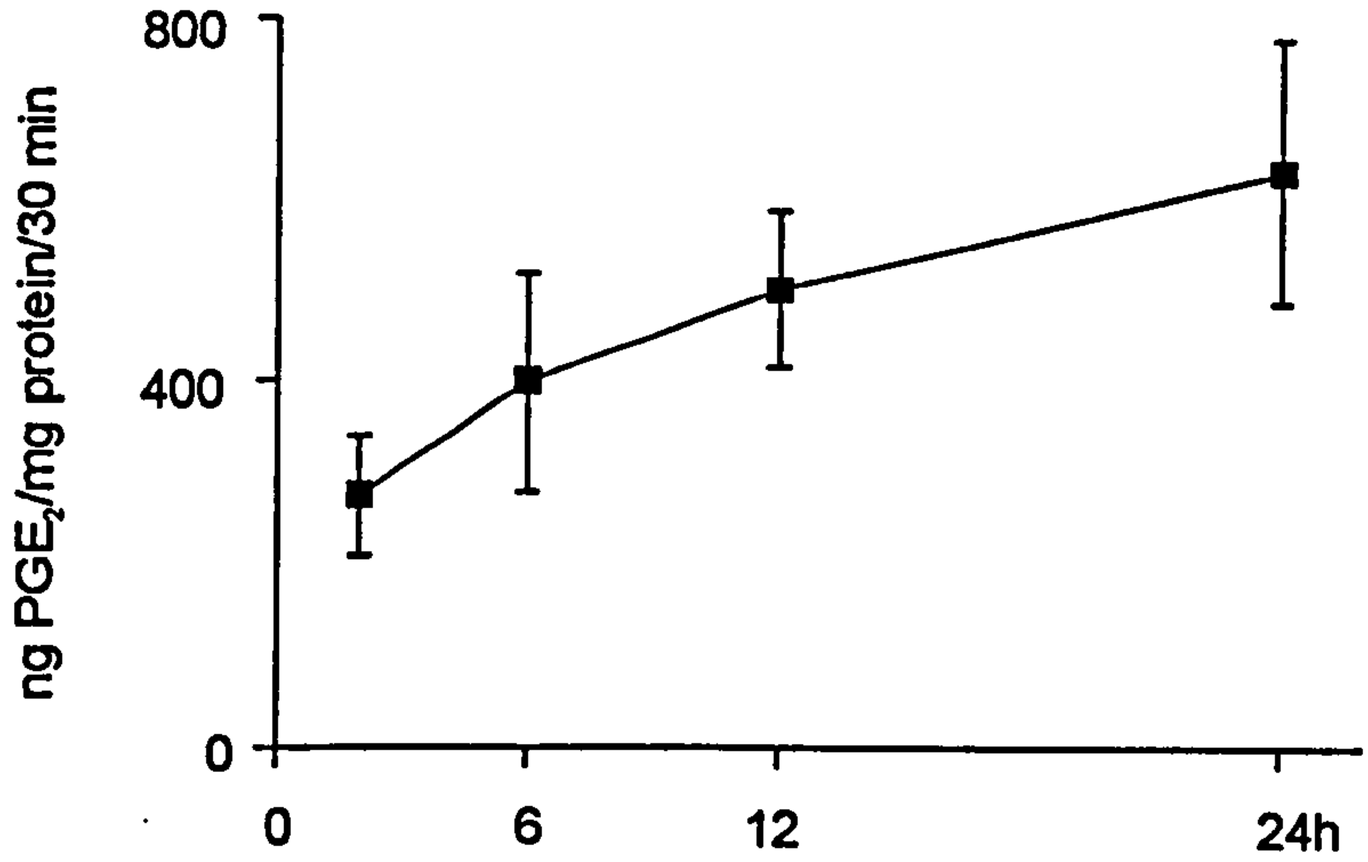

Figure 3.14 Time course of COX activity in inflammatory cells in the BSA-induced pleurisy
Rats were sensitised with BSA into the tail, then challenged with BSA in the pleural cavity 12 days later. Data is expressed as mean ± standard error of the mean (n=6 per time point).

3.4 Rat methylated BSA-induced pleurisy

3.4.1 Exudate volume and inflammatory cell counts

Challenge with methylated BSA in the pleural cavity of rats resulted in a cell mediated inflammatory reaction that caused influx of inflammatory cells and exudate into the pleural cavity, which peaked at 24h (Figure 3.15). At 2h, the pleural cavity of rats contained 0.5 ± 0.07ml of exudate and 4.8 ± 0.8 $x10^6$ inflammatory cells, both parameters increased at 6h and 12h and peaked at 24h with 3.5 ± 0.8ml of exudate and 59.1 ± 8.4 $x10^6$ inflammatory cells being removed from the pleural cavity. After 24h this cell mediated reaction waned with both parameters being reduced by 48h (0.6 ± 0.76ml and 43.3 ±10.1 $x10^6$ cells).

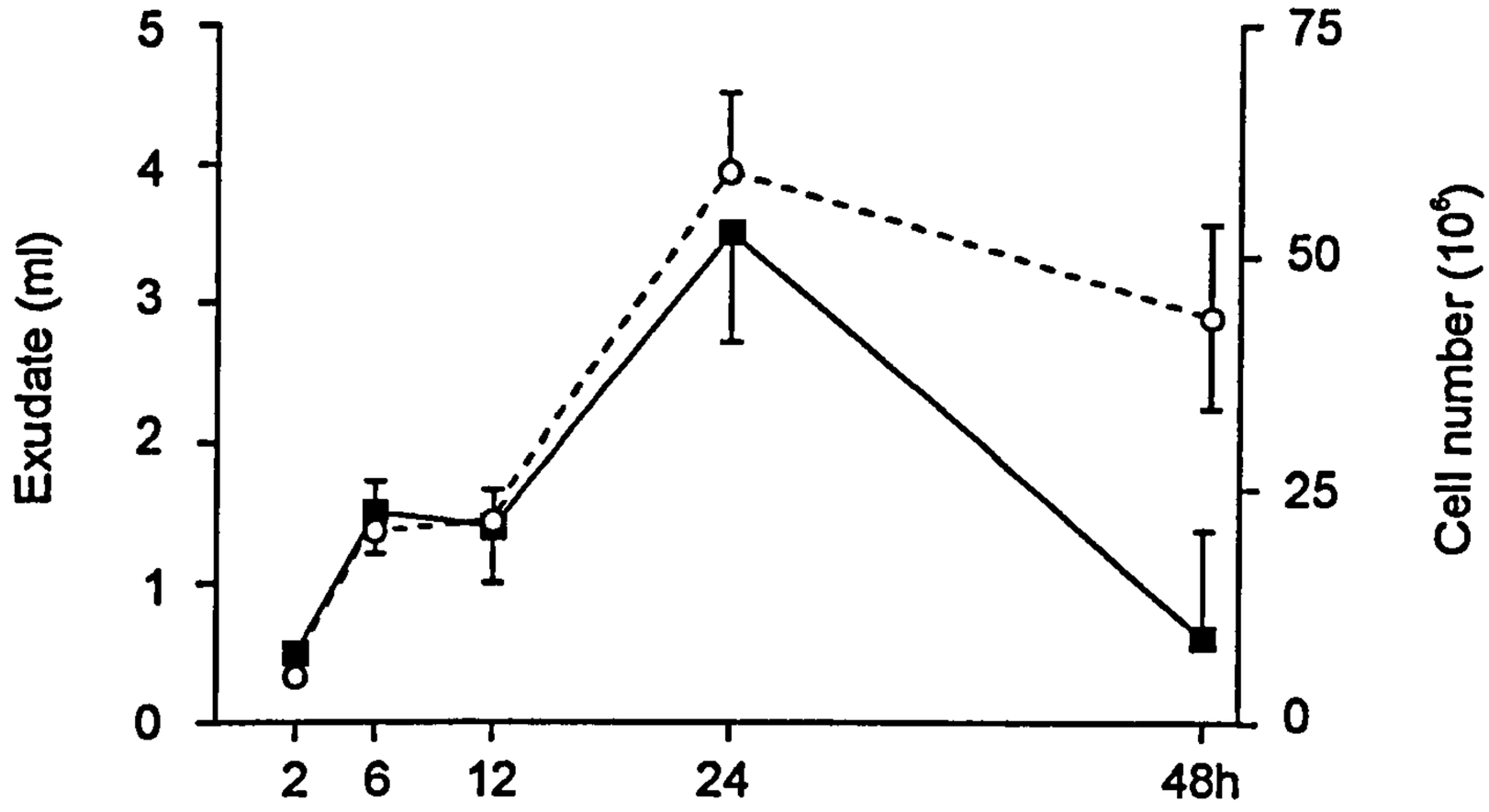

Figure 3.15 Time course of inflammation in the methylated BSA-induced pleurisy. *Exudate volume is represented by ■ and inflammatory cell influx by o in Wistar rats challenged with methylated BSA into the pleural cavity, 12 days after sensitisation with methylated BSA into the tail. Data is expressed as mean ± standard error of the mean (n=15 per time point).*

Differential counts of inflammatory cell smears stained with Harris' hematoxylin and eosin showed a PMN dominant reaction up to 12hrs, with MN cells being the predominant cell type at the peak of inflammation (from 24h onwards), Table 3.4.

	Time after intrapleural methylated BSA challenge (h)				
	2	6	12	24	48
PMNs	77%	71%	83%	46%	4%
MNs	23%	29%	17%	54%	96%

Table 3.4 Differential counts of inflammatory cell smears in the methylated BSA-induced pleurisy. *Rats were sensitised with methylated BSA into the tail, then challenged with methylated BSA in the pleural cavity 12 days later. Cell smears were stained with haematoxylin and eosin. n=4 per time point.*

3.4.2 iNOS protein expression in inflammatory cells

iNOS protein was expressed throughout the time course of rats challenged intrapleurally with methylated BSA (Figure 3.16). iNOS protein expression increased up to 12h, where it was maximal, then waned thereafter.

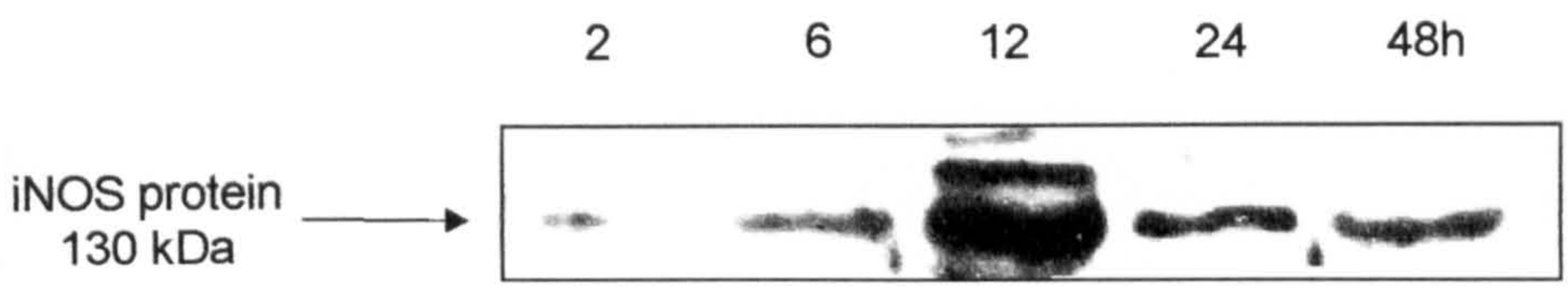

Figure 3.16 iNOS protein expression in the methylated BSA-induced pleurisy. *iNOS expression was determined by Western blotting of cells form inflammatory exudates from rats sensitised into the tail with methylated BSA and challenged 12 days later with methylated BSA intrapleurally. A typical blot*

3.4.3 Levels of nitrite in cell-free inflammatory exudates

Twelve hours after intrapleural challenge with BSA, nitrite levels in cell free exudates were maximal (19.7 ± 1.8μM, Figure 3.17), correlating with the peak in iNOS protein expression (Figure 3.16) and activity (Figure 3.18). At 2h, 6h, 24h and 48h nitrite levels were 0.4 ± 0.4, 4.8± 0.5, 1.3 ±0.2 and 0.1 ± 0.1μM, respectively.

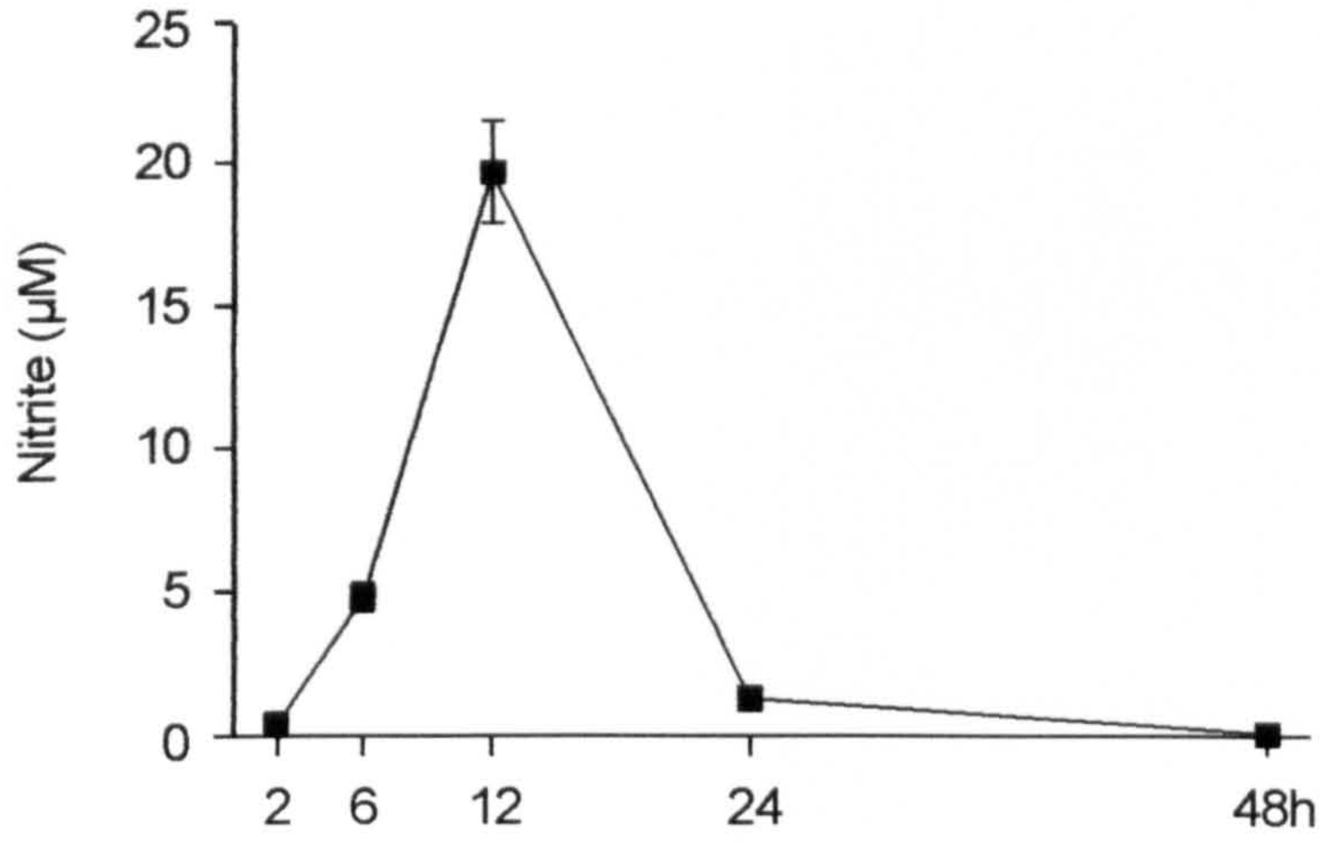

Figure 3.17 Time course of nitrite accumulation in the methylated BSA-induced pleurisy. *Rats were sensitised with methylated BSA into the tail, then challenged with methylated BSA in the pleural cavity 12 days later. Data is expressed as mean ± standard error of the mean (n=6 per time point).*

3.4.4 iNOS enzyme activity in inflammatory cell pellets

Twelve hours after intrapleural challenge with methylated BSA iNOS activity was maximal (1139 ± 63 pMol citrulline/mg protein/30 min, Figure 3.18). The 2h and 6h levels were 54 ± 26 and 119 ± 68 pMol citrulline/mg protein/30 min. After 12h, iNOS activity declined rapidly to baseline at 48h (10 ± 6 pMol citrulline/mg protein/30 min). cNOS activity was not detectable in this model at the time points measured.

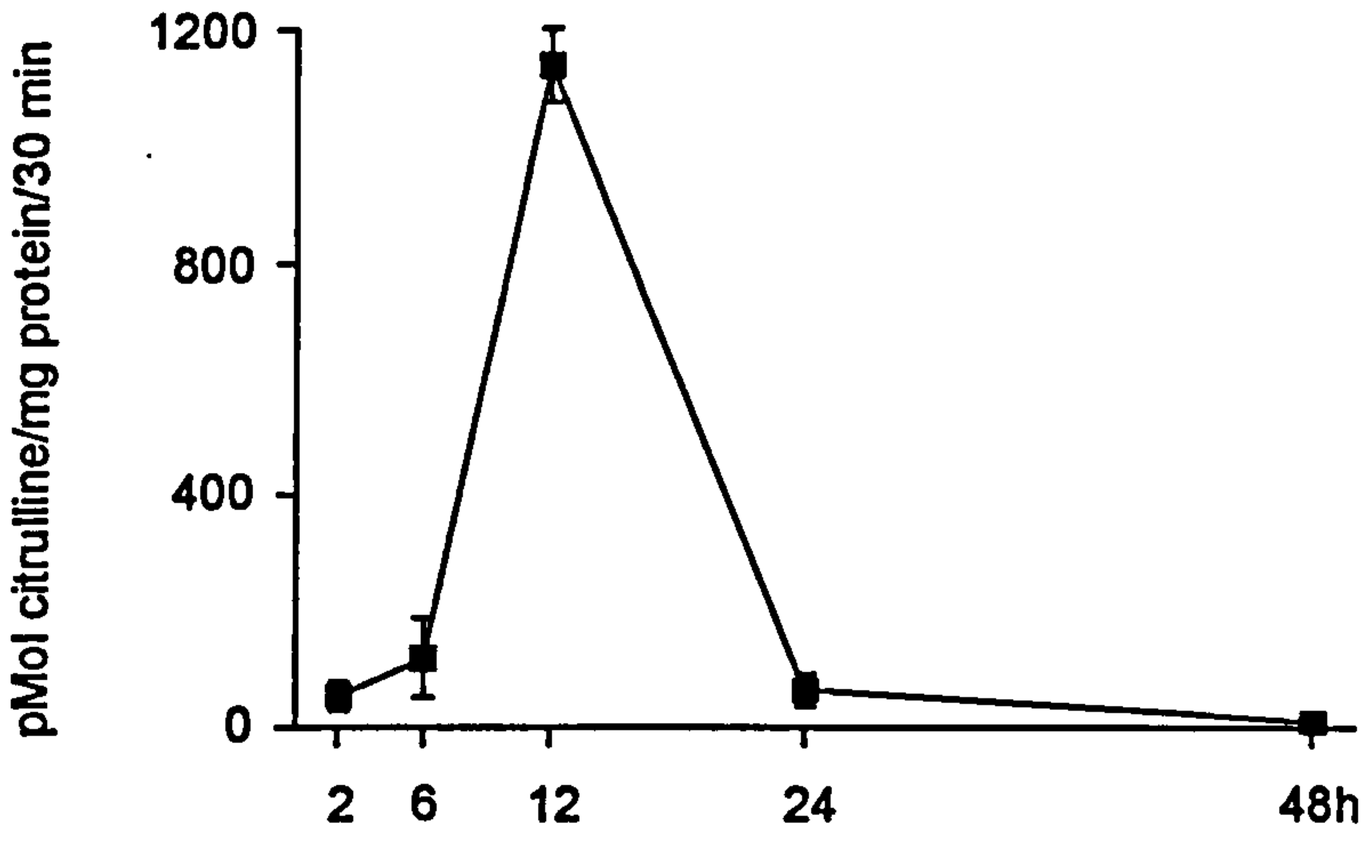

Figure 3.18 Time course of iNOS activity in the methylated BSA-induced pleurisy. *Rats were sensitised with methylated BSA into the tail, then challenged with methylated BSA in the pleural cavity 12 days later. Data is expressed as mean ± standard error of the mean (n=6 per time point).*

3.4.5 Arginase enzyme activity in inflammatory cell pellets

In the methylated BSA-challenged pleurisy, arginase levels were detectable throughout the time course (Figure 3.19). Arginase activity at 2h was 1.833 ±0.191 mU/mg protein/min, increasing at 6h, 12h and 24h to a peak at 48h (5.676 ± 0.651 mU/mg protein/min).

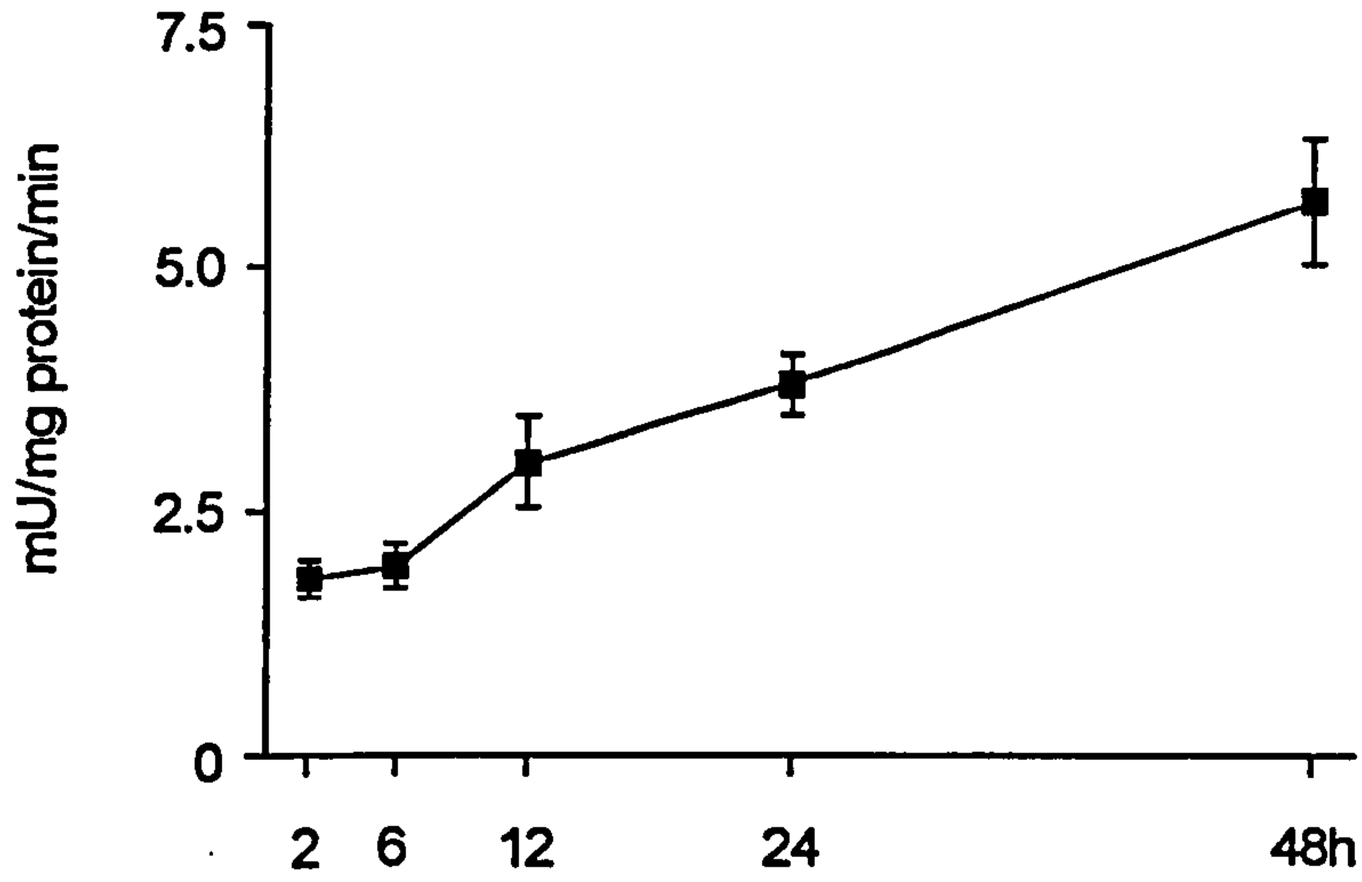

Figure 3.19 Time course of arginase activity in the methylated BSA-induced pleurisy. *Rats were sensitised with methylated BSA into the tail, then challenged with methylated BSA in the pleural cavity 12 days later. Data is expressed as mean ± standard error of the mean (n=6 per time point).*

3.4.6 COX activity in inflammatory cell pellets

In this type IV, cell mediated delayed hypersensitivity reaction, COX activity increased from 2h (16 ± 4) to a maximum at 48h (53 ± 8 ng PGE_2/mg protein/30min, Figure 3.20)..

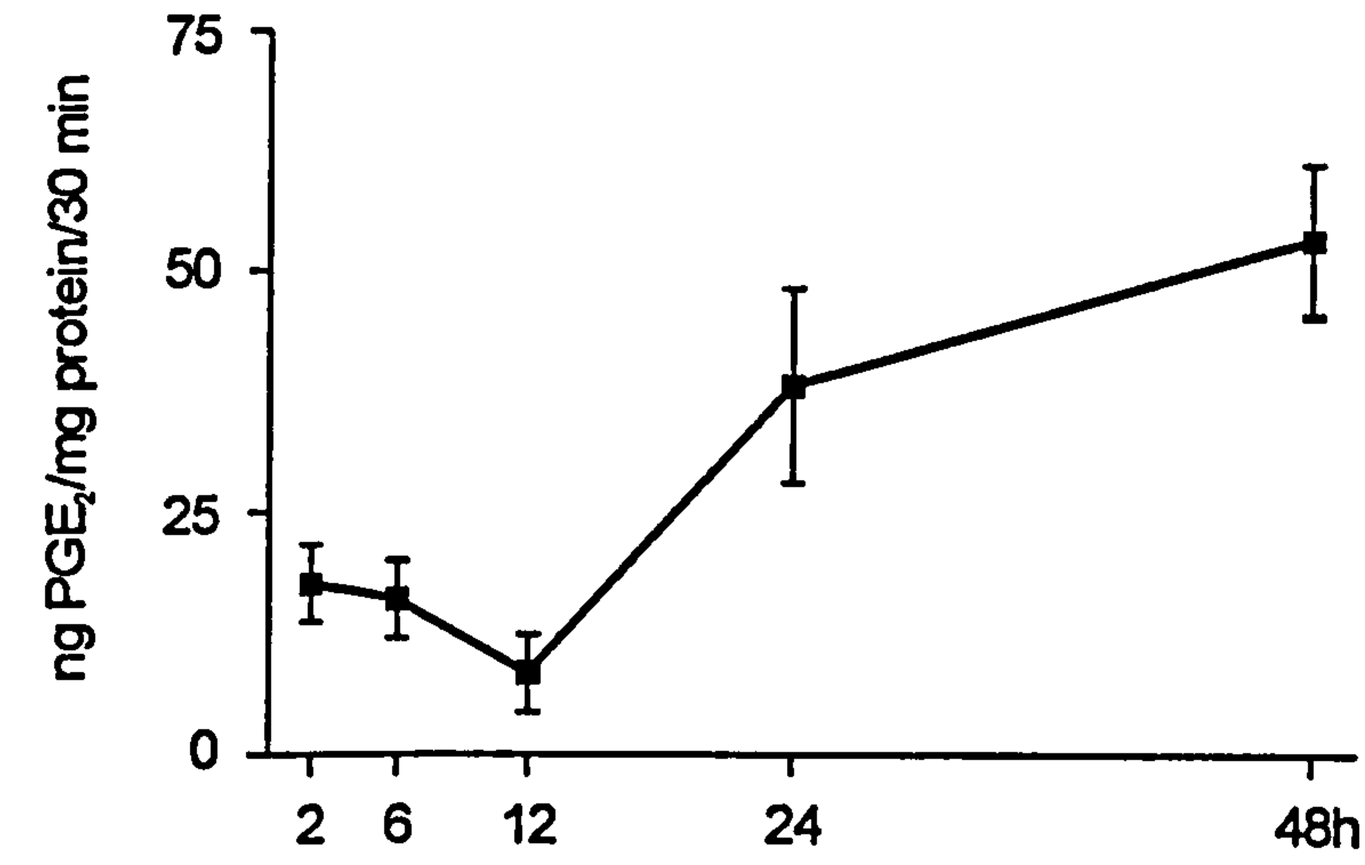

Figure 3.20 Time course of COX activity in the methylated BSA-induced pleurisy. *Rats were sensitised with methylated BSA into the tail, then challenged with methylated BSA in the pleural cavity 12 days later. Data is expressed as mean ± standard error of the mean (n=6 per time point).*

3.5 Murine chronic granulomatous tissue air pouch

3.5.1 Granulomatous tissue basic histology, dry weight, carmine content, and vascularity

The resulting inflammation after *M. tb* and croton oil injection has three phases acute, chronic and a resolving stage. Granuloma dry weight was 48.9 ± 4.2 mg at day 3 (Figure 3.21a), which increased at day 5 (69.0 ± 3.5 mg) and peaked at day 7 (82.8 ± 3.0 mg). After day 7 granuloma dry weight deceased to 38.4 ± 1.8 mg at 28 days.

The vascular component of the granulomatous tissue, as measured by carmine content, was 438 ± 27 µg at day 3 (Figure 3.21a), this rose to a peak at day 5 (688 ± 57 µg), then decreased steadily over the ensuing 23 days, being 463 ± 41 µg at day 28.

Vascular index was measured as a parameter of angiogenesis and expressed as µg carmine per mg granuloma dry weight (Figure 3.21a). The vascular index was 6.42 ± 0.26 µg carmine/mg tissue at day 3, this peaked at day 5 (9.76 ± 0.67 µg carmine/mg tissue), then deceased to a plateau over the rest of the time course, being 7.51 ± 0.73 µg carmine/mg tissue at 28 days.

Histology examination of the air pouch demonstrated PMNs were the dominant cell type at day 3, with smaller numbers of macrophages and lymphocytes and the occasional fibroblast with capillaries surrounded by extracellular matrix. By day 7 the granuloma was highly vascularised with numerous PMNs and macrophages present in the loose connective tissue of the dermis and the occasional intact and degranulated mast cell was observed (Figure 3.21b). A region of active fibrogenesis was observed above the skeletal muscle and below the skin with a high collagen content (red coloration, Figure 3.21c). By 28 days the granulomatous tissue was highly organised consisting of fibroblasts and the occasional inflammatory cell.

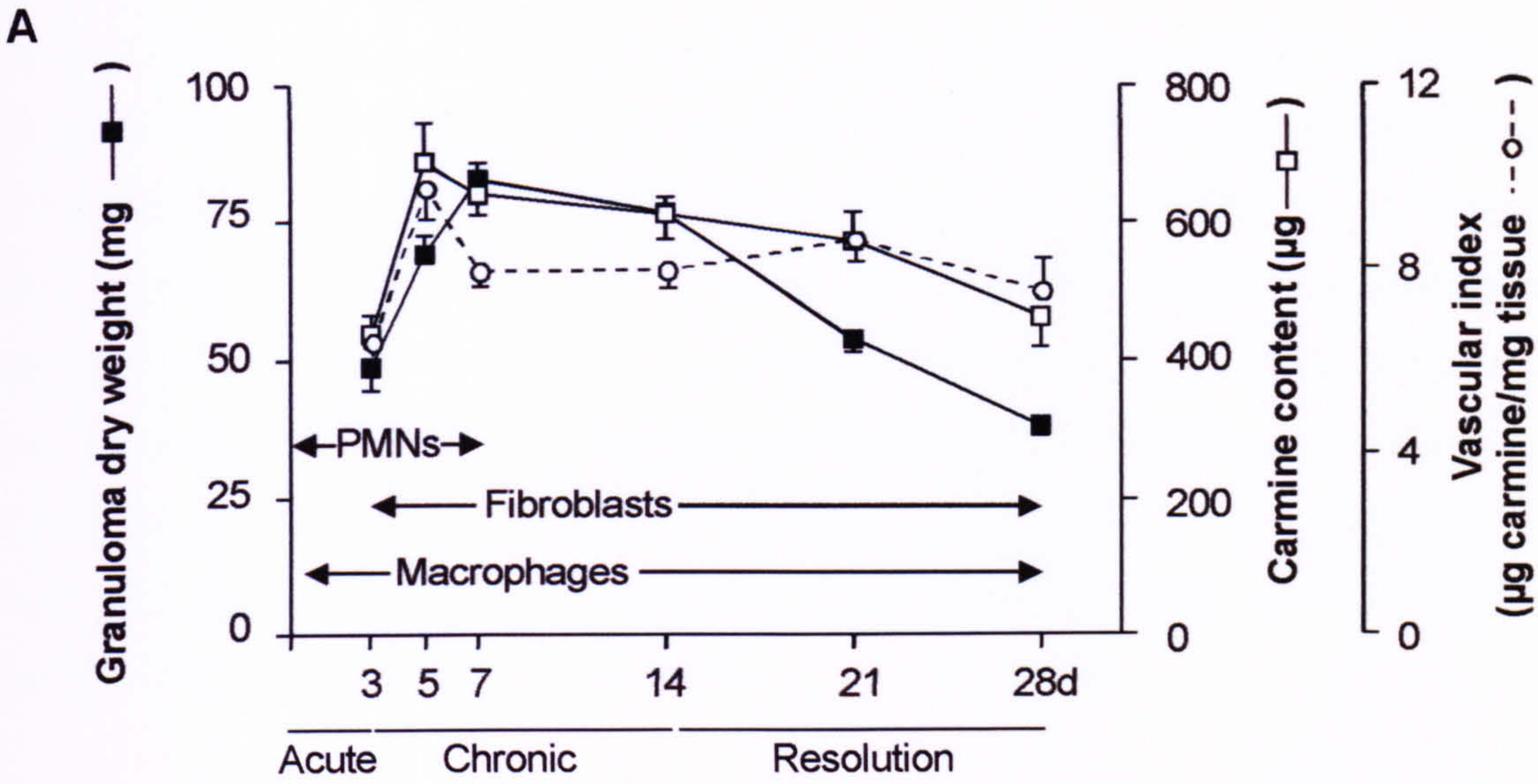

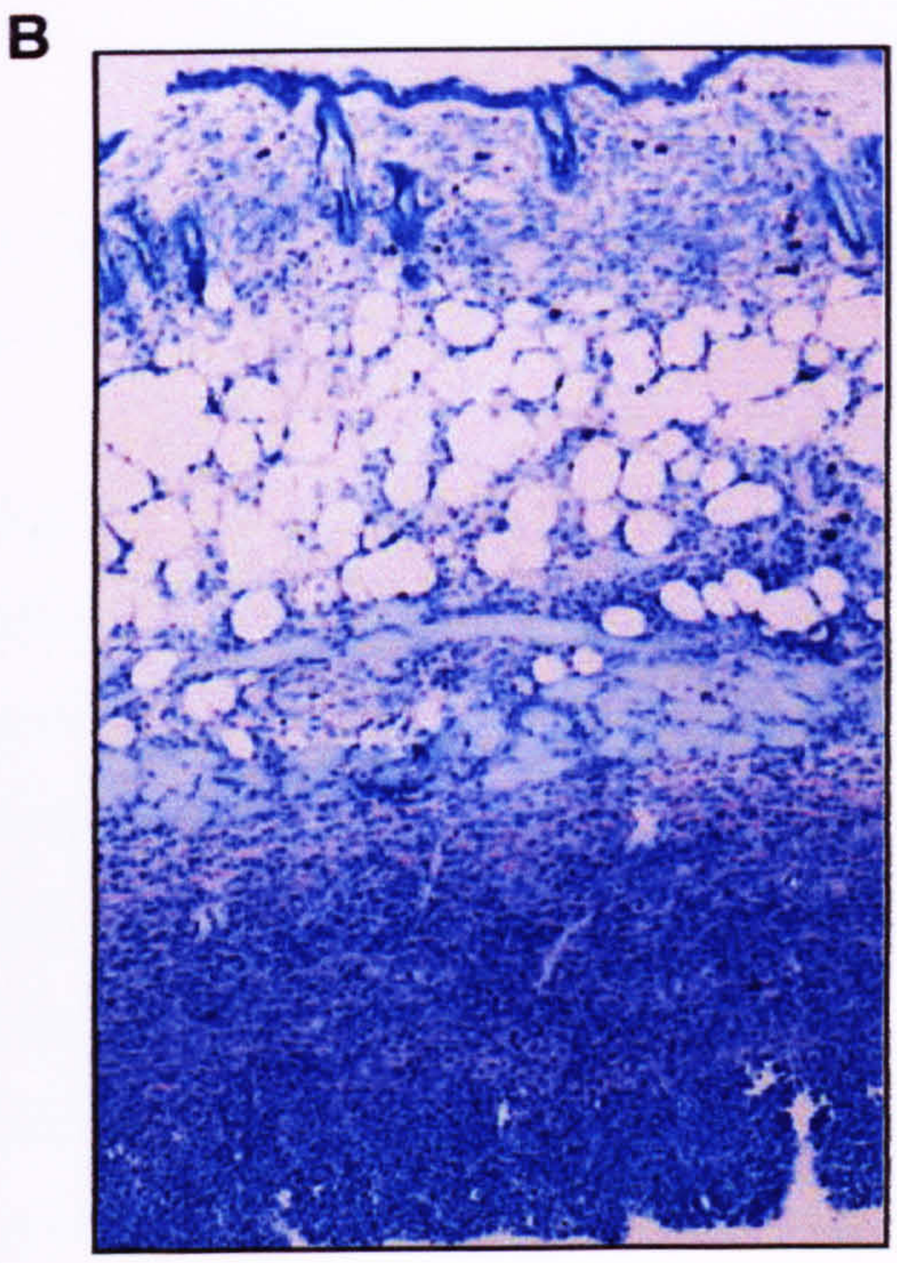

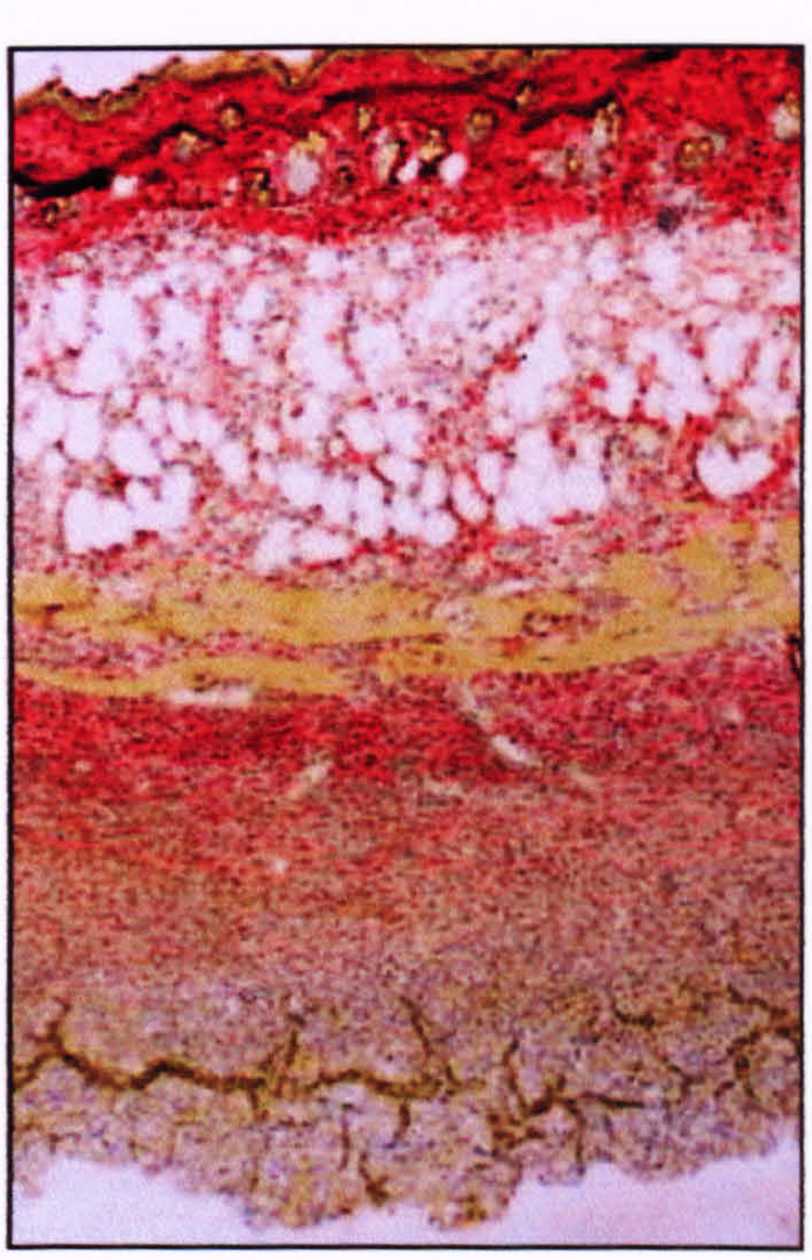

Figure 3.21 Inflammation, angiogenesis and histological examination of the murine chronic granulomatous tissue air pouch. *Panel A is a time course of grauloma dry weight (■), carmine content (□), vascular index (○) and cell type influx into the mouse croton oil-induced chronic granulomatous tissue air pouch. Data is expressed as mean ± standard error of the mean (n=8 per time point). Panel B shows a 7 day air pouch stained with toluidine blue and Panel C Van Gieson. Panel B and C magnification x100.*

3.5.2 iNOS protein expression

iNOS protein expression was detected in homogenates of granuloma tissue throughout the time course of this chronic inflammatory model as determined by Western blot analysis (Figure 3.22). During the early stages of the air pouch (up to 3 days) it is extremely difficult to separate the air pouch from the overlying dermis and the material obtained was not sufficient for Western blot analysis. As can be seen from Figure 3.22, iNOS protein expression was most intense at day 7, a time where macrophage influx into the air pouch lining was maximal. This was reduced at subsequent time points (14, 21 and 28 days), although iNOS protein expression was still detectable.

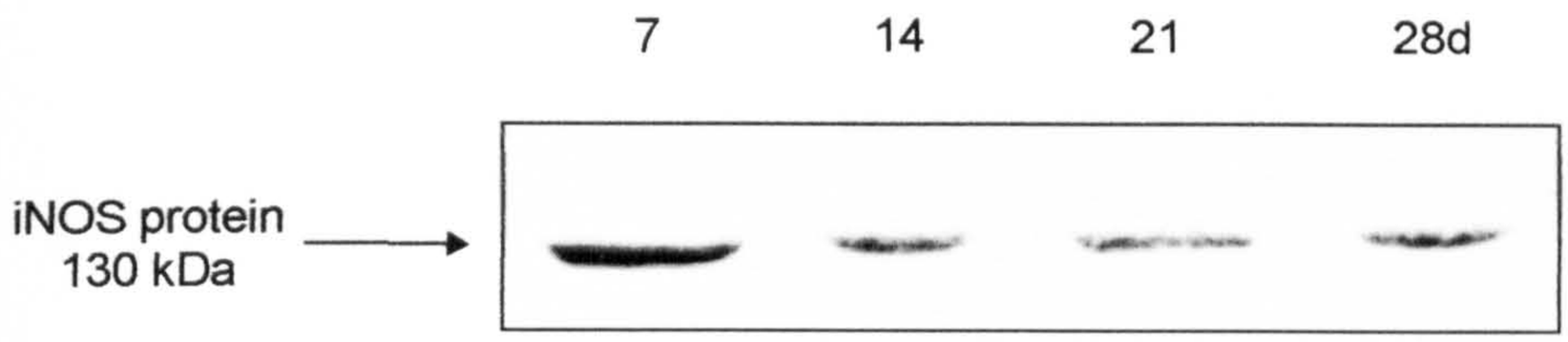

Figure 3.22 iNOS protein expression of the murine chronic granulomatous tissue air pouch. *As determined by Western blotting at days 7, 14, 21 and 28.*

3.5.3 Levels of nitrite in cell-free inflammatory exudates

Nitrite accumulation in cell-free exudate extracted from the air pouch cavity was measured at 6, 12 and 24h, 3, 5 and 7days (Figure 3.23). It was impossible to measure nitrite levels at 14, 21 and 28 days due to limitations in extracting exudate from the air pouch at these time points. Nitrite production first became detectable at 12h (0.4 ± 0.3 μM), however most of the samples investigated at this time point were below the level of detection of the assay. Levels of nitrite rose consistently from 24h (5.0 ± 3.7 μM) reaching a peak at 7 days of 80.4 ± 6.6 μM.

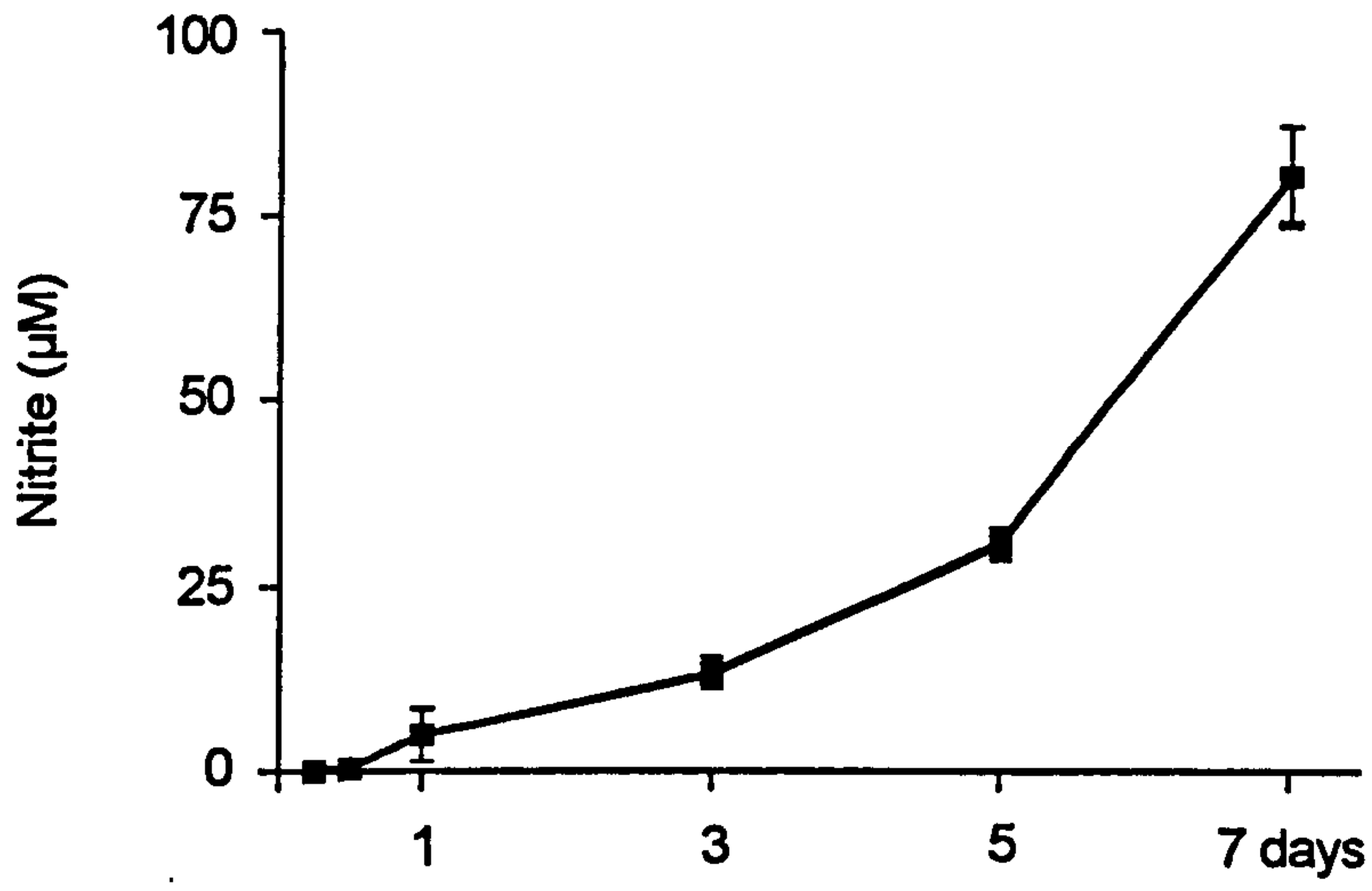

Figure 3.23 Time course of nitrite accumulation in exudates taken from the murine chronic granulomatous tissue air pouch. *Data is expressed as mean ± standard error of the mean (n=5-8 per time point).*

3.5.4 NOS enzyme activity

NOS enzyme activity was measured in homogenates of granulomatous tissue (Figure 3.24), iNOS activity in skin and air pouches without the injection of FCA/croton oil mixture below the detection limit of the assay. Levels of iNOS activity were low during the acute phase of this chronic inflammatory model, being 173 ± 89 pMol citrulline/mg protein/30 min at 3 days. At day 5 iNOS activity increased to 260 ± 60 pMol citrulline/mg protein/30 min and peaked at day 7 (805 ± 268 pMol citrulline/mg protein/30 min), after which activity returned to basal levels (80 ± 23 pMol citrulline/mg protein/30 min at 28 days).

cNOS activity of skin and air pouches without the injection of FCA/croton oil mixture was 52 ± 17 pMol citrulline/mg protein/30 min and probably reflected the vascular component contained within the overlying skin rather than the very thin air pouch membrane. cNOS activity (Figure 3.24) was detectable at 6 and 12h (72 ± 13 and 47 ± 18 pMol citrulline/mg protein/30 min, respectively), rising to a peak at 24h (153 ± 34 pMol citrulline/mg protein/30 min). cNOS activity was reduced at 3 days (38 ± 14 pMol citrulline/mg protein/30 min), then elevated at day 5 (146 ± 34 pMol citrulline/mg protein/30 min), reaching a second peak at

day 7 (175 ± 56 pMol citrulline/mg protein/30 min), after which levels returned to baseline, being 29 ± 8 pMol citrulline/mg protein/30 min at 28 days.

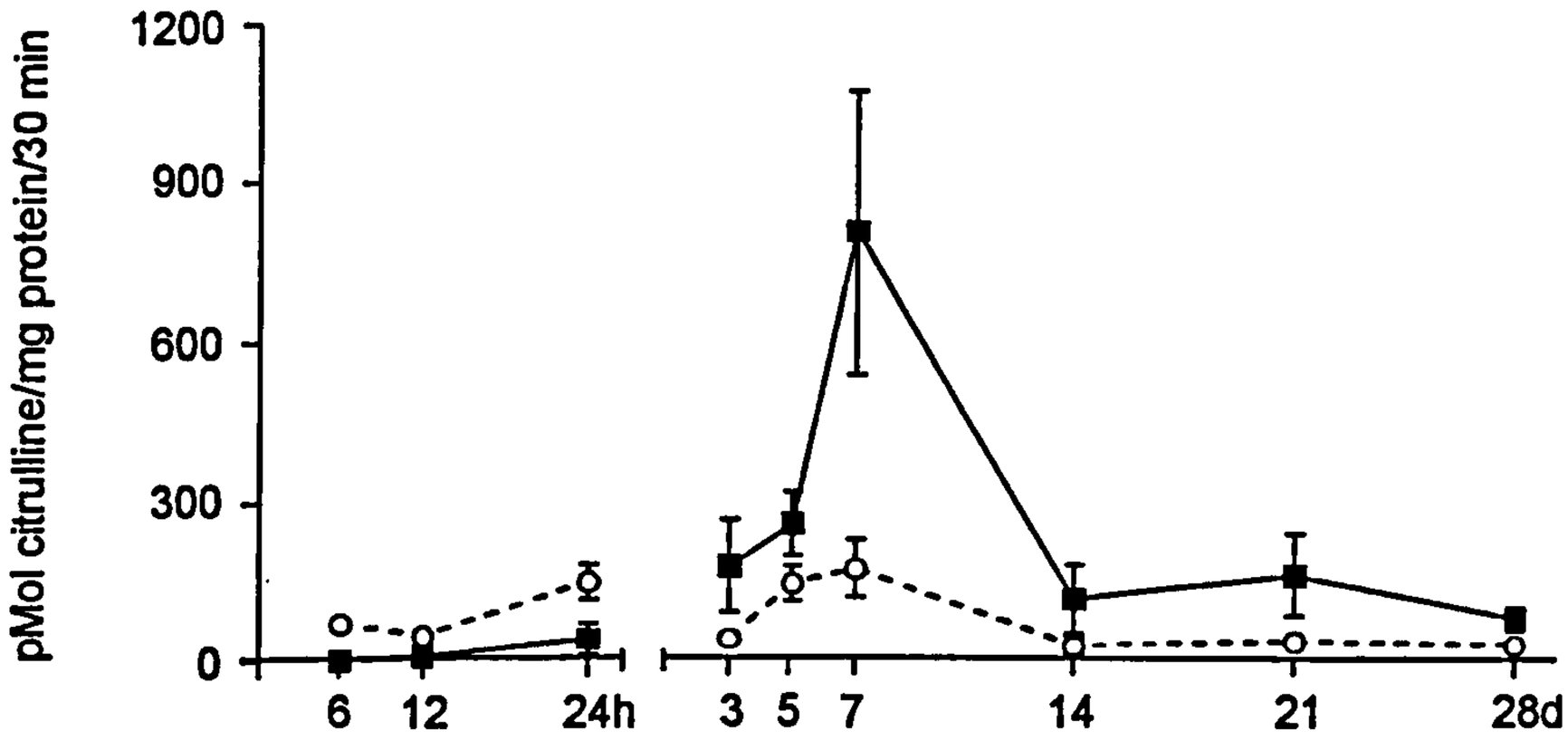

Figure 3.24 Time course of iNOS and cNOS activity in tissue homogenates taken from the mouse croton oil-induced chronic granulomatous tissue air pouch. *iNOS activity is represented by ■ and cNOS activity by o. Data is expressed as mean ± standard error of the mean (n=8 per time point).*

3.5.5 Temporal and spatial expression of iNOS protein

Up to 14 days iNOS protein staining was selectively associated with monocyte/macrophages in blood vessels and in loose connective tissue of the subdermis. Occasionally positive stained monocytes were observed in the lumen of vessels in this area. As the granuloma developed iNOS positively stained macrophages were associated with the fibrotic region of tissue. Endothelial cells of blood vessels in the subdermal region were lightly stained , with arterioles staining most intensely. Neutrophils present in the lower border of the granulomatous tissue (nearest the cavity) were also lightly stained for iNOS (Figure 3.25).

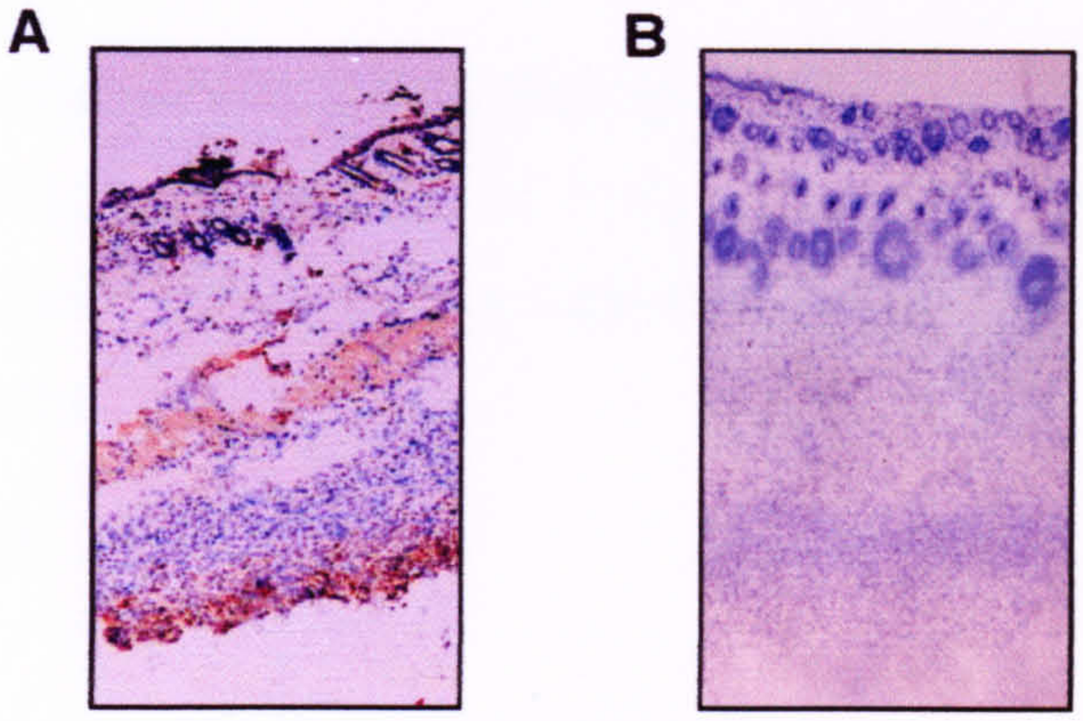

Figure 3.25 Immunohistochemical analysis of iNOS protein in a 7 day air pouch. *Panel A is a 7 day granulomatous tissue air pouch stained with a specific rabbit anti-murine iNOS antibody and in Panel B iNOS antibody was replaced with normal rabbit IgG and acted as a negative control.*

3.5.6 Arginase enzyme activity

Arginase activity was measured in homogenates of chronic granulomatous tissue (Figure 3.26) and was detected at 6, 12, 24h and 3 days (26.4 ± 9.8 mU/mg protein/min). Arginase activity then peaked at day 5 (97.2 ± 9.7 mU/mg protein/min) then waned thereafter, being 41.3 ± 6.4 mU/mg protein/min at 28 days.

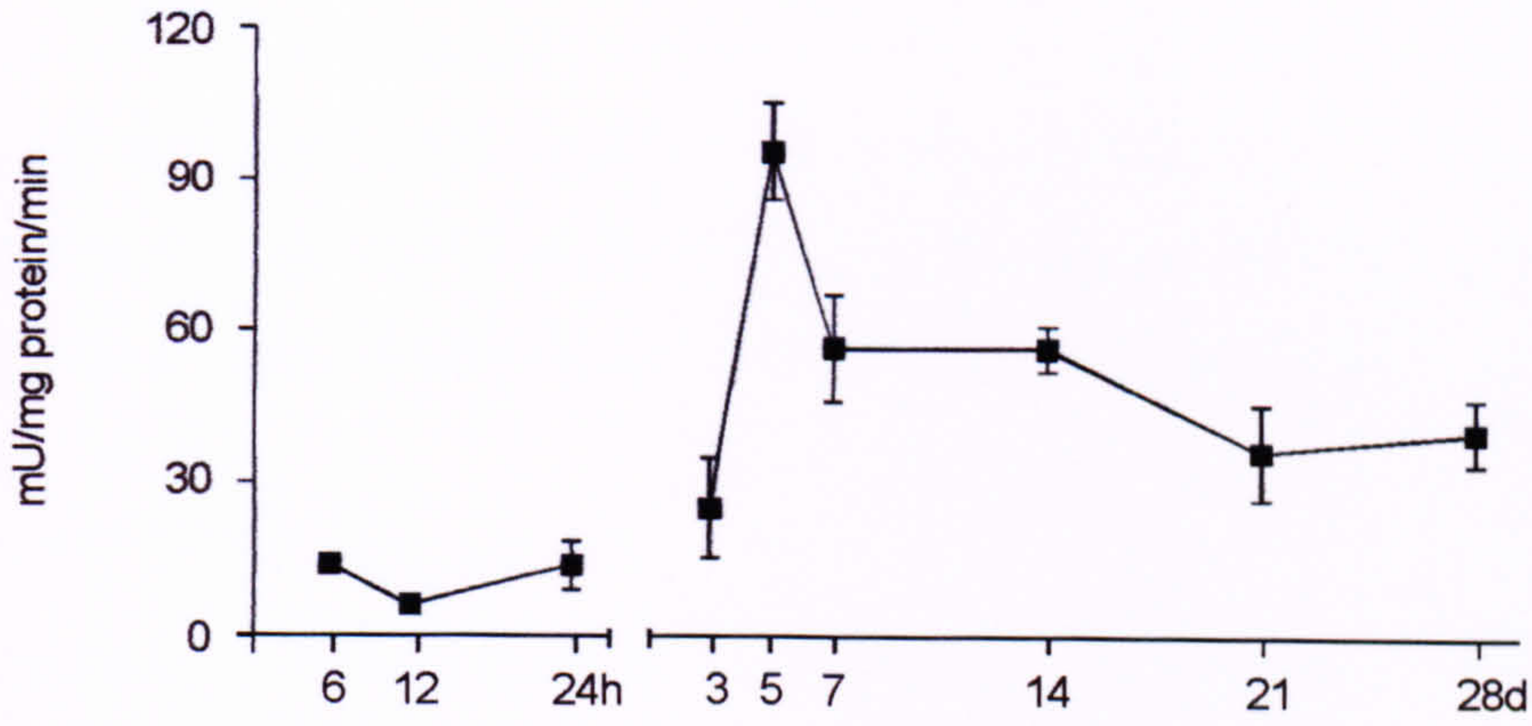

Figure 3.26 Time course of arginase activity in tissue homogenates taken from the mouse croton oil-induced chronic granulomatous tissue air pouch*. Data is expressed as mean ± standard error of the mean (n=8 per time point).*

3.5.7 COX activity

Cyclooxygenase activity was detected throughout the time course of this chronic model (Figure 3.27), being highest at 3 and 5 days (66 ±5 and 76 ± 8 ng PGE_2/mg protein/30min, respectively), then diminishing thereafter to 34 ± 7 ng PGE_2/mg protein/30min at 28 days.

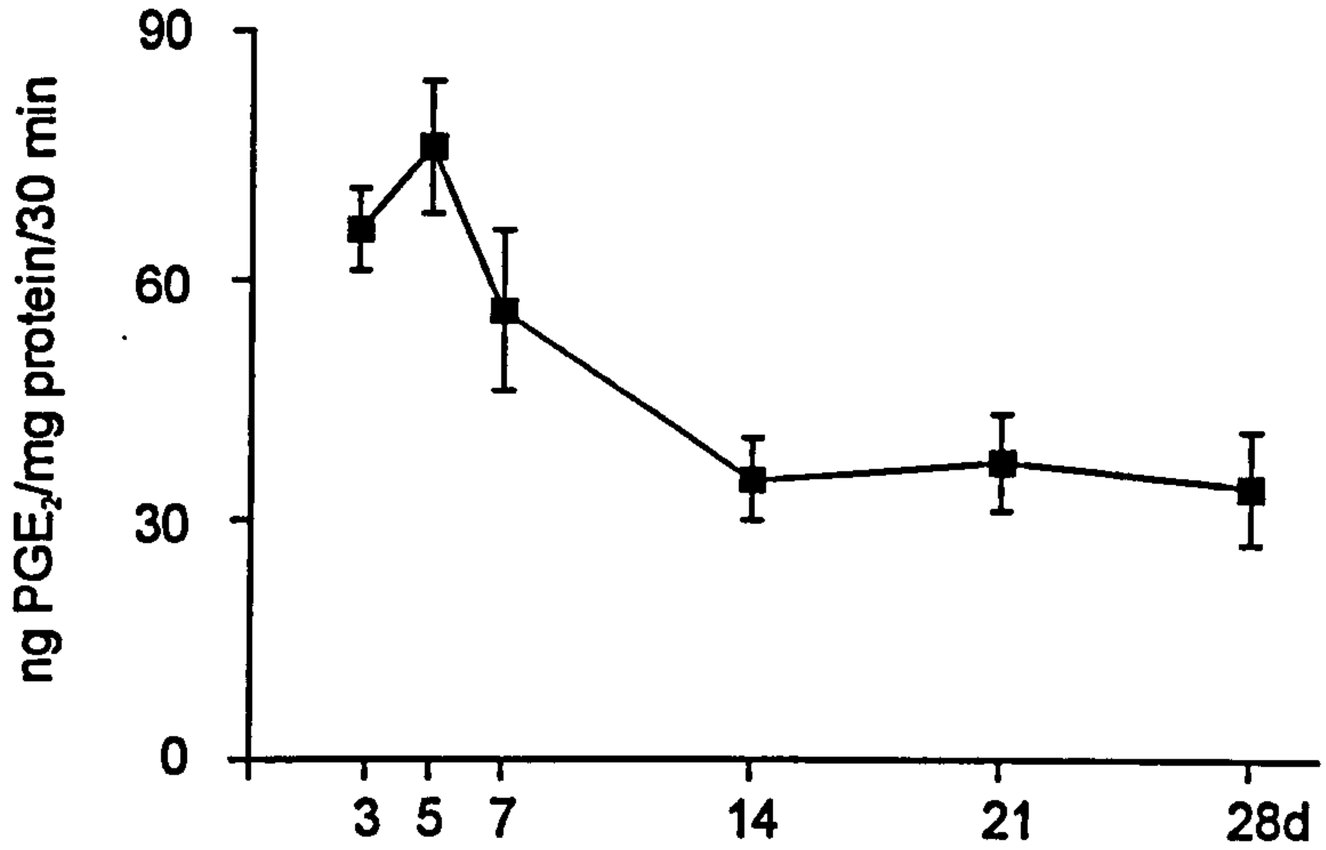

Figure 3.27 Time course of cyclooxygenase activity in tissue homogenates taken from the mouse croton oil-induced chronic granulomatous tissue air pouch. *Data is expressed as mean ± standard error of the mean (n=6 per time point).*

3.6 Summary of findings

(1) In the carrageenin pleurisy model, inflammatory exudate and cell numbers peaked at 24h and waned by 48h. iNOS protein expression was detectable in this inflammatory model between 2 and 48h, with the major peak being at 6h. This correlated with maximal levels of iNOS activity. Two peaks in nitrite were observed, the first at 0.5h and the second at 6h. Immunocytochemical analysis of cell smears revealed that both MNs and PMNs stained positively for iNOS protein, with the most intense staining associated with MNs at 6 and 48h. Arginase activity in this model was very low, however a peak in activity was measurable at 6h. In contrast, PGE_2 was maximal at 2h with predominant levels of 6 keto $PGF_{1\alpha}$ being detected at 6h.

(2) In the BSA-induced immediate hypersensitivity reaction, iNOS protein expression, iNOS activity, nitrite, cell numbers and exudate volume all peaked at the early time points and declined to baseline by 48h. In contrast, arginase and COX activity peaked during the resolution stages of this model.

(3) In the methylated BSA-induced DTH reaction, inflammatory parameters were maximal at 24h with exudate volume being negligible by 48h, however there was still a considerable number of inflammatory cells in the pleural washouts. iNOS activity, iNOS protein expression and nitrite were all maximal at 12h. Arginase and COX activity were maximal during the resolution stage of inflammation.

(4) In the murine chronic granulomatous tissue air pouch, iNOS protein expression was maximal at 7days, but was also detectable at the other time points measured. iNOS activity, nitrite, arginase activity and COX activity were also maximal between 5 and 7 days. All these different enzymic pathways peaked at a time where granuloma dry weight was maximal. Interestingly, cNOS activity peaked at 24h this was prior to the peak in vascularity. The majority of

the staining for iNOS in the granuloma was associated with influxing inflammatory cells.

CHAPTER 4

4.1 Introduction

In Chapter 3, the expression of iNOS protein and NOS enzyme activity were demonstrated in immune and non-immune models of acute inflammation and in a model of chronic inflammation. These parameters were mapped in conjunction wth the expression of COX and arginase activity. In this chapter, the effects of NO inhibition using a number of NOS inhibitors was investigated in a non-immune model of acute inflammation, the carrageenin-induced pleurisy.

Non L-arginine analogue based NOS inhibitors, including aminoguanidine (Griffiths *et al.*, 1993), S(2-aminoethyl)-isothiourea (AE-ITU; Garvey *et al.*, 1994; Southan *et al.*, 1995) and N-(3-(aminomethyl)-benzyl) acetamide (1400W; Garvey *et al.*, 1997) will be used in the carrageenin-induced pleurisy model to inhibit NO production from iNOS. These compounds are reported to have a greater selectivity and higher potency for iNOS than ecNOS *in vitro* and *in vivo* compared to most L-arginine analogues. Therefore, these more selective iNOS inhibitors will be used and compared to a standard L-arginine analogue, N^G-monomethyl-L-arginine (L-NMMA), in the carrageenin-induced pleurisy. Previously published studies have demonstrated an anti-inflammatory effect of NOS inhibitors when administered away from the inflammatory site in models of acute inflammation (Ialenti *et al.*, 1992; Tracey *et al.*, 1995; Salvemini *et al.*, 1996), but in some cases these anti-inflammatory actions were reversed by vasodilators (Najafipour *et al.*, 1993; Ridger *et al.*, 1997). Therefore, one possible mechanism of action of these systemically administered NOS inhibitors may be to inhibit ecNOS resulting in vasoconstriction followed by a reduction in blood delivery to the inflamed site. This sequence of events may ultimately lead to reduced cellular diapedesis and exudation and thus be interpreted as anti-inflammatory. In this present chapter a comparison was made between the administration of both selective and non-selective inhibitors into and away from the inflammatory site. The effect of NOS inhibition was also assessed on possible interactions with the COX, arginase and HSP in the carrageenin-induced acute inflammation.

4.2 NOS inhibition in the carrageenin-induced pleurisy.

4.2.1 Effect of intrapleural injection of NOS inhibitors at 1h.

The initial peak of nitrite in inflammatory exudate was detectable at 1h (Section 3.2.4), this would suggest that the principle source of NO at this time was from the post capillary endothelial cells lining the pleural cavity and not from an inducible source. Initially, the contribution of NO to the developing inflammatory response was determined by administration of NOS inhibitors directly into the pleural cavity immediately prior to carrageenin injection.

AE-ITU at 3 and 10mg/kg significantly increased exudate volume (0.25 ± 0.02ml, 0.24 ± 0.02ml, respectively) and inflammatory cell influx (5.4 ± 0.5 x10^6, 5.4 ± 0.7 x10^6 cells, respectively) when compared to untreated controls (0.13 ± 0.02ml, 2.9 ± 0.5 x10^6 for exudate and cells respectively; Figure 4.1A, B). 1400W at 10mg/kg also significantly elevated exudate volume (0.23 ± 0.04ml) compared to saline controls (0.07 ± 0.03ml) but was without effect on inflammatory cell numbers (Figure 4.1A,B). Figure 4.1C demonstrates that both AE-ITU and 1400W reduced nitrite levels significantly at 10mg/kg (11.3 ± 1.1, 13.3 ± 0.8µM, respectively) when compared to control values (16.6 ± 1.1, 20.6 ± 1.4µM, respectively). Given their lack of specificity, it is likely that AE-ITU and 1400W also inhibited ecNOS at the dosing levels used. Finally, L-NIO (10mg/kg) increased exudate volume (0.34 ± 0.05ml, compared to controls 0.10 ± 0.03ml) whereas inflammatory cell numbers were unchanged (Figure 4.1A, B). At this time point the ecNOS inhibitor L-NIO (1, 10mg/kg) was more potent than the two iNOS inhibitors at reducing nitrite levels at 1h (13.4 ± 0.8, 11.22 ± 0.6µM, respectively) compared to saline treated animals (16.1 ± 0.6µM; Figure 4.1 C).

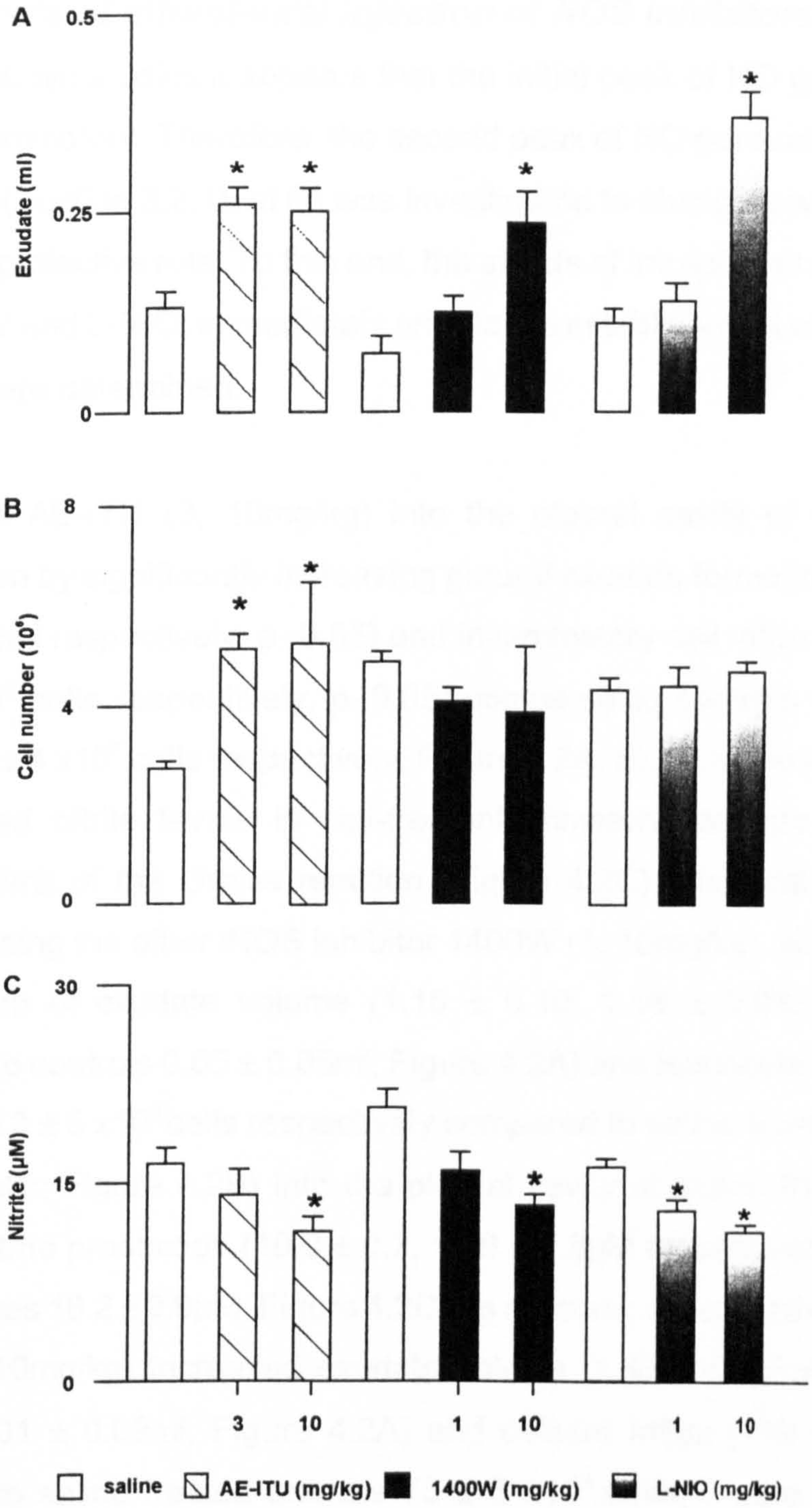

Figure 4.1 Effects of NOS inhibitors injected locally on a rat carrageenin-induced pleurisy at 1h. *AE-ITU, 1400W or L-NIO were injected directly into the pleural cavity of rats immediately before carrageenin injection. Thereafter, their effects on (A) exudate volume, (B) cell number and (C) nitrite in pleural exudates was determined 1h after carrageenin injection. Data is expressed as mean ± standard error of the mean (n=6-8 per group) from separate experiments for each NOS inhibitor used. * $p \leq 0.05$ in comparison to saline controls.*

4.2.2 Effects of intrapleural injection of NOS inhibitors at 6h.

From the above studies it appears that the initial peak of NO generation at 1h is anti-inflammatory. Therefore, the second peak of NO generation, apparently from iNOS (Section 3.2.4), at 6h was investigated to elucidate whether this had a similarly protective role. To this end, the effects of intrapleural injection of AE-ITU,1400W and L-NIO, immediately prior to the establishment of a carrageenin pleurisy, were determined.

Injection of AE-ITU (3, 10mg/kg) into the pleural cavity of rats worsened inflammation by significantly increasing pleural exudate formation (1.47 ± 0.09, 1.46 ± 0.12ml respectively; $p \leq 0.05$) and inflammatory cell influx (109 ± 7 $x10^6$, 99 ± 8 $x10^6$ cells respectively, $p \leq 0.05$) compared to controls values (1.00 ± 0.06ml, 75 ± 4 $x10^6$ cells respectively, Figure 4.2A, B). Both these doses of AE-ITU reduced nitrite levels in cell-free inflammatory exudate to below the detection limit of the Greiss reaction (Figure 4.2C). Identical findings were observed using the other iNOS inhibitor 1400W (1, 10mg/kg), which caused an exacerbation of exudate volume (1.18 ± 0.10, 1.16 ± 0.08ml respectively compared to controls 0.65 ± 0.05ml; Figure 4.2A) and leucocyte migration (103 ± 8 $x10^6$, 113 ± 5 $x10^6$ cells respectively compared to saline treated animals 79 ± 2 $x10^6$ cells; Figure 4.2B) into the pleural cavity at doses that significantly inhibited nitrite production (10.0 ± 0.2, 10.6 ± 0.8µM respectively compared to control values 16.2 ± 0.9µM; Figure 4.2C). In contrast, although the highest dose of L-NIO (10mg/kg) increased exudate volume (1.45 ± 0.07ml compared to controls 1.01 ± 0.09ml; Figure 4.2A) and cellular influx (112 ± 7 $x10^6$ cells compared to saline treated animals 75 ± 5 $x10^6$ cells; Figure 4.2B) into the pleural cavity and significantly reduced nitrite levels (7.8 ± 0.4µM compared to control values 14.5 ± 0.5µM, $p \leq 0.05$; Figure 4.2C), L-NIO was not as potent at 6h compared to that observed at 1h.

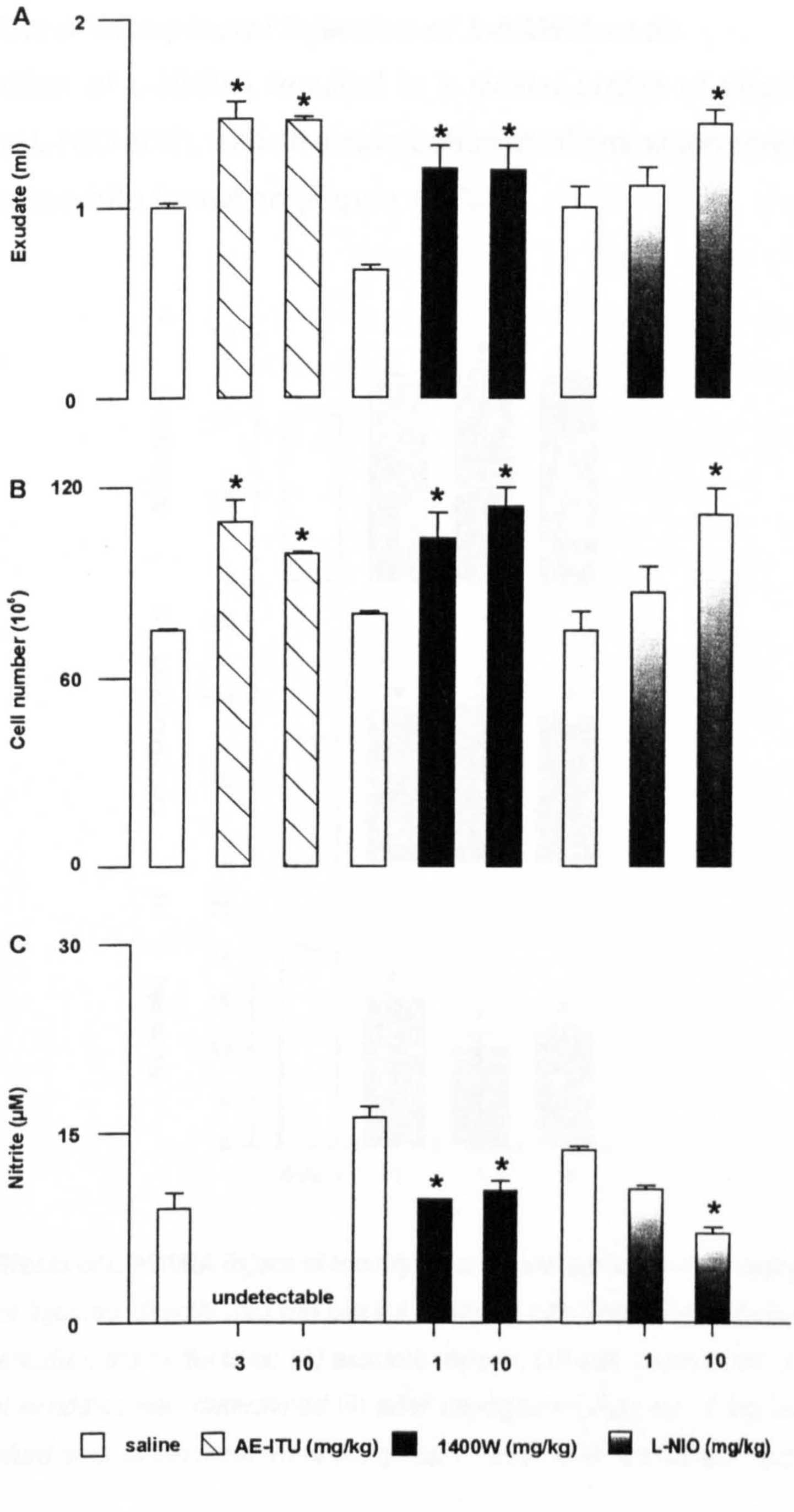

Figure 4.2 Effects of NOS inhibitors injected locally on a rat carrageenin-induced pleurisy at 6h. *AE-ITU, 1400W or L-NIO were injected directly into the pleural cavity of rats immediately before carrageenin injection. Thereafter, their effects on (A) exudate volume, (B) cell number and (C) nitrite levels in the pleural exudates was determined 6h after carrageenin injection. Data is expressed as mean ± standard error of the mean (n=8 per group) from separate experiments for each NOS inhibitor used. * $p \leq 0.05$ in comparison to saline controls.*

4.2.3 Effect of intrapleural injection of L-NMMA at 6h

Local injection of L-NMMA resulted in a similar profile of effect as AE-ITU, 1400W and L-NIO at 6h, with an exacerbation of inflammation concominant with a reduction in nitrite formation (Figure 4.3A-C)

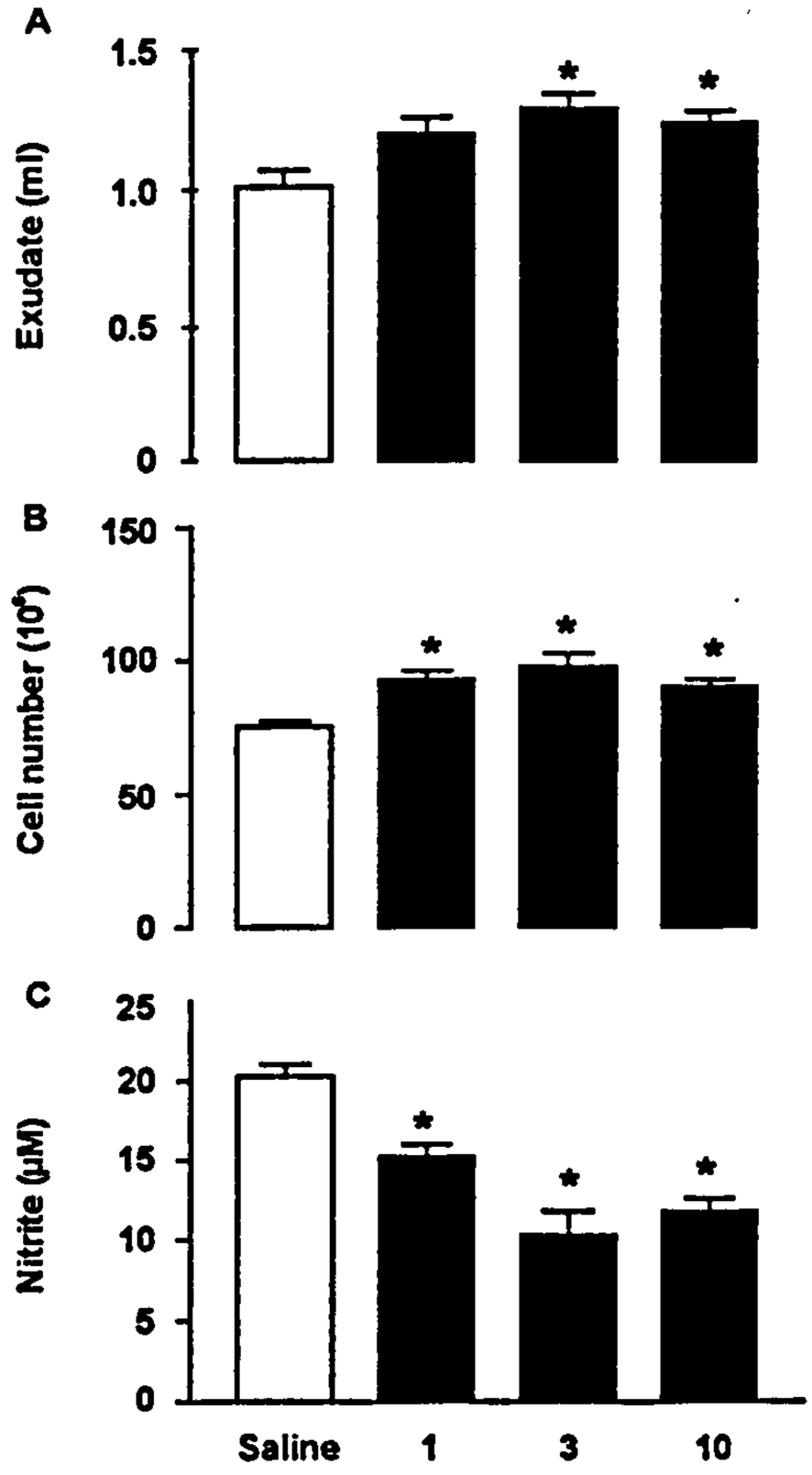

Figure 4.3 Effects of L-NMMA injected locally on a rat carrageenin-induced pleurisy at 6h. *L-NMMA was injected directly into the pleural cavity of rats immediately before carrageenin injection. Thereafter, their effects on (A) exudate volume, (B) cell number and (C) nitrite levels in the pleural exudates was determined 6h after carrageenin injection. Data is expressed as mean ± standard error of the mean (n=6 per group). * p≤0.05 in comparison to saline controls.*

4.2.4 Effect of intrapleural injection of DPTA NoNoate at 6h

Since inhibition of NO caused an increased carrageenin-induced inflammation, it was postulated that further increasing local levels of this free radical may be of therapeutic benefit and would help confirm a direct anti-inflammatory action for NO. Therefore in a parallel experiment the NO donor, DPTA NoNoate (6h ½

life), was administered locally. This compound was used because of its slow profile of release. Most donors like sodium nitroprusside release NO rapidly, therefore there effects would be immediate and may be detrimental through a sizable rapid release of NO. Injection of DPTA NoNoate (0.1, 1mg/kg) into the pleural cavity of rats resulted in a significant reduction ($p \leq 0.05$) in both exudate volume (0.79 ± 0.27, 0.59 ± 0.59ml respectively compared to control values 0.97 ± 0.24ml) and leucocyte influx (57 ± 19 $x10^6$, 52 ± 7 $x10^6$ cells respectively compared to saline treated animals 129 ± 8 $x10^6$ cells) into the pleural cavity of rats with carrageenin-induced inflammation (Figure 4.4A, B)

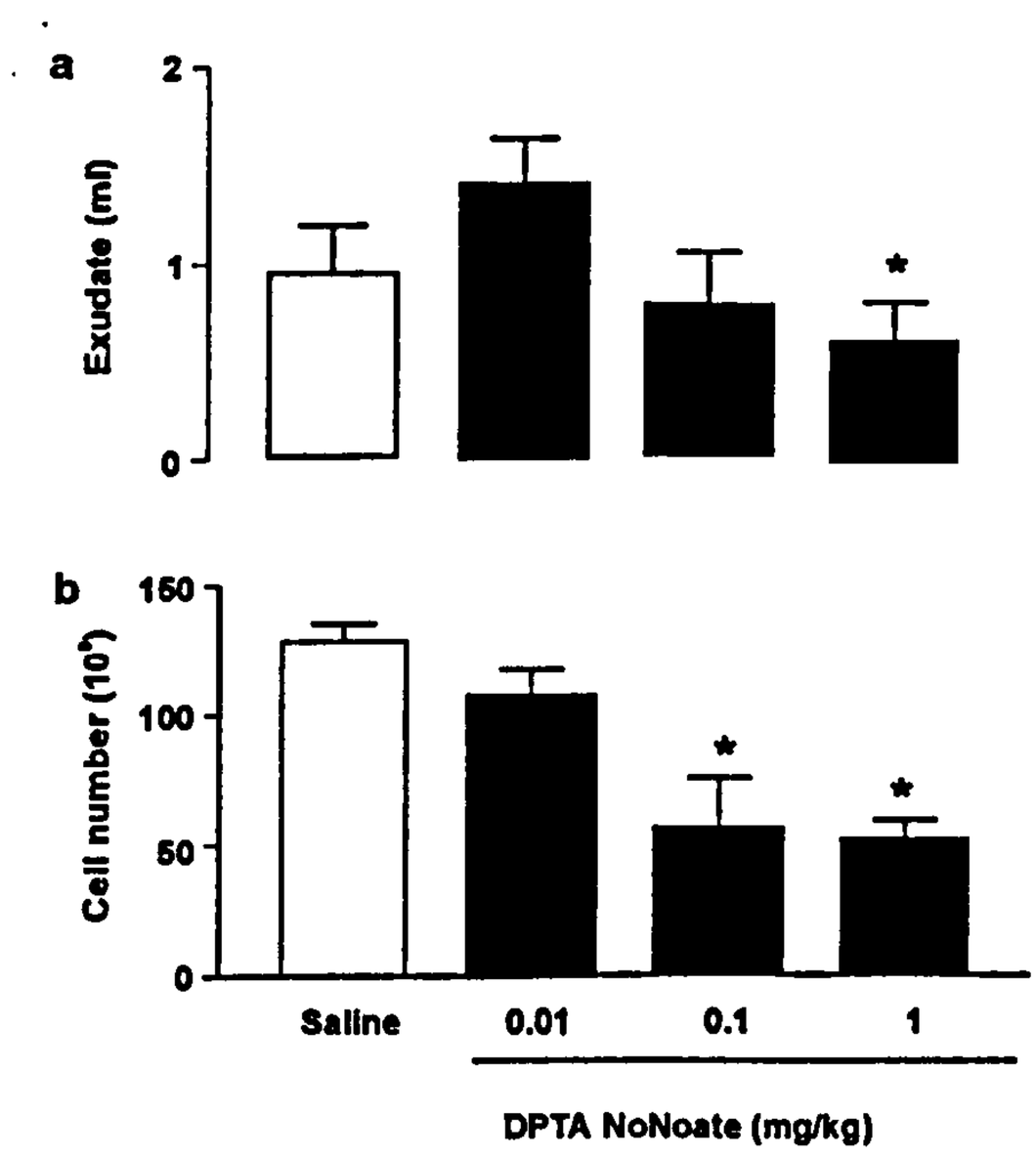

Figure 4.4 Effects on pleural inflammation at 6h after the administration of an NO donor locally. *DPTA NoNoate was injected directly into the pleural cavity of rats immediately prior to carrageenin. 6h after carrageenin injection the effects of this slow releasing NO donor was examined on (A) exudate volume and (B) cell number in pleural exudates. Data is expressed as mean ± standard error of the mean (n=8 per group). * $p \leq 0.05$ in comparison to saline controls.*

4.2.5 Effect of early intrapleural injection of NOS inhibitors on the resolution of inflammation

As demonstrated above NOS inhibition exacerbated inflammation at 1 and 6h. Therefore, was this elevated inflammatory response a consequence of a transient increase in inflammation at this early phase that results in a knock on

effect that results in a delay in inflammatory resolution? To discern this, AE-ITU was administered into the pleural cavity immediately prior to carrageenin injection (as above) and its effects on inflammation was determined at 36h, a time point where the inflammation is resolving, and at 72h, a time point at which this model is usually resolved.

Injection of AE-ITU or L-NMMA (3, 30mg/kg) into the pleural cavity of rats again resulted in an aggravation of both exudate volume (40-50%; $p \leq 0.05$) and inflammatory cell influx (30-40%; $p \leq 0.05$) at 36h, Figure 4.5A, B. Nitrite was measured at this time point however, all values were below the detection limit of the assay..

At 72h local injection of AE-ITU (3, 10mg/kg) into the pleural cavity of rats still resulted in an elevated exudate volume, being significant at the higher dose (0.39 ± 0.17ml compared to control values 0.03 ± 0.02ml) and inflammatory cell influx ($57 \pm 9 \times 10^6$ cells compared to saline treated animals $13 \pm 4 \times 10^6$ cells), Figure 4.6A, B. Nitrite was measured at this time point however, all values were below the detection limit of the assay.

Thus, from these experiments it appears that early production of NO plays a critical role in determining the outcome of this inflammatory response.

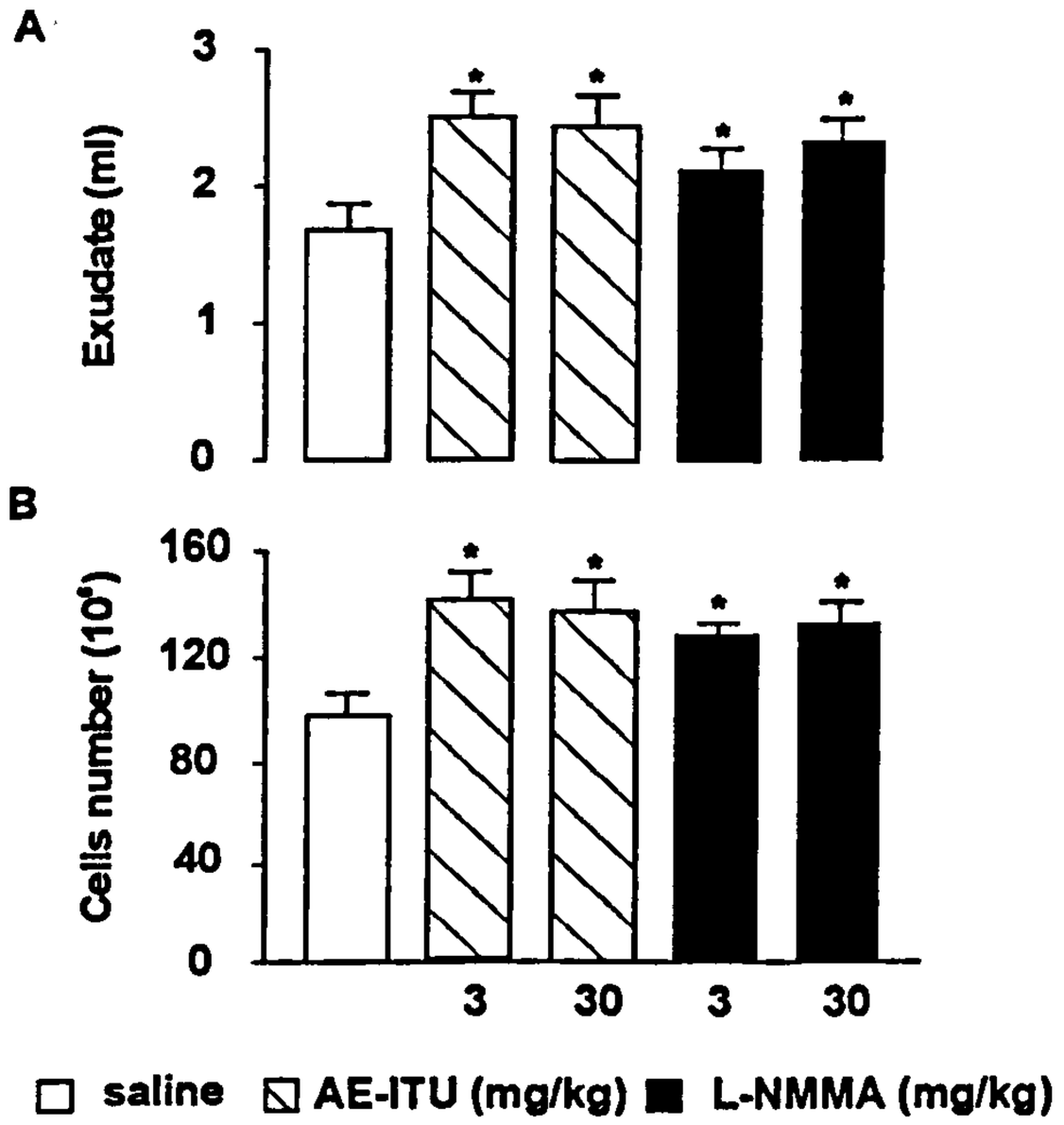

Figure 4.5 Effects of early NOS inhibition on inflammatory resolution (36h) in the rat carrageenin-induced pleurisy. *AE-ITU was injected directly into the pleural cavity of rats immediately prior to carrageenin injection. 36h later, at the start of the resolving stage, the consequence of early NOS inhibition was examined on (A) exudate volume and (B) cell number. Data is expressed as mean ± standard error of the mean (n=6-8 per group). * p≤0.05 in comparison to saline controls.*

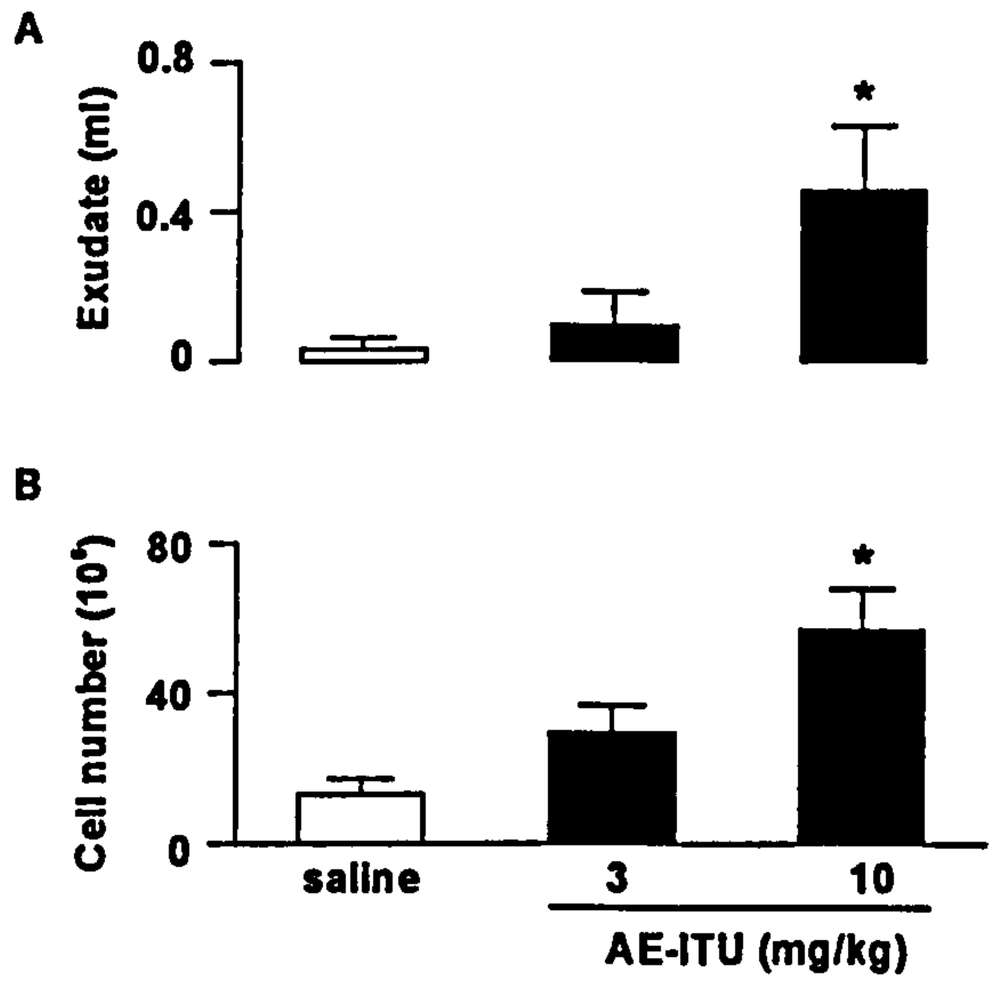

Figure 4.6 Effects of early NOS inhibition on inflammatory resolution (72h) in the rat carrageenin -induced pleurisy. *AE-ITU was injected directly into the pleural cavity of rats immediately prior to carrageenin injection. 72h later, at resolution, the consequence of early NOS inhibition was examined on (A) exudate volume and (B) cell number. Data is expressed as mean ± standard error of the mean (n=6 per group). * p≤0.05 in comparison to saline controls.*

4.2.6 Effects of the systemic injection of NOS inhibitors

A fundamental question still needs to be addressed, whether there is a differential effect on inflammation by administering NOS inhibitors locally versus systemically. In order to determine this, the effect on inflammation at 6 and 36h of AE-ITU and L-NMMA when injected into the peritoneal cavity at the time of carrageenin injection was examined.

AE-ITU had no effect on exudate formation at 3 or 30mg/kg but significantly ($p \leq 0.05$) reduced cellular influx (78 ± 9 $x10^6$, 67 ± 7 $x10^6$ cells respectively compared to saline treated animals 104 ± 6 $x10^6$ cells) at 6h, while reducing nitrite levels to 4.2 ± 0.4, 3.2 ± 0.3μM, respectively, compared to control values 9.8 ± 0.1μM (Figure 4.7A-C).

Similar results were obtained with L-NMMA on exudate formation at 3 or 30mg/kg. However, at the highest dose (300mg/kg) L-NMMA significantly ($p \leq 0.05$) reduced exudate volume (0.50 ± 0.06ml compared to saline controls 1.32 ± 0.08ml). Once again leucocyte influx was inhibited at all doses tested (3, 30, 300mg/kg), 78 ± 13 $x10^6$, 74 ± 4 $x10^6$, 48 ± 6 $x10^6$ cells respectively compared to saline treated animals 104 ± 6 $x10^6$ cells at 6h. Nitrite formation was significantly inhibited at all doses tested ($p \leq 0.05$, Figure 4.7A-C).

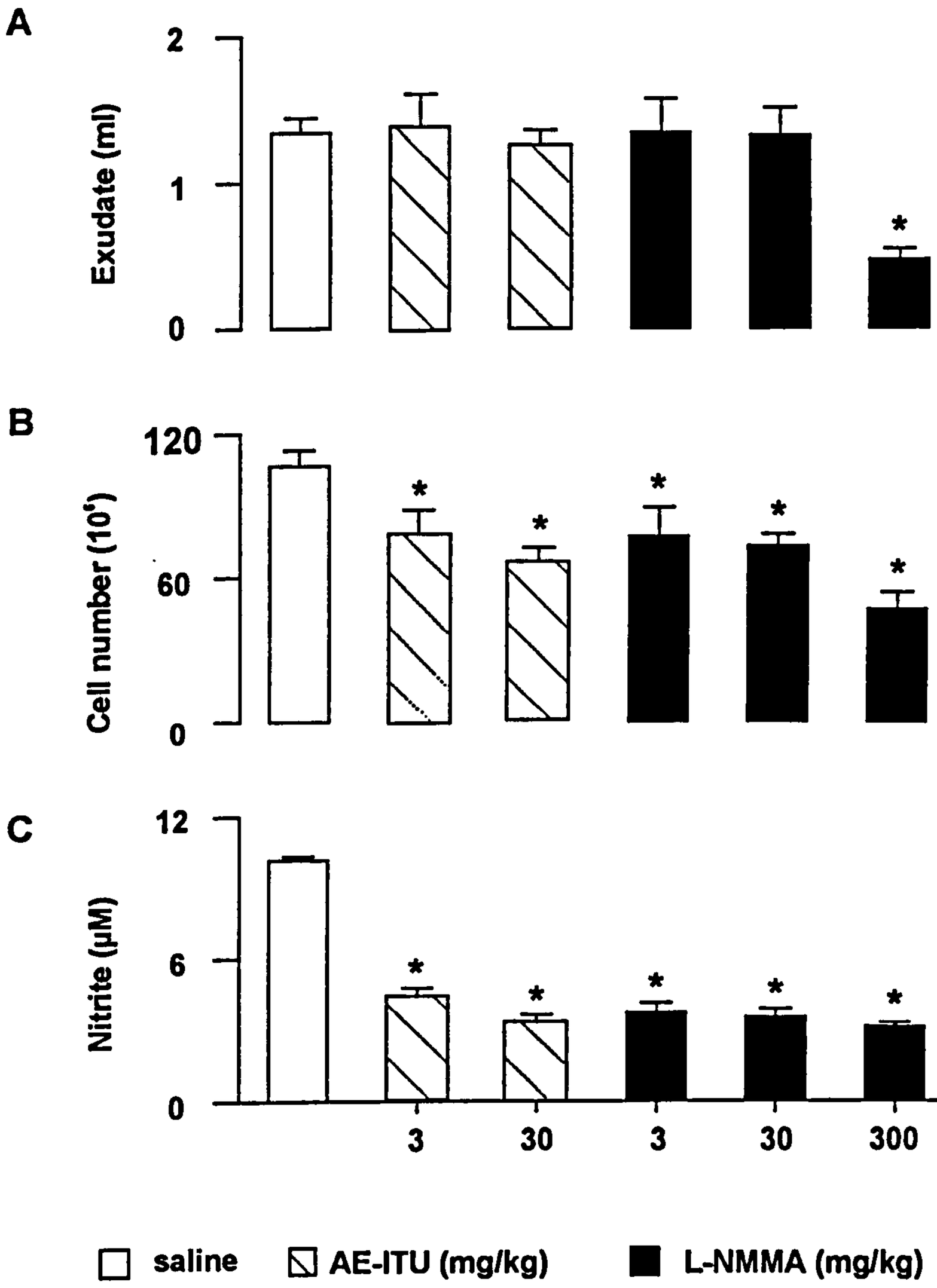

Figure 4.7 Effects of NOS inhibitors injected systemically on a rat carrageenin-induced pleurisy at 6h. *Either AE-ITU or L-NMMA was injected into the peritoneal cavity just prior to intrapleural carrageenin injection. 6h later the effects of these NOS inhibitors was determined on (A) exudate volume, (B) cell number and (C) nitrite in pleural exudates. Data is expressed as mean ± standard error of the mean (n=8 per group). * p≤0.05 in comparison to saline controls.*

The systemic administration of the NOS inhibitors, AE-ITU and L-NMMA at 36h resulted in a significant ($p \leq 0.05$) suppression of both exudate volume (11-50%) and inflammatory cell influx (30-76%) into the pleural cavity of rats, Figure 4.8A, B.

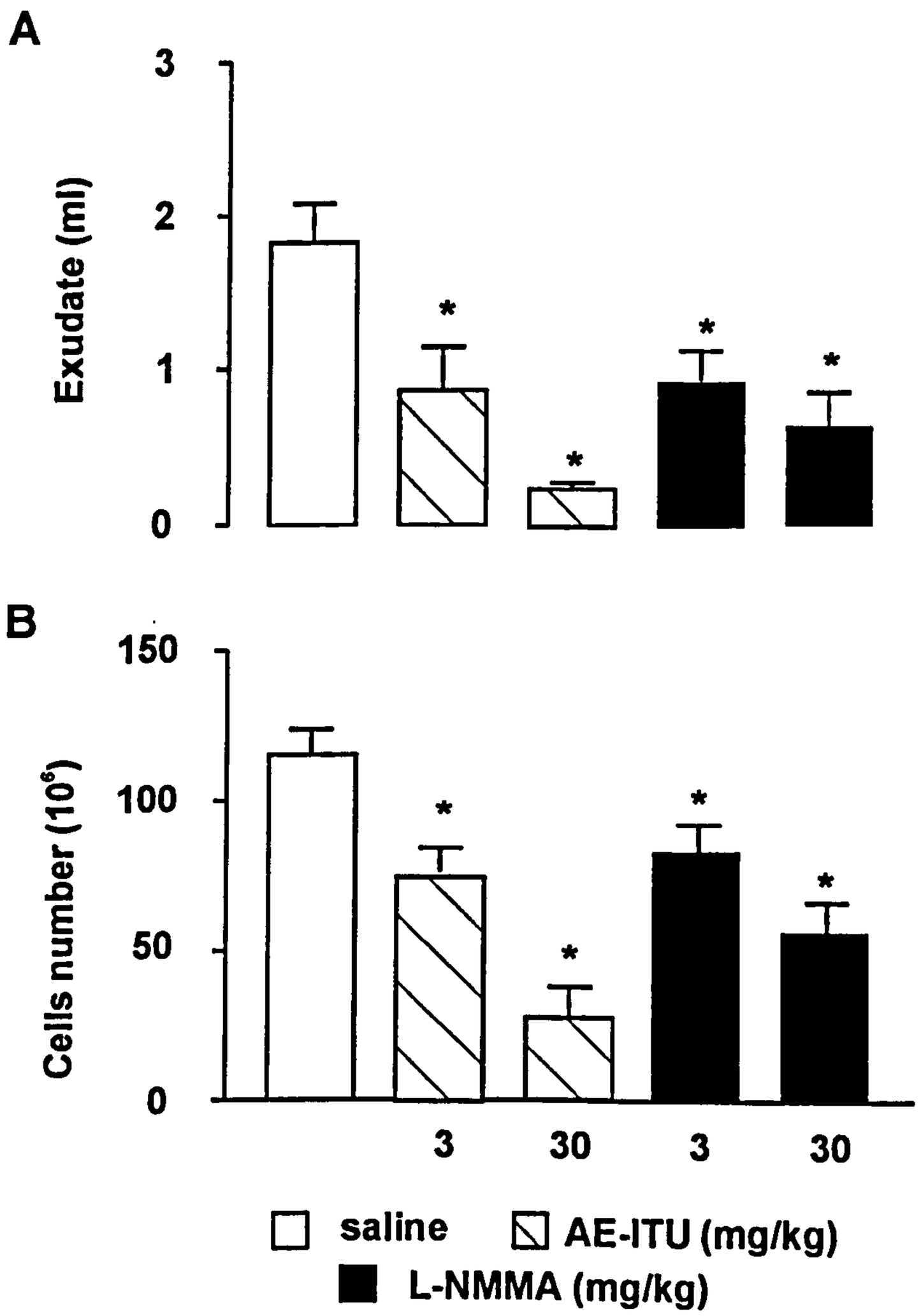

Figure 4.8 Effects of NOS inhibitors injected systemically on a rat carrageenin-Induced pleurisy at 36h. *Either AE-ITU or L-NMMA was injected into the peritoneal cavity just prior to intrapleural carrageenin injection. 36h later the effects of these NOS inhibitors was determined on (A) exudate volume, (B) cell number and (C) nitrite in pleural exudates. Data is expressed as mean ± standard error of the mean (n=8 per group). * p≤0.05 in comparison to saline controls.*

Therefore, at 6 and 36h systemic (i.p.) administration of NOS inhibitors caused an inhibition of inflammation. conversely, local injection of NOS inhibitors into the pleural cavity immediately prior to carrageenin injection, increased exudate volume and inflammatory cell number at 6h and 36h. These findings present highly conflicting outcomes on inflammation depending on whether NOS inhibitors are administered either locally or systemically.

4.2.7 Effect of NOS inhibitors in the pleural cavity in the absence of carrageenin

To show that AE-ITU (3mg/kg) and 1400W (10mg/kg) did not exacerbate inflammation simply as a result of direct irritation we injected these drugs, as well as saline, into the pleural cavity in the absence of carrageenin. Neither drug caused measurable exudate formation or an increase in cellular influx (Table 4.1)

		Time after carrageenin-injection (h)			
		1		6	
NOS inhibitor	Dose (mg/kg)	Exudate (ml)	Cells (10^6)	Exudate (ml)	Cells (10^6)
Saline	-	0.11 ± 0.05	2.4 ± 0.7	0.04 ± 0.04	2.1 ± 1.7
AE-ITU	3	0.10 ± 0.07	2.5 ± 1.5	0.03 ± 0.03	2.0 ± 1.4
1400W	10	0.11 ± 0.04	2.2 ± 0.5	0.04 ± 0.04	1.8 ± 1.3

Table 4.1 A determination of the non-specific, irritant effects of iNOS selective inhibitors on the non-inflamed pleural cavity at 1 and 6h. *Data is expressed as mean ± standard error of the mean (n=6 per group per time point).*

Moreover, cationic compounds, including NOS inhibitors, may cause non-specific mast cell degranulation due to their strongly charged nature. Therefore, N^G-nitro-D-arginine methyl ester (D-NAME) the inactive enantiomer of the non-specific cationic NOS inhibitor L-NAME, was injected intrapleurally at the same molarity as AE-ITU (3, 10mg/kg; 1.9, 6.3μM respectively) and caused no increase in inflammatory parameters at 1 or 6h (Figure 4.9). As a final control experiment, using the MTT assay for the assessment of cell viability, we found that neither AE-ITU nor L-NMMA, when injected intrapleurally, caused toxicity to influxing inflammatory cells in the pleural cavity at 6h (Table 4.2).

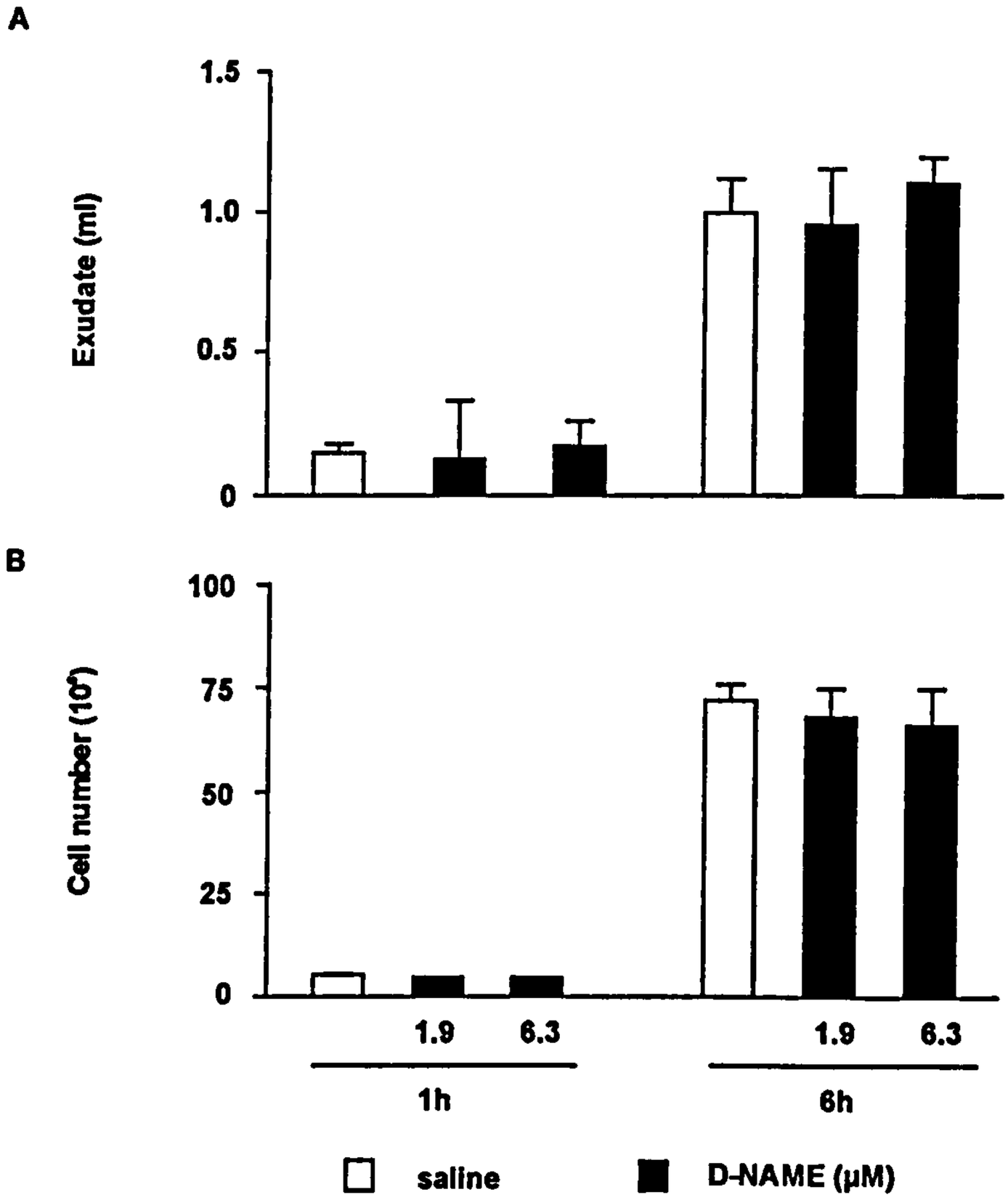

Figure 4.9 A determination of the non-specific, irritant effects of NOS inhibitors during Inflammation. *D-NAME was injected directly into the pleural cavity of rats immediately prior to carrageenin. 1 and 6h after carrageenin injection the effects of this inactive enantomer of the NOS inhibitor L-NAME was assessed in (A) exudate volume and (B) cell number in pleural exudates. Data is expressed as mean ± standard error of the mean (n=8/6per group).*

NOS inhibitor	Dose (mg/kg)	Change in MTT content of cells as expressed as a percentage of saline control
AE-ITU	3	104 ± 12
	10	101 ± 4
L-NMMA	3	98 ± 6
	10	105 ± 5

Table 4.2 Effect of the NOS inhibitors AE-ITU and L-NMMA on cell viability. *Viability was assessed by the MTT assay, 6h post-carrageenin injection. Data is expressed as a percentage of control (n=5 per group).*

4.2.8 Effect of intrapleural injection of NOS inhibitors at 2h post carrageenin

In attempt to specifically inhibit iNOS enzyme activity, AE-ITU was injected into the pleural cavity 2h after carrageenin injection, a time point at which iNOS protein expression is first evident (refer to Figure 3.2). Inflammatory exudates were collected at 6h, the peak in iNOS related NO production. In line with previous data in this chapter, where NOS inhibitors were injected locally, nitrite was significantly reduced (2.9 ± 0.4μM compared to controls 11.9 ± 3.3μM) but exudate volume (2.65 ± 0.1ml compared to controls 1.84 ± 0.29ml) and inflammatory cell numbers (163 ± 4 x10^6cells compared to controls 133 ± 5 x10^6 cells) were significantly increased (Figure 4.10).

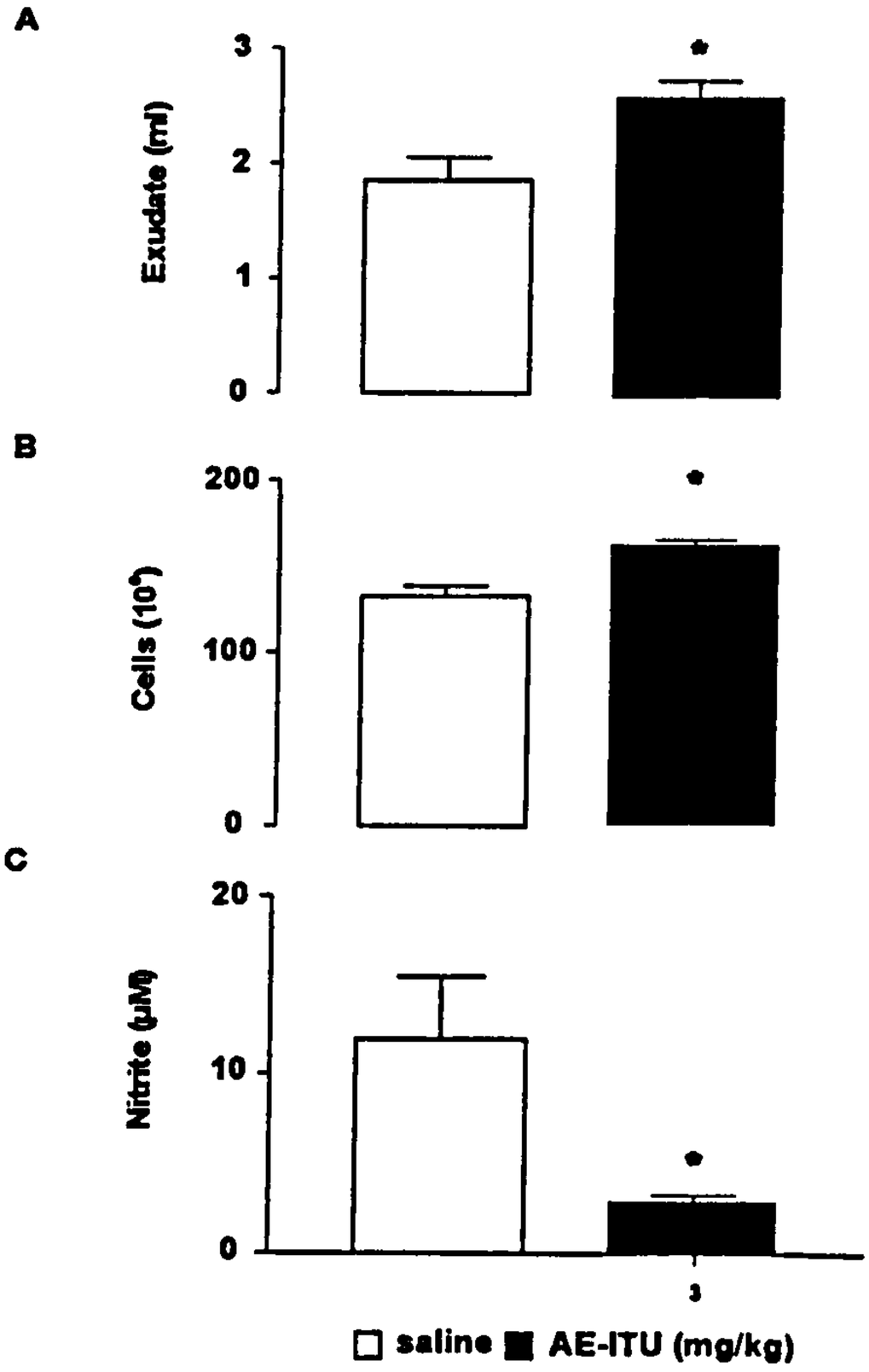

Figure 4.10 Therapeutic effects of NOS inhibition in the carrageenin-induced pleurisy at 6h. *AE-ITU was injected into the pleural cavity 2h after carrageenin injection. 6h after carrageenin injection its effects on (A) exudate volume, (B) cell number and (C) nitrite accumulation was determined. Data is expressed as mean ± standard error of the mean(n=6 per group). * p≤0.05 in comparison to saline controls.*

4.2.9 Histamine involvement in the increase in inflammatory parameters at 1h

In an attempt to elucidate the mechanisms by which inhibition of NO synthesis worsens inflammation, levels of the most likely pro-inflammatory mediators were measured after treatment with AE-ITU. As shown in Figure 4.11 and by others (Capasso *et al.*, 1975), mast cell-derived histamine (Section 3.15) peaked in this model between 0.5-1h after carrageenin injection.

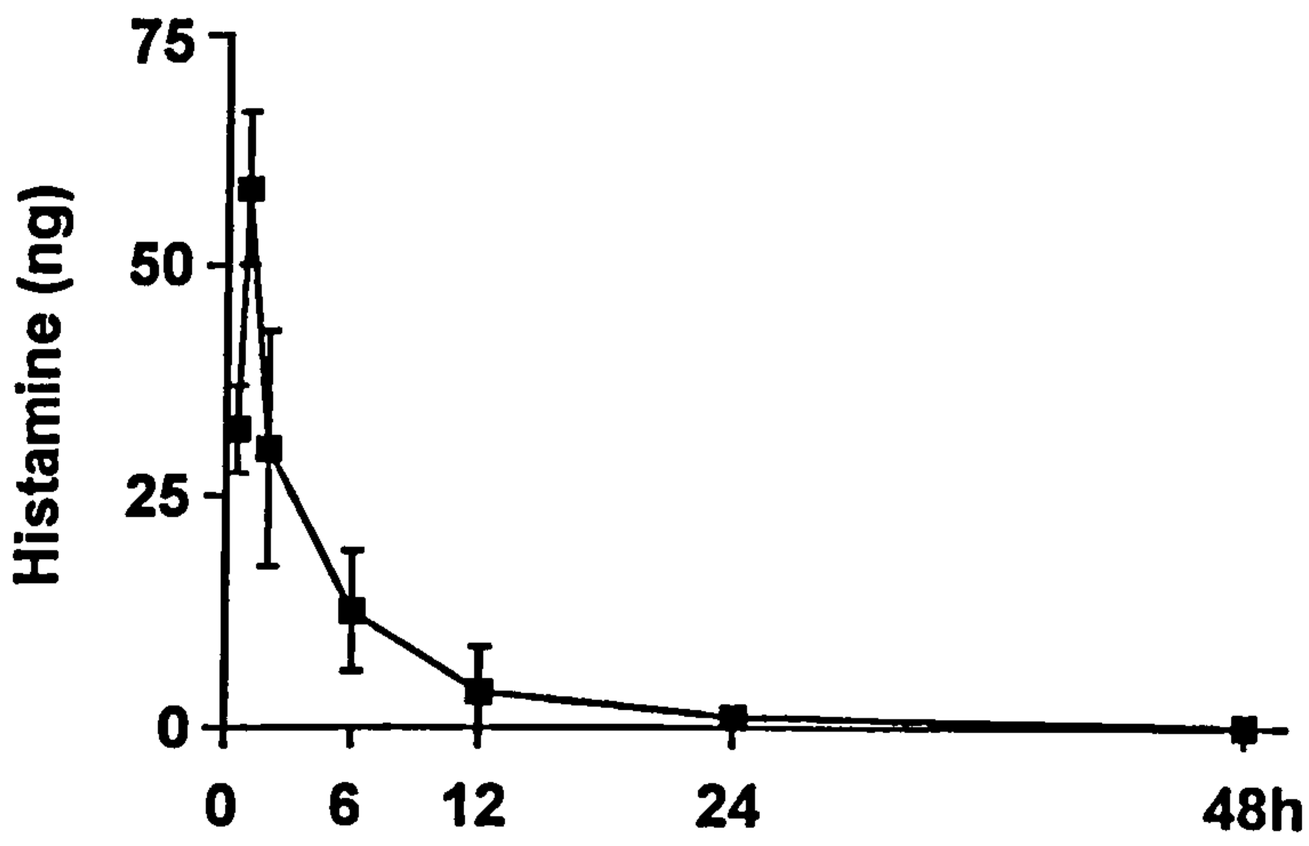

Figure 4.11 Time course of histamine levels in cell-free inflammatory exudates from rats with a carrageenin-induced pleurisy. *Data is expressed as mean ± standard error of the mean (n=8 per time point).*

In addition, histamine mediates oedema formation (Capasso *et al.*, 1975) and NO stabilises mast cells, thereby preventing histamine release (Salvemini *et al.*, 1991, Brooks *et al.*, 1999) therefore, levels of this acute inflammatory mediator were measured after NOS inhibition in cell-free inflammatory exudates. AE-ITU (10mg/kg) significantly increased ($p \geq 0.05$) histamine release into cell-free inflammatory exudates at 1h, 65.2 ± 7.3ng compared with saline controls (43.8 ± 1.5ng; Figure 4.12).

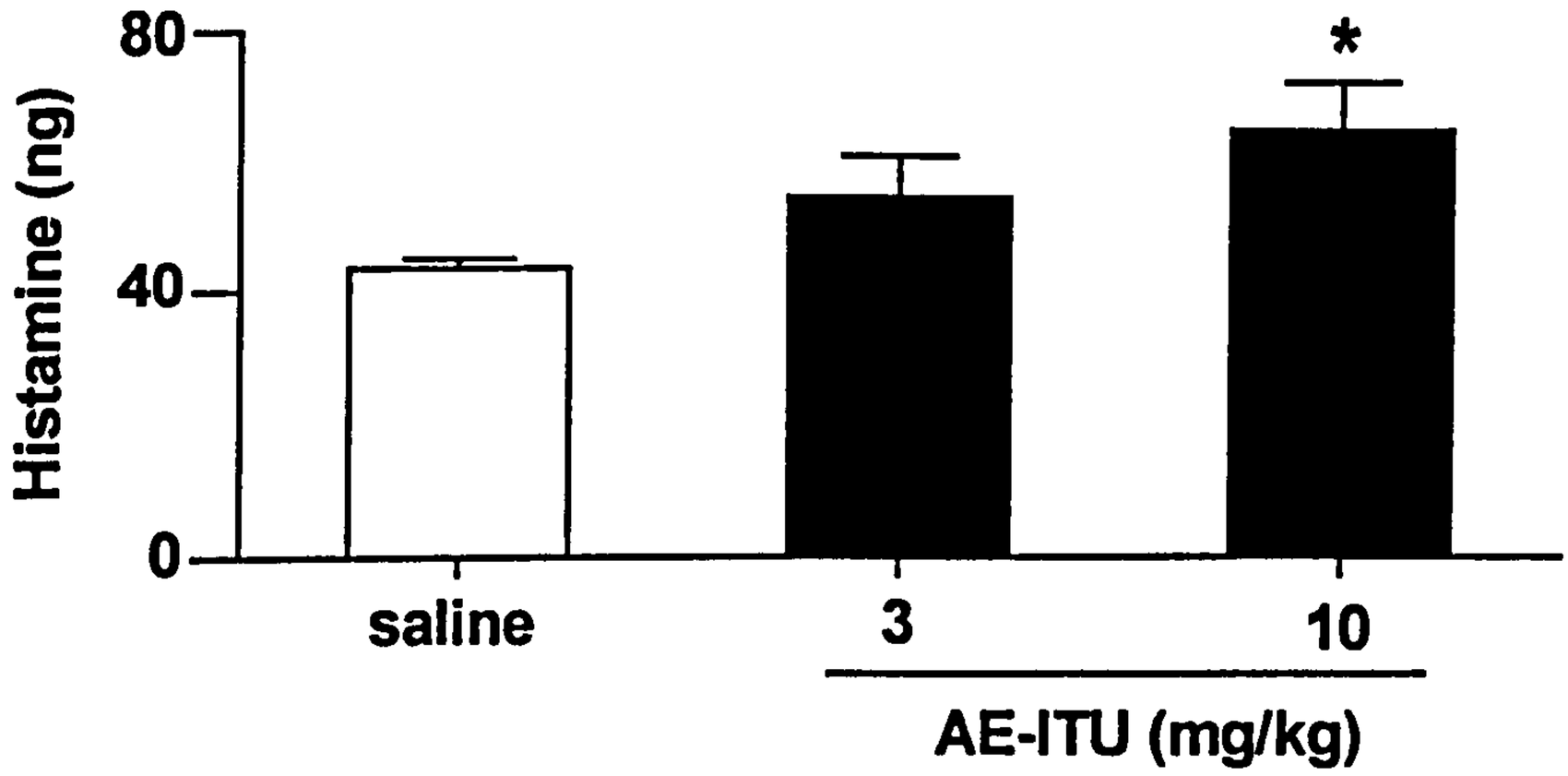

Figure 4.12 Effects of local NOS inhibition on histamine levels in the rat carrageenin-induced pleurisy. *AE-ITU was injected into the pleural cavity immediately prior to carrageenin injection. 1h later histamine levels was determined in cell-free exudates.Data is expressed as mean ± standard error of the mean (n=8 per group). * p≤0.05 in comparison to saline controls.*

This increase in histamine after AE-ITU treatment was accompanied by a decrease in mast cell numbers (the cellular source of histamine) as counted after toluidine blue staining (2.24.5), presumably as a consequence of increased cellular degranulation (Table 4.3; Figure 4.13 A, B).

Treatment	Mean percentage of Total cells	% change compared with controls
control	0.92	-
AE-ITU (3mg/kg)	0.30	67
AE-ITU (10mg/kg)	0.26	72

Table 4.3 Effect of AE-ITU treatment on mast cell numbers recovered from the pleural cavity. *Data is also expressed as the percentage change compared to control in a 1h carrageenin-induced pleurisy after AE-ITU treatment. Data is expressed as both mean percentage of mast cells per total cells and as a percentage change compared to control values (n=6 cell smears from 6 rats).*

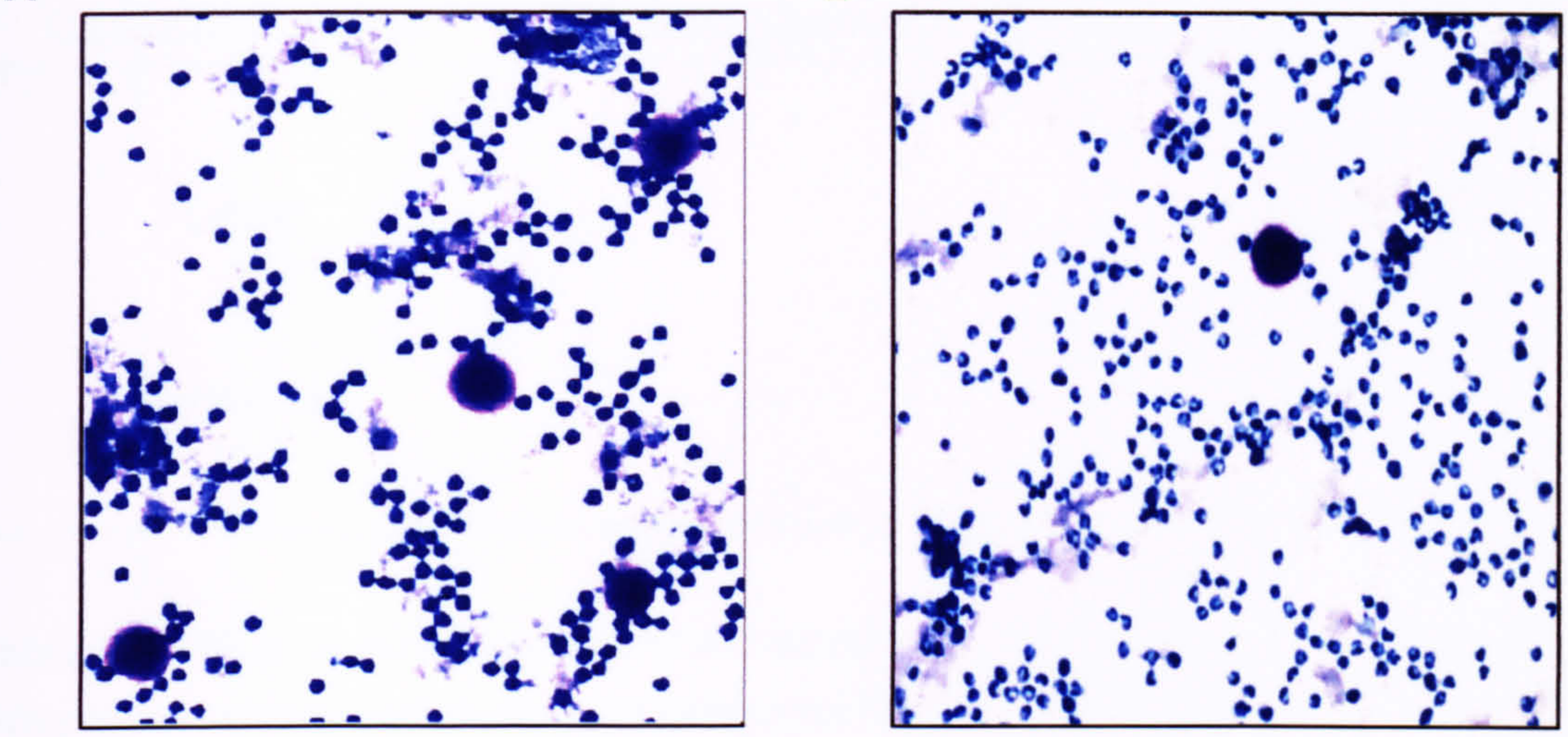

Figure 4.13 Effect of AE-ITU on mast cell degranulation in a 1h carrageenin-induced pleurisy. *Panel A shows a 1h cell smear stained with toludine blue from rats treated with carrageenin and saline and Panel B shows a 1h cell smear stained with toludine blue from rats treated with carrageenin and AE-ITU (10mg/kg). Panel A and B magnification x20.*

To confirm the involvement of mast cell derived histamine at 1h in the carrageenin-induced pleurisy animals were depleted of histamine using CMP 48/80. Two published methods were compared for their effectiveness in depleting histamine levels prior to and after carrageenin injection. In the first method (Diaz *et al.*, 1996) mast cells were degranulated locally at the site of inflammation by injection of 12µg CMP 48/80 into the pleural cavity. Animals were sacrificed 3 days later prior to and 1h after carrageenin-injection. In the second method (Di Rosa *et al.*, 1971) mast cells were depleted systemically by i.p injection of CMP 48/80 (3 days of 0.6mg /kg twice daily and 1 day 1.2mg/kg twice daily) after treatment animals were left for 2 days before histamine levels were analysed prior to and 1h after carrageenin injection (Table 4.3).

Depletion method	Carrageenin	Histamine levels (ng)
-	+	4.38 ± 1.5
Local	-	71.7 ± 7.2
	+	107 ± 15.7
Systemic	-	≤ 1
	+	≤ 1

Table 4.4 Effect of local and systemic depletion of mast cells before and 1h after intrapleural carrageenin challenge on histamine levels in cell-free inflammatory exudates.

As demonstrated in Table 4.3, the best method for depleting mast cell amines from the pleural cavity was to use the systemic depletion method, therefore was used in all subsequent experiments. The increase in exudate volume observed at 1h with AE-ITU (3, 10mg/kg) was partially attenuated by histamine depletion at dosing levels that significantly reduced exudate nitrate formation (14.1 ± 1.1,8.2 ± 1.0μM, respectively, compared to saline 14.6 ± 1.3μM and saline + CMP 48/80 16.6 ± 1.3μM; contrast Figures 4.1 and 4.14). Although there was an expected reduction in exudate formation in animals treated with CMP 48/80 alone (Figure 4.15 A), there was no change in cell numbers (Figure 4.14 B). This observation is consistent with the fact that histamine mediates oedema formation and not cell migration. AE-ITU (3, 10mg/kg) injection still caused a significant increase in inflammatory cell influx into the pleural cavity (5.1 ± 0.5, 6.2 ± 0.6 $x10^6$ cells respectively compared to both saline 4.1 ± 0.8 $x10^6$ cells and saline + CMP 48/80 4.2 ± 0.2 $x10^6$ cells; Figure 4.14 B).

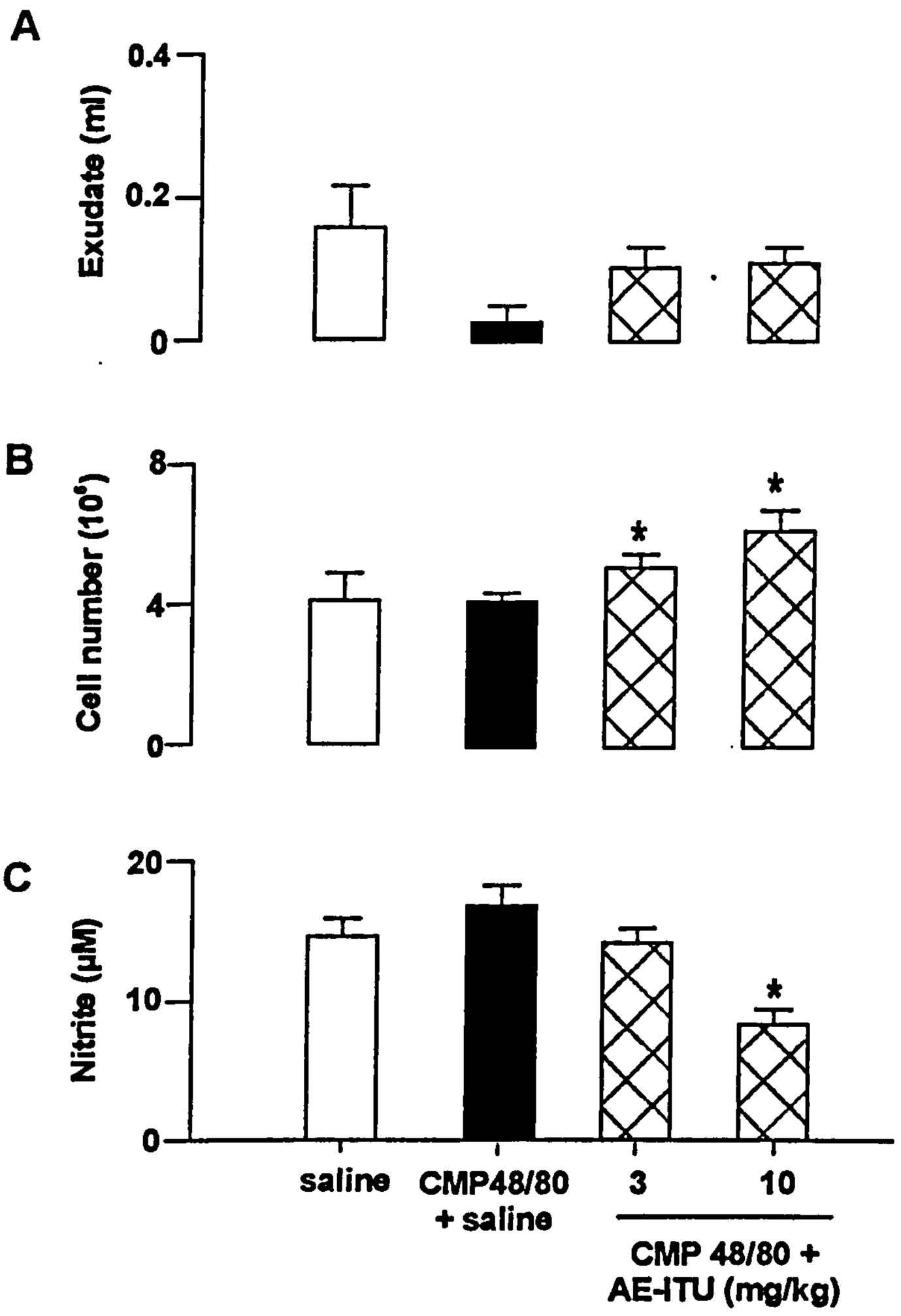

Figure 4.14 The effects of mast cell depletion on the exacerbation of inflammation after intrapleural injection of AE-ITU. *Panel (A) exudate volume (B) cell number and (C) nitrite production was ascertained in the pleural cavity 1h after depletion of mast cells using CMP 48/80. Data is expressed as mean ± standard error of the mean (n=8 per group). * p≤0.05 in comparison to saline controls.*

4.2.10 CINC involvement in the increase in inflammatory parameters at 1h

Another candidate for investigation was CINC, a potent neutrophil chemoattractant (Watanabe *et al.*, 1991). CINC levels in the pleural cavity peaked at 1h (1656 ± 304pg) in cell-free inflammatory exudate and delined over the time course of the pleurisy (Figure 4.15A).

Intrapleural injection of AE-ITU (3,10 mg/kg) caused a significant increase in CINC in cell-free pleural exudates (2444 ± 84, 2332 ± 131pg respectively compared with control values 1830 ± 28pg; Figure 4.15 B). It is worth noting that mast cell depletion with CMP 48/80 had no effect on AE-ITU's increases in CINC or on the overall levels of CINC measured (data not shown).

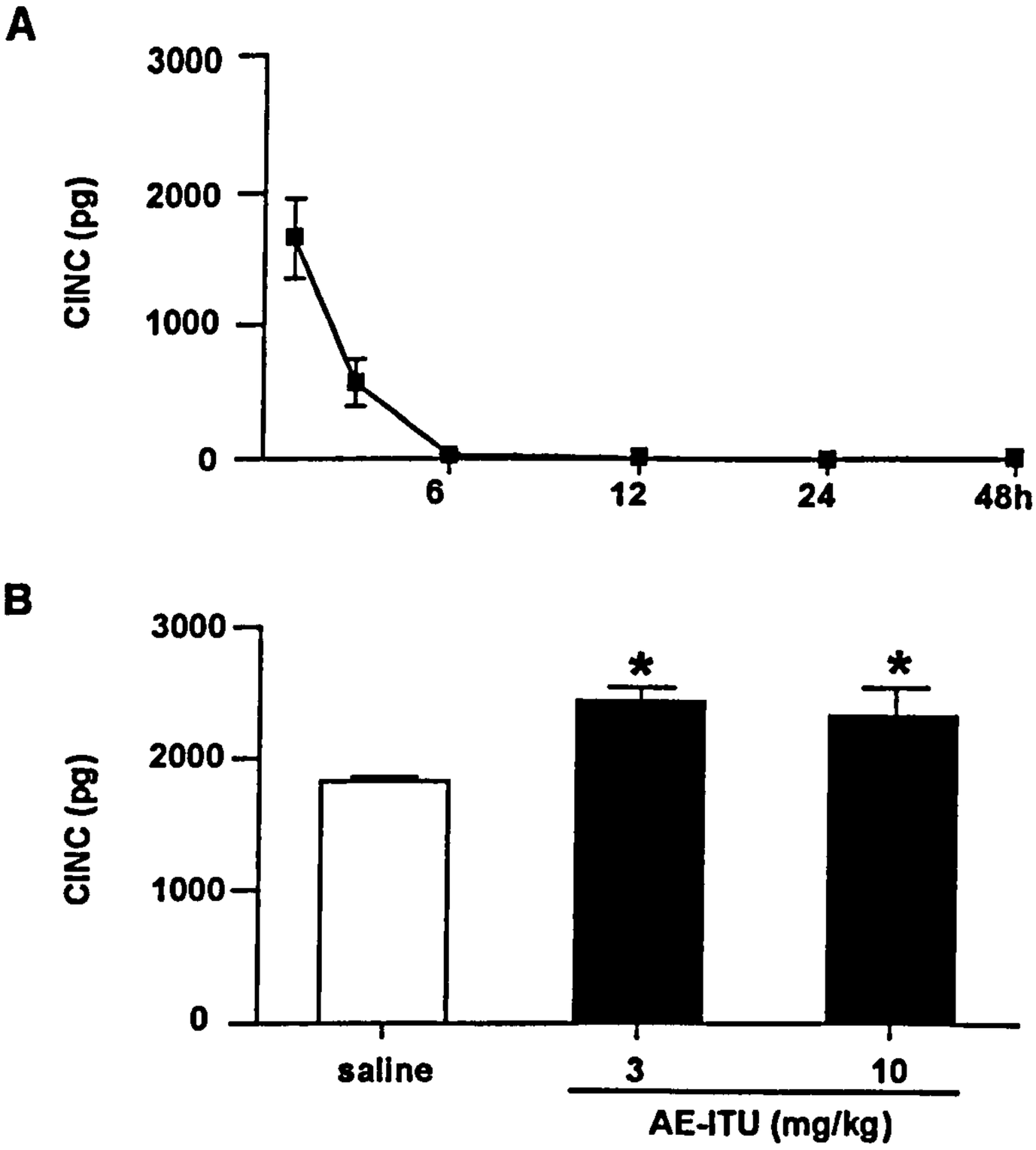

Figure 4.15 Effects of local NOS inhibition on levels of CINC in the rat carrageenin-induced pleurisy. *The profile of CINC was determined in the cell-free inflammatory exudate by ELISA (a). Thereafter, the effects of AE-ITU, injected into the pleural cavity immediately prior to carrageenin injection, was examined on CINC levels 1h after carrageenin injection (b). Data is expressed as mean ± standard error of the mean (n=6-8 per group). * p≤0.05 in comparison to saline controls.*

4.2.11 Eicosanoid involvement in the increase in inflammatory parameters at 6h

An additional explanation for exacerbated inflammation after NOS inhibition could be enhanced eicosanoid synthesis, particularly as NO has been suggested to modulate COX activity, as covered in the introduction and

dicussion. Thus, given the pro-inflammatory properties of some eicosanoids and their abundance in the carrageenin-induced pleurisy up to 6h (Tomlinson *et al.*, 1994), we examined the effects of NOS inhibition on inflammatory cell COX activity as well as cell-free exudate levels of PGE_2, 6-keto $PGF_{1\alpha}$ (Table 4.4) and the neutrophil chemoattractant, LTB_4. Surprisingly, AE-ITU (3mg/kg) had no effect on either COX activity in inflammatory cell pellets or on levels of PGE_2 and 6-keto $PGF_{1\alpha}$. Interestingly, however, exudate levels of LTB_4 were significantly increased in comparison to controls (Table 4.4).

	Saline	AE-ITU (3mg/kg)
COX activity (ng mg protein^{-1} 30min^{-1})	4.4 ± 1.4	5.8 ± 1
PGE_2 (pg)	637 ± 87	852 ± 77
6-Keto $PGF_{1\alpha}$ (pg)	1631 ± 364	1483 ± 328
LTB_4 (pg)	64 ± 7	91 ± 10*

Table 4.5 Effects of local NOS inhibition on eicosanoid production in the rat carrageenin-induced pleurisy at 6h. *AE-ITU (3mg/kg) was injected into the pleural cavity of rats immediately prior to carrageenin injection. 6h later levels of eicosanoids was determined in the cell-free inflammatory exudate. Data is expressed as mean ± standard error of the mean (n=6-8 per group). * $p \leq 0.05$ in comparison to saline controls.*

4.2.12 Effects of NOS inhibition on TAOS and SSA in inflammatory cells and cell-free exudates

In a series of final experiments TAOS and SSA activity were measured as an indirect indication of superoxide and other oxidant species formation. Changes in these two parameters provide an alternative mechanism for the hypothesis that during inflammation NO may indeed have a protective role. Administered immediately prior to the induction of inflammation, AE-ITU (3, 10mg/kg) significantly reduced both TAOS (Table 4.5) and SSA (Table 4.6) in cells and cell-free exudates at 1h and 6h in comparison to saline controls.

	Cells (µM L-ascorbate equivalent antioxidant capacity/mg protein)		Exudate (µM L-ascorbate equivalent antioxidant capacity/mg protein)	
	1h	6h	1h	6h
Control	1997 ± 366	466 ± 57	89.8 ± 5.2	100.1 ± 2.0
AE-ITU (3mg/kg)	288 ± 73 *	73 ± 12 *	64.4 ± 2.2 *	65.3 ± 1.7 *
AE-ITU (10mg/kg)	578 ± 86 *	169 ± 32 *	56.2 ± 2.1 *	76.1 ± 2.2 *

Table 4.6 Effect of NOS inhibition on TAOS of inflammatory cells and cell-free exudates in the carrageenin-induced pleurisy at 1h and 6h. *AE-ITU was injected into the pleural cavity of rats immediately prior to carrageenin injection. 1 and 6h later total antioxidant status was determined in both inflammatory cells and cell-free inflammatory exudate. Data is expressed as mean ± standard error of the mean (n=8-10 per group). * $p \leq 0.05$ in comparison to saline controls.*

	Cells (change in rate/mg protein)		**Exudate** (change in rate)	
	1h	6h	1h	6h
Control	0.42 ± 0.07	0.16 ± 0.02	0.011 ± 0.001	0.010 ± 0.001
AE-ITU (3mg/kg)	0.18 ± 0.02 *	0.03 ± 0.02 *	0.005 ± 0.001 *	0.003 ± 0.001 *
AE-ITU (10mg/kg)	0.21 ± 0.02 *	0.08 ± 0.01 *	0.003 ± 0.001 *	0.005 ± 0.001 *

Table 4.7 Effect of NOS inhibition on SSA of inflammatory cells and cell-free exudates in the carrageenin-induced pleurisy at 1h and 6h. *AE-ITU was injected into the pleural cavity of rats immediately prior to carrageenin injection. 1 and 6h later, superoxide scavenging ability was determined in both inflammatory cells and cell-free inflammatory exudate. Data is expressed as mean ± standard error of the mean (n=8-10 per group). * $p \leq 0.05$ in comparison to saline controls.*

4.2.13 Effect of NOS inhibition on inflammatory cell profile and apoptosis at 6h

Since there was a significant increase in the PMN chemoattractants CINC and LTB_4 at 1 and 6h respectively, differential counts were performed to assess whether this resulted in a change in the composition of inflammatory cells obtained at 6h. As can be seen in Table 4.7 the percentage of PMNs in the inflammatory exudate was elevated after treatment with AE-ITU (3, 10mg/kg).

	Treatment		
Cell type	**Saline**	**AE-ITU (3mg/kg)**	**AE-TU (10mg/kg)**
PMN	88.4%	89.5%	91.3%
Macrophage	9.7%	8.9%	7.2%
Other	1.9%	1.6%	1.5%

Table 4.8 Effect of AE-ITU on inflammatory cell profile in a 6h carrageenin-induced pleurisy. *Where, other represents mast cell, eosinophils, lymphocytes and mesothelial cells. Data is expressed as percentages of total inflammatory cell number of n=4 rats per group.*

In addition, NO has been widely reported to induce accelerated PMN apoptosis in a number of different animal species (Uchida *et al.*, 1997, Fortenberry et al., 1998, Blaylock et al., 1998, Ward et al, 2000, Misso et al., 2000). Since in this series of experiments NO inhibitors increased inflammatory cell numbers it was hypothesised that inhibition of NO may retard the rate of apoptosis thereby increasing the cells present in the inflammatory exudates. Apoptosis was measured in cell smears taken from animals 6h after AE-ITU (3, 10mg/kg) or saline and carrageenin injection. The TUNEL method (Section 2.24) was used to determine apoptosis in these samples. AE-ITU at both 3 and 10mg/kg had no effect on the percentage of apoptotic cells present in the cell smears compared to vehicle and carrageenin (5% of total cells; *n=6* per treatment). An example of an apoptotic body at 6h is presented in Figure 4.16.

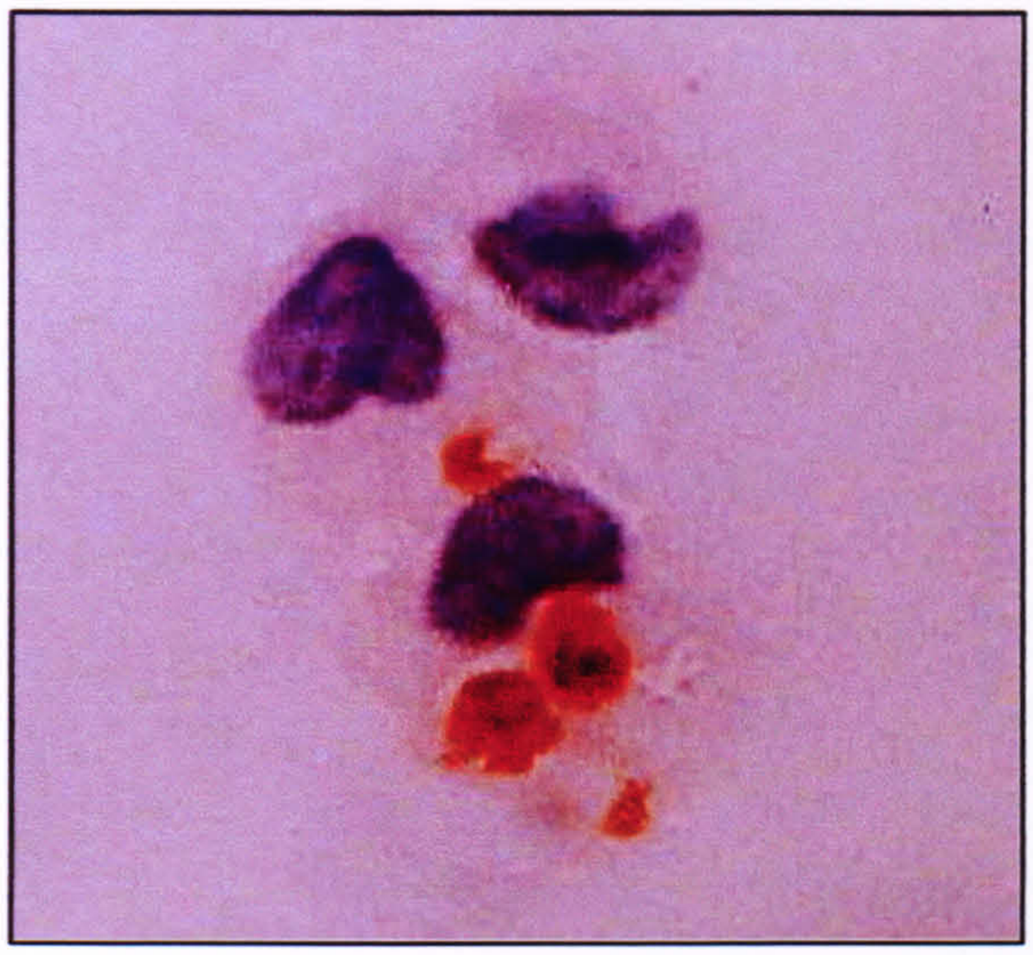

Figure 4.16 Apoptosis in the carrageenin-induced pleurisy at 6h. *Panel showing apoptotic bodies from a 6h cell smear taken from rats treated with saline and carrageenin. Magnification x100.*

4.2.14 Effect of NOS inhibition on HSP 72 and HO-1 levels in inflammatory cells at 72h

At 72h, an increase in inflammation was still observed after AE-ITU inhibition of NO. Therefore, markers of oxidative and cellular stress, HSP 72 and HO-1, were investigated in inflammatory cells taken from the pleural cavity at 72h.

Western blot analysis of HSP 72 in inflammatory cells taken from the pleural cavity at 72h resulted in a significant increase in HSP 72 protein after AE-ITU (3, 10mg/kg) treatment as assessed by densitometry (29.5 ± 4.3, 37.6 ± 8.7 arbitrary units compared to saline controls 11.7 ± 2.8 arbitrary units; Figure 4.17 A, B)

Although HSP 72 protein expression was significantly increased no effect on HO-1 protein levels were detected at this time point (Figure 4.17 C, D)

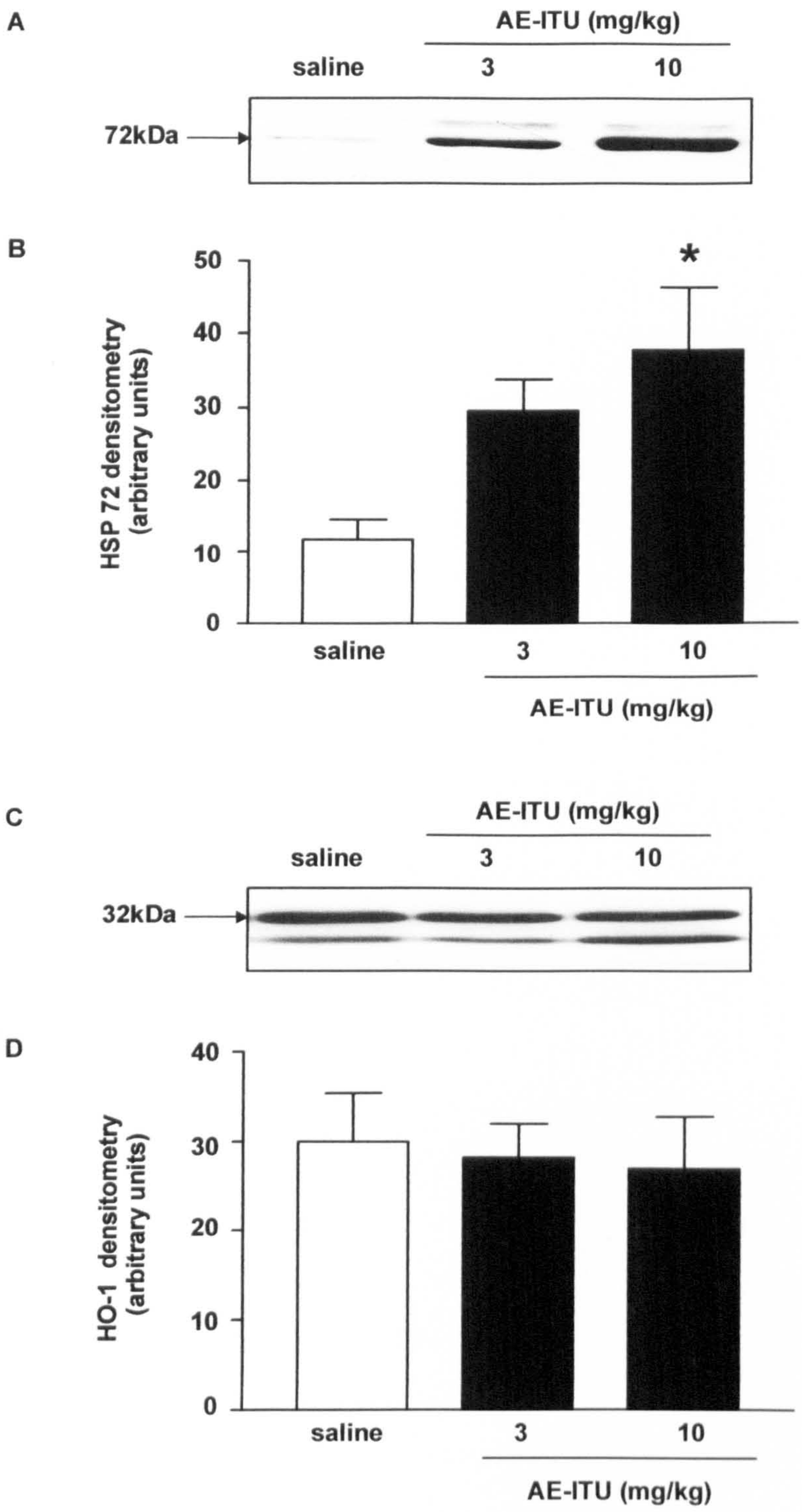

Figure 4.17 Expression of HSP 72 and HO-1 protein in inflammatory cells taken from the pleural cavity of male wistar rats at 72h. *Panel (A) is a representative Western blot of HSP 72, (B) densitometrical analysis of HSP 72 Western blots expressed as arbitrary units, (C) is a representative Western blot of HO-1, (B) densitometrical analysis of HO-1 Western blots expressed as arbitrary units. In panels B and D, data is expressed as mean ± standard error of the mean (n=6 per group). *p≤0.05 in comparison to saline controls.*

4.3 Summary of findings

(1) In the carrageenin-induced pleurisy injection of NOS inhibitors, regardless of selectivity between isoforms, resulted in an increase in exudate volume and inflammatory cell number in the pleural cavity of treated animals at 1,6 and 36h. Furthermore, this observed increase in inflammation during the normal time course of this inflammatory model resulted in a prolonged pathology as seen at 72h.

(2) In contrast, administering NOS inhibitors systemically ameliorated the severity of inflammation throughout the reaction and is in keeping with data presented in the literature where NOS inhibitors were given away from the site of inflammation.

(3) Local inhibition of NO synthesis in the pleural cavity of rats resulted in an augmentation of the pro-inflammatory mediators CINC and LTB_4 which would in part explain the elevated proportion of PMNs observed in the pleural cavity at 6h after carrageenin injection. In addition, local administration of NOS inhibitors in this model resulted in a decrease in intact mast cells and an increase in histamine levels, which may be partly responsible for the increase in exudate volume after NOS inhibition since, prior depletion of mast cells ameliorated this effect.

(4) Local inhibition of NO also resulted in a significant reduction in antioxidant levels in cells and cell-free exudate at both 1 and 6h taken from the pleural cavity. This may be reflective of an increase in oxidative stress in this cavity after NOS inhibition. In addition, an increase in HSP 72 immunoreactivity, a marker of cellular stress, was observed at 72h

CHAPTER 5

CHAPTER 5. *NO inhibition in the murine chronic granulomatous tissue air pouch*

5.1 Introduction

In the rat carrageenin-induced pleurisy local inhibition of NO production exacerbated inflammation and prolonged resolution. This led to the conclusion that NO was protective in this model. Therefore these studies were extended to a model of chronic inflammation to establish whether or not a similar protective role for NO could be assigned to the development of a chronic inflammatory lesion. The tools used for this study included NOS inhibitors and genetic deletion of the iNOS gene. The effects of NOS inhibition was evaluated on granuloma dry weight, vascularity, NOS pathway and arginase activity and prostaglandin production.

In Chapter 3, it was demonstrated that iNOS protein expression, iNOS activity, nitrite, arginase activity and COX activity were maximal between 5 and 7 days. Maximal expression of these different pathways were at a time where granuloma formation was at a peak. cNOS activity was highest at 24h, a time prior to maximal vascularity. The majority of iNOS staining was immunolocalised to influxing inflammatory cells in the granuloma, with the majority of NO production being formed from the iNOS isoform. Therefore, the effects of NOS inhibition in this croton oil -induced chronic granulomatous tissue air pouch model were assessed at various time points up to 28 days.

5.2 Effect of NOS inhibition in the murine croton oil-induced chronic granulomatous tissue air pouch

5.2.1 Effect of oral administration of aminoguanidine on the nitric oxide pathway

Measurement of nitrite levels was only possible at up to 7 days, therefore the effect of aminoguanidine on nitrite levels was assessed at 0.25, 0.5, 1, 5 and 7 days. Nitrite levels were below the detection limit of the assay prior to the day 1 time point. However, at 1, 5 and 7 days aminoguanidine (150mg/kg) significantly decreased nitrite levels in cell free exudate by 100, 53 and 35% (Figure 5.1).

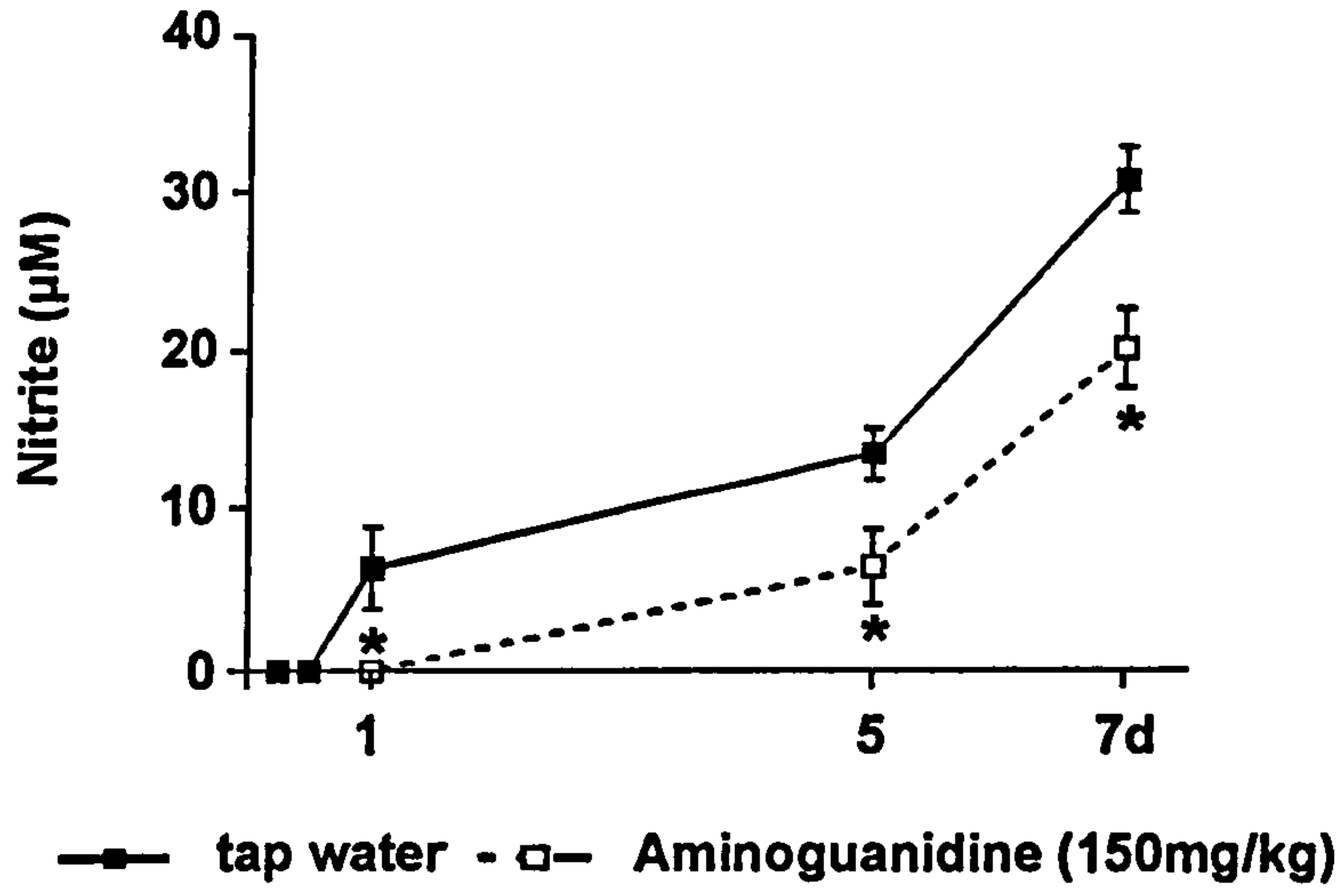

Figure 5.1 Effect of the relatively selective iNOS inhibitor aminoguanidine on nitrite levels in cell-free exudates from the murine croton oil-induced chronic granulomatous tissue air pouch. *Aminoguanidine was dissolved in tap water and given to mice every day (0-28 days). Data is expressed as mean ± standard error of the mean (n=5 per treatment group and per time point). *p≤0.05 in comparison to control values.*

Aminoguanidine (150mg/kg) was assessed on NOS enzyme activity in the granuloma. Aminoguanidine (150mg/kg) had no effect on iNOS enzyme activity in granulomatous tissue of treated mice at 0.25, 0.5, 1, 5, 7, 14, 21 and 28 days, compared to saline controls; 0 ± 0, 0 ± 0, 41 ± 31, 190 ± 74, 501 ± 105, 241 ± 68, 165 ± 78, 174 ± 90 pmol citruline/mg protein/30min (Figure 5.2A).

Similarly to iNOS, cNOS activity was unaffected by aminoguanidine treatment throughout the time course compared with tap water controls 24 ± 7, 47 ± 17, 153 ± 34, 67 ± 24, 159 ± 36, 68 ± 14, 44 ± 8, 58 ± 19 pmol citruline/mg protein/30min; Figure 5.2B).

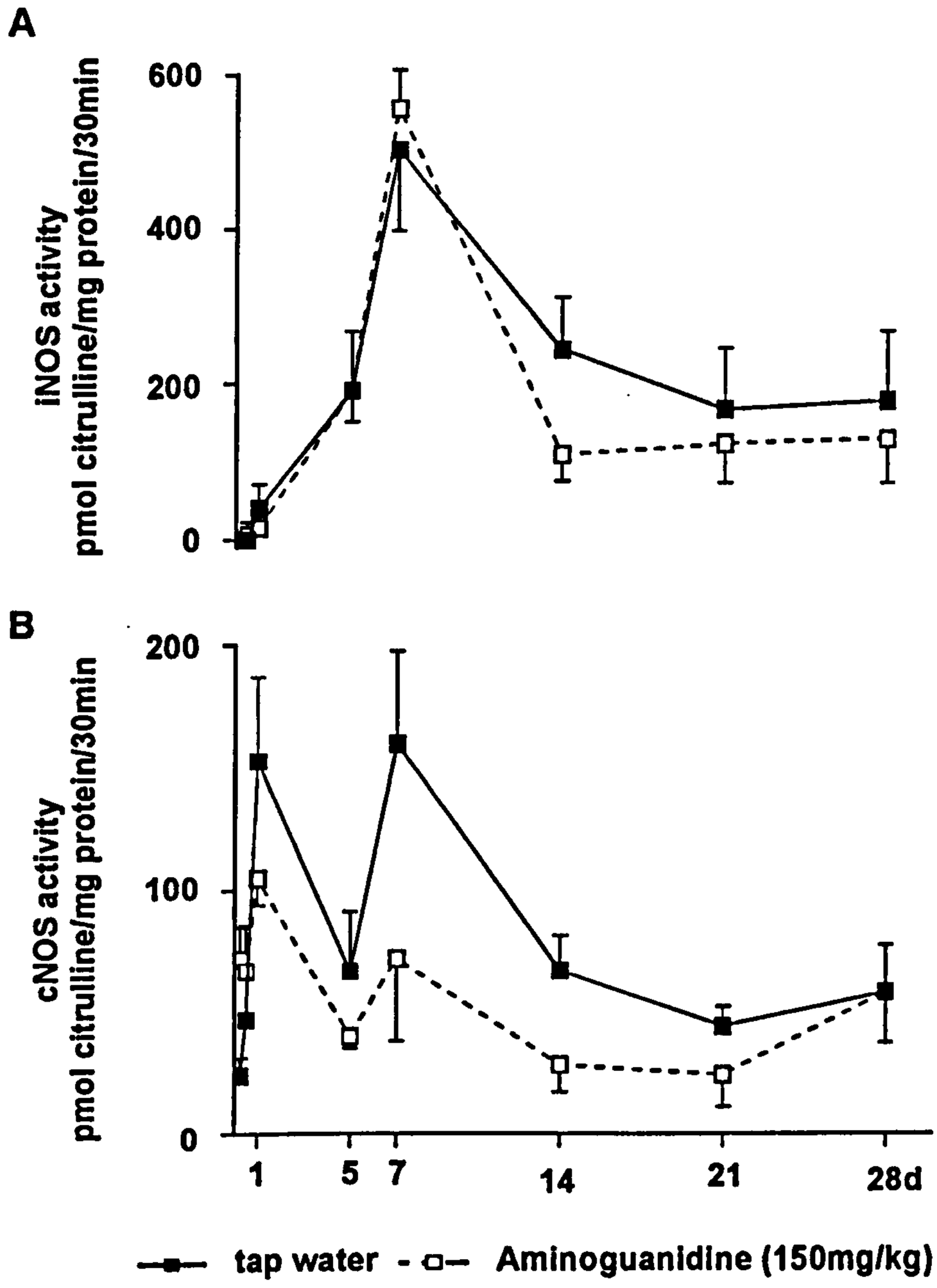

Figure 5.2 Effect of the selective iNOS inhibitor aminoguanidine on iNOS and cNOS enzyme activity in granulomatous tissue. *Where panel (A) is iNOS activity and (B) cNOS activity. Aminoguanidine was dissolved in tap water and given to mice every day (0-28 days). Data is expressed as mean ± standard error of the mean (n=5 per treatment group and per time point).*

Supporting the findings on iNOS activity in the granuloma, aminoguanidine at 5, 7 and 14 days had no effect on the expression of iNOS protein (Figure 5.3)

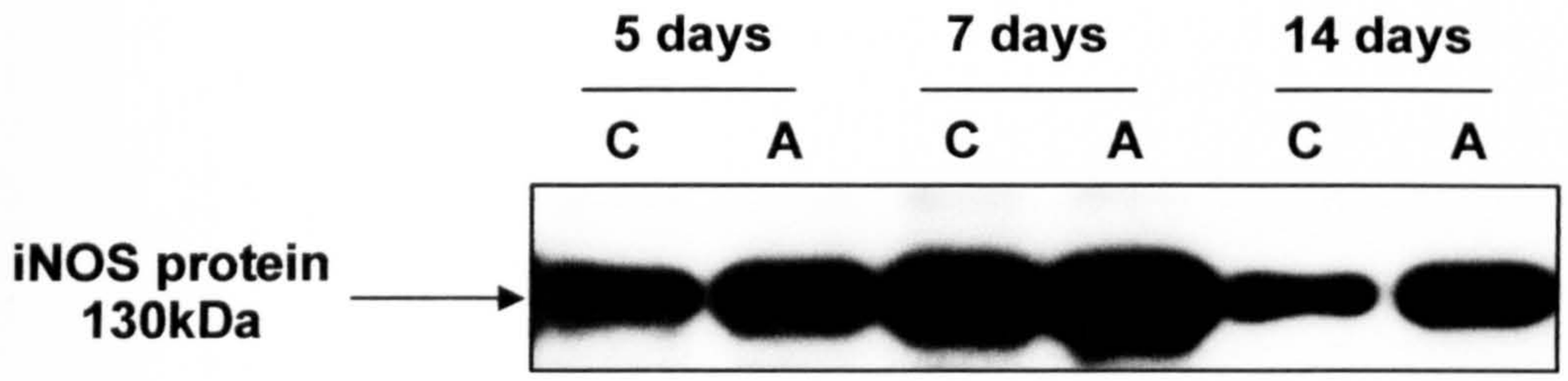

Figure 5.3 Effect of the selective iNOS inhibitor aminoguanidine on iNOS protein expression in granulomatous tissue. *iNOS protein expression was assessed at 5, 7 and 14 days post initiation. C represents control samples (tap water) and A aminoguanidine (150mg/kg) treated animals.*

5.2.2 Effect of oral administration of aminoguanidine on the arginase activity

Regulatory effects of the NOS inhibition on arginase activity were evaluated in this chronic model.

Similar to the effects on the iNOS, arginase activity was not affected by inhibition of NO production by aminoguanidine, with levels in the tap water controls being; 7.0 ± 0.9, 4.5 ± 0.4, 13.5 ± 3.8, 113.8 ± 31.4, 71.5 ± 16.5, 49.6 ± 5.2, 24.5 ± 3.8, 22.4 ± 5.1 mU urea/mg protein/min (Figure 5.4).

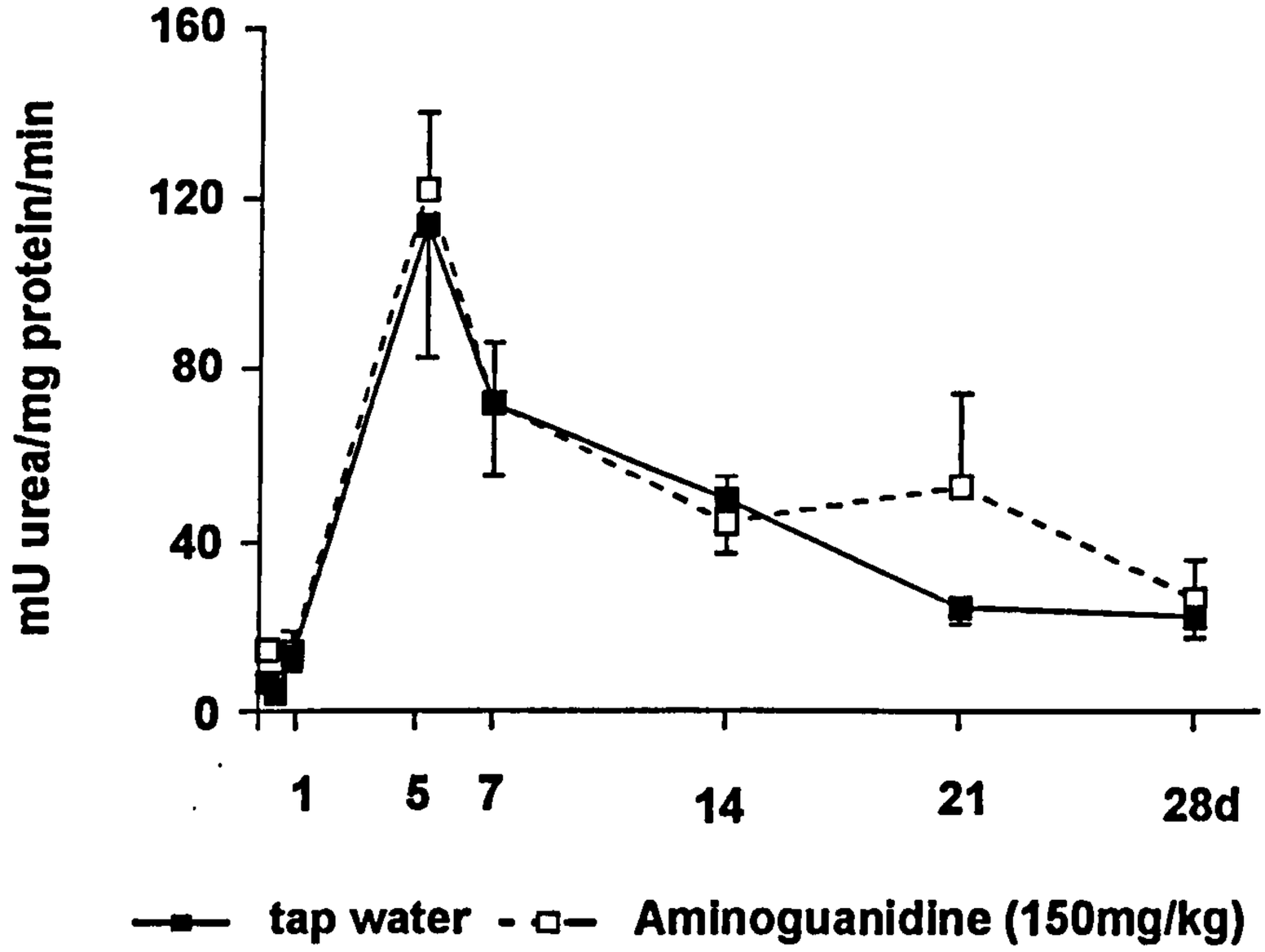

Figure 5.4 Effect of the selective iNOS inhibitor aminoguanidine on arginase activity in the murine croton oil-induced chronic granulomatous tissue air pouch. *Aminoguanidine was dissolved in tap water and given to mice every day (0-28 days). Data is expressed as mean ± standard error of the mean (n=5 per treatment group and per time point).*

5.2.3 Effect of oral administration of aminoguanidine on granulomatous tissue dry weight, carmine content and vascularity

Effect of aminoguanidine (150mg/kg) was assessed on granulomatous tissue dry weight, carmine content and vascularity at 7 and 14 days. 7 days of aminoguanidine treatment significantly reduced ($p \leq 0.05$) granulomatous tissue dry weight (83.8 ± 4.8 mg) compared to tap water controls (111.4 ± 8.5 mg; Figure 5.5A). By 14 days granuloma dry weights in treated (66.6 ± 6.8 mg) and control animals (68.0 ± 5.6 mg) were similar. The vascular component of this granulomatous tissue as measured by carmine content was also significantly reduced by aminoguanidine treatment to 435 ± 40 µg carmine compared to control values, 822 ± 99 µg carmine (Figure 5.5B). As with the dry weight measurements the reduction observed at 7 days was no longer evident by 14 days, with control values being 286 ± 21 µg carmine and aminoguanidine treated animals containing 368 ± 52 µg carmine. Angiogenesis in the chronic air pouch was measured as a ratio between camine content and granuloma dry

weight and referred to as the vascular index. Control tissues had a vascular index of 7.51 ± 0.77 µg carmine/mg tissue (Figure 5.5C), this was significantly reduced by aminoguanidine treatment to 5.19 ± 0.41 µg at 7 days. By 14 days of aminoguanidine treatment, the vascular index of controls (0.24 ± 0.02 µg carmine/mg tissue) and aminoguanidine treated (0.20 ±0.03 µg carmine/mg tissue) rats were again similar.

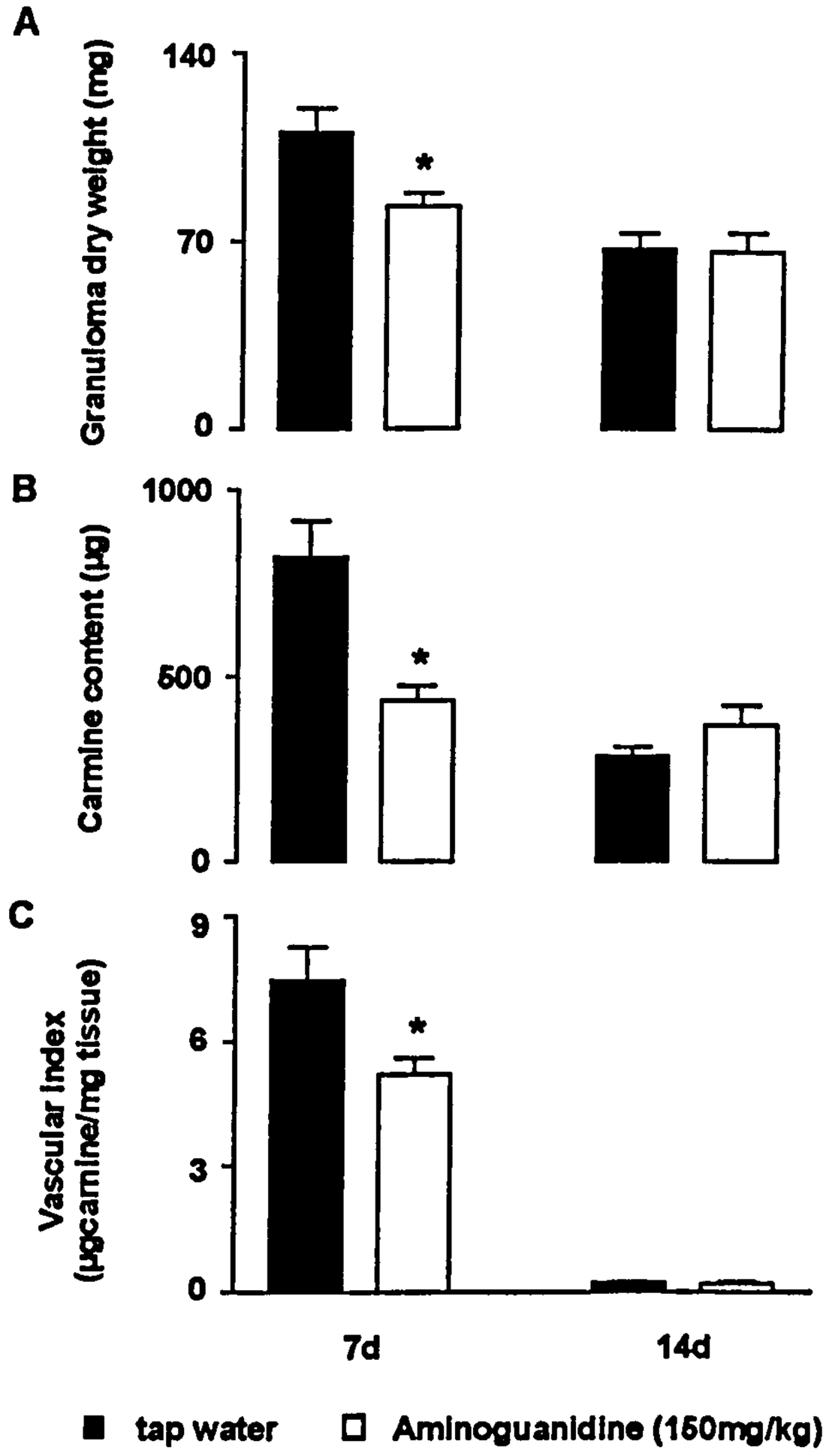

Figure 5.5 Effect of the selective iNOS inhibitor aminoguanidine on granulomatous tissue formation and angiogenesis in the murine croton oil-induced chronic granulomatous tissue air pouch. *Where, granuloma dry weight (A), carmine content (B) and vascular index (C). Aminoguanidine was dissolved in tap water and given to mice every day (0-14 days). Data is expressed as mean ± standard error of the mean (n=12 per treatment group and per time point). *p≤0.05 in comparison to control values.*

The decrease in the vascular content of the granuloma was confirmed by morphometric analysis of PECAM (CD 31) staining of endothelial cells within the granuloma, where aminoguanidine treatment reduced the number of immunopositive cells by 19%. Again like with carmine analysis, the reduction observed was only transient, with no differences in vascular volume at 14 days between aminoguanidine treated animals and controls (data not shown).

5.2.4 Effect of local injection of AE-ITU on nitrite, granuloma dry weight, carmine content and vascularity

In the acute model (Chapter 4), NOS inhibition had a differential effect on inflammation depending on the route of administration. Systemic inhibition caused a significant decrease in inflammatory parameters, whereas local injection of NOS inhibitors increased inflammation. Therefore, the effect of local injection of the iNOS selective inhibitor AE-ITU (3, 30mg/kg) was assessed on nitrite and lesion formation in the chronic granulomatous tissue air pouch at 7 days. AE-ITU was dissolved in sterile saline and injected intrapouch from day 0-7.

Intrapouch injection of AE-ITU significantly ($p \leq 0.05$) reduced nitrite levels in cell-free inflammatory exudates at 30mg/kg (8.4 ±1.5μM), whereas at 3mg/kg AE-ITU it was without effect compared to saline controls (18.0 ± 2.7μM; Figure 5.6A).

In addition, intrapouch injection of AE-ITU significantly reduced the dry mass of the granuloma, again with AE-ITU being significant at 30mg/kg (52 ± 6 mg), whereas at 3mg/kg there was no effect compared to saline treated animals (75 ± 8 mg; Figure 5.6B).

Intrapouch injection of AE-ITU had no effect on the vascular content of the air pouch (Figure 5.6C). However, this resulted in a significant increase in the vascular index of the granulomatous tissue only at the 30mg/kg dose (13.11 ± 2.17 μg carmine/mg tissue) compared to saline controls (7.59 ± 1.22 μg carmine/mg tissue; Figure 5.6D).

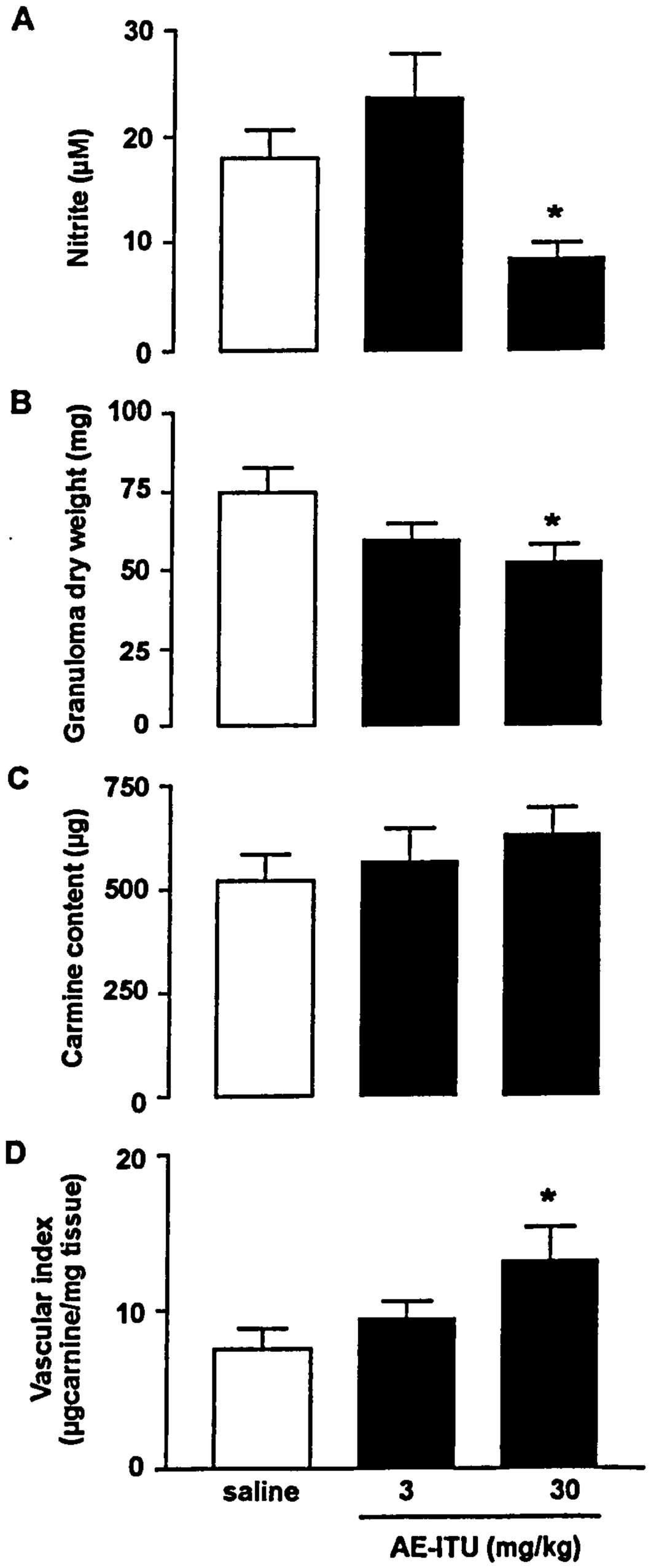

Figure 5.6 Effect of the selective iNOS inhibitor AE-ITU on granulomatous tissue formation, angiogenesis and nitrite formation in the murine croton oil-induced chronic granulomatous tissue air pouch. *Where, (A)is nitrite accumulation,(B) granuloma dry weight, (C) carmine content and (D) vascular index. AE-ITU was dissolved in saline and injected intrapouch every day (0-7 days). Data is expressed as mean ± standard error of the mean (n=5-8 per treatment group). *p≤0.05 in comparison to control values.*

5.3 Effect of iNOS gene deletion in the murine croton oil-induced chronic granulomatous tissue air pouch

Pharmacological inhibition of iNOS revealed an inhibitory effect on the formation of granulomatous tissue at 7days, when administered both systemically and locally. A differential effect on vascular index was observed when iNOS inhibitors were given orally or intrapouch. Systemic inhibition of NO resulted in a decrease in vascular index, whereas local inhibition caused a significant increase although the NOS inhibitors used were different. As with the carrageenin-induced pleurisy in the rat (Chapter 4), these contrary effects may have resulted from a degree of inhibition of ecNOS both systemically and within the granuloma or by virtue of the different NOS inhibitors and concentrations of these compounds used. Therefore, in an attempt to resolve this complex issue, iNOS deficient mice were employed as a tool to differentiate between inhibition of iNOS and ecNOS.

5.3.1 Effect on granulomatous tissue dry weight, carmine content and vascularity in the granuloma

Initially, SV129 mice (wild type controls for iNOS knockout mice) were examined for their response to croton oil and Freunds complete adjuvant mixture (5, 7 and 14 days). This was carried out to establish whether these in bred mice reacted similarly to the outbred Swiss albino mice (T_0 mice), the normal species used in this model.

SV129 mice had a granuloma dry weight of 44.0 ± 3.5, 70.0 ± 9.7 and 37.3 ± 5.5 mg at 5, 7 and 14 days respectively (Figure 5.7A). The vascular component of this granulomatous tissue as measured by carmine content was 260 ± 33, 555 ± 68 and 173 ± 31 µg carmine at 5, 7 and 14 days respectively (Figure 5.7B). This resulted in a vascular index of 6.01 ± 0.95, 8.15 ± 1.13 and 4.58 ± 0.22 µg carmine/mg tissue at 5, 7 and 14 days respectively (Figure 5.7C).

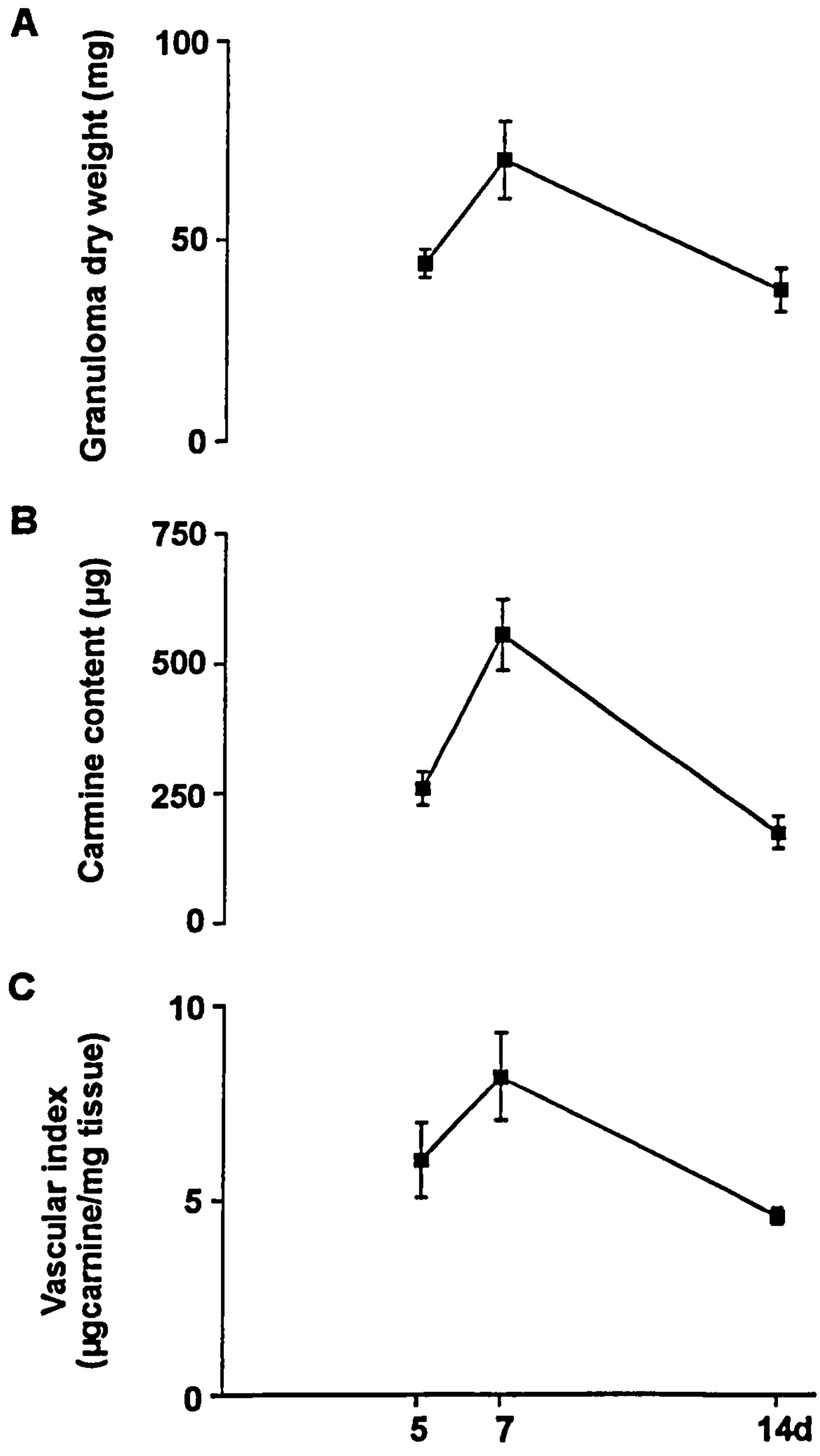

Figure 5.7 The profile of granulomatous tissue formation and angiogenesis in the murine croton oil-induced chronic granulomatous tissue air pouch in wild type mice (sv129). *Granuloma dry weight (A), carmine content (B) and vascular index (C) in sv129 mice at 5, 7 and 14 days. Data is expressed as mean ± standard error of the mean (n=3 per time point).*

Since, the profile of inflammation was similar in sv129 and T_0 mice the effect of iNOS deletion was assessed in this chronic inflammatory model at 7 days, the peak in the inflammatory response.

iNOS gene deletion significantly ($p \leq 0.05$) reduced the dry mass of the granuloma to (86.1 ± 5.5 mg), with control values being 118.8 ± 10.4 mg (Figure 5.8A). whereas iNOS knockout mice had the same vascular content as wild type control (Figure 5.8B).

However, this resulted in a significant increase in the vascular index of the granulomatous tissue in iNOS knockout animals (10.56 ± 0.58 µg carmine/mg tissue) compared with sv129 mice (7.04 ± 0.41 µg carmine/mg tissue; Figure 5.8C).

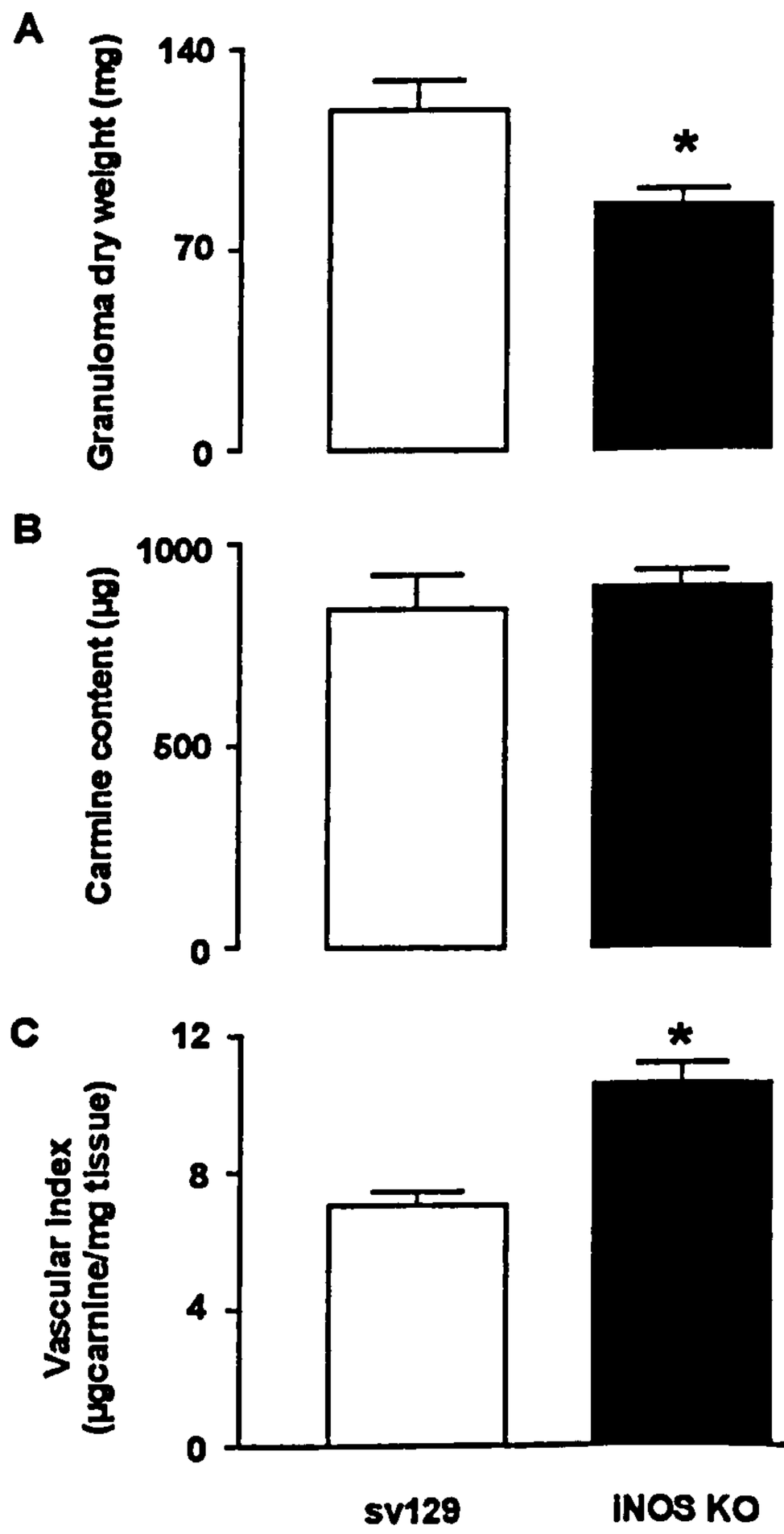

Figure 5.8 Effect of iNOS gene deletion on granulomatous tissue formation and angiogenesis in the murine croton oil-induced chronic granulomatous tissue air pouch. *Where, (A)is granuloma dry weight, (B) carmine content and (C) vascular index. Data is expressed as mean ± standard error of the mean (n=8 per group). *$p \leq 0.05$ in comparison to control values.*

Morphometric analysis of PECAM (CD 31) staining showed that there was an increase (16%) in the number vessels as a percentage of total granuloma area, when compared to wild type controls. Representative pictures of the section analysed are depicted in Figure 5.9. With (A) representing sv129 control animals and (B) being iNOS deficient mice. In general CD 31 staining can be seen in larger vessels in the skin and in capillaries that are present in the granulomatous tissue during its formation.

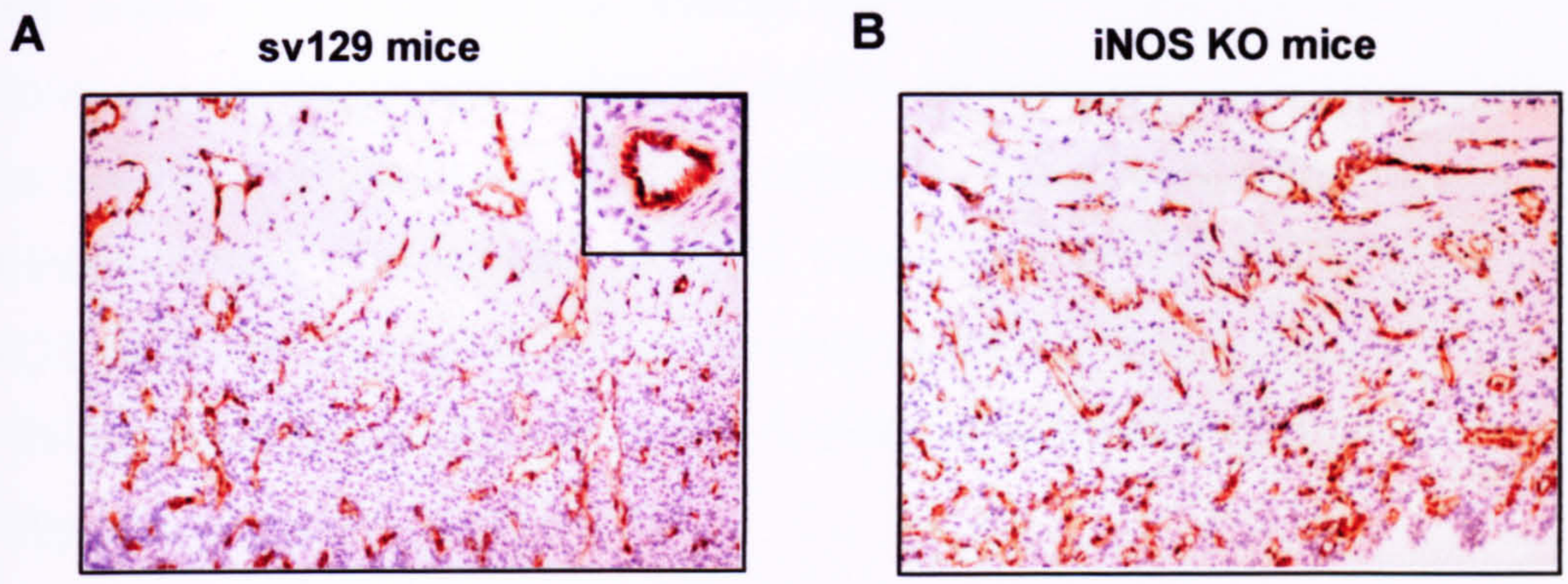

Figure 5.9 Spacial expression of PECAM (CD 31) staining in the granuloma taken from iNOS knockout and wild type mice*. Where, (A) is sv129 mice and (B) iNOS knockout mice 7 days after induction of granuloma formation with 0.1% croton oil in Freund's complete adjuvant. For the morphometric analysis n=6 animals were used. The magnification of the major panels is x63, with the insert in (A) showing a high power picture of a vessel and its endothelial cells (magnification x200).*

5.3.2 Effect on the nitric oxide pathway

The effect of iNOS gene deletion was assessed on iNOS activity, nitrite, iNOS protein expression and iNOS cellular localisation in the granuloma. iNOS gene deletion reduced nitrite levels close to baseline values (4.6 ± 1.3μM), compared to wild type controls (35.2 ± 3.6μM).

Similarly, iNOS activity was reduced to the detection limit of the assay in iNOS knockout mice (996 ± 289 pmol citrulline/mg protein/30 min) when compared to sv129 mice (185 ± 54 pmol citrulline/mg protein/30 min).

Interestingly, cNOS (ecNOS and nNOS) levels were unaffected, this was

surprising since some compensation from ecNOS and nNOS was expected, with iNOS knockout mice producing 119 ± 33 pmol citrulline/mg protein/30 min and control animals 93 ± 25 pmol citrulline/mg protein/30 min (Figure 5.10).

Western blot analysis of iNOS knockout mice and sv129 showed that both types of mice produced similar levels of iNOS protein (Figure 5.11A). The antibody used for the detection of iNOS was purchased from Santa Cruz, it was raised to amino acids 1126-1144 at the carboxy terminus of iNOS. A blast search was performed and it was found that this amino acid sequence is not present on either eNOS or nNOS. In addition, Chandrasekar and colleagues (1998) showed that this antibody was specific to iNOS, showing no cross-reactivity with either ecNOS or nNOS. Therefore, it was concluded that the iNOS protein detected in the iNOS knockout animals was non-functional since little product or enzyme activity was detected (Figure 5.10).

Spatial analysis of iNOS protein expression in the wild type (Figure 5.11B) and iNOS gene deleted animals (Figure 5.11C) at 7 days revealed a similar distribution of both the functional and non-functional protein within the skin and regions of the granuloma. The most intense staining of iNOS was associated with infuxing inflammatory cells in vessels in the skin and at the lower regions of the granuloma furthest from the skin. NADPH diaphorase staining (old method for detection of iNOS) revealed a slight reduction in staining in iNOS knockout mice (5.11E) compared with wild type controls (Figure 5.11D). However the number of stained cells per section was too low for morphometric analysis to be meanigful.

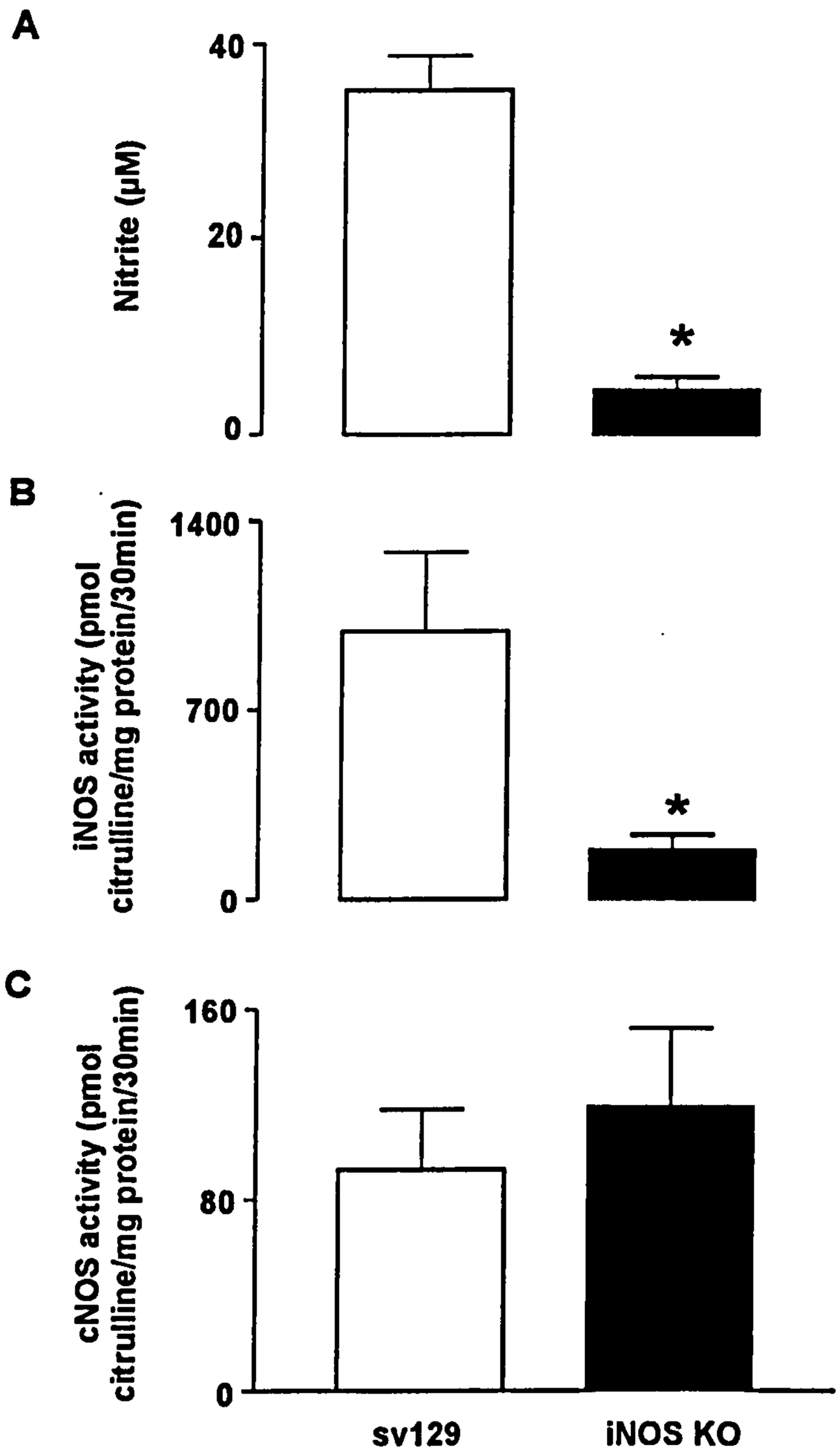

Figure 5.10 Effect of iNOS gene deletion on the NOS pathway in the murine croton oil-induced chronic granulomatous tissue air pouch. *Where, (A) is nitrite in cell-free exudate, (B) iNOS activity and (C) cNOS activity in the granuloma. Data is expressed as mean ± standard error of the mean (n=8 per group). *p≤0.05 in comparison to control values.*

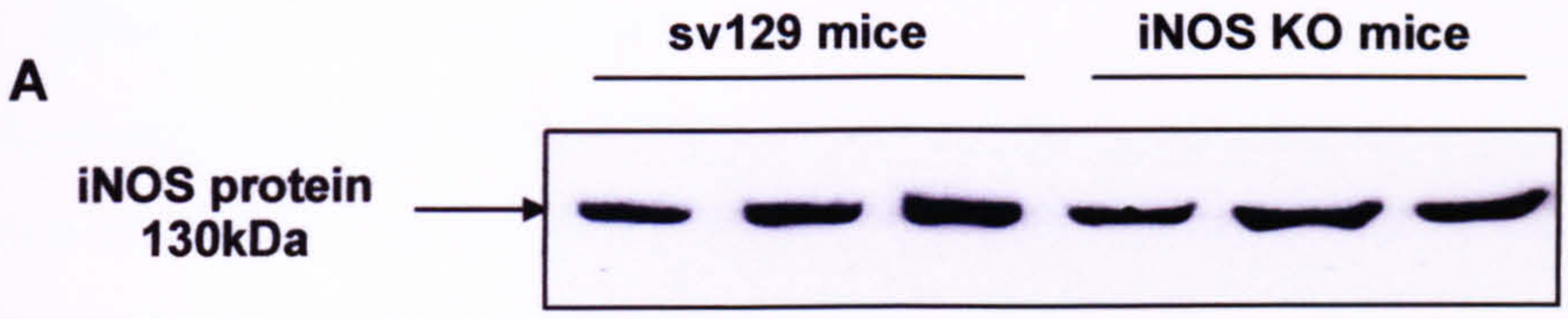

Figure 5.11 Quantitative and spacial analysis of iNOS protein expression in sv129 and iNOS knockout mice. *(A) is a representative Western blot (1 of 2) for iNOS protein in sV129 and iNOS knockout animal 7 days post injection of croton-oil in Freund's complete adjuvant. Where (B) is immunohistochemical analysis of iNOS protein expression in a 7 day air pouch of sv129 mice and (C) is immunohistochemical analysis of iNOS protein expression in a 7 day air pouch of iNOS gene deleted animals. (D) is NADPH diaphorase staining in a 7 day air pouch of sv129 mice, where the arrows indicate positively labeled cells for NADPH diaphorase activity and (E) is NADPH diaphorase staining in a 7 day air pouch of iNOS knockout mice . In (A) n=3 different animals were used, whereas panels B and C, D and E are Magnification x234. All immunohistochemistry pictures are representative of n=3 mice.*

5.3.3 Effect on the arginase

At 7 days arginase protein expression was slightly increased in iNOS knockout animals compared to controls (Figure 5.12A). This was also reflected in a significant increase ($p \geq 0.05$; Figure 5.12B) in arginase activity at this time point in iNOS gene deleted animals with an activity level of 179 ± 15 mU urea/mg protein/min compared to sv129 control mice (105 ± 9 mU urea/mg protein/min). The distribution of arginase staining in the granulomatous tissue was similar to iNOS, being associated with macrophages within the granuloma closest to the inflammatory stimulus and furthest from the skin (data not shown)

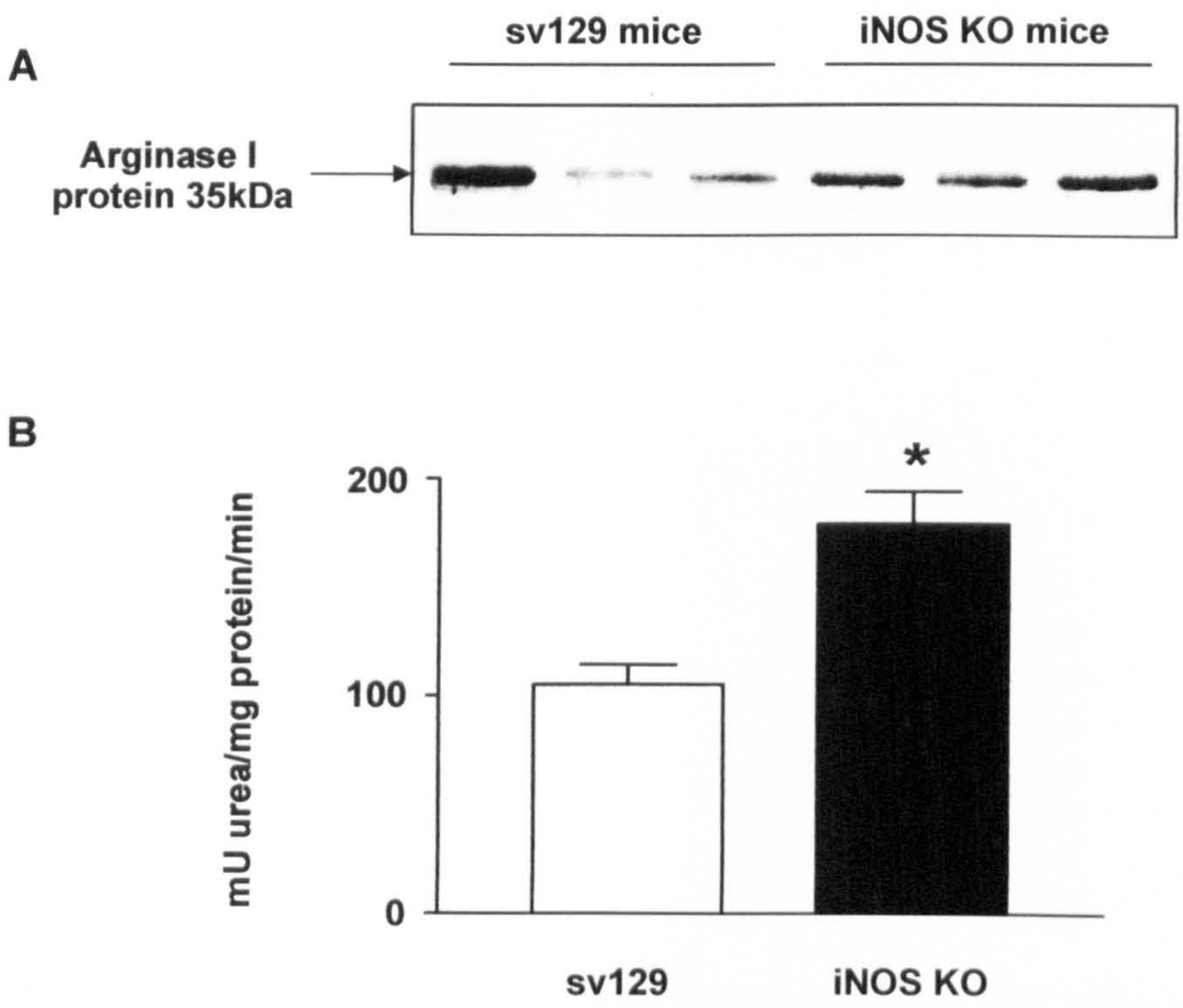

Figure 5.12 The effects of iNOS gene deletion on the expression of arginase in the murine croton oil-induced chronic granulomatous tissue air pouch. *Where, (A) is arginase I protein expression and (B) arginase activity in iNOS knockout mice compared to sv129 controls at 7 days. Data is expressed as mean ± standard error of the mean (n=8 per group). *$p \leq 0.05$ in comparison to control values.*

5.3.4 Effect on the general histological appearance of the air pouch

The general histological appearance of the air pouches from iNOS knockout and sv129 mice were very similar at 7 days. The granuloma was highly vascularised

with numerous PMNs and macrophages present in the loose connective tissue of the dermis and the occasional intact and degranulated mast cell was observed (Figure 5.13A, B). A region of active was observed above the skeletal muscle and below the skin and a high collagen content (vivid red coloration, Figure 5.13C, D)

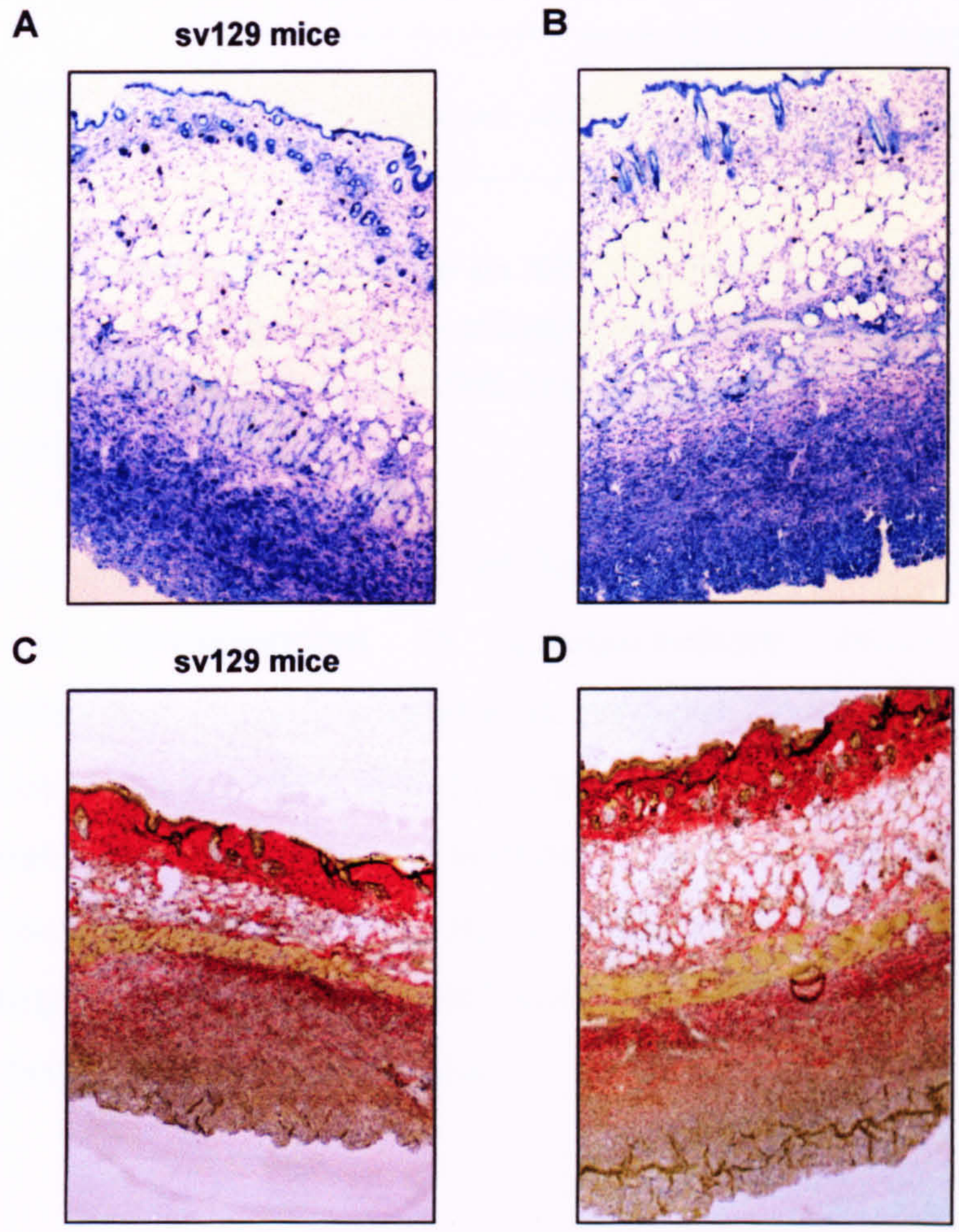

Figure 5.13 Effect of iNOS gene deletion on the histological appearance of the granuloma in the murine croton oil-induced chronic granulomatous tissue air pouch *Panel A (sv129 mice) and Panel B (iNOS knockout mice) shows a 7 day air pouch stained with toludine blue and Panel C (sv129 mice) and panel D (iNOS knockout mice) are Van Gieson stains. Panels A, B, C and D magnification x63.*

5.3.5 Effect on HSP protein expression

The effect of iNOS gene deletion was investigated on the expression of the heat shock proteins 70 and 32 (HO-1), since again it has been suggested that NO can modulate protein expression of these cellular chaperones (results section

Chapter 4 and Willis *et al.*, 1995). Densitometrical analysis of Western blots of of HSP 72 in both sv129 and iNOS knockout mice demonstrated no significant differences between the intensity of HSP 72 protein staining between the two groups of animals (Figure 5.14).

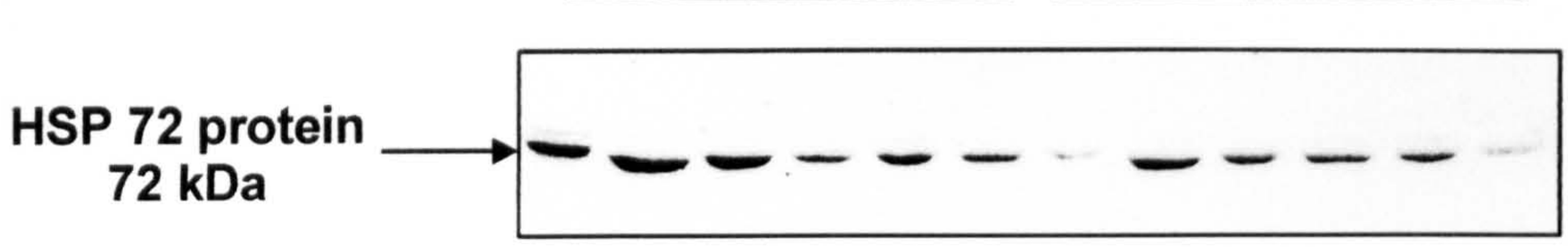

Figure 5.14 Effect of iNOS gene deletion on HSP 72 protein expression in the murine croton oil-induced chronic granulomatous tissue air pouch*. at 7 days after induction of granuloma formation with 0.1% croton oil in Freund's complete adjuvant. Protein expression in n=6 animal per group.*

Western blot analysis of HO-1 was not sensitive enough to pick up protein expression in homogenates of granulomatous tissue. Therefore, immunohistochemical analysis was used to compare the expression of HO-1 in iNOS knockout and sv129 mice. Immunolocalisation of HO-1 expression in these animals revealed that the majority of staining was associated with macrophage like cells (Figure 5.15) in the granuloma adjacent to the muscle layer that separates the granuloma spatially from the skin. Once again similar staining was observed in both iNOS and sv129 mice.

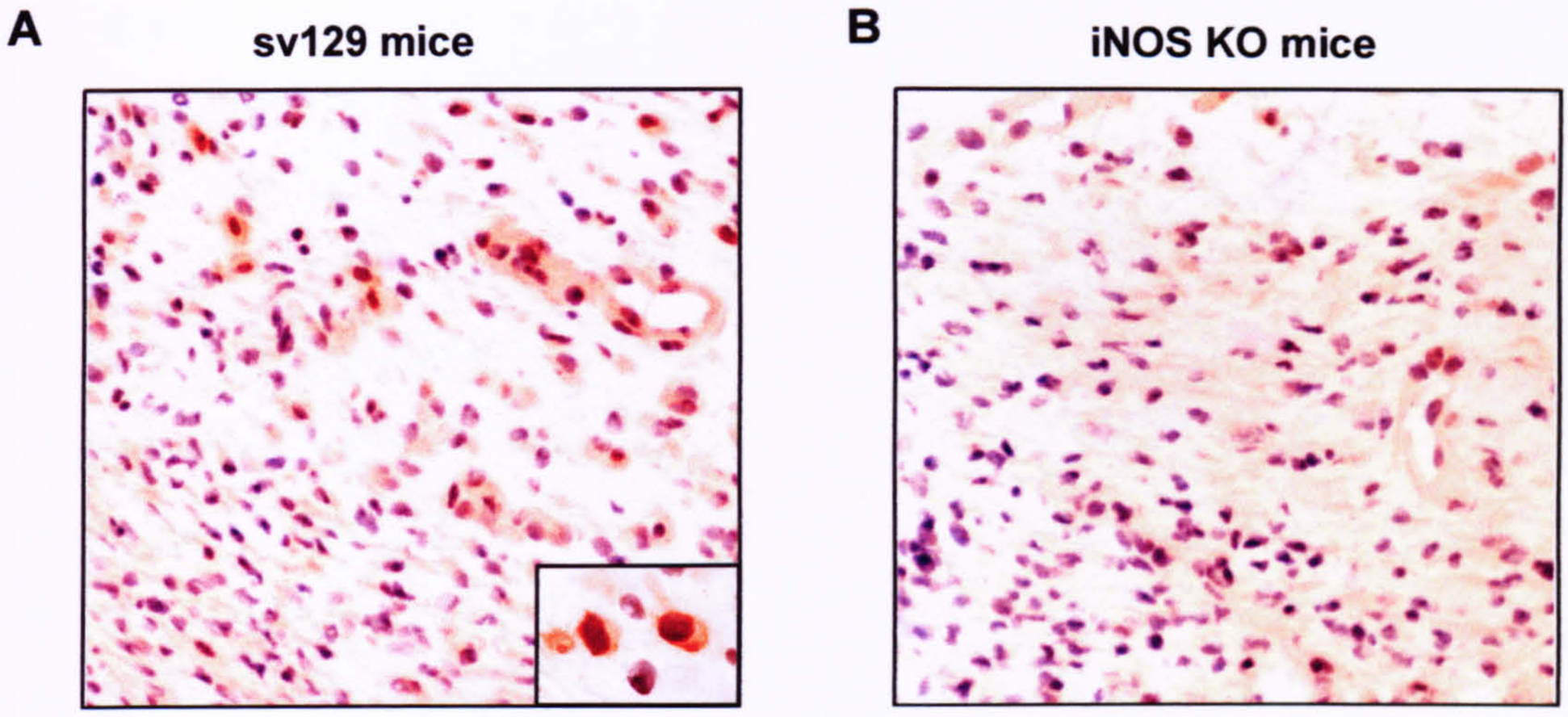

***Figure 5.15 Spacial expression of HO-1 staining in sv129 and iNOS knockout mice**. Where, (A)represents sv129 mice and (B) iNOS knockout mice 7 days after induction of granuloma formation with 0.1% croton oil in Freund's complete adjuvant. The magnification of the major panels is x63, with the insert in (A) showing a high power picture of a macrophage immunostained for HO-1 (magnification x200).*

5.3.6 Effect on COX-2 expression

The expression of COX-2 was analysed in iNOS knockout mice and sv129 controls. Densitometrical analysis revealed that iNOS gene deletion reduced the expression of COX-2 protein in this model, although this reduction didn't quite reach significance (Figure 5.16).

***Figure 5.16 Effect of iNOS gene deletion on COX-2 protein expression in the murine chronic granulomatous tissue air pouch.** Western blot analysis was performed on granulomatous tissue, 7 days after induction of granuloma formation with 0.1% croton oil in Freund's complete adjuvant. Protein expression in n=3 animal per group.*

5.4 Summary of findings

(1) Oral administration of aminoguanidine significantly decreased nitrite levels between 1-7 days. However no effect on iNOS, cNOS and arginase enzyme activity or iNOS protein expression was observed. However at 5 days hemeoxygenase activity was significantly increased. Systemic inhibition of NO production resulted in a significant decrease in granuloma dry weight, carmine content and vascular index of granulomas dissected from aminoguanidine treated mice. Similarly, local injection of AE-ITU (30mg/kg) significantly reduced nitrite and granulomatous tissue dry weight. However, carmine content was unaffected, leading to a significant increase in the vascular index.

(2) iNOS gene deletion had similar effects on inflammation to local administration of the selective iNOS inhibitor AE-ITU. Granuloma dry weight was significantly reduced without effect on carmine content of the granuloma. This resulted in a significant increase in the vascular index, which was confirmed by a 16% increase in CD31 immunostaining compared to wild type controls. Not surprisingly, nitrite and iNOS enzyme activity was reduced to the detection limits of the assays used. In addition, the general histological appearance of the air pouch in iNOS knockout and sv129 mice was similar with little to no effect on the spatial distribution of HO-1 and protein expression of COX-2. Arginase I protein expression and total arginase activity were significantly increased by iNOS gene deletion suggesting a possible regulatory effect of NO on arginase activity.

APPENDIX I

Abramson, S., H. Korchak, R. Ludewig, H. Edelson, K. Haines, R. I. Levin, R. Herman, L. Rider, S. Kimmel, and G. Weissmann. 1985. Modes of action of aspirin-like drugs. *Proc Natl Acad Sci U S A 82:7227.*

Abramson, S. B. 1992. Treatment of gout and crystal arthropathies and uses and mechanisms of action of nonsteroidal anti-inflammatory drugs. *Curr Opin Rheumatol 4:295.*

Aeberhard, E. E., S. A. Henderson, N. S. Arabolos, J. M. Griscavage, F. E. Castro, C. T. Barrett, and L. J. Ignarro. 1995. Nonsteroidal anti-inflammatory drugs inhibit expression of the inducible nitric oxide synthase gene. *Biochem Biophys Res Commun 208:1053.*

Albina, J. E., C. D. Mills, W. L. Henry, Jr., and M. D. Caldwell. 1990. Temporal expression of different pathways of 1-arginine metabolism in healing wounds. *J Immunol 144:3877.*

Albina, J. E., S. Cui, R. B. Mateo, and J. S. Reichner. 1993. Nitric oxide-mediated apoptosis in murine peritoneal macrophages. *J Immunol 150:5080.*

Amin, A. R., P. Vyas, M. Attur, J. Leszczynska-Piziak, I. R. Patel, G. Weissmann, and S. B. Abramson. 1995. The mode of action of aspirin-like drugs: effect on inducible nitric oxide synthase. *Proc Natl Acad Sci U S A 92:7926.*

Amon, U., M. Nitschke, D. Dieckmann, B. F. Gibbs, C. Wehrhahan, and H. H. Wolff. 1994. Activation and inhibition of mediator release from skin mast cells: a review of in vitro experiments. *Clin Exp Allergy 24:1098.*

Andrade, J., M. Conde, F. Sobrino, and F. J. Bedoya. 1993. Activation of peritoneal macrophages during the prediabetic phase in low-dose streptozotocin-treated mice. *FEBS Lett 327:32.*

Antunes, E., M. Mariano, G. Cirino, S. Levi, and G. de Nucci. 1990. Pharmacological characterization of polycation-induced rat hind-paw oedema. *Br J Pharmacol 101:986.*

Appleton, I., A. Tomlinson, P. R. Colville-Nash, and D. A. Willoughby. 1993. Temporal and spatial immunolocalization of cytokines in murine chronic granulomatous tissue. Implications for their role in tissue development and repair processes [see comments]. *Lab Invest 69:405.*

Appleton, I., A. Tomlinson, and D. A. Willoughby. 1997. Induction of cyclooxygenase and nitric oxide in inflammation. *Adv Pharmacol 35:27.*

Arnold, W. P., C. K. Mittal, S. Katsuki, and F. Murad. 1977. Nitric oxide activates guanylate cyclase and increases guanosine 3':5'- cyclic monophosphate levels in various tissue preparations. *Proc Natl Acad Sci U S A 74:3203.*

Asahi, M., J. Fujii, K. Suzuki, H. G. Seo, T. Kuzuya, M. Hori, M. Tada, S. Fujii, and N. Taniguchi. 1995. Inactivation of glutathione peroxidase by nitric oxide. Implication for cytotoxicity. *J Biol Chem 270:21035.*

Auphan, N., J. A. DiDonato, C. Rosette, A. Helmberg, and M. Karin. 1995. Immunosuppression by glucocorticoids: inhibition of NF-kappa B activity through induction of I kappa B synthesis. *Science 270:286.*

Baeuerle, P. A., and D. Baltimore. 1988. I kappa B: a specific inhibitor of the NF-kappa B transcription factor. *Science 242:540.*

Baeuerle, P. A. 1991. The inducible transcription activator NF-kappa B: regulation by distinct protein subunits. *Biochim Biophys Acta 1072:63.*

Balla, J., H. S. Jacob, G. Balla, K. Nath, J. W. Eaton, and G. M. Vercellotti. 1993. Endothelial-cell heme uptake from heme proteins: induction of sensitization and desensitization to oxidant damage. *Proc Natl Acad Sci U S A 90:9285.*

Barthlen, W., C. Klemens, S. Rogenhofer, J. Stadler, N. Unbehaun, and B. Holzmann. 2000. Critical role of nitric oxide for proliferation and apoptosis of bone- marrow cells under septic conditions. *Ann Hematol 79:249.*

Beckman, J. S., T. W. Beckman, J. Chen, P. A. Marshall, and B. A. Freeman. 1990. Apparent hydroxyl radical production by peroxynitrite: implications for endothelial injury from nitric oxide and superoxide. *Proc Natl Acad Sci U S A 87:1620.*

Bellmann, K., M. Jaattela, D. Wissing, V. Burkart, and H. Kolb. 1996. Heat shock protein hsp70 overexpression confers resistance against nitric oxide. *FEBS Lett 391:185.*

Bianchi, M., P. Ulrich, O. Bloom, M. Meistrell, 3rd, G. A. Zimmerman, H. Schmidtmayerova, M. Bukrinsky, T. Donnelley, R. Bucala, B. Sherry, and et al. 1995. An inhibitor of macrophage arginine transport and nitric oxide production (CNI-1493) prevents acute inflammation and endotoxin lethality. *Mol Med 1:254.*

Bieganski, T., J. Kusche, W. Lorenz, R. Hesterberg, C. D. Stahlknecht, and K. D. Feussner. 1983. Distribution and properties of human intestinal diamine oxidase and its relevance for the histamine catabolism. *Biochim Biophys Acta 756:196.*

Blantz, R. C., J. Satriano, F. Gabbai, and C. Kelly. 2000. Biological effects of arginine metabolites. *Acta Physiol Scand 168:21.*

Blaylock, M. G., B. H. Cuthbertson, H. F. Galley, N. R. Ferguson, and N. R. Webster. 1998. The effect of nitric oxide and peroxynitrite on apoptosis in human polymorphonuclear leukocytes. *Free Radic Biol Med 25:748.*

Bogle, R. G., A. R. Baydoun, J. D. Pearson, S. Moncada, and G. E. Mann. 1992. L-arginine transport is increased in macrophages generating nitric oxide. *Biochem J 284:15.*

Bolotina, V. M., S. Najibi, J. J. Palacino, P. J. Pagano, and R. A. Cohen. 1994. Nitric oxide directly activates calcium-dependent potassium channels in vascular smooth muscle. *Nature 368:850.*

Bolz, S. S., and U. Pohl. 1997. Indomethacin enhances endothelial NO release--evidence for a role of PGI2 in the autocrine control of calcium-dependent autacoid production. *Cardiovasc Res 36:437.*

Boucher, J. L., C. Moali, and J. P. Tenu. 1999. Nitric oxide biosynthesis, nitric oxide synthase inhibitors and arginase competition for L-arginine utilization. *Cell Mol Life Sci 55:1015.*

Boughton-Smith, N. K., A. M. Deakin, and B. J. Whittle. 1992. Actions of nitric oxide on the acute gastrointestinal damage induced by PAF in the rat. *Agents Actions Spec:C3.*

Boughton-Smith, N. K., S. M. Evans, C. J. Hawkey, A. T. Cole, M. Balsitis, B. J. Whittle, and S. Moncada. 1993a. Nitric oxide synthase activity in ulcerative colitis and Crohn's disease. *Lancet 342:338.*

Boughton-Smith, N. K., S. M. Evans, B. J. Whittle, and S. Moncada. 1993b. Induction of nitric oxide synthase in rat intestine and its association with tissue injury. *Agents Actions 38:C125.*

Boxer, L. A., and J. E. Smolen. 1988. Neutrophil granule constituents and their release in health and disease. *Hematol Oncol Clin North Am 2:101.*

Bradford, M. M. 1976. A rapid and sensitive method for the quantitation of microgram quantities of protein utilizing the principle of protein-dye binding. *Anal Biochem 72:248.*
Bredt, D. S., P. M. Hwang, C. E. Glatt, C. Lowenstein, R. R. Reed, and S. H. Snyder. 1991. Cloned and expressed nitric oxide synthase structurally resembles cytochrome P-450 reductase. *Nature 351:714.*

Brooks, A. C., C. J. Whelan, and W. M. Purcell. 1999. Reactive oxygen species generation and histamine release by activated mast cells: modulation by nitric oxide synthase inhibition. *Br J Pharmacol 128:585.*

Bulut, V., A. Severn, and F. Y. Liew. 1993. Nitric oxide production by murine macrophages is inhibited by prolonged elevation of cyclic AMP. *Biochem Biophys Res Commun 195:1134.*

Calabrese, V., A. Copani, D. Testa, A. Ravagna, F. Spadaro, E. Tendi, V. G. Nicoletti, and A. M. Giuffrida Stella. 2000. Nitric oxide synthase induction in astroglial cell cultures: effect on heat shock protein 70 synthesis and oxidant/antioxidant balance. *J Neurosci Res 60:613.*

Capasso, F., C. J. Dunn, S. Yamamoto, D. A. Deporter, J. P. Giroud, and D. A. Willoughby. 1975a. Pharmacological mediators of various immunological and non-immunological inflammatory reactions produced in the pleural cavity. *Agents Actions 5:528.*

Capasso, F., C. J. Dunn, S. Yamamoto, D. A. Willoughby, and J. P. Giroud. 1975b. Further studies on carrageenan-induced pleurisy in rats. *J Pathol 116:117.*

Chang, C. I., J. C. Liao, and L. Kuo. 1998. Arginase modulates nitric oxide production in activated macrophages. *Am J Physiol 274:H342.*

Chartrain, N. A., D. A. Geller, P. P. Koty, N. F. Sitrin, A. K. Nussler, E. P. Hoffman, T. R. Billiar, N. I. Hutchinson, and J. S. Mudgett. 1994. Molecular cloning, structure, and chromosomal localization of the human inducible nitric oxide synthase gene. *J Biol Chem 269:6765.*

Chayen, J., and L. Bitensky. 1971. Lysosomal enzymes and inflammation with particular reference to rheumatoid diseases. *Ann Rheum Dis 30:522.*

Chen, K., and M. D. Maines. 2000. Nitric oxide induces heme oxygenase-1 via mitogen-activated protein kinases ERK and p38. *Cell Mol Biol (Noisy-le-grand) 46:609.*

Chiesi, M., and R. Schwaller. 1995. Inhibition of constitutive endothelial NO-synthase activity by tannin and quercetin. *Biochem Pharmacol 49:495.*

Chu, S. C., H. P. Wu, T. C. Banks, N. T. Eissa, and J. Moss. 1995. Structural diversity in the 5'-untranslated region of cytokine- stimulated human inducible nitric oxide synthase mRNA. *J Biol Chem 270:10625.*

Chu, S. C., J. Marks-Konczalik, H. P. Wu, T. C. Banks, and J. Moss. 1998. Analysis of the cytokine-stimulated human inducible nitric oxide synthase (iNOS) gene: characterization of differences between human and mouse iNOS promoters. *Biochem Biophys Res Commun 248:871.*

Clancy, R. M., and S. B. Abramson. 1992. Novel synthesis of S-nitrosoglutathione and degradation by human neutrophils. *Anal Biochem 204:365.*

Closs, E. I., C. R. Lyons, C. Kelly, and J. M. Cunningham. 1993. Characterization of the third member of the MCAT family of cationic amino acid transporters. Identification of a domain that determines the transport properties of the MCAT proteins. *J Biol Chem 268:20796.*

Cobb, J. P., C. Natanson, W. D. Hoffman, R. F. Lodato, S. Banks, C. A. Koev, M. A. Solomon, R. J. Elin, J. M. Hosseini, and R. L. Danner. 1992. N omega-amino-L-arginine, an inhibitor of nitric oxide synthase, raises vascular resistance but increases mortality rates in awake canines challenged with endotoxin. *J Exp Med 176:1175.*

Colville-Nash, P. R., and D. W. Gilroy. 2000. Cyclooxygenase enzymes as targets for the therapeutic intervention in inflammation. *Drug News and Perspectives 13:587.*

Connor, J. R., P. T. Manning, S. L. Settle, W. M. Moore, G. M. Jerome, R. K. Webber, F. S. Tjoeng, and M. G. Currie. 1995. Suppression of adjuvant-induced arthritis by selective inhibition of inducible nitric oxide synthase. *Eur J Pharmacol 273:15.*

Cook, H. T., A. Jansen, S. Lewis, P. Largen, M. O'Donnell, D. Reaveley, and V. Cattell. 1994. Arginine metabolism in experimental glomerulonephritis: interaction between nitric oxide synthase and arginase. *Am J Physiol 267:F646.*

Corbett, J. A., R. G. Tilton, K. Chang, K. S. Hasan, Y. Ido, J. L. Wang, M. A. Sweetland, J. R. Lancaster, Jr., J. R. Williamson, and M. L. McDaniel. 1992. Aminoguanidine, a novel inhibitor of nitric oxide formation, prevents diabetic vascular dysfunction. *Diabetes 41:552.*

Corbett, J. A., A. Mikhael, J. Shimizu, K. Frederick, T. P. Misko, M. L. McDaniel, O. Kanagawa, and E. R. Unanue. 1993. Nitric oxide production in islets from nonobese diabetic mice: aminoguanidine-sensitive and -resistant stages in the immunological diabetic process. *Proc Natl Acad Sci U S A 90:8992.*

Corraliza, I. M., M. L. Campo, G. Soler, and M. Modolell. 1994. Determination of arginase activity in macrophages: a micromethod. *J Immunol Methods 174:231.*

Corraliza, I. M., G. Soler, K. Eichmann, and M. Modolell. 1995. Arginase induction by suppressors of nitric oxide synthesis (IL-4, IL- 10 and PGE2) in murine bone-marrow-derived macrophages. *Biochem Biophys Res Commun 206:667.*

Corrigan, C. J., and A. B. Kay. 1996. T-cell/eosinophil interactions in the induction of asthma. *Eur Respir J Suppl 22:72s.*

Corson, M. A., N. L. James, S. E. Latta, R. M. Nerem, B. C. Berk, and D. G. Harrison. 1996. Phosphorylation of endothelial nitric oxide synthase in response to fluid shear stress. *Circ Res 79:984.*

Croen, K. D. 1993. Evidence for antiviral effect of nitric oxide. Inhibition of herpes simplex virus type 1 replication. *J Clin Invest 91:2446.*

Curtis, J. F., N. G. Reddy, R. P. Mason, B. Kalyanaraman, and T. E. Eling. 1996. Nitric oxide: a prostaglandin H synthase 1 and 2 reducing cosubstrate that does not stimulate cyclooxygenase activity or prostaglandin H synthase expression in murine macrophages. *Arch Biochem Biophys 335:369.*

Darley-Usmar, V., H. Wiseman, and B. Halliwell. 1995. Nitric oxide and oxygen radicals: a question of balance. *FEBS Lett 369:131.*

David, P., H. Mayan, H. Cohen, D. M. Tal, and S. J. Karlish. 1992. Guanidinium derivatives act as high affinity antagonists of Na+ ions in occlusion sites of Na+,K(+)-ATPase. *J Biol Chem 267:1141.*

De Caterina, R., P. Libby, H. B. Peng, V. J. Thannickal, T. B. Rajavashisth, M. A. Gimbrone, Jr., W. S. Shin, and J. K. Liao. 1995. Nitric oxide decreases cytokine-induced endothelial activation. Nitric oxide selectively reduces endothelial expression of adhesion molecules and proinflammatory cytokines. *J Clin Invest 96:60.*

de Vera, M. E., R. A. Shapiro, A. K. Nussler, J. S. Mudgett, R. L. Simmons, S. M. Morris, Jr., T. R. Billiar, and D. A. Geller. 1996. Transcriptional regulation of human inducible nitric oxide synthase (NOS2) gene by cytokines: initial analysis of the human NOS2 promoter. *Proc Natl Acad Sci U S A 93:1054.*

Deakin, A. M., A. N. Payne, B. J. Whittle, and S. Moncada. 1995. The modulation of IL-6 and TNF-alpha release by nitric oxide following stimulation of J774 cells with LPS and IFN-gamma. *Cytokine 7:408.*

Deuel, T. F., R. S. Kawahara, T. A. Mustoe, and A. F. Pierce. 1991. Growth factors and wound healing: platelet-derived growth factor as a model cytokine. *Annu Rev Med 42:567.*

Devi, L., S. Petanceska, R. Liu, B. Arbabha, M. Bansinath, and U. Garg. 1994. Regulation of neuropeptide-processing enzymes by nitric oxide in cultured astrocytes. *J Neurochem 62:2387.*

Di Rosa, M., J. P. Giroud, and D. A. Willoughby. 1971. Studies on the mediators of the acute inflammatory response induced in rats in different sites by carrageenan and turpentine. *J Pathol 104:15.*

Di Rosa, M., A. Ialenti, A. Ianaro, and L. Sautebin. 1996. Interaction between nitric oxide and cyclooxygenase pathways. *Prostaglandins Leukot Essent Fatty Acids 54:229.*

Diaz, B. L., M. F. Serra, A. C. Alves, A. L. Pires, F. M. Correa, R. S. Cordeiro, M. A. Martins, and P. M. e Silva. 1996. Alloxan diabetes reduces pleural mast cell numbers and the subsequent eosinophil influx induced by allergen in sensitized rats. *Int Arch Allergy Immunol 111:36.*

Diaz-Flores, L., R. Gutierrez, and H. Varela. 1994. Angiogenesis: an update. *Histol Histopathol 9:807.*

Ding, A., C. F. Nathan, J. Graycar, R. Derynck, D. J. Stuehr, and S. Srimal. 1990. Macrophage deactivating factor and transforming growth factors-beta 1 - beta 2 and - beta 3 inhibit induction of macrophage nitrogen oxide synthesis by IFN-gamma. *J Immunol 145:940.*

Djukanovic, R. 2000. The role of co-stimulation in airway inflammation. *Clin Exp Allergy 30 Suppl 1:46.*

Dong, C., and R. A. Flavell. 2001. Th1 and Th2 cells. *Curr Opin Hematol 8:47.*

Doni, M. G., B. J. Whittle, R. M. Palmer, and S. Moncada. 1988. Actions of nitric oxide on the release of prostacyclin from bovine endothelial cells in culture. *Eur J Pharmacol 151:19.*

Drapier, J. C., and J. B. Hibbs, Jr. 1988. Differentiation of murine macrophages to express nonspecific cytotoxicity for tumor cells results in L-arginine-dependent inhibition of mitochondrial iron-sulfur enzymes in the macrophage effector cells. *J Immunol 140:2829.*

Duncan, M. R., and B. Berman. 1989. Differential regulation of collagen, glycosaminoglycan, fibronectin, and collagenase activity production in cultured human adult dermal fibroblasts by interleukin 1-alpha and beta and tumor necrosis factor-alpha and beta. *J Invest Dermatol 92:699.*

Duncan, M. R., and B. Berman. 1989. Differential regulation of glycosaminoglycan, fibronectin, and collagenase production in cultured human dermal fibroblasts by interferon-alpha, -beta, and -gamma. *Arch Dermatol Res 281:11.*

Durante, W., L. Liao, I. Iftikhar, W. E. O'Brien, and A. I. Schafer. 1996. Differential regulation of L-arginine transport and nitric oxide production by vascular smooth muscle and endothelium. *Circ Res 78:1075.*

Eissa, N. T., A. J. Strauss, C. M. Haggerty, E. K. Choo, S. C. Chu, and J. Moss. 1996. Alternative splicing of human inducible nitric-oxide synthase mRNA. tissue-specific regulation and induction by cytokines. *J Biol Chem 271:27184.*

Farrell, A. J., D. R. Blake, R. M. Palmer, and S. Moncada. 1992. Increased concentrations of nitrite in synovial fluid and serum samples suggest increased nitric oxide synthesis in rheumatic diseases. *Ann Rheum Dis 51:1219.*

Fehsel, K., K. D. Kroncke, K. L. Meyer, H. Huber, V. Wahn, and V. Kolb-Bachofen. 1995. Nitric oxide induces apoptosis in mouse thymocytes. *J Immunol 155:2858.*

Feldberg, W., and J. Talesnik. 1953. Reduction of tissue histamine by copound 48/80. *J Physiol 120:550.*

Feldman, P. L., O. W. Griffith, H. Hong, and D. J. Stuehr. 1993. Irreversible inactivation of macrophage and brain nitric oxide synthase by L-NG-methylarginine requires NADPH-dependent hydroxylation. *J Med Chem 36:491.*

Fernvik, E., J. Lundahl, and G. Hallden. 2000. The impact of eotaxin- and IL-5-induced adhesion and transmigration on eosinophil activity markers. *Inflammation 24:73.*

Fitch, F. W., R. Stack, P. Fields, D. W. Lancki, and D. C. Cronin. 1995. Regulation of T lymphocyte subsets. *Ciba Found Symp 195:68.*

Fleming, I., J. Bauersachs, B. Fisslthaler, and R. Busse. 1998. Ca2+-independent activation of the endothelial nitric oxide synthase in response to tyrosine phosphatase inhibitors and fluid shear stress. *Circ Res 82:686.*

Florey, H. W. 1970. *General pathology*. Lloyd-Luke, London.

Fortenberry, J. D., M. L. Owens, M. R. Brown, D. Atkinson, and L. A. Brown. 1998. Exogenous nitric oxide enhances neutrophil cell death and DNA fragmentation. *Am J Respir Cell Mol Biol 18:421.*

Frevert, C. W., S. Huang, H. Danaee, J. D. Paulauskis, and L. Kobzik. 1995. Functional characterization of the rat chemokine KC and its importance in neutrophil recruitment in a rat model of pulmonary inflammation. *J Immunol 154:335.*

Fujii, E., K. Irie, Y. Uchida, F. Tsukahara, and T. Muraki. 1994. Possible role of nitric oxide in 5-hydroxytryptamine-induced increase in vascular permeability in mouse skin. *Naunyn Schmiedebergs Arch Pharmacol 350:361.*

Fujimoto, Y., S. Tagano, K. Ogawa, S. Sakuma, and T. Fujita. 1998. Comparison of the effects of nitric oxide and peroxynitrite on the 12- lipoxygenase and cyclooxygenase metabolism of arachidonic acid in rabbit platelets. *Prostaglandins Leukot Essent Fatty Acids 59:95.*

Fukahori, M., K. Ichimori, H. Ishida, H. Nakagawa, and H. Okino. 1994. Nitric oxide reversibly suppresses xanthine oxidase activity. *Free Radic Res 21:203.*

Fukuto, J. M., G. C. Wallace, R. Hszieh, and G. Chaudhuri. 1992. Chemical oxidation of N-hydroxyguanidine compounds. Release of nitric oxide, nitroxyl and possible relationship to the mechanism of biological nitric oxide generation. *Biochem Pharmacol 43:607.*

Fukuto, J. M., D. J. Stuehr, P. L. Feldman, M. P. Bova, and P. Wong. 1993. Peracid oxidation of an N-hydroxyguanidine compound: a chemical model for the oxidation of N omega-hydroxyl-L-arginine by nitric oxide synthase. *J Med Chem 36:2666.*

Furchgott, R. F., and J. V. Zawadzki. 1980. The obligatory role of endothelial cells in the relaxation of arterial smooth muscle by acetylcholine. *Nature 288:373.*

Furchgott, R. F. 1983. Role of endothelium in responses of vascular smooth muscle. *Circ Res 53:557.*

Furchgott, R. F., and P. M. Vanhoutte. 1989. Endothelium-derived relaxing and contracting factors. *Faseb J 3:2007.*

Furfine, E. S., M. F. Harmon, J. E. Paith, and E. P. Garvey. 1993. Selective inhibition of constitutive nitric oxide synthase by L-NG- nitroarginine. *Biochemistry 32:8512.*

Gaboury, J., R. C. Woodman, D. N. Granger, P. Reinhardt, and P. Kubes. 1993. Nitric oxide prevents leukocyte adherence: role of superoxide. *Am J Physiol 265:H862.*

Gaboury, J. P., X. F. Niu, and P. Kubes. 1996. Nitric oxide inhibits numerous features of mast cell-induced inflammation. *Circulation 93:318.*

Gaillard, T., A. Mulsch, R. Busse, H. Klein, and K. Decker. 1991. Regulation of nitric oxide production by stimulated rat Kupffer cells. *Pathobiology 59:280.*

Gaillard, T., A. Mulsch, H. Klein, and K. Decker. 1992. Regulation by prostaglandin E2 of cytokine-elicited nitric oxide synthesis in rat liver macrophages. *Biol Chem Hoppe Seyler 373:897.*

Garcia-Cardena, G., P. Martasek, B. S. Masters, P. M. Skidd, J. Couet, S. Li, M. P. Lisanti, and W. C. Sessa. 1997. Dissecting the interaction between nitric oxide synthase (NOS) and caveolin. Functional significance of the nos caveolin binding domain in vivo. *J Biol Chem 272:25437.*

Garside, P., A. K. Hutton, A. Severn, F. Y. Liew, and A. M. Mowat. 1992. Nitric oxide mediates intestinal pathology in graft-vs.-host disease. *Eur J Immunol 22:2141.*

Garvey, E. P., J. A. Oplinger, G. J. Tanoury, P. A. Sherman, M. Fowler, S. Marshall, M. F. Harmon, J. E. Paith, and E. S. Furfine. 1994. Potent and selective inhibition of human nitric oxide synthases. Inhibition by non-amino acid isothioureas. *J Biol Chem 269:26669.*

Garvey, E. P., J. A. Oplinger, E. S. Furfine, R. J. Kiff, F. Laszlo, B. J. Whittle, and R. G. Knowles. 1997. 1400W is a slow, tight binding, and highly selective inhibitor of inducible nitric-oxide synthase in vitro and in vivo. *J Biol Chem 272:4959.*

Gilroy, D. W. and P. R. Colville-Nash. 2000. New insights into the role of COX-2 in inflammation. *J Mol Med 78:121.*

Giraldelo, C. M., A. Zappellini, M. N. Muscara, I. M. De Luca, S. Hyslop, G. Cirino, R. Zatz, G. De Nucci, and E. Antunes. 1994. Effect of arginine analogues on rat hind paw oedema and mast cell activation in vitro. *Eur J Pharmacol 257:87.*

Goodwin, J. S., R. P. Messner, and G. T. Peake. 1978. Prostaglandin suppression of mitogen-stimulated lymphocytes in vitro. Changes with mitogen dose and preincubation. *J Clin Invest 62:753.*

Gopalakrishna, R., Z. H. Chen, and U. Gundimeda. 1993. Nitric oxide and nitric oxide-generating agents induce a reversible inactivation of protein kinase C activity and phorbol ester binding. *J Biol Chem 268:27180.*

Granger, D. N., and P. Kubes. 1994. The microcirculation and inflammation: modulation of leukocyte- endothelial cell adhesion. *J Leukoc Biol 55:662.*

Greenblatt, E. P., A. L. Loeb, and D. E. Longnecker. 1993. Marked regional heterogeneity in the magnitude of EDRF/NO-mediated vascular tone in awake rats. *J Cardiovasc Pharmacol 21:235.*

Grega, G. J., S. W. Adamski, and E. Svensjo. 1985. Is there evidence for venular large junctional gap formation in inflammation? *Microcirc Endothelium Lymphatics 2:211.*

Griffiths, M. J., M. Messent, R. J. MacAllister, and T. W. Evans. 1993. Aminoguanidine selectively inhibits inducible nitric oxide synthase. *Br J Pharmacol 110:963.*

Griscavage, J. M., S. Wilk, and L. J. Ignarro. 1995. Serine and cysteine proteinase inhibitors prevent nitric oxide production by activated macrophages by interfering with transcription of the inducible NO synthase gene. *Biochem Biophys Res Commun 215:721.*

Griscavage, J. M., S. Wilk, and L. J. Ignarro. 1996. Inhibitors of the proteasome pathway interfere with induction of nitric oxide synthase in macrophages by blocking activation of transcription factor NF-kappa B. *Proc Natl Acad Sci U S A 93:3308.*

Grody, W. W., G. J. Dizikes, and S. D. Cederbaum. 1987. Human arginase isozymes. *Isozymes Curr Top Biol Med Res 13:181.*

Gross, S. S., D. J. Stuehr, K. Aisaka, E. A. Jaffe, R. Levi, and O. W. Griffith. 1990. Macrophage and endothelial cell nitric oxide synthesis: cell-type selective inhibition by NG-aminoarginine, NG-nitroarginine and NG- methylarginine. *Biochem Biophys Res Commun 170:96.*

Gross, S. S., E. A. Jaffe, R. Levi, and R. G. Kilbourn. 1991. Cytokine-activated endothelial cells express an isotype of nitric oxide synthase which is tetrahydrobiopterin-dependent, calmodulin-independent and inhibited by arginine analogs with a rank-order of potency characteristic of activated macrophages. *Biochem Biophys Res Commun 178:823.*

Gross, S. S., and R. Levi. 1992. Tetrahydrobiopterin synthesis. An absolute requirement for cytokine- induced nitric oxide generation by vascular smooth muscle. *J Biol Chem 267:25722.*

Gross, S. S., and M. S. Wolin. 1995. Nitric oxide: pathophysiological mechanisms. *Annu Rev Physiol 57:737.*

Gruetter, C. A., B. K. Barry, D. B. McNamara, D. Y. Gruetter, P. J. Kadowitz, and L. Ignarro. 1979. Relaxation of bovine coronary artery and activation of coronary arterial guanylate cyclase by nitric oxide, nitroprusside and a carcinogenic nitrosoamine. *J Cyclic Nucleotide Res 5:211.*

Gryglewski, R. J., R. M. Palmer, and S. Moncada. 1986. Superoxide anion is involved in the breakdown of endothelium-derived vascular relaxing factor. *Nature 320:454.*

Guidot, D. M., M. J. Repine, B. M. Hybertson, and J. E. Repine. 1995. Inhaled nitric oxide prevents neutrophil-mediated, oxygen radical- dependent leak in isolated rat lungs. *Am J Physiol 269:L2.*

Gurjar, M. V., R. V. Sharma, and R. C. Bhalla. 1999. eNOS gene transfer inhibits smooth muscle cell migration and MMP-2 and MMP-9 activity. *Arterioscler Thromb Vasc Biol 19:2871.*

Habib, A., C. Creminon, Y. Frobert, J. Grassi, P. Pradelles, and J. Maclouf. 1993. Demonstration of an inducible cyclooxygenase in human endothelial cells using antibodies raised against the carboxyl-terminal region of the cyclooxygenase-2. *J Biol Chem 268:23448.*

Hambleton, P., and P. Miller. 1988. Studies on immunological air pouch inflammation in the rat. *Int Arch Allergy Appl Immunol 87:70.*

Harbrecht, B. G., T. R. Billiar, J. Stadler, A. J. Demetris, J. B. Ochoa, R. D. Curran, and R. L. Simmons. 1992. Nitric oxide synthesis serves to reduce hepatic damage during acute murine endotoxemia. *Crit Care Med 20:1568.*

Hasan, K., B. J. Heesen, J. A. Corbett, M. L. McDaniel, K. Chang, W. Allison, B. H. Wolffenbuttel, J. R. Williamson, and R. G. Tilton. 1993. Inhibition of nitric oxide formation by guanidines. *Eur J Pharmacol 249:101.*

Hayashi, Y., M. Nishio, Y. Naito, H. Yokokura, Y. Nimura, H. Hidaka, and Y. Watanabe. 1999. Regulation of neuronal nitric-oxide synthase by calmodulin kinases. *J Biol Chem 274:20597.*

Hecker, M., C. Schott, B. Bucher, R. Busse, and J. C. Stoclet. 1995. Increase in serum NG-hydroxy-L-arginine in rats treated with bacterial lipopolysaccharide. *Eur J Pharmacol 275:R1.*

Hibbs, J. B., Jr., R. R. Taintor, and Z. Vavrin. 1987a. Macrophage cytotoxicity: role for L-arginine deiminase and imino nitrogen oxidation to nitrite. *Science 235:473.*

Hibbs, J. B., Jr., Z. Vavrin, and R. R. Taintor. 1987b. L-arginine is required for expression of the activated macrophage effector mechanism causing selective metabolic inhibition in target cells. *J Immunol 138:550.*

Hibbs, J. B., Jr., R. R. Taintor, Z. Varin, D. L. Granger, J.-C. Drapier, I. J. Amber, and J. R. Lancaster, Jr. 1990. Synthesis of nitric oxide from a terminal guanidino notrogen atom of L-arginine: a molecular mechanism regulating cellular proliferation that targets intracellular iron. In *Nitric oxide from L-arginine: A bioregulatory system.* S. Moncada, and E. A. Higgs, eds. Elsevier, Amsterdam, p. 189.

Hickey, M. J., K. A. Sharkey, E. G. Sihota, P. H. Reinhardt, J. D. Macmicking, C. Nathan, and P. Kubes. 1997. Inducible nitric oxide synthase-deficient mice have enhanced leukocyte- endothelium interactions in endotoxemia. *Faseb J 11:955.*

Hightower, L. E. 1991. Heat shock, stress proteins, chaperones, and proteotoxicity. *Cell 66:191.*

Hirata, K., R. Kuroda, T. Sakoda, M. Katayama, N. Inoue, M. Suematsu, S. Kawashima, and M. Yokoyama. 1995. Inhibition of endothelial nitric oxide synthase activity by protein kinase C. *Hypertension 25:180.*

Hobbs, A. J., J. M. Fukuto, and L. J. Ignarro. 1994. Formation of free nitric oxide from l-arginine by nitric oxide synthase: direct enhancement of generation by superoxide dismutase. *Proc Natl Acad Sci U S A 91:10992.*

Hogaboam, C. M., K. Jacobson, S. M. Collins, and M. G. Blennerhassett. 1995. The selective beneficial effects of nitric oxide inhibition in experimental colitis. *Am J Physiol 268:G673.*

Hogg, N., R. J. Singh, and B. Kalyanaraman. 1996. The role of glutathione in the transport and catabolism of nitric oxide. *FEBS Lett 382:223.*

Hotter, G., D. Closa, N. Prats, F. Pi, E. Gelpi, and J. Rosello-Catafau. 1997. Free radical enhancement promotes leucocyte recruitment through a PAF and LTB4 dependent mechanism. *Free Radic Biol Med 22:947.*

Hrabak, A., M. Idei, and A. Temesi. 1994. Arginine supply for nitric oxide synthesis and arginase is mainly exogenous in elicited murine and rat macrophages. *Life Sci 55:797.*

Hrabak, A., T. Bajor, A. Temesi, and G. Meszaros. 1996. The inhibitory effect of nitrite, a stable product of nitric oxide (NO) formation, on arginase. *FEBS Lett 390:203.*

Hrabak, A., T. Bajor, G. J. Southan, A. L. Salzman, and C. Szabo. 1997. Comparison of the inhibitory effect of isothiourea and mercapto- alkylguanidine derivatives on the alternative pathways of arginine metabolism in macrophages. *Life Sci 60:L395.*

Hutcheson, I. R., B. J. Whittle, and N. K. Boughton-Smith. 1990. Role of nitric oxide in maintaining vascular integrity in endotoxin- induced acute intestinal damage in the rat. *Br J Pharmacol 101:815.*

Ialenti, A., A. Ianaro, S. Moncada, and M. Di Rosa. 1992. Modulation of acute inflammation by endogenous nitric oxide. *Eur J Pharmacol 211:177.*

Ialenti, A., A. Ianaro, P. Maffia, L. Sautebin, and M. Di Rosa. 2000. Nitric oxide inhibits leucocyte migration in carrageenin-induced rat pleurisy [In Process Citation]. *Inflamm Res 49:411.*

Ianaro, A., D. Xu, C. A. O'Donnell, M. Di Rosa, and F. Y. Liew. 1995. Expression of TGF-beta in attenuated Salmonella typhimurium: oral administration leads to the reduction of inflammation, IL-2 and IFN- gamma, but enhancement of IL-10, in carrageenin-induced oedema in mice. *Immunology 84:8.*

Ignarro, L. J., H. Lippton, J. C. Edwards, W. H. Baricos, A. L. Hyman, P. J. Kadowitz, and C. A. Gruetter. 1981. Mechanism of vascular smooth muscle relaxation by organic nitrates, nitrites, nitroprusside and nitric oxide: evidence for the involvement of S-nitrosothiols as active intermediates. *J Pharmacol Exp Ther 218:739.*

Ignarro, L. J., J. N. Degnan, W. H. Baricos, P. J. Kadowitz, and M. S. Wolin. 1982. Activation of purified guanylate cyclase by nitric oxide requires heme. Comparison of heme-deficient, heme-reconstituted and heme-containing forms of soluble enzyme from bovine lung. *Biochim Biophys Acta 718:49.*

Ignarro, L. J., G. M. Buga, K. S. Wood, R. E. Byrns, and G. Chaudhuri. 1987. Endothelium-derived relaxing factor produced and released from artery and vein is nitric oxide. *Proc Natl Acad Sci U S A 84:9265.*

Ignarro, L. J. 1990. Biosynthesis and metabolism of endothelium-derived nitric oxide. *Annu Rev Pharmacol Toxicol 30:535.*

Imai, T., Y. Hirata, K. Kanno, and F. Marumo. 1994. Induction of nitric oxide synthase by cyclic AMP in rat vascular smooth muscle cells. *J Clin Invest 93:543.*

Iuvone, T., R. Camuccio, and M. Di Rosa. 1994. Modulation of granuloma formation by endogenous nitric oxide. *Eur J Pharmacol 265:89.*

Jakschik, B. A., and L. H. Lee. 1980. Enzymatic assembly of slow reacting substance. *Nature 287:51.*

Jenkinson, C. P., W. W. Grody, and S. D. Cederbaum. 1996. Comparative properties of arginases. *Comp Biochem Physiol B Biochem Mol Biol 114:107.*

Joly, G. A., M. Ayres, F. Chelly, and R. G. Kilbourn. 1994. Effects of NG-methyl-L-arginine, NG-nitro-L-arginine, and aminoguanidine on constitutive and inducible nitric oxide synthase in rat aorta. *Biochem Biophys Res Commun 199:147.*

Jorens, P. G. 1995. Modulation of nitric oxide synthase activity in macrophages. *Mediators in Inflammation 4:75.*

Kaling, M., W. Kugler, K. Ross, C. Zoidl, and G. U. Ryffel. 1991. Liver-specific gene expression: A-activator-binding site, a promoter module present in vitellogenin and acute-phase genes. *Mol Cell Biol 11:93.*

Kallmann, B. A., R. Malzkorn, and H. Kolb. 1999. Exogenous nitric oxide modulates cytokine production in human leukocytes. *Life Sci 65:1787.*

Kane, L. P., P. G. Andres, K. C. Howland, A. K. Abbas, and A. Weiss. 2001. Akt provides the CD28 costimulatory signal for up-regulation of IL-2 and IFN-gamma but not TH2 cytokines. *Nat Immunol 2:37.*

Kanyo, Z. F., L. R. Scolnick, D. E. Ash, and D. W. Christianson. 1996. Structure of a unique binuclear manganese cluster in arginase. *Nature 383:554.*

Katsuyama, K., M. Shichiri, F. Marumo, and Y. Hirata. 1998. NO inhibits cytokine-induced iNOS expression and NF-kappaB activation by interfering with phosphorylation and degradation of IkappaB-alpha. *Arterioscler Thromb Vasc Biol 18:1796.*

Kepka-Lenhart, D., L. C. Chen, and S. M. Morris, Jr. 1996. Novel actions of aspirin and sodium salicylate: discordant effects on nitric oxide synthesis and induction of nitric oxide synthase mRNA in a murine macrophage cell line. *J Leukoc Biol 59:840.*

Kerwin, J. F., Jr., J. R. Lancaster, Jr., and P. L. Feldman. 1995. Nitric oxide: a new paradigm for second messengers. *J Med Chem 38:4343.*

Kharitonov, V. G., V. S. Sharma, R. B. Pilz, D. Magde, and D. Koesling. 1995. Basis of guanylate cyclase activation by carbon monoxide. *Proc Natl Acad Sci U S A 92:2568.*

Kiang, J. G., and G. C. Tsokos. 1998. Heat shock protein 70 kDa: molecular biology, biochemistry, and physiology. *Pharmacol Ther 80:183.*

Kim, Y. M., M. E. de Vera, S. C. Watkins, and T. R. Billiar. 1997. Nitric oxide protects cultured rat hepatocytes from tumor necrosis factor-alpha-induced apoptosis by inducing heat shock protein 70 expression. *J Biol Chem 272:1402.*

Klatt, P., K. Schmidt, and B. Mayer. 1992. Brain nitric oxide synthase is a haemoprotein. *Biochem J 288:15.*

Knowles, R. G., M. Merrett, M. Salter, and S. Moncada. 1990. Differential induction of brain, lung and liver nitric oxide synthase by endotoxin in the rat. *Biochem J 270:833.*

Knowles, R.G., and S. Moncada. 1994. Nitric oxide synthases in mammals. *Biochem J 298:249.*

Koide, M., Y. Kawahara, I. Nakayama, T. Tsuda, and M. Yokoyama. 1993. Cyclic AMP-elevating agents induce an inducible type of nitric oxide synthase in cultured vascular smooth muscle cells. Synergism with the induction elicited by inflammatory cytokines. *J Biol Chem 268:24959.*

Koller, M., T. Hensler, B. Konig, G. Prevost, J. Alouf, and W. Konig. 1993. Induction of heat-shock proteins by bacterial toxins, lipid mediators and cytokines in human leukocytes. *Zentralbl Bakteriol 278:365.*

Konig, W., M. Koller, and J. Brom. 1992. Priming mechanisms and induction of heat shock proteins in human polymorphonuclear granulocytes induced by eicosanoids and cytokines. *Eicosanoids 5:S39.*

Kopp, E., and S. Ghosh. 1994. Inhibition of NF-kappa B by sodium salicylate and aspirin [see comments]. *Science 265:956.*

Kopp, E., and S. Ghosh. 1994. Inhibition of NF-kappa B by sodium salicylate and aspirin. *Science 265:956.*

Koshland, D. E., Jr. 1992. The molecule of the year. *Science 258:1861.*

Kroll, M. H., and A. I. Schafer. 1989. Biochemical mechanisms of platelet activation. *Blood 74:1181.*

Kubes, P., M. Suzuki, and D. N. Granger. 1991. Nitric oxide: an endogenous modulator of leukocyte adhesion. *Proc Natl Acad Sci U S A 88:4651.*

Kubes, P., and S. Kanwar. 1994. Histamine induces leukocyte rolling in post-capillary venules. A P- selectin-mediated event. *J Immunol 152:3570.*

Kubes, P., I. Kurose, and D. N. Granger. 1994. NO donors prevent integrin-induced leukocyte adhesion but not P- selectin-dependent rolling in postischemic venules. *Am J Physiol 267:H931.*

Kubes, P. 2000. Inducible nitric oxide synthase: a little bit of good in all of us. *Gut 47:6.*

Kunz, D., G. Walker, W. Eberhardt, U. K. Messmer, A. Huwiler, and J. Pfeilschifter. 1997. Platelet-derived growth factor and fibroblast growth factor differentially regulate interleukin 1beta- and cAMP-induced nitric oxide synthase expression in rat renal mesangial cells. *J Clin Invest 100:2800.*

Kurose, I., R. Wolf, M. B. Grisham, and D. N. Granger. 1994. Modulation of ischemia/reperfusion-induced microvascular dysfunction by nitric oxide. *Circ Res 74:376.*

Kurose, I., R. Wolf, M. B. Grisham, and D. N. Granger. 1995. Effects of an endogenous inhibitor of nitric oxide synthesis on postcapillary venules. *Am J Physiol 268:H2224.*

Kurumbail, R. G., A. M. Stevens, J. K. Gierse, J. J. McDonald, R. A. Stegeman, J. Y. Pak, D. Gildehaus, J. M. Miyashiro, T. D. Penning, K. Seibert, P. C. Isakson, and W. C. Stallings. 1996. Structural basis for selective inhibition of cyclooxygenase-2 by anti-inflammatory agents. *Nature 384:644.*

Kwon, N. S., C. F. Nathan, and D. J. Stuehr. 1989. Reduced biopterin as a cofactor in the generation of nitrogen oxides by murine macrophages. *J Biol Chem 264:20496.*

Kwon, N. S., C. F. Nathan, C. Gilker, O. W. Griffith, D. E. Matthews, and D. J. Stuehr. 1990. L-citrulline production from L-arginine by macrophage nitric oxide synthase. The ureido oxygen derives from dioxygen. *J Biol Chem 265:13442.*

Kwon, N. S., D. J. Stuehr, and C. F. Nathan. 1991. Inhibition of tumor cell ribonucleotide reductase by macrophage-derived nitric oxide. *J Exp Med 174:761.*

Laight, D. W., T. Andrews, A. Hej-Yehia, C. M. J., and E. E. Anngard. 1997. Microassay of superoxide anion scavenging activity. *Environ Toxicol Pharmacol 3:65.*

Laight, D. W., P. T. Gunnarsson, A. V. Kaw, E. E. Anngard, and C. M. J. 1999. Physiological assay of plasma total antioxidant status in a model of endothelial dysfunction in the rat following experimental oxidant stress. *Environ Toxicol Pharmacol 7:27.*

Lambert, L. E., J. P. Whitten, B. M. Baron, H. C. Cheng, N. S. Doherty, and I. A. McDonald. 1991. Nitric oxide synthesis in the CNS endothelium and macrophages differs in its sensitivity to inhibition by arginine analogues. *Life Sci 48:69.*

Lambert, L. E., J. F. French, J. P. Whitten, B. M. Baron, and I. A. McDonald. 1992. Characterization of cell selectivity of two novel inhibitors of nitric oxide synthesis. *Eur J Pharmacol 216:131.*

Lander, H. M., P. K. Sehajpal, and A. Novogrodsky. 1993. Nitric oxide signaling: a possible role for G proteins. *J Immunol 151:7182.*

Laszlo, F., S. M. Evans, and B. J. Whittle. 1995. Aminoguanidine inhibits both constitutive and inducible nitric oxide synthase isoforms in rat intestinal microvasculature in vivo. *Eur J Pharmacol 272:169.*

Laubach, V. E., C. X. Zhang, S. W. Russell, W. J. Murphy, and P. A. Sherman. 1997. Analysis of expression and promoter function of the human inducible nitric oxide synthase gene in DLD-1 cells and monkey hepatocytes. *Biochim Biophys Acta 1351:287.*

Lee, T. H., H. J. Ryu, P. W. Chung, W. S. Lim, and M. Y. Chung. 1987. The prevalence of diabetic complications in Korea. *J Med Assoc Thai 70 Suppl 2:173.*

Lefer, A. M., M. R. Siegfried, and X. L. Ma. 1993. Protection of ischemia-reperfusion injury by sydnonimine NO donors via inhibition of neutrophil-endothelium interaction. *J Cardiovasc Pharmacol 22:S27.*

Lei, S. Z., Z. H. Pan, S. K. Aggarwal, H. S. Chen, J. Hartman, N. J. Sucher, and S. A. Lipton. 1992. Effect of nitric oxide production on the redox modulatory site of the NMDA receptor-channel complex. *Neuron 8:1087.*

Leone, A. M., R. M. Palmer, R. G. Knowles, P. L. Francis, D. S. Ashton, and S. Moncada. 1991. Constitutive and inducible nitric oxide synthases incorporate molecular oxygen into both nitric oxide and citrulline. *J Biol Chem 266:23790.*

Lepoivre, M., F. Fieschi, J. Coves, L. Thelander, and M. Fontecave. 1991. Inactivation of ribonucleotide reductase by nitric oxide. *Biochem Biophys Res Commun 179:442.*

Lewis, A. J., J. Parker, J. DiLuigi, L. J. Datko, and R. P. Carlson. 1981. Immunomodulation of delayed hypersensitivity to methylated bovine serum albumin (MBSA) in mice using subliminal and normal sensitization procedures. *J Immunopharmacol 3:289.*

Liew, F. Y. 1993. The role of nitric oxide in parasitic diseases. *Ann Trop Med Parasitol 87:637.*

Lin, W. W., B. C. Chen, Y. W. Hsu, C. M. Lee, and S. K. Shyue. 1999. Modulation of inducible nitric oxide synthase induction by prostaglandin E2 in macrophages: distinct susceptibility in murine J774 and RAW 264.7 macrophages. *Prostaglandins Other Lipid Mediat 58:87.*

Lopez-Farre, A., C. Caramelo, A. Esteban, M. L. Alberola, I. Millas, M. Monton, and S. Casado. 1995. Effects of aspirin on platelet-neutrophil interactions. Role of nitric oxide and endothelin-1. *Circulation 91:2080.*

Lopez-Farre, A., A. Riesco, E. Digiuni, J. R. Mosquera, C. Caramelo, L. S. de Miguel, I. Millas, T. de Frutos, M. R. Cernadas, M. Monton, J. Alonso, and S. Casado. 1996. Aspirin-stimulated nitric oxide production by neutrophils after acute myocardial ischemia in rabbits. *Circulation 94:83.*

Lorsbach, R. B., W. J. Murphy, C. J. Lowenstein, S. H. Snyder, and S. W. Russell. 1993. Expression of the nitric oxide synthase gene in mouse macrophages activated for tumor cell killing. Molecular basis for the synergy between interferon-gamma and lipopolysaccharide. *J Biol Chem 268:1908.*

Lotz, M. 1993. Interleukin-6. *Cancer Invest 11:732.*

Lowenstein, C. J., E. W. Alley, P. Raval, A. M. Snowman, S. H. Snyder, S. W. Russell, and W. J. Murphy. 1993. Macrophage nitric oxide synthase gene: two upstream regions mediate induction by interferon gamma and lipopolysaccharide. *Proc Natl Acad Sci U S A 90:9730.*

Lowry, R. P., T. Takeuchi, H. Cremisi, and B. Konieczny. 1993. Th2-like effectors may function as antigen-specific suppressor cells in states of transplantation tolerance. *Transplant Proc 25:324.*

Ma, X. L., A. S. Weyrich, D. J. Lefer, and A. M. Lefer. 1993. Diminished basal nitric oxide release after myocardial ischemia and reperfusion promotes neutrophil adherence to coronary endothelium. *Circ Res 72:403.*

Ma, Z., S. Ramanadham, J. A. Corbett, A. Bohrer, R. W. Gross, M. L. McDaniel, and J. Turk. 1996. Interleukin-1 enhances pancreatic islet arachidonic acid 12-lipoxygenase product generation by increasing substrate availability through a nitric oxide-dependent mechanism. *J Biol Chem 271:1029.*

Maeda, H., T. Akaike, M. Yoshida, and M. Suga. 1994. Multiple functions of nitric oxide in pathophysiology and microbiology: analysis by a new nitric oxide scavenger. *J Leukoc Biol 56:588.*

Makino, S., and T. Fukuda. 1995. Eosinophils and allergy in asthma. *Allergy Proc 16:13.*

Malawista, S. E., R. R. Montgomery, and G. van Blaricom. 1992. Evidence for reactive nitrogen intermediates in killing of staphylococci by human neutrophil cytoplasts. A new microbicidal pathway for polymorphonuclear leukocytes. *J Clin Invest 90:631.*

Mannaioni, P. F., E. Masini, A. Pistelli, D. Salvemini, and J. R. Vane. 1991. Mast cells as a source of superoxide anions and nitric oxide-like factor: relevance to histamine release. *Int J Tissue React 13:271.*

Marletta, M. A. 1994a. Nitric oxide synthase: aspects concerning structure and catalysis. *Cell 78:927.*

Marletta, M. A. 1994b. Approaches toward selective inhibition of nitric oxide synthase. *J Med Chem 37:1899.*

Marotta, P., L. Sautebin, and M. Di Rosa. 1992. Modulation of the induction of nitric oxide synthase by eicosanoids in the murine macrophage cell line J774. *Br J Pharmacol 107:640.*

Martin, E., C. Nathan, and Q. W. Xie. 1994. Role of interferon regulatory factor 1 in induction of nitric oxide synthase. *J Exp Med 180:977.*

Mauel, J., A. Ransijn, S. B. Corradin, and Y. Buchmuller-Rouiller. 1995. Effect of PGE2 and of agents that raise cAMP levels on macrophage activation induced by IFN-gamma and TNF-alpha. *J Leukoc Biol 58:217.*

Mayer, B., M. John, and E. Bohme. 1990. Purification of a Ca2+/calmodulin-dependent nitric oxide synthase from porcine cerebellum. Cofactor-role of tetrahydrobiopterin. *FEBS Lett 277:215.*

Mayer, B., F. Brunner, and K. Schmidt. 1993. Inhibition of nitric oxide synthesis by methylene blue. *Biochem Pharmacol 45:367.*

McCafferty, D. M., J. S. Mudgett, M. G. Swain, and P. Kubes. 1997. Inducible nitric oxide synthase plays a critical role in resolving intestinal inflammation. *Gastroenterology 112:1022.*

McCall, T. B., N. K. Boughton-Smith, R. M. Palmer, B. J. Whittle, and S. Moncada. 1989. Synthesis of nitric oxide from L-arginine by neutrophils. Release and interaction with superoxide anion. *Biochem J 261:293.*

McCall, T. B., M. Feelisch, R. M. Palmer, and S. Moncada. 1991. Identification of N-iminoethyl-L-ornithine as an irreversible inhibitor of nitric oxide synthase in phagocytic cells. *Br J Pharmacol 102:234.*

McCartney-Francis, N., J. B. Allen, D. E. Mizel, J. E. Albina, Q. W. Xie, C. F. Nathan, and S. M. Wahl. 1993. Suppression of arthritis by an inhibitor of nitric oxide synthase. *J Exp Med 178:749.*

McInnes, I. B., B. P. Leung, M. Field, X. Q. Wei, F. P. Huang, R. D. Sturrock, A. Kinninmonth, J. Weidner, R. Mumford, and F. Y. Liew. 1996. Production of nitric oxide in the synovial membrane of rheumatoid and osteoarthritis patients. *J Exp Med 184:1519.*

McMillan, K., D. S. Bredt, D. J. Hirsch, S. H. Snyder, J. E. Clark, and B. S. Masters. 1992. Cloned, expressed rat cerebellar nitric oxide synthase contains stoichiometric amounts of heme, which binds carbon monoxide. *Proc Natl Acad Sci U S A 89:11141.*

Medeiros, M. V., I. M. Binhara, H. Moreno Junior, R. Zatz, G. De Nucci, and E. Antunes. 1995. Effect of chronic nitric oxide synthesis inhibition on the inflammatory responses induced by carrageenin in rats. *Eur J Pharmacol 285:109.*

Meerpohl, H. G., and T. Bauknecht. 1986. Role of prostaglandins on the regulation of macrophage proliferation and cytotoxic functions. *Prostaglandins 31:961.*

Mellion, B. T., L. J. Ignarro, E. H. Ohlstein, E. G. Pontecorvo, A. L. Hyman, and P. J. Kadowitz. 1981. Evidence for the inhibitory role of guanosine 3', 5'-monophosphate in ADP-induced human platelet aggregation in the presence of nitric oxide and related vasodilators. *Blood 57:946.*

Michel, T., G. K. Li, and L. Busconi. 1993. Phosphorylation and subcellular translocation of endothelial nitric oxide synthase. *Proc Natl Acad Sci U S A 90:6252.*

Michell, B. J., J. E. Griffiths, K. I. Mitchelhill, I. Rodriguez-Crespo, T. Tiganis, S. Bozinovski, P. R. de Montellano, B. E. Kemp, and R. B. Pearson. 1999. The Akt kinase signals directly to endothelial nitric oxide synthase. *Curr Biol 9:845.*

Middleton, S. J., M. Shorthouse, and J. O. Hunter. 1993. Increased nitric oxide synthesis in ulcerative colitis [see comments]. *Lancet 341:465.*

Milano, S., F. Arcoleo, M. Dieli, R. D'Agostino, P. D'Agostino, G. De Nucci, and E. Cillari. 1995. Prostaglandin E2 regulates inducible nitric oxide synthase in the murine macrophage cell line J774. *Prostaglandins 49:105.*

Miller, M. J., S. Chotinaruemol, H. Sadowska-Krowicka, J. L. Kakkis, U. K. Munshi, X. J. Zhang, and D. A. Clark. 1993. Nitric oxide: the Jekyll and Hyde of gut inflammation. *Agents Actions 39:C180.*

Mills, C. D., J. Shearer, R. Evans, and M. D. Caldwell. 1992. Macrophage arginine metabolism and the inhibition or stimulation of cancer. *J Immunol 149:2709.*

Mills, C. D., K. Kincaid, J. M. Alt, M. J. Heilman, and A. M. Hill. 2000. M-1/M-2 macrophages and the Th1/Th2 paradigm. *J Immunol 164:6166.*

Misko, T. P., W. M. Moore, T. P. Kasten, G. A. Nickols, J. A. Corbett, R. G. Tilton, M. L. McDaniel, J. R. Williamson, and M. G. Currie. 1993. Selective inhibition of the inducible nitric oxide synthase by aminoguanidine. *Eur J Pharmacol 233:119.*

Misso, N. L., C. D. Peacock, D. N. Watkins, and P. J. Thompson. 2000. Nitrite generation and antioxidant effects during neutrophil apoptosis. *Free Radic Biol Med 28:934.*

Mitchell, J. A., P. Akarasereenont, C. Thiemermann, R. J. Flower, and J. R. Vane. 1993. Selectivity of nonsteroidal antiinflammatory drugs as inhibitors of constitutive and inducible cyclooxygenase. *Proc Natl Acad Sci U S A 90:11693.*

Moilanen, E., P. Vuorinen, H. Kankaanranta, T. Metsa-Ketela, and H. Vapaatalo. 1993. Inhibition by nitric oxide-donors of human polymorphonuclear leucocyte functions. *Br J Pharmacol 109:852.*

Molina y Vedia, L., B. McDonald, B. Reep, B. Brune, M. Di Silvio, T. R. Billiar, and E. G. Lapetina. 1992. Nitric oxide-induced S-nitrosylation of glyceraldehyde-3-phosphate dehydrogenase inhibits enzymatic activity and increases endogenous ADP-ribosylation. *J Biol Chem 267:24929.*

Moncada, S., and J. R. Vane. 1979. Mode of action of aspirin-like drugs. *Adv Intern Med 24:1*

Moncada, S., R. M. Palmer, and E. A. Higgs. 1989. Biosynthesis of nitric oxide from L-arginine. A pathway for the regulation of cell function and communication. *Biochem Pharmacol 38:1709.*

Moncada, S., R. M. Palmer, and E. A. Higgs. 1991. Nitric oxide: physiology, pathophysiology, and pharmacology. *Pharmacol Rev 43:109.*

Moore, P. K., P. Wallace, Z. Gaffen, S. L. Hart, and R. C. Babbedge. 1993. Characterization of the novel nitric oxide synthase inhibitor 7-nitro indazole and related indazoles: antinociceptive and cardiovascular effects. *Br J Pharmacol 110:219.*

Moore, A. R., and M. Brown. 1996. The effects of a novel formulation of cyclosporin on antibody and cell mediated imunne reactions in the pleural cavity of rats. *4th International workshop on hyaluronan in drug delivery 4:116.*

Morbidelli, L., C. H. Chang, J. G. Douglas, H. J. Granger, F. Ledda, and M. Ziche. 1996. Nitric oxide mediates mitogenic effect of VEGF on coronary venular endothelium. *Am J Physiol 270:H411.*

Morimoto, R. I., K. D. Sarge, and K. Abravaya. 1992. Transcriptional regulation of heat shock genes. A paradigm for inducible genomic responses. *J Biol Chem 267:21987.*

Mosmann, T. R., and S. Sad. 1996. The expanding universe of T-cell subsets: Th1, Th2 and more. *Immunol Today 17:138.*

Movat, H. Z. 1987. The role of histamine and other mediators in microvascular changes in acute inflammation. *Can J Physiol Pharmacol 65:451.*

Muhl, H., D. Kunz, and J. Pfeilschifter. 1994. Expression of nitric oxide synthase in rat glomerular mesangial cells mediated by cyclic AMP. *Br J Pharmacol 112:1.*

Mulligan, M. S., S. Moncada, and P. A. Ward. 1992. Protective effects of inhibitors of nitric oxide synthase in immune complex-induced vasculitis. *Br J Pharmacol 107:1159.*

Mulsch, A., P. Mordvintcev, A. F. Vanin, and R. Busse. 1991. The potent vasodilating and guanylyl cyclase activating dinitrosyl- iron(II) complex is stored in a protein-bound form in vascular tissue and is released by thiols. *FEBS Lett 294:252.*

Mulsch, A., B. Schray-Utz, P. I. Mordvintcev, S. Hauschildt, and R. Busse. 1993. Diethyldithiocarbamate inhibits induction of macrophage NO synthase. *FEBS Lett 321:215.*

Musch, M. W., M. M. Billah, and M. I. Siegel. 1987. Antigen-and ionophore-stimulated synthesis of platelet-activating factor by the cloned mast cell line, MC9. *Biochem Biophys Res Commun 144:1243.*

Myers, P. R., R. L. Minor, Jr., R. Guerra, Jr., J. N. Bates, and D. G. Harrison. 1990. Vasorelaxant properties of the endothelium-derived relaxing factor more closely resemble S-nitrosocysteine than nitric oxide. *Nature 345:161.*

Naito, M., S. Umeda, T. Yamamoto, H. Moriyama, H. Umezu, G. Hasegawa, H. Usuada, L. D. Shultz, and K. Takahashi. 1996. Development, differentiation, and phenotypic heterogeneity of murine tissue macrophages. *J Leukoc Biol 59:133.*

Najafipour, H., and W. R. Ferrell. 1993. Nitric oxide modulates sympathetic vasoconstriction and basal blood flow in normal and acutely inflamed rabbit knee joints. *Exp Physiol 78:615.*

Nathan, C. 1992. Nitric oxide as a secretory product of mammalian cells. *Faseb J 6:3051.*

Nathan, C., and Q. W. Xie. 1994. Regulation of biosynthesis of nitric oxide. *J Biol Chem 269:13725.*

Neuzil, J., and R. Stocker. 1993. Bilirubin attenuates radical-mediated damage to serum albumin. *FEBS Lett 331:281.*

Nishimura, H., M. Emoto, K. Kimura, and Y. Yoshikai. 1997. Hsp70 protects macrophages infected with Salmonella choleraesuis against TNF-alpha-induced cell death. *Cell Stress Chaperones 2:50.*

O'Garra, A., and K. Murphy. 1994. Role of cytokines in determining T-lymphocyte function. *Curr Opin Immunol 6:458.*

Osawa, Y., and J. C. Davila. 1993. Phencyclidine, a psychotomimetic agent and drug of abuse, is a suicide inhibitor of brain nitric oxide synthase. *Biochem Biophys Res Commun 194:1435.*

Ou, P., and S. P. Wolff. 1993. Aminoguanidine: a drug proposed for prophylaxis in diabetes inhibits catalase and generates hydrogen peroxide in vitro. *Biochem Pharmacol 46:1139.*

Oyanagui, Y. 1994. Nitric oxide and superoxide radical are involved in both initiation and development of adjuvant arthritis in rats. *Life Sci 54:L285.*

Padgett, E. L., and S. B. Pruett. 1995. Rat, mouse and human neutrophils stimulated by a variety of activating agents produce much less nitrite than rodent macrophages. *Immunology 84:135.*

Palluy, O., and M. Rigaud. 1996. Nitric oxide induces cultured cortical neuron apoptosis. *Neurosci Lett 208:1.*

Palmer, R. M., A. G. Ferrige, and S. Moncada. 1987. Nitric oxide release accounts for the biological activity of endothelium-derived relaxing factor. *Nature 327:524.*

Pan, J., K. L. Burgher, A. M. Szczepanik, and G. E. Ringheim. 1996. Tyrosine phosphorylation of inducible nitric oxide synthase: implications for potential post-translational regulation. *Biochem J 314:889.*

Park, J. H., S. H. Chang, K. M. Lee, and S. H. Shin. 1996. Protective effect of nitric oxide in an endotoxin-induced septic shock. *Am J Surg 171:340.*

Park, S. K., H. L. Lin, and S. Murphy. 1997. Nitric oxide regulates nitric oxide synthase-2 gene expression by inhibiting NF-kappaB binding to DNA. *Biochem J 322:609.*

Paton, W. D. M. 1951. Compound 48/80: a potent histamine liberator. *Br J Pharmacol 6:499.*

Peterson, D. A., D. C. Peterson, S. Archer, and E. K. Weir. 1992. The non specificity of specific nitric oxide synthase inhibitors. *Biochem Biophys Res Commun 187:797.*

Peunova, N., and G. Enikolopov. 1993. Amplification of calcium-induced gene transcription by nitric oxide in neuronal cells. *Nature 364:450.*

Polla, B. S., A. M. Healy, W. C. Wojno, and S. M. Krane. 1987. Hormone 1 alpha,25-dihydroxyvitamin D3 modulates heat shock response in monocytes. *Am J Physiol 252:C640.*

Pollock, J. S., U. Forstermann, J. A. Mitchell, T. D. Warner, H. H. Schmidt, M. Nakane, and F. Murad. 1991. Purification and characterization of particulate endothelium-derived relaxing factor synthase from cultured and native bovine aortic endothelial cells. *Proc Natl Acad Sci U S A 88:10480.*

Polte, T., A. Abate, P. A. Dennery, and H. Schroder. 2000. Heme oxygenase-1 is a cGMP-inducible endothelial protein and mediates the cytoprotective action of nitric oxide. *Arterioscler Thromb Vasc Biol 20:1209.*

Radomski, M. W., R. M. Palmer, and S. Moncada. 1987a. Comparative pharmacology of endothelium-derived relaxing factor, nitric oxide and prostacyclin in platelets. *Br J Pharmacol 92:181.*

Radomski, M. W., R. M. Palmer, and S. Moncada. 1987b. The role of nitric oxide and cGMP in platelet adhesion to vascular endothelium. *Biochem Biophys Res Commun 148:1482.*

Radomski, M. W., R. M. Palmer, and S. Moncada. 1987c. Endogenous nitric oxide inhibits human platelet adhesion to vascular endothelium. *Lancet 2:1057.*

Radomski, M. W., R. M. Palmer, and S. Moncada. 1987d. The anti-aggregating properties of vascular endothelium: interactions between prostacyclin and nitric oxide. *Br J Pharmacol 92:639.*

Regnault, C., M. Roch-Arveiller, I. Florentin, J. P. Giroud, E. Postaire, and M. Delaforge. 1996. Kinetic evaluation of nitric oxide production in pleural exudate after induction of two inflammatory reactions in the rat. *Inflammation 20:613.*

Ribeiro, S. P., J. Villar, G. P. Downey, J. D. Edelson, and A. S. Slutsky. 1994. Sodium arsenite induces heat shock protein-72 kilodalton expression in the lungs and protects rats against sepsis. *Crit Care Med 22:922.*

Riches, D. W., and D. R. Stanworth. 1982. Evidence for a mechanism for the initiation of acid hydrolase secretion by macrophages that is functionally independent of alternative pathway complement activation. *Biochem J 202:639.*

Ridger, V. C., E. R. Pettipher, C. E. Bryant, and S. D. Brain. 1997. Effect of the inducible nitric oxide synthase inhibitors aminoguanidine and L-N6-(1-iminoethyl)lysine on zymosan-induced plasma extravasation in rat skin. *J Immunol 159:383.*

Ridley, M. G., G. Kingsley, C. Pitzalis, and G. S. Panayi. 1990. Monocyte activation in rheumatoid arthritis: evidence for in situ activation and differentiation in joints. *Br J Rheumatol 29:84.*

Risau, W. 1990. Angiogenic growth factors. *Prog Growth Factor Res 2:71.*

Rodenas, J., M. T. Mitjavila, and T. Carbonell. 1998. Nitric oxide inhibits superoxide production by inflammatory polymorphonuclear leukocytes. *Am J Physiol 274:C827.*

Romanska, H. M., T. S. Ikonen, A. E. Bishop, R. E. Morris, and J. M. Polak. 2000. Up-regulation of inducible nitric oxide synthase in fibroblasts parallels the onset and progression of fibrosis in an experimental model of post-transplant obliterative airway disease. *J Pathol 191:71.*

Rosenthal, A. S., and E. M. Shevach. 1973. Function of macrophages in antigen recognition by guinea pig T lymphocytes. I. Requirement for histocompatible macrophages and lymphocytes. *J Exp Med 138:1194.*

Rotzinger, S., C. M. Aragon, F. Rogan, S. Amir, and Z. Amit. 1995. The nitric oxide synthase inhibitor NW-nitro-L-arginine methylester attenuates brain catalase activity in vitro. *Life Sci 56:1321.*

Ryan, G. B., and G. Majno. 1977. Acute inflammation. A review. *Am J Pathol 86:183.*

Ryan, J. A., and L. E. Hightower. 1996. Stress proteins as molecular biomarkers for environmental toxicology. *Exs 77:411.*

Sakurai, H., H. Kohsaka, M. F. Liu, H. Higashiyama, Y. Hirata, K. Kanno, I. Saito, and N. Miyasaka. 1995. Nitric oxide production and inducible nitric oxide synthase expression in inflammatory arthritides. *J Clin Invest 96:2357.*

Salvemini, D., G. de Nucci, R. J. Gryglewski, and J. R. Vane. 1989. Human neutrophils and mononuclear cells inhibit platelet aggregation by releasing a nitric oxide-like factor. *Proc Natl Acad Sci U S A 86:6328.*

Salvemini, D., E. Masini, A. Pistelli, P. F. Mannaioni, and J. R. Vane. 1991. Nitric oxide: a regulatory mediator of mast cell reactivity. *J Carrdiovasc Pharmacol 17:S258.*

Salvemini, D., T. P. Misko, J. L. Masferrer, K. Seibert, M. G. Currie, and P. Needleman. 1993. Nitric oxide activates cyclooxygenase enzymes. *Proc Natl Acad Sci U S A 90:7240.*

Salvemini, D., P. T. Manning, B. S. Zweifel, K. Seibert, J. Connor, M. G. Currie, P. Needleman, and J. L. Masferrer. 1995. Dual inhibition of nitric oxide and prostaglandin production contributes to the antiinflammatory properties of nitric oxide synthase inhibitors. *J Clin Invest 96:301.*

Salvemini, D., Z. Q. Wang, P. S. Wyatt, D. M. Bourdon, M. H. Marino, P. T. Manning, and M. G. Currie. 1996. Nitric oxide: a key mediator in the early and late phase of carrageenan- induced rat paw inflammation. *Br J Pharmacol 118:829.*

Samali, A., and T. G. Cotter. 1996. Heat shock proteins increase resistance to apoptosis. *Exp Cell Res 223:163.*

Sautebin, L., A. Ialenti, A. Ianaro, and M. Di Rosa. 1995. Endogenous nitric oxide increases prostaglandin biosynthesis in carrageenin rat paw oedema. *Eur J Pharmacol 286:219.*

Seed MP, Gilroy D, Paul-Clark MJ, Tomlinson A, Willoughby DA. 1999. The role of the inducible enzymes cycloxygenase-2, nitric oxide synthase, and heme oxygenase in inflammation angiogenesis. In "Inducible enzymes in inflammation". Eds. Willoughby D.A., and Tomlinson A. Birkhauser Press.

Schaffer, M. R., U. Tantry, S. S. Gross, H. L. Wasserburg, and A. Barbul. 1996. Nitric oxide regulates wound healing. *J Surg Res 63:237.*

Schmidt, H. H., R. Seifert, and E. Bohme. 1989. Formation and release of nitric oxide from human neutrophils and HL-60 cells induced by a chemotactic peptide, platelet activating factor and leukotriene B4. *FEBS Lett 244:357.*

Schmidt, H. H., and U. Walter. 1994. NO at work. *Cell 78:919.*

Seiler, N., F. N. Bolkenius, and B. Knodgen. 1985. The influence of catabolic reactions on polyamine excretion. *Biochem J 225:219.*

Sherman, M. P., E. E. Aeberhard, V. Z. Wong, J. M. Griscavage, and L. J. Ignarro. 1993. Pyrrolidine dithiocarbamate inhibits induction of nitric oxide synthase activity in rat alveolar macrophages. *Biochem Biophys Res Commun 191:1301.*

Shimpo, M., U. Ikeda, Y. Maeda, K. Ohya, Y. Murakami, and K. Shimada. 2000. Effects of aspirin-like drugs on nitric oxide synthesis in rat vascular smooth muscle cells. *Hypertension 35:1085.*

Shute, J. 1992. Basophil migration and chemotaxis. *Clin Exp Allergy 22:321.*

Sin, Y. M., A. D. Sedgwick, E. P. Chea, and D. A. Willoughby. 1986. Mast cells in newly formed lining tissue during acute inflammation: a six day air pouch model in the mouse. *Ann Rheum Dis 45:873.*

Smith, W. L., and L. J. Marnett. 1991. Prostaglandin endoperoxide synthase: structure and catalysis. *Biochim Biophys Acta 1083:1.*

Snyder, G. D., R. W. Holmes, J. N. Bates, and B. J. Van Voorhis. 1996. Nitric oxide inhibits aromatase activity: mechanisms of action. *J Steroid Biochem Mol Biol 58:63.*

Sorkin, E., V. J. Stecher, and J. F. Borel. 1970. Chemotaxis of leucocytes and inflammation. *Ser Haematol 3:131.*

Southan, G. J., C. Szabo, and C. Thiemermann. 1995. Isothioureas: potent inhibitors of nitric oxide synthases with variable isoform selectivity. *Br J Pharmacol 114:510.*

Spector, G. W., and D. A. Willoughby. 1968. The histroy of inflammation. In *The pharmacology of inflammation.* G. W. Spector, and D. A. Willoughby, eds. The English University Press, London, p. 1.

Stadler, J., T. R. Billiar, R. D. Curran, D. J. Stuehr, J. B. Ochoa, and R. L. Simmons. 1991. Effect of exogenous and endogenous nitric oxide on mitochondrial respiration of rat hepatocytes. *Am J Physiol 260:C910.*

Stamler, J. S., D. I. Simon, J. A. Osborne, M. E. Mullins, O. Jaraki, T. Michel, D. J. Singel, and J. Loscalzo. 1992a. S-nitrosylation of proteins with nitric oxide: synthesis and characterization of biologically active compounds. *Proc Natl Acad Sci U S A 89:444.*

Stamler, J. S., D. J. Singel, and J. Loscalzo. 1992b. Biochemistry of nitric oxide and its redox-activated forms. *Science 258:1898.*

Stamler, J. S. 1994. Redox signaling: nitrosylation and related target interactions of nitric oxide. *Cell 78:931.*

Stefanovic-Racic, M., K. Meyers, C. Meschter, J. W. Coffey, R. A. Hoffman, and C. H. Evans. 1995. Comparison of the nitric oxide synthase inhibitors methylarginine and aminoguanidine as prophylactic and therapeutic agents in rat adjuvant arthritis. *J Rheumatol 22:1922.*

Stocker, R., Y. Yamamoto, A. F. McDonagh, A. N. Glazer, and B. N. Ames. 1987. Bilirubin is an antioxidant of possible physiological importance. *Science 235:1043.*

Stuehr, D. J., and M. A. Marletta. 1985. Mammalian nitrate biosynthesis: mouse macrophages produce nitrite and nitrate in response to Escherichia coli lipopolysaccharide. *Proc Natl Acad Sci U S A 82:7738.*

Stuehr, D. J., and C. F. Nathan. 1989. Nitric oxide. A macrophage product responsible for cytostasis and respiratory inhibition in tumor target cells. *J Exp Med 169:1543.*

Stuehr, D. J., N. S. Kwon, C. F. Nathan, O. W. Griffith, P. L. Feldman, and J. Wiseman. 1991. N omega-hydroxy-L-arginine is an intermediate in the biosynthesis of nitric oxide from L-arginine. *J Biol Chem 266:6259.*

Stuehr, D. J., H. J. Cho, N. S. Kwon, M. F. Weise, and C. F. Nathan. 1991. Purification and characterization of the cytokine-induced macrophage nitric oxide synthase: an FAD- and FMN-containing flavoprotein. *Proc Natl Acad Sci U S A 88:7773.*

Stuehr, D. J., and O. W. Griffith. 1992. Mammalian nitric oxide synthases. *Adv Enzymol Relat Areas Mol Biol 65:287.*

Stuehr, D. J., H. M. Abu-Soud, D. L. Rousseau, P. L. Feldman, and J. Wang. 1995. Control of electron transfer in neuronal nitric oxide synthase by calmodulin, substrate, substrate analogs, and nitric oxide. *Adv Pharmacol 34:207.*

Suschek, C., H. Rothe, K. Fehsel, J. Enczmann, and V. Kolb-Bachofen. 1993. Induction of a macrophage-like nitric oxide synthase in cultured rat aortic endothelial cells. IL-1 beta-mediated induction regulated by tumor necrosis factor-alpha and IFN-gamma. *J Immunol 151:3283.*

Swierkosz, T. A., J. A. Mitchell, T. D. Warner, R. M. Botting, and J. R. Vane. 1995. Co-induction of nitric oxide synthase and cyclo-oxygenase: interactions between nitric oxide and prostanoids. *Br J Pharmacol 114:1335.*

Szabo, C., G. J. Southan, C. Thiemermann, and J. R. Vane. 1994. The mechanism of the inhibitory effect of polyamines on the induction of nitric oxide synthase: role of aldehyde metabolites. *Br J Pharmacol 113:757.*

Takiguchi, M., T. Matsubasa, Y. Amaya, and M. Mori. 1989. Evolutionary aspects of urea cycle enzyme genes. *Bioessays 10:163.*

Tayeh, M. A., and M. A. Marletta. 1989. Macrophage oxidation of L-arginine to nitric oxide, nitrite, and nitrate. Tetrahydrobiopterin is required as a cofactor. *J Biol Chem 264:19654.*

Taylor-Robinson, A. W., F. Y. Liew, A. Severn, D. Xu, S. J. McSorley, P. Garside, J. Padron, and R. S. Phillips. 1994. Regulation of the immune response by nitric oxide differentially produced by T helper type 1 and T helper type 2 cells. *Eur J Immunol 24:980.*

Terada, L. S. 1996. Hypoxia-reoxygenation increases O2-. efflux which injures endothelial cells by an extracellular mechanism. *Am J Physiol 270:H945.*

Thiemermann, C. 1995. Selective inhibition of the activity of inducible nitric oxide synthase in septic shock. *Prog Clin Biol Res 392:383.*

Thornton, F. J., M. R. Schaffer, M. B. Witte, L. L. Moldawer, S. L. MacKay, A. Abouhamze, C. L. Tannahill, and A. Barbul. 1998. Enhanced collagen accumulation following direct transfection of the inducible nitric oxide synthase gene in cutaneous wounds. *Biochem Biophys Res Commun 246:654.*

Tissot, M., M. D'Asniere, M. Solier, J. P. Giroud, and R. Engler. 1984. Study of the evolution of acute phase reactants and of thromboxane and prostacyclin during calcium pyrophosphate-induced pleurisy in the rat. *Agents Actions 14:82.*

Tissot, M., D. Regoli, and J. P. Giroud. 1985. Bradykinin levels in inflammatory exudates. *Inflammation 9:419.*

Toda, N., T. Matsumoto, and K. Yoshida. 1992. Comparison of hypoxia-induced contraction in human, monkey, and dog coronary arteries. *Am J Physiol 262:H678.*

Tomlinson, A., I. Appleton, A. R. Moore, D. W. Gilroy, D. Willis, J. A. Mitchell, and D. A. Willoughby. 1994. Cyclo-oxygenase and nitric oxide synthase isoforms in rat carrageenin- induced pleurisy. *Br J Pharmacol 113:693.*

Tracey, W. R., M. Nakane, J. Kuk, G. Budzik, V. Klinghofer, R. Harris, and G. Carter. 1995. The nitric oxide synthase inhibitor, L-NG-monomethylarginine, reduces carrageenan-induced pleurisy in the rat. *J Pharmacol Exp Ther 273:1295.*

Tsai, A. 1994. How does NO activate hemeproteins? *FEBS Lett 341:141.*

Tsunawaki, S., M. Sporn, A. Ding, and C. Nathan. 1988. Deactivation of macrophages by transforming growth factor-beta. *Nature 334:260.*

Tucker, A., I. F. McMurtry, A. F. Alexander, J. T. Reeves, and R. F. Grover. 1977. Lung mast cell density and distribution in chronically hypoxic animals. *J Appl Physiol 42:174.*

Uchida, T., T. Yamashita, A. Araki, H. Watanabe, and F. Sendo. 1997. rIFN-gamma-activated rat neutrophils induce tumor cell apoptosis by nitric oxide. *Int J Cancer 71:231.*

Ueki, Y., S. Miyake, Y. Tominaga, and K. Eguchi. 1996. Increased nitric oxide levels in patients with rheumatoid arthritis. *J Rheumatol 23:230.*

Urban, M. B., R. Schreck, and P. A. Baeuerle. 1991. NF-kappa B contacts DNA by a heterodimer of the p50 and p65 subunit. *Embo J 10:1817.*

Vane, J. R., J. A. Mitchell, I. Appleton, A. Tomlinson, D. Bishop-Bailey, J. Croxtall, and D. A. Willoughby. 1994. Inducible isoforms of cyclooxygenase and nitric-oxide synthase in inflammation. *Proc Natl Acad Sci U S A 91:2046.*

Vane, J. R., and R. M. Botting. 1997. Mechanism of action of aspirin-like drugs. *Semin Arthritis Rheum 26:2.*

Vasquez-Vivar, J., B. Kalyanaraman, P. Martasek, N. Hogg, B. S. Masters, H. Karoui, P. Tordo, and K. A. Pritchard, Jr. 1998. Superoxide generation by endothelial nitric oxide synthase: the influence of cofactors. *Proc Natl Acad Sci U S A 95:9220.*

Vega, V. L., M. Maldonado, L. Mardones, V. Manriquez, E. Vivaldi, J. Roa, and P. H. Ward. 1998. Inhibition of nitric oxide synthesis aggravates hepatic oxidative stress and enhances superoxide dismutase inactivation in rats subjected to tourniquet shock. *Shock 9:320.*

Verdon, C. P., B. A. Burton, and R. L. Prior. 1995. Sample pretreatment with nitrate reductase and glucose-6-phosphate dehydrogenase quantitatively reduces nitrate while avoiding interference by NADP+ when the Griess reaction is used to assay for nitrite. *Anal Biochem 224:502.*

Vodovotz, Y., C. Bogdan, J. Paik, Q. W. Xie, and C. Nathan. 1993. Mechanisms of suppression of macrophage nitric oxide release by transforming growth factor beta. *J Exp Med 178:605.*

Wahl, L. M., S. M. Wahl, S. E. Mergenhagen, and G. R. Martin. 1975. Collagenase production by lymphokine-activated macrophages. *Science 187:261.*

Wallerath, T., I. Gath, W. E. Aulitzky, J. S. Pollock, H. Kleinert, and U. Forstermann. 1997. Identification of the NO synthase isoforms expressed in human neutrophil granulocytes, megakaryocytes and platelets. *Thromb Haemost 77:163.*

Wang, Y., W. R. Mathews, D. M. Guido, A. Farhood, and H. Jaeschke. 1995. Inhibition of nitric oxide synthesis aggravates reperfusion injury after hepatic ischemia and endotoxemia. *Shock 4:282.*

Ward, C., T. H. Wong, J. Murray, I. Rahman, C. Haslett, E. R. Chilvers, and A. G. Rossi. 2000. Induction of human neutrophil apoptosis by nitric oxide donors: evidence for a caspase-dependent, cyclic-GMP-independent, mechanism. *Biochem Pharmacol 59:305.*

Warrens, A. N., and R. I. Lecher. 1992. Key molecular events in the induction and expression of the immune response. In *The molecular biology of the immune response.* A. W. Thomson, ed. John Wiley and Sons, Chichester, p. 1.

Watanabe, K., F. Koizumi, Y. Kurashige, S. Tsurufuji, and H. Nakagawa. 1991. Rat CINC, a member of the interleukin-8 family, is a neutrophil- specific chemoattractant in vivo. *Exp Mol Pathol 55:30.*

Watanabe, Y., K. Terashima, and H. Hidaka. 1996. Neuronal nitric oxide synthase specific autophosphorylation in baculovirus/Sf9 insect cell system. *Biochem Biophys Res Commun 219:638.*

Wedmore, C. V., and T. J. Williams. 1981. Control of vascular permeability by polymorphonuclear leukocytes in inflammation. *Nature 289:646.*

Wei, X. Q., I. G. Charles, A. Smith, J. Ure, G. J. Feng, F. P. Huang, D. Xu, W. Muller, S. Moncada, and F. Y. Liew. 1995. Altered immune responses in mice lacking inducible nitric oxide synthase. *Nature 375:408.*

Weinberg, J. B., D. L. Granger, D. S. Pisetsky, M. F. Seldin, M. A. Misukonis, S. N. Mason, A. M. Pippen, P. Ruiz, E. R. Wood, and G. S. Gilkeson. 1994. The role of nitric oxide in the pathogenesis of spontaneous murine autoimmune disease: increased nitric oxide production and nitric oxide synthase expression in MRL-lpr/lpr mice, and reduction of spontaneous glomerulonephritis and arthritis by orally administered NG-monomethyl-L- arginine. *J Exp Med 179:651.*

Weisz, A., L. Cicatiello, and H. Esumi. 1996. Regulation of the mouse inducible-type nitric oxide synthase gene promoter by interferon-gamma, bacterial lipopolysaccharide and NG- monomethyl-L-arginine. *Biochem J 316:209.*

Werb, Z., and S. Gordon. 1975. Elastase secretion by stimulated macrophages. Characterization and regulation. *J Exp Med 142:361.*

White, K. A., and M. A. Marletta. 1992. Nitric oxide synthase is a cytochrome P-450 type hemoprotein. *Biochemistry 31:6627.*

Willis, R. A., A. K. Nussler, K. M. Fries, D. A. Geller, and R. P. Phipps. 1994. Induction of nitric oxide synthase in subsets of murine pulmonary fibroblasts: effect on fibroblast interleukin-6 production. *Clin Immunol Immunopathol 71:231.*

Willis, D., A. Tomlinson, R. Frederick, M. J. Paul-Clark, and D. A. Willoughby. 1995. Modulation of heme oxygenase activity in rat brain and spleen by inhibitors and donors of nitric oxide. *Biochem Biophys Res Commun 214:1152.*

Willis, D. 1999. Overview of HO-1 in inflammatory pathologies. In *Inducible enzymes in the inflammatory response*, Vol. 4. D. A. Willoughby, and A. Tomlinson, eds. Birkhauser Verlag, Basel-Boston-Berlin, p. 55.

Wink, D. A., K. S. Kasprzak, C. M. Maragos, R. K. Elespuru, M. Misra, T. M. Dunams, T. A. Cebula, W. H. Koch, A. W. Andrews, J. S. Allen, and et al. 1991. DNA deaminating ability and genotoxicity of nitric oxide and its progenitors. *Science 254:1001.*

Wink, D. A., and J. Laval. 1994. The Fpg protein, a DNA repair enzyme, is inhibited by the biomediator nitric oxide in vitro and in vivo. *Carcinogenesis 15:2125.*

Winkler, J. D., C. M. Sung, W. C. Hubbard, and F. H. Chilton. 1993. Influence of arachidonic acid on indices of phospholipase A2 activity in the human neutrophil. *Biochem J 291:825.*

Witte, M. B., M. R. Schaffer, and A. Barbul. 1996. Phenotypic induction of nitric oxide is critical for synthetic function in wound fibroblasts. *Surgical Forum:703.*

Wolff, D. J., and B. J. Gribin. 1994. The inhibition of the constitutive and inducible nitric oxide synthase isoforms by indazole agents. *Arch Biochem Biophys 311:300.*

Wright, C. D., A. Mulsch, R. Busse, and H. Osswald. 1989. Generation of nitric oxide by human neutrophils. *Biochem Biophys Res Commun 160:813.*

Wu, G. 1995. Nitric oxide synthesis and the effect of aminoguanidine and NG-monomethyl-L-arginine on the onset of diabetes in the spontaneously diabetic BB rat. *Diabetes 44:360.*

Wu, T. W., K. P. Fung, J. Wu, C. C. Yang, and R. D. Weisel. 1996. Antioxidation of human low density lipoprotein by unconjugated and conjugated bilirubins. *Biochem Pharmacol 51:859.*

Xie, W. 1992. Mitogen-inducible prostaglandin G/H synthase: a new target for nonsteroidal antiinflammatory drugs. *Drug Development Research 25:249.*

Xu, Q., Y. Hu, R. Kleindienst, and G. Wick. 1997. Nitric oxide induces heat-shock protein 70 expression in vascular smooth muscle cells via activation of heat shock factor 1. *J Clin Invest 100:1089.*

Young, L. H., C. C. Liu, S. Joag, S. Rafii, and J. D. Young. 1990. How lymphocytes kill. *Annu Rev Med 41:45.*

Ziche, M., L. Morbidelli, R. Choudhuri, H. T. Zhang, S. Donnini, H. J. Granger, and R. Bicknell. 1997. Nitric oxide synthase lies downstream from vascular endothelial growth factor-induced but not basic fibroblast growth factor-induced angiogenesis. *J Clin Invest 99:2625.*

Ziche, M., A. Parenti, F. Ledda, P. Dell'Era, H. J. Granger, C. A. Maggi, and M. Presta. 1997. Nitric oxide promotes proliferation and plasminogen activator production by coronary venular endothelium through endogenous bFGF. *Circ Res 80:845.*

APPENDIX II

Abstracts

Northeast ADR, Eastham D, **Paul-Clark MJ**,. Burnand KG. 1993. A comparison between foot plethysmography and light reflection rheography in patients with healed venous ulcers. *Venous Forum Annual Meeting.*

Willis D, Tomlinson A, Frederick R, **Paul-Clark MJ**, Willoughby DA. 1995. The effect of arginine analogues and an NO donor on heme oxygenase in rat tissue homogenates. *Inflammation Research 44(S3):S235.*

Gilroy DW, Tomlinson A, Appleton I, **Paul-Clark MJ**, Willoughby DA. 1995. Effects of aspirin on cyclooxygenase (COX) and nitric oxide synthase (NOS) in chronic inflammation. *Inflammation Research 44(S3):S271.*

Brown JR, Willis D, Moore AR, **Paul-Clark MJ**, Willoughby DA. 1995. Apoptosis, heat shock protein 70kDa and tumour supressor p53 in a model of acute inflammation in the rat. *2nd World Congress on Inflammation*, Brighton.

Paul-Clark MJ, Tomlinson A, Gilroy DW, Willis D, Willoughby DA. 1998. Nitric oxide synthase inhibitors exacerbate acute inflammation in rat carrageenin-induced pleurisy. *Oral presentation. Pathological Society of Great Britain and Ireland, Winter meeting; 6-8th January.*

Paul-Clark MJ, Lim LHK, Del Soldato P, Burgaud J-L, Flower RJ and Perretti M. 2000. NCX-1015, a novel derivative of prednisolone with enhanced anti-inflammatory properties. *British Journal of Pharmacology 129: 98P.*

Paul-Clark MJ, Lim LHK, Del Soldato P, Burgaud J-L, Flower RJ and Perretti M. 2000. A nitro-derivative of prednisolone (NCX-1015) possesses higher anti-inflammatory activities. *FASEB 14 (4): 491.8.*

Paul-Clark MJ, Gilroy DW, Willoughby DA and Tomlinson A. 2001. Opposing effects of NOS inhibitors depending on their administration route. *5th World Congress on Inflammation, Edinburgh; Abstract number 04/03*

Paul-Clark MJ, Mancini L , Burgaud J-L, Flower RJ and Perretti M. 2001. Local and systemic effects of nitro-prednisolone (NCX-1015) in experimental arthritis. *5th World Congress on Inflammation, Edinburgh; Abstract number W14/02*

Roviezzo F, **Paul-Clark MJ**, Del Soldato P, Flower RJ and Perretti M. 2001. Enhanced activation of the glucocorticoid receptor by nitro- prednisolone (NCX-1015). *5th World Congress on Inflammation, Edinburgh; Abstract number W14/03*

Paul-Clark MJ, Howat D, Flower RJ, Moore PK and Perretti M. 2001. Nitro-paracetamol (NCX-701) exhibits anti-inflammatory activity in the zymosan air pouch. *5th World Congress on Inflammation, Edinburgh; Abstract number 09/01*

Papers

Willis D, Tomlinson A, Frederick R, **Paul-Clark MJ**, Willoughby DA. 1995. Modulation of heme oxygenase activity in rat brain and spleen by inhibitors and donors of nitric oxide. *Biochem Biophys Res Commun 214:1152.*

Gilroy DW, Colville-Nash PR, Willis D, Chivers J, **Paul-Clark MJ**, Willoughby DA. 1999. Inducible cyclooxygenase may have anti-inflammatory properties. *Nat Med 5:698.*

Paul-Clark MJ, Del Soldato P, Fiorucci S, Flower RJ, Perretti M. 2000. 21-NO-prednisolone is a novel nitric oxide-releasing derivative of prednisolone with enhanced anti-inflammatory properties. *Br J Pharmacol 131:1345.*

Paul-Clark MJ, Gilroy DW, Willis D, Willoughby DA, Tomlinson A. 2001. Nitric oxide synthase inhibitors have opposite effects on acute inflammation depending on their route of administration. *J Immunol 166:1169.*

Oliani SM, **Paul-Clark MJ**, Christian HC, Flower RJ, Perretti M. 2001. Neutrophil interaction with inflamed postcapillary venule endothelium alters annexin 1 expression. *Am J Pathol 158:603.*

Contributions to other publications

Colville-Nash PR, Clarke AE, Sy-Yed I, Gilroy DW, **Paul-Clark MJ**, Tomlinson A, Willoughby DA. Control of inducible nitric oxide synthase in murine macrophages by diclofenac and hyaluronic acid. *The Royal Society of Medicine*; Round Table Series **45**:127-146. (1996)

Seed MP, Gilroy D, **Paul-Clark MJ**, Tomlinson A, Willoughby DA. The role of the inducible enzymes cycloxygenase-2, nitric oxide synthase, and heme oxygenase in inflammation angiogenesis. In "Inducible enzymes in inflammation". Eds. Willoughby D.A., and Tomlinson A. Birkhauser Press. (1998).

CHAPTER 6

6.1 Introduction

Numerous investigations have shown *in vitro* and *in vivo* that products from the COX and NOS pathways can directly affect the activity of their respective enzymes (Swierkosz *et al.*, 1995; Curtis *et al.*, 1996; Lin., *et al* 1999). Moreover, some NSAIDs including aspirin (Amin *et al.*, 1995; Aeberhard *et al.*, 1995; Colville-Nash *et al.*, 1996) have been shown *in vitro* to inhibit iNOS mRNA, protein and NO production. Therefore, the inhibition of NO by aspirin may be an additional mechanism accounting for its anti-inflammatory actions and may explain the differences observed in NSAIDs capacity to inhibit neutrophil function (Abramson *et al.*, 1985), COX activity (Mitchell *et al.*, 1993) NF-κB activation (Kopp and Ghosh, 1994) and neurogenic inflammation (Abramson, 1992). Therefore, the effect of COX inhibition on the nitric oxide pathway was investigated using aspirin *in vivo*, using the complement mediated carrageenin-induced pleurisy and the murine croton-oil-induced chronic granulomatous tissue air pouch. In addition, the effect of COX inhibition was further investigated *in vitro* using two immortalised cell lines, murine derived J774.2 macrophages and hybrid endothelial cells derived from human umbilical veins, EA.hy926, to further assess actions of aspirin on the generation of nitric oxide.

6.2 Effects of aspirin on iNOS and NO production in the carrageenin-induced pleurisy

6.2.1 Inflammatory parameters at 6h.

Aspirin dose-dependently reduced exudate volume by 15, 33, 27, 36, 41 and 67% at 10, 20, 50, 100, 200 and 500mg/kg respectively compared with control values (1.25 ± 0.10ml). A significant reduction ($p \leq 0.05$) was seen at 20, 100, 200 and 500mg/kg (Figure 6.1A).

Similar effects were observed on inflammatory cell number by 13, 40, 50, 39, 42 and 46% at 20, 50, 100, 200 and 500mg/kg compared to control values (120 ± 5 $x10^6$ cells; Figure 6.1B). A significant reduction ($p \leq 0.05$) was seen at 20, 50, 100, 200 and 500mg/kg.

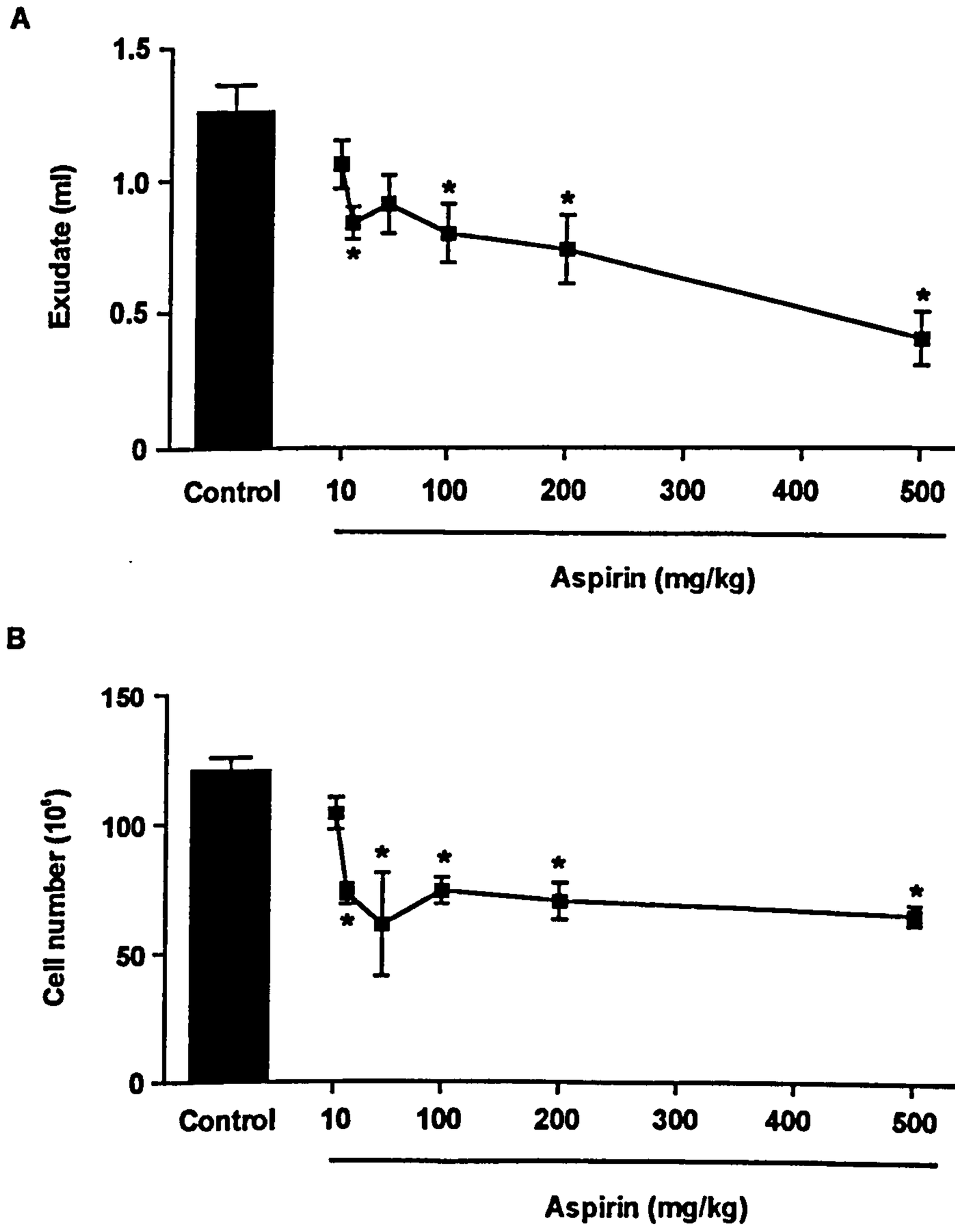

Figure 6.1 Effect of oral administration of aspirin on inflammatory parameters in the carrageenin-induced pleurisy. *Where (A) is Exudate volume and (B) inflammatory cells recovered from the pleural cavity. Data is expressed as mean ± standard error of the mean (n=6 per group). *p≤0.05 in comparison to saline controls.*

6.2.2 PGE_2 levels at 6h

Since the principle mechanism by which aspirin exerts its anti inflammatory effect is by the inhibition of PGE_2 production, levels of this prostanoid were determined in cell-free inflammatory exudates at 6h. Aspirin dose-dependently reduced exudate PGE_2 levels by 30, 67, 67, 77, 91 and 95% at 10, 20, 50, 100, 200 and 500mg/kg respectively compared with control values (166 ± 40 pg). A

significant reduction ($p \leq 0.05$) was seen at 20, 50, 100, 200 and 500mg/kg (Figure 6.2).

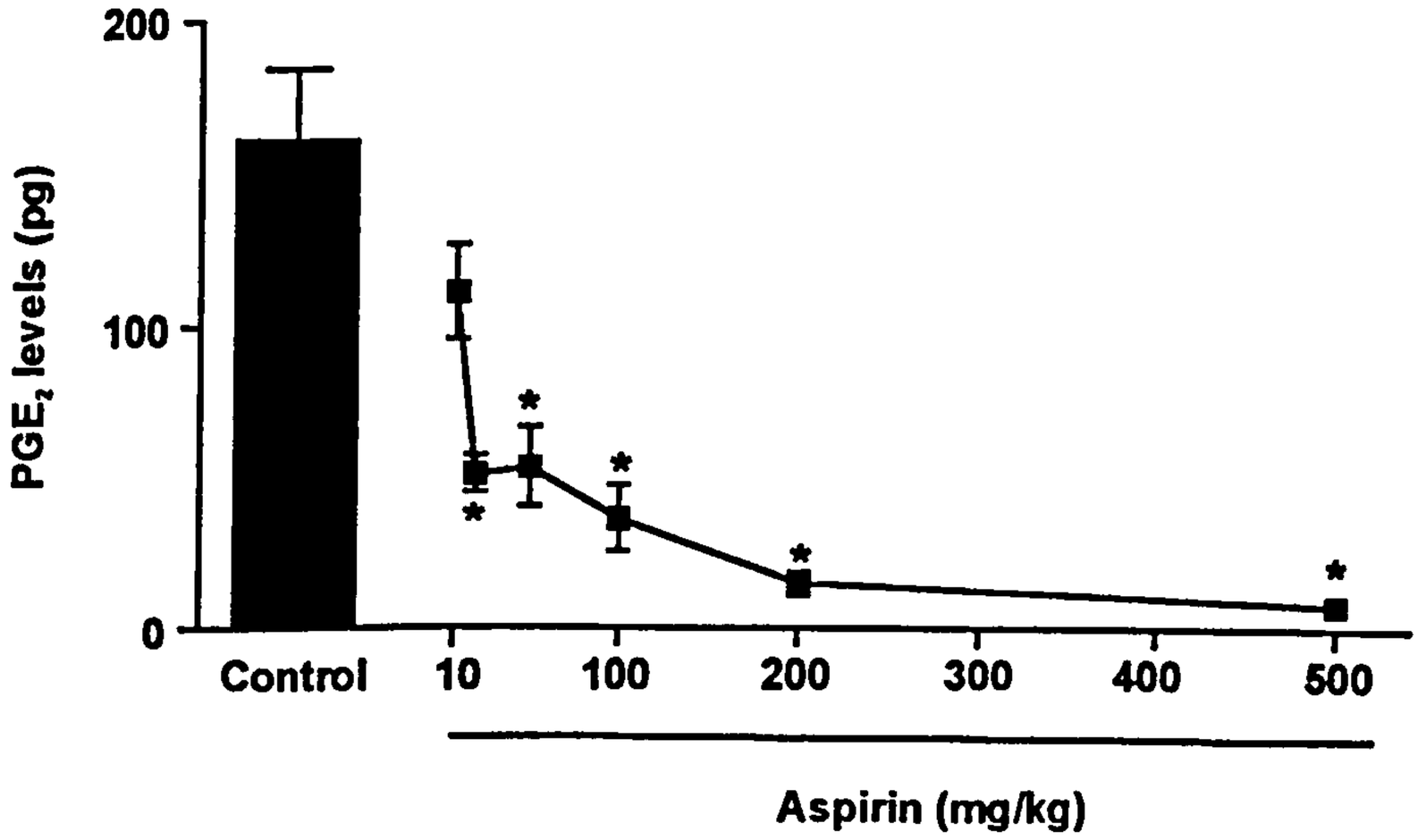

Figure 6.2 Effect of oral administration of aspirin on PGE_2 levels in the carrageenin-induced pleurisy at 6h. *Data is expressed as mean ± standard error of the mean (n=6 per group). *$p \leq 0.05$ in comparison to saline controls.*

6.2.3 Nitric oxide pathway at 6h

Oral administration of aspirin resulted in a dose-dependent increase in nitrite, iNOS protein and iNOS activity at 6h. Nitrite levels were significantly increased ($p \leq 0.05$) at 100, 200 and 500mg/kg by 178, 270 and 280%, respectively compared with controls (12.9 ± 1.4μM; Figure 6.3A).

Similarly, iNOS protein expression was elevated significantly ($p \leq 0.05$) at 100, 200 and 500mg/kg by 313, 285 and 257%, respectively compared with control values (19.2 ± 10.9 arbitrary units; Figure 6.3B)

Again iNOS activity was increased significantly ($p \leq 0.05$) by aspirin treatment a 100, 200 and 500mg/kg by120, 126 and 118% compared with control values (448 ± 80 pmol citrulline/mg protein/30 min; Figure 6.3C).

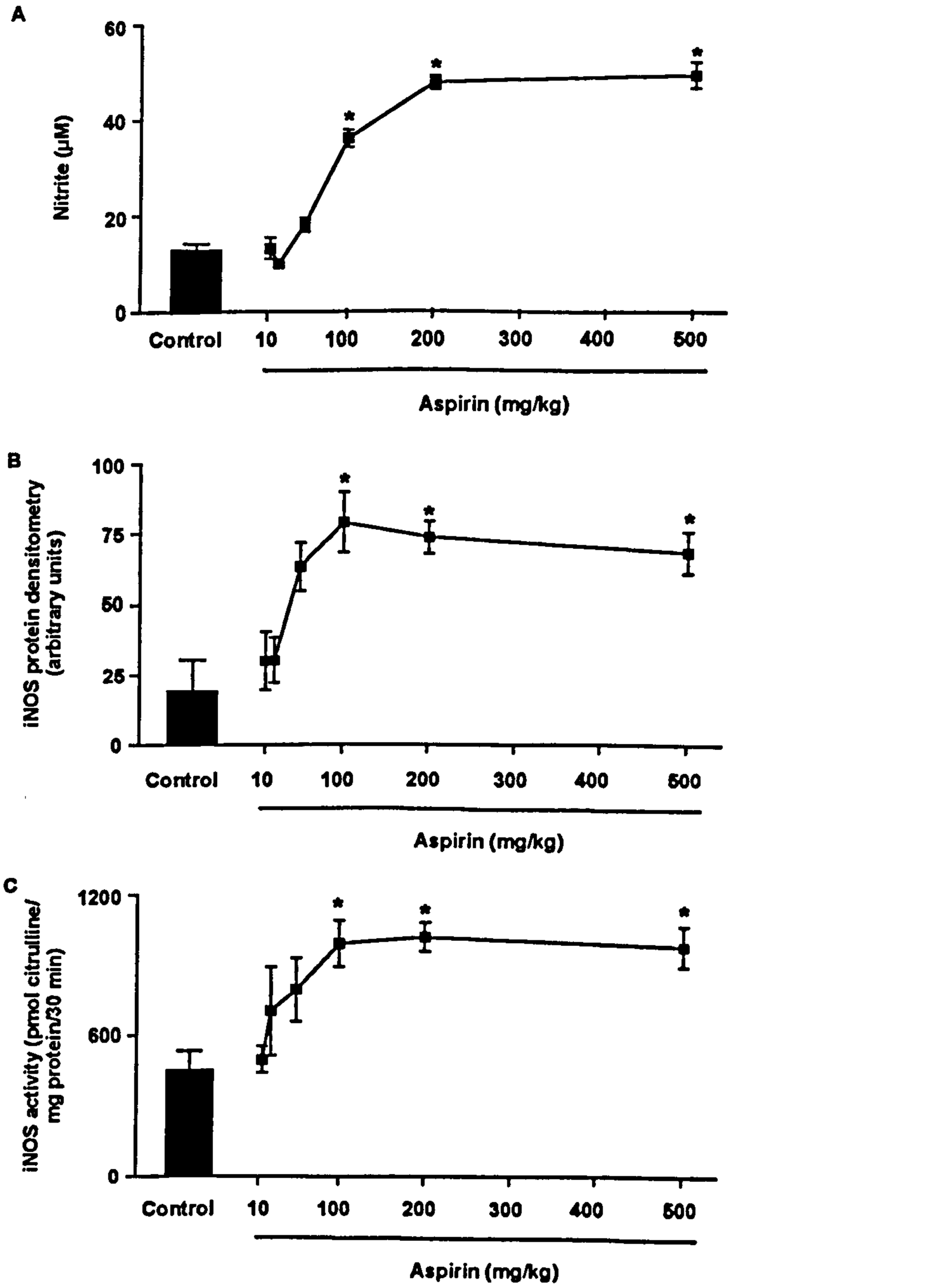

Figure 6.3 Effect of oral administration of aspirin on the nitric oxide pathway in the carrageenin-induced pleurisy at 6h. *Where (A) is nitrite, (B) densitometry of iNOS protein expression and (C) iNOS activity. Data is expressed as mean ± standard error of the mean (n=6 per group). *p≤0.05 in comparison to saline controls.*

6.2.4 Effect of oral administration of aspirin and intrapleural injection of AE-ITU at 6h

Oral administration of aspirin significantly reduced exudate volume and inflammatory cell number whilst elevating levels of NO. In addition to this data,

intrapleural injection of NOS inhibitors significantly increased inflammatory parameters whilst significantly reducing nitrite levels. Therefore it was suggested that NO might be anti-inflammatory in the carrageenin-induced pleural model. Hence, to determine if aspirin exerted it's anti-inflammatory effect, at least in part by elevating NO, both aspirin and AE-ITU were given prior to carrageenin injection and the effect on inflammation and NO production was measured at 6h.

Animals that were dosed orally with gum tragacanth and injected intrapleurally with saline had an exudate level of 1.32 ± 0.06ml. Exudate levels were significantly reduced ($p \leq 0.05$) in rats treated with aspirin (200mg/kg) orally and saline intrapleurally (0.85 ± 0.13ml). The reduction in exudate volume observed with aspirin was reversed by intrapleural injection of AE-ITU (3, 10mg/kg), being 1.30 ± 0.11, 1.48 ± 0.14ml respectively (Figure 6.4A).

Animals that were dosed orally with gum tragacanth and injected intrapleurally with saline had 104 ± 7 $x10^6$ cells transmigrate into the pleural cavity. Inflammatory cell number was significantly reduced ($p \leq 0.05$) in rats treated with aspirin (200mg/kg) orally and saline intrapleurally (53 ± 9 $x10^6$ cells). The reduction in cellular influx observed with aspirin was reversed by intrapleural injection of AE-ITU (3, 10mg/kg), being 92 ± 6 and 107 ± 8 $x10^6$ cells respectively (Figure 6.4B).

Animals that were dosed orally with gum tragacanth (t= -1h) and injected intrapleurally with saline produced 17.3 ± 0.3μM nitrite in cell free exudates. Nitrite levels were significantly increased ($p \leq 0.05$) in rats treated with aspirin (200mg/kg) orally and saline intrapleurally (58.7 ± 1.3μMl). The increase in nitrite levels observed with aspirin was ameliorated by intrapleural injection of AE-ITU (3, 10mg/kg), being 17.3 ± 3.9 and 10.2 ± 0.7μm respectively (Figure 6.4C).

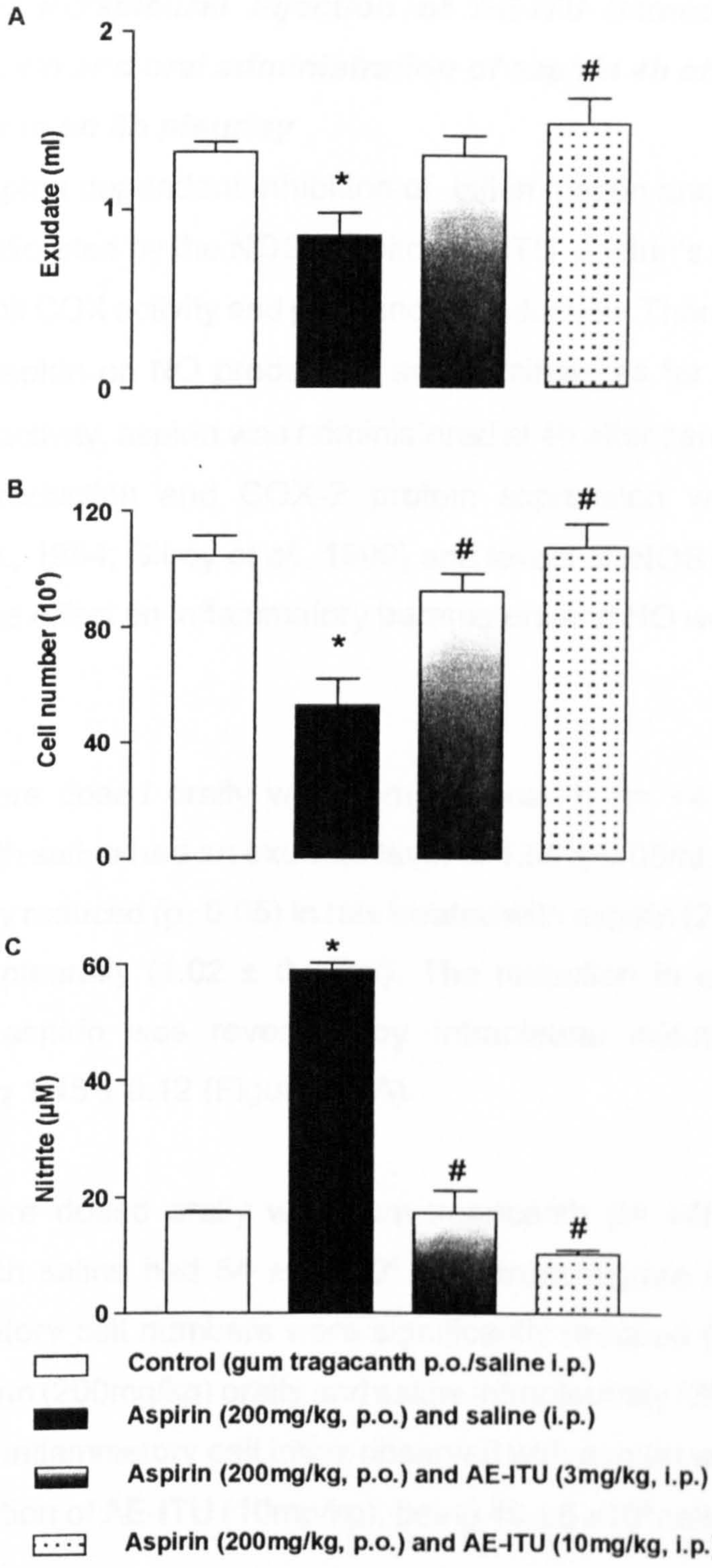

Figure 6.4 Effects of aspirin dosed orally and AE-ITU injected locally on inflammation in the carrageenin-induced pleurisy at 6h. *Either AE-ITU or saline was injected directly into the pleural cavity of rats immediately before carrageenin injection. Aspirin or gum tragacanth was dosed orally 1h before carrageenin injection. Thereafter, their effects on (A) exudate volume, (B) cell number and (C) nitrite in pleural exudates was determined 6h after carrageenin injection. Data is expressed as mean ± standard error of the mean (n=6 per group). * $p \leq 0.05$ in comparison to saline controls, #$p \leq 0.05$ in comparison to aspirin (200mg/kg, p.o.) and saline (i.p.)*

6.2.5 Effect of intrapleural injection of AE-ITU immediately prior to carrageenin and oral administration of aspirin 4h after carrageenin injection in an 8h pleurisy

Although the aspirin dependent inhibition of inflammation and increase in NO levels were ameliorated by the NOS inhibitor AE-ITU, aspirin's main action is to irreversibly inhibit COX activity and prostanoid production. Therefore, to confirm the effects of aspirin on NO production and eliminate as far as possible the effects on COX activity, aspirin was administered at 4h after carrageenin, a time where PGE_2 production and COX-2 protein expression were decreasing (Tomlinson *et al.*, 1994; Gilroy *et al.*, 1999) and levels of iNOS protein were on the increase. The effect on inflammatory parameters and NO were assessed at 8h.

Animals that were dosed orally with gum tragacanth (t= +4h) and injected intrapleurally with saline had an exudate level of 1.58 ± 0.05ml. Exudate levels were significantly reduced ($p \leq 0.05$) in rats treated with aspirin (200mg/kg) orally and saline intrapleurally (1.02 ± 0.07ml). The reduction in exudate volume observed with aspirin was reversed by intrapleural injection of AE-ITU (10mg/kg), being 1.45 ± 0.12 (Figure 6.5A).

Animals that were dosed orally with gum tragacanth (t= +4h) and injected intrapleurally with saline had 54 ± 3 $x10^6$ cells transmigrate into the pleural cavity. Inflammatory cell numbers were significantly reduced ($p \leq 0.05$) in rats treated with aspirin (200mg/kg) orally and saline intrapleurally (36 ± 2 $x10^6$cells). The reduction in inflammatory cell influx observed with aspirin was reversed by intrapleural injection of AE-ITU (10mg/kg), being 49 ± 5 $x10^6$ cells(Figure 6.5B).

Animals that were dosed orally with gum tragacanth (t= +4h) and injected intrapleurally with saline produced 15.0 ± 0.6μM nitrite in cell free exudates. Nitrite levels were significantly increased ($p \leq 0.05$) in rats treated with aspirin (200mg/kg) orally and saline intrapleurally (54.7 ± 2.3μMl). The increase in

nitrite levels observed with aspirin were ameliorated by intrapleural injection of AE-ITU (10mg/kg), being 12.8 ± 0.9μm (Figure 6.5C).

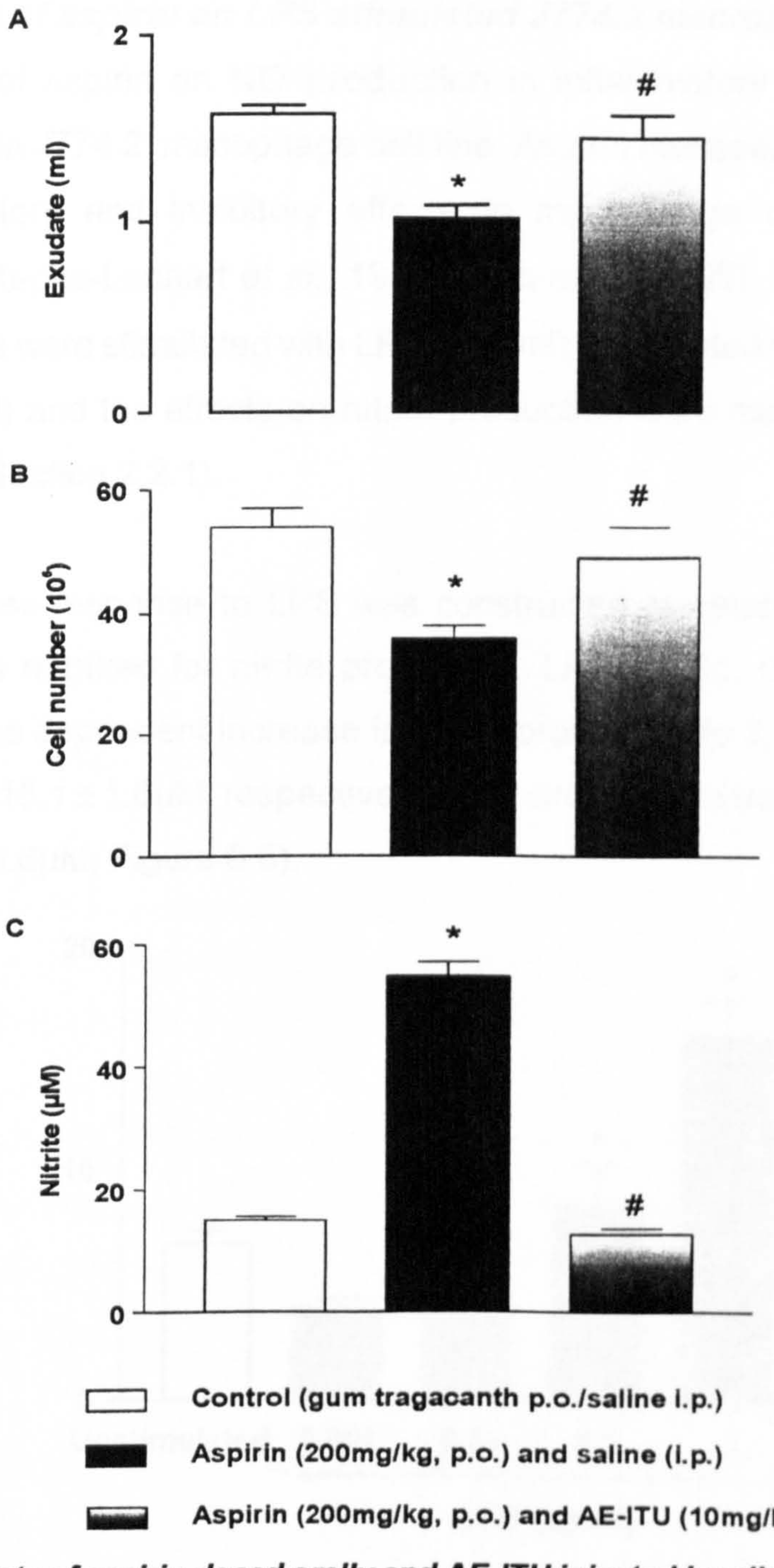

Figure 6.5 Effects of aspirin dosed orally and AE-ITU injected locally on inflammation at 8h in the carrageenin-induced pleurisy. *Either AE-ITU or saline were injected directly into the pleural cavity of rats immediately before carrageenin injection. Aspirin or gum tragacanth was dosed orally 4h after carrageenin injection. Thereafter, their effects on (A) exudate volume, (B) cell number and (C) nitrite in pleural exudates was determined 8h after carrageenin injection. Data is expressed as mean ± standard error of the mean (n=6 per group). * $p \leq 0.05$ in comparison to saline controls, #$p \leq 0.05$ in comparison to aspirin (200mg/kg, p.o.) and saline (i.p.)*

6.3 Effects of aspirin on LPS stimulated J774.2 macrophages and A23187 stimulated EA.hy926 endothelial cells

6.3.1 Effect of aspirin on LPS stimulated J774.2 macrophages

The effects of aspirin on NO production in inflammatory cells was further investigated in J774.2 macophage cell line. Aspirin has been reported to have both stimulatory and inhibitory effects in macrophage cell lines on NO production (Kepka-Lenhart *et al.*, 1996; Amin *et al.*, 1995). Therefore, J774.2 macrophages were stimulated with LPS (1µg/ml) and treated with aspirin (3, 10, 30, 100µg/ml) and the effects on nitrite production were measured 24h post-stimulation (Section 2.2.1).

Initially, a dose-response to LPS was constructed to establish the optimum concentration required for nitrite production. LPS (0.001, 0.01, 0.1, 1µg/ml) caused a dose dependent increase in nitrite production to 3.9 ± 0.6, 3.9 ± 0.4, 8.6 ± 1.8 and 16.1 ± 1.6µM, respectively, compared to cells treated with medium alone (6.8 ± 0.6µM; Figure 6.6).

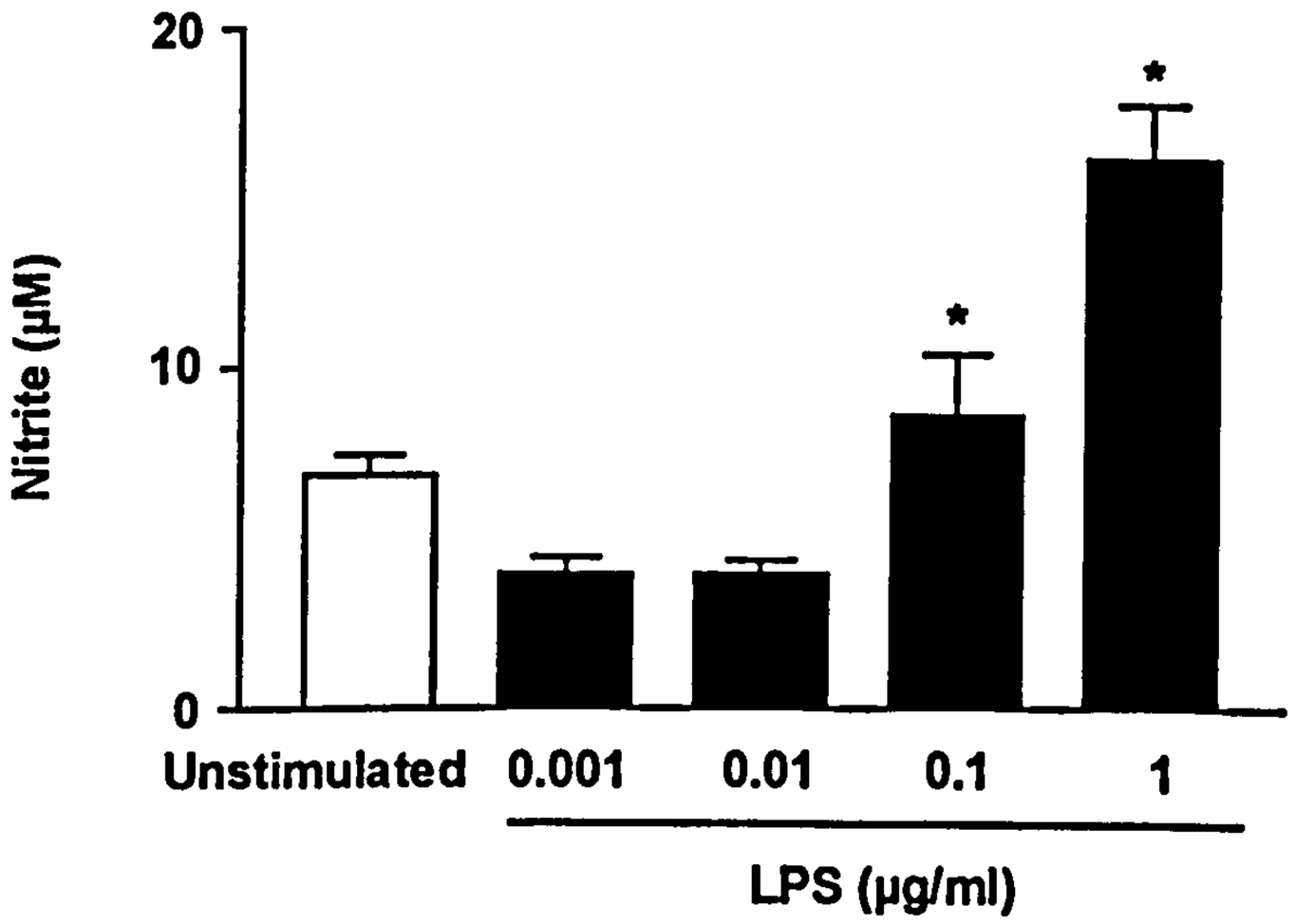

Figure 6.6 Effects of LPS stimulation on nitrite production in J774.2 macrophages after 24h. *Data is expressed as mean ± s.e.m. (n=8 per dose). *p≤0.05 in comparison to LPS-stimulated controls.*

Unstimulated J774.2 macrophages produced very little nitrite (0.6 ± 0.3μM); this was significantly elevated by LPS (1μg/ml) stimulation to 5.9 ± 0.1μM. Aspirin treatment at 30 and 100μg/ml significantly elevated nitrite levels in these cell by 10 and 22%, respectively, compared to LPS stimulated cells (Figure 6.7).

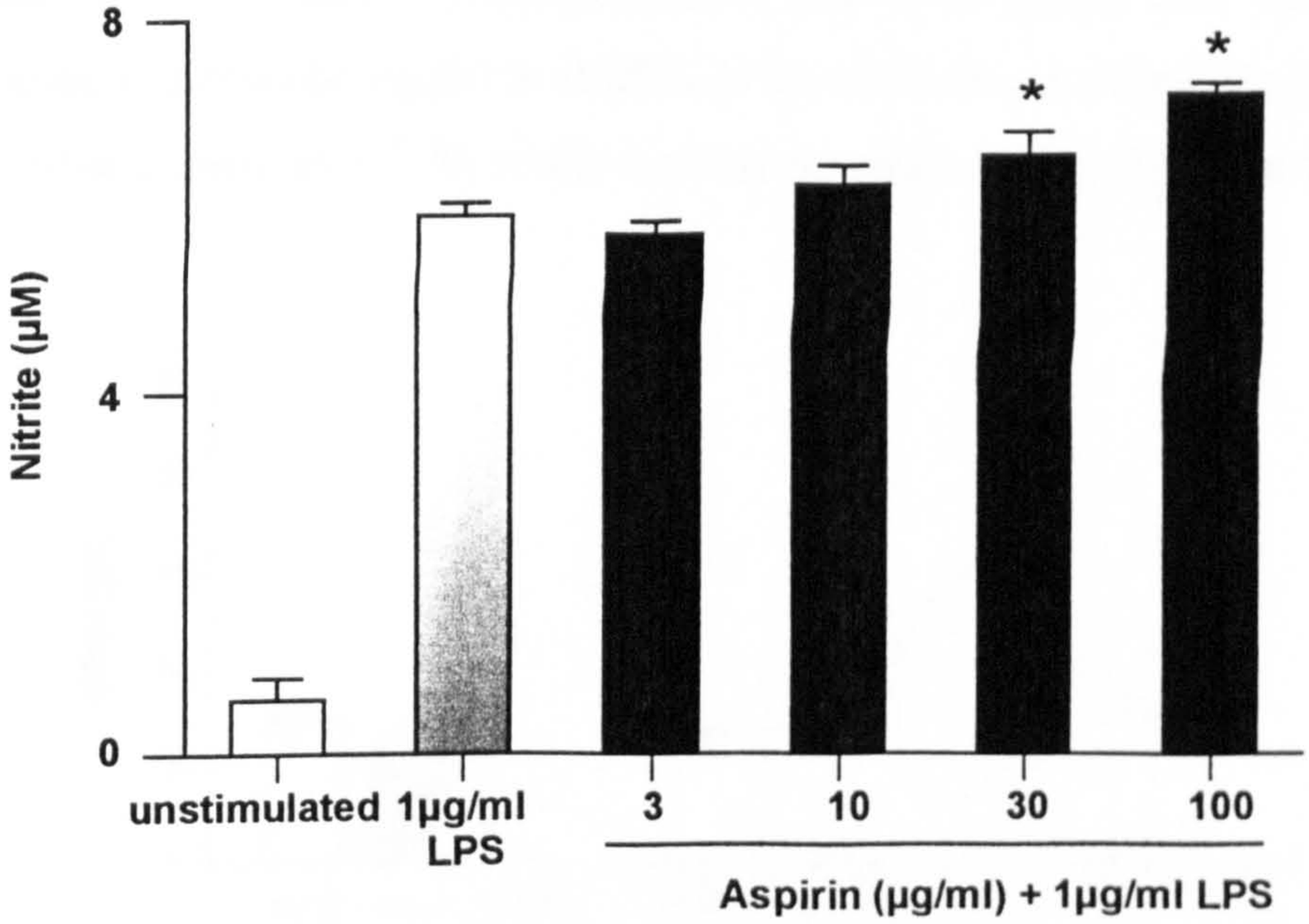

Figure 6.7 Effects of concomitant administration of aspirin and LPS in J774.2.2 macrophages at 24h on nitrite production*. Data is expressed as mean ± s.e.m. (n=10 per dose). *p≤0.05 in comparison to LPS-stimulated controls.*

6.3.2 Effects of A23187 stimulation on EA.hy926 endothelial cells

Other cells that maybe a target for aspirin and its potential induction of NO are endothelial cells. For these experiments the immortalised endothelial cell line EA.hy926 was used.

The effect of the calcium ionophore A23187 was assessed on cellular viability and nitrite production to obtain a profile of effect for this particular stimulus on EA.hy926 endothelial cells and to optimise the concentrations required for nitrite production. After 24h stimulation cells were assessed for the above parameters.

EA.hy926 cells were stimulated with different concentrations of the calcium ionophore A23187 (0.005, 0.01, 0.05, 0.1, 0.5, 1, 2.5, 5μM), this caused a

significant increase in nitrite levels in the cell-free supernatant at 0.1, 0.5 and 1μM by 67, 231 and 67%, respectively, when compared to vehicle control groups (5.9 ± 0.3μM), medium control values were 7.4 ± 0.5μM (Figure 6.8A). Cell viability was assessed using the MTT method (Section 2.21) in the same experiments. At A23817 concentrations 2.5 and 5μM, cell viability was significantly reduced being 60 and 50% of control values respectively. Vehicle control values were 91 ± 3 % of the normal medium control (Figure 6.8B)

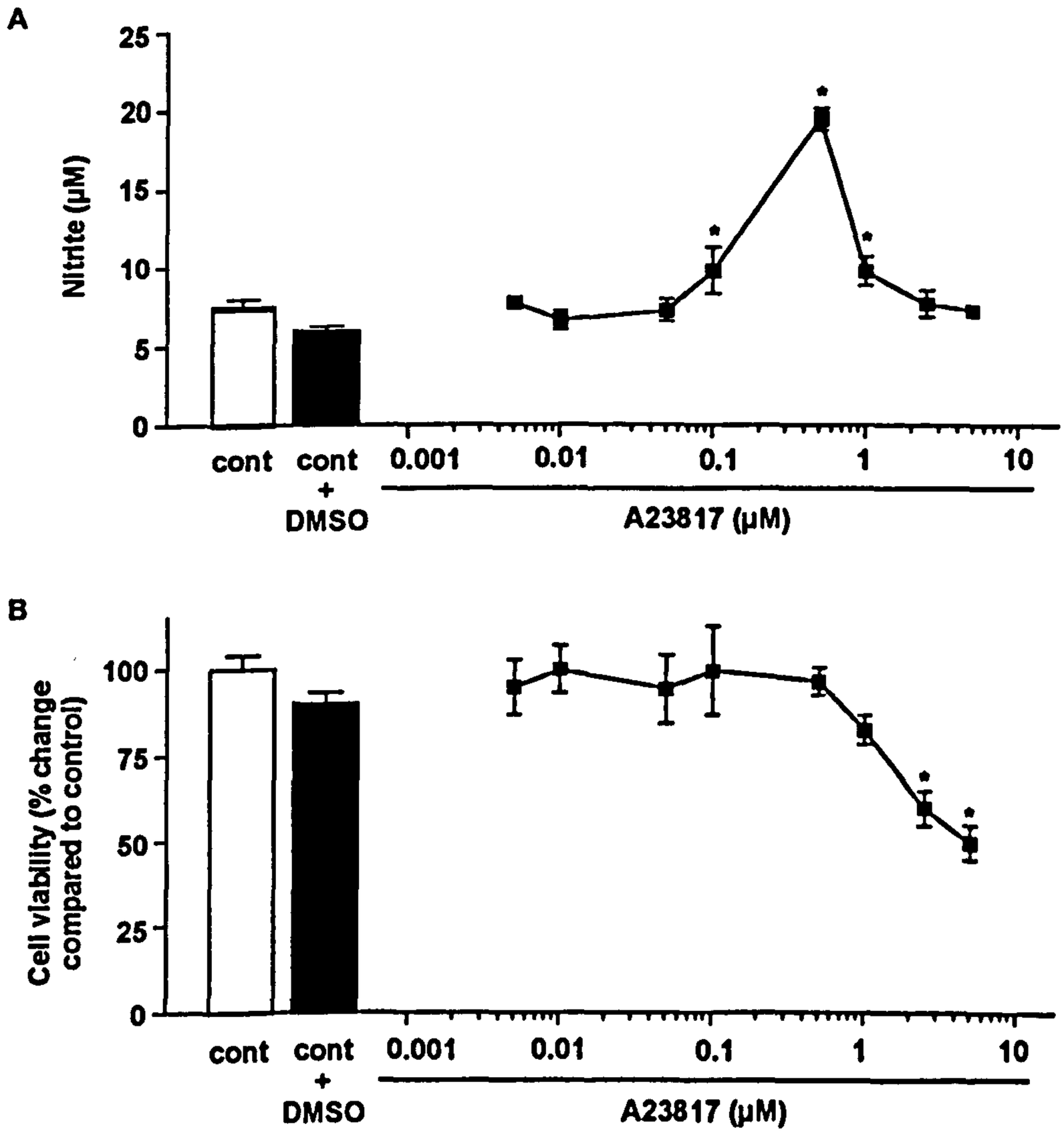

Figure 6.8 Effects of A23187 stimulation on nitrite production and cell viability in EA.hy926 endothelial cells after 24h. *Data is expressed as mean ± s.e.m. (combination of two experiments with n=8 per dose). *p≤0.05 in comparison to control + DMSO.*

A time course of A23187 stimulation was carried out to assess whether 24h was the optimal time point for the measurement of nitrite formation. A concentration

of 0.5μM A23187 was used in this and all subsequent experiments because this concentration caused maximal nitrite production with little effect on cell viability.

The effect of A23187 (0.5μg/ml) stimulation was assessed at 15 min, 1, 2, 6, 12, 24h. This resulted in a time dependent increase in nitrite levels being maximally elevated at 24h (25.3 ± 1.6μM) compared to vehicle control (11.6 ± 3.0μM; Figure 6.9).

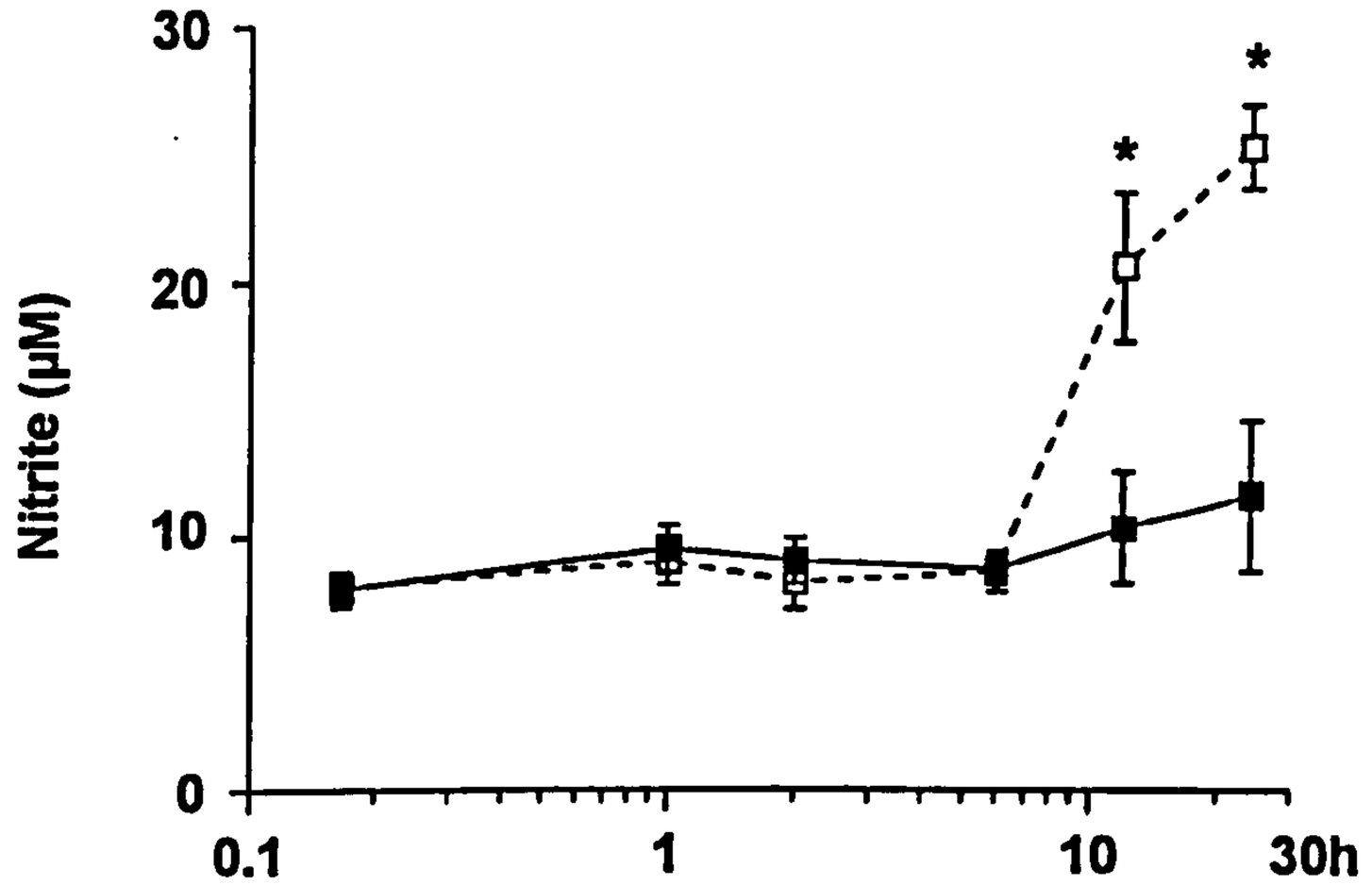

Figure 6.9 Effects of A23187 stimulation on nitrite production in EA.hy926 endothelial cells between 10min and 24h. *Data is expressed as mean ± s.e.m. (n=6 per time point). *p≤0.05 in comparison to vehicle controls.*

In subsequent studies a 24h time point was used, since it was the peak in nitrite concentrations out of the time points measured.

6.3.3 Effects of aspirin on A23187 stimulated EA.hy926 endothelial cells

The effect of concomitant administration of aspirin (0.03-3μM) and A23187 (0.5μg/ml) was assessed in endothelial cells on iNOS protein expression, nitrite, iNOS and cNOS activity and cell viability. Unlike the response seen in inflammatory pellets from the carrageenin-induced pleurisy, iNOS protein expression from EA.hy926 endothelial cells didn't change (Figure 6.10A).

However nitrite levels were significantly elevated ($p \leq 0.05$) by aspirin treatment at 0.3µg/ml with the level being 23.9 ± 1.8µM compared to both A23187 (0.5µM; 7.9 ± 2.9µM nitrite) alone and vehicle treated control cells (0.7 ± 0.1µM nitrite; Figure 6.10B).

Similarly iNOS activity was significantly elevated ($p \leq 0.05$) by aspirin treatment at 0.3µg/ml, being 174 ± 24 pMol citrulline/mg protein/30 min compared to both A23187 (0.5µM; 91 ± 10 pMol citrulline/mg protein/30 min) alone and vehicle treated control cells (33 ± 10 pMol citrulline/mg protein/30 min; Figure 6.10C).

Stimulation of EA.hy926 cells with A23187 (0.5µM) caused an inhibition of ecNOS; however some activity was detected at an aspirin dose of 0.3µg/ml (33 ± 28 pMol citrulline/mg protein/30 min) which was similar to vehicle treated control values (44 ± 14 pMol citrulline/mg protein/30 min; Figure 6.10D).

Aspirin (0.03, 0.1, 0.3, 1, 3µg/ml) had no effect on cell viability of EA.hy926 endothelial cells after A23817 stimulation (Figure 5.28E).

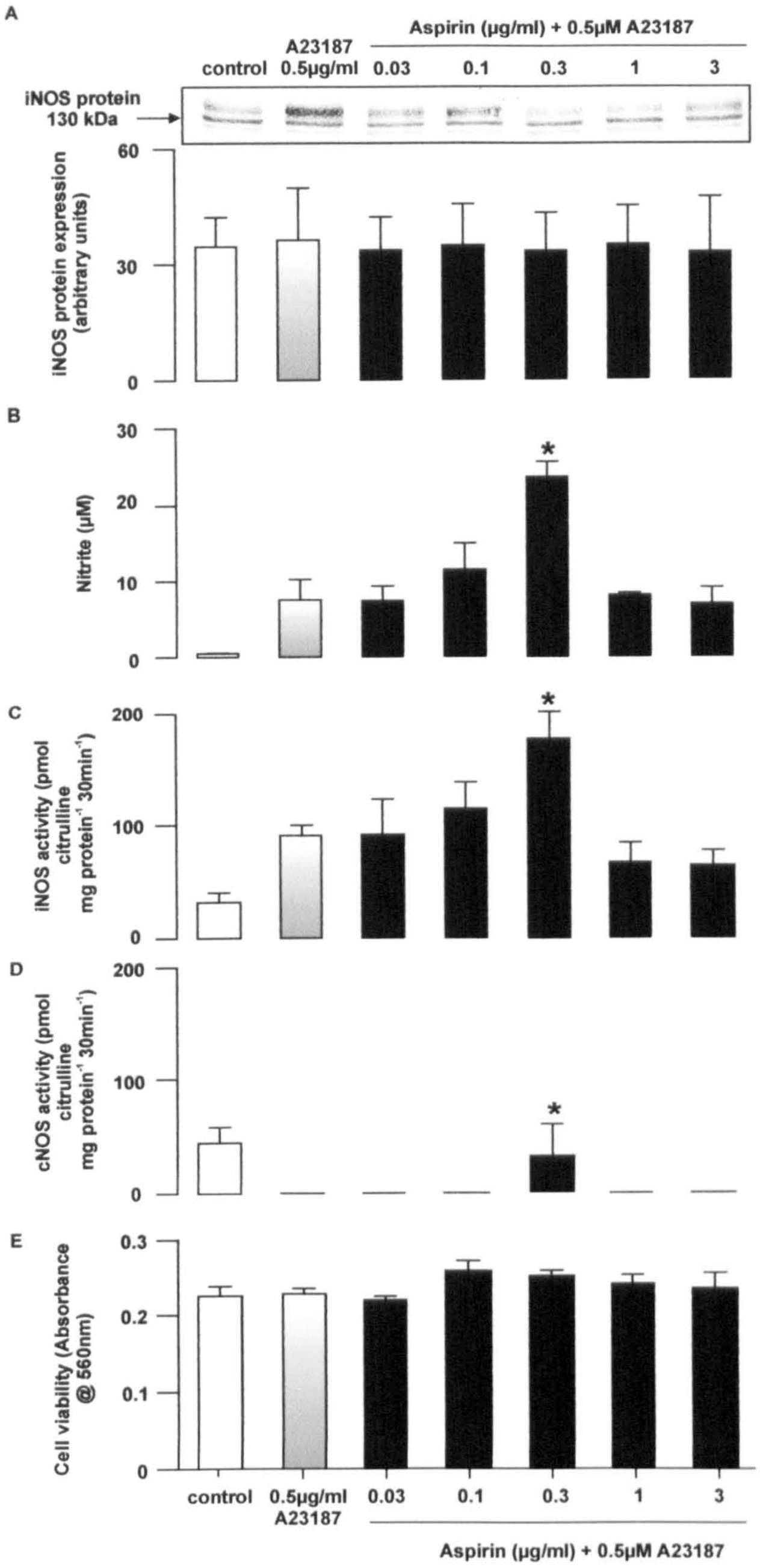

Figure 6.10 Effect of concomitant administration of aspirin and A23187 on the nitric oxide pathway and cell viability in EA.hy926 endothelial cells. *Where (A) is densitometry of iNOS protein expression (inserted panel is a representitive Western blot), (B) nitrite, (C) iNOS activity, (D) cNOS activity and (E) cell viability after 24h of stimulation. Data is expressed as mean ± standard error of the mean (2 experiments, n=8 per group each experiment for nitrite, iNOS and cNOS activity: cell viability 1 experiment, n=8 per gorup: iNOS Western blots 1 experiment n=4 per gorup). *p≤0.05 in comparison to A23187 stimulated cells.*

6.4 Effect of aspirin in the murine croton oil-induced granulomatous tissue air pouch

6.4.1 iNOS enzyme activity and granulomatous tissue dry weight in a 7 day chronic air pouch

The NSAID aspirin (10, 200mg/kg), was dosed orally from 3 days after the induction of inflammation. Its effects were assessed on granuloma dry weight and nitric oxide production at 7 days in this model of chronic inflammation.

Oral administration of aspirin had no effect on granulomatous tissue dry weight at 7 days, however, at a dose of 10mg/kg significantly increased iNOS activity at 7 days (Table 6.1).

NSAID	dose	n	Granuloma dry weight (mg)	iNOS activity (pmol citrulline/mg protein/30 min)
control	-	22	74 ± 8	297 ± 68
aspirin	10	22	73 ± 6	814 ± 371*
	200	22	67 ± 7	435 ± 141

Table 6.1 Effects of oral administration of aspirin in the murine croton oil-induced chronic granulomatous tissue air pouch. *The effects of aspirin were assessed on granuloma dry weight and iNOS activity at 7 days . Data is expressed as mean ± s.e.m. of n animals per group. * $p \leq 0.05$ in comparison to control mice.*

6.4.2 A further examination of the effects of aspirin on the iNOS protein expression and activity at 7 days.

The effects of aspirin (10, 100, 200mg/kg) were further investigated at 7 days in this model, with iNOS protein expression and activity being determined in the same samples. As previously described iNOS activity was significantly increased with aspirin (10mg/kg; Figure 6.11B). Values were 133 ± 19, 111 ± 7 and 103 ± 20 pmol citrulline/mg protein/30min at 10, 100 and 200 mg/kg of aspirin, respectively, compared with gum tragacanth treated controls (90 ± 10 pmol citrulline/mg protein/30min). However, there was no effect on iNOS protein

expression (Figure 6.11A), suggesting that in the murine croton oil-induced chronic granulomatous tissue air pouch aspirin increased iNOS enzyme activity without affecting protein expression. However, Western blot analysis may not have been sensitive enough to detect changes in iNOS protein expression in this tissue, since only a subpopulation of influxing macrophages in the granuloma are immunopossitive for iNOS at this time point.

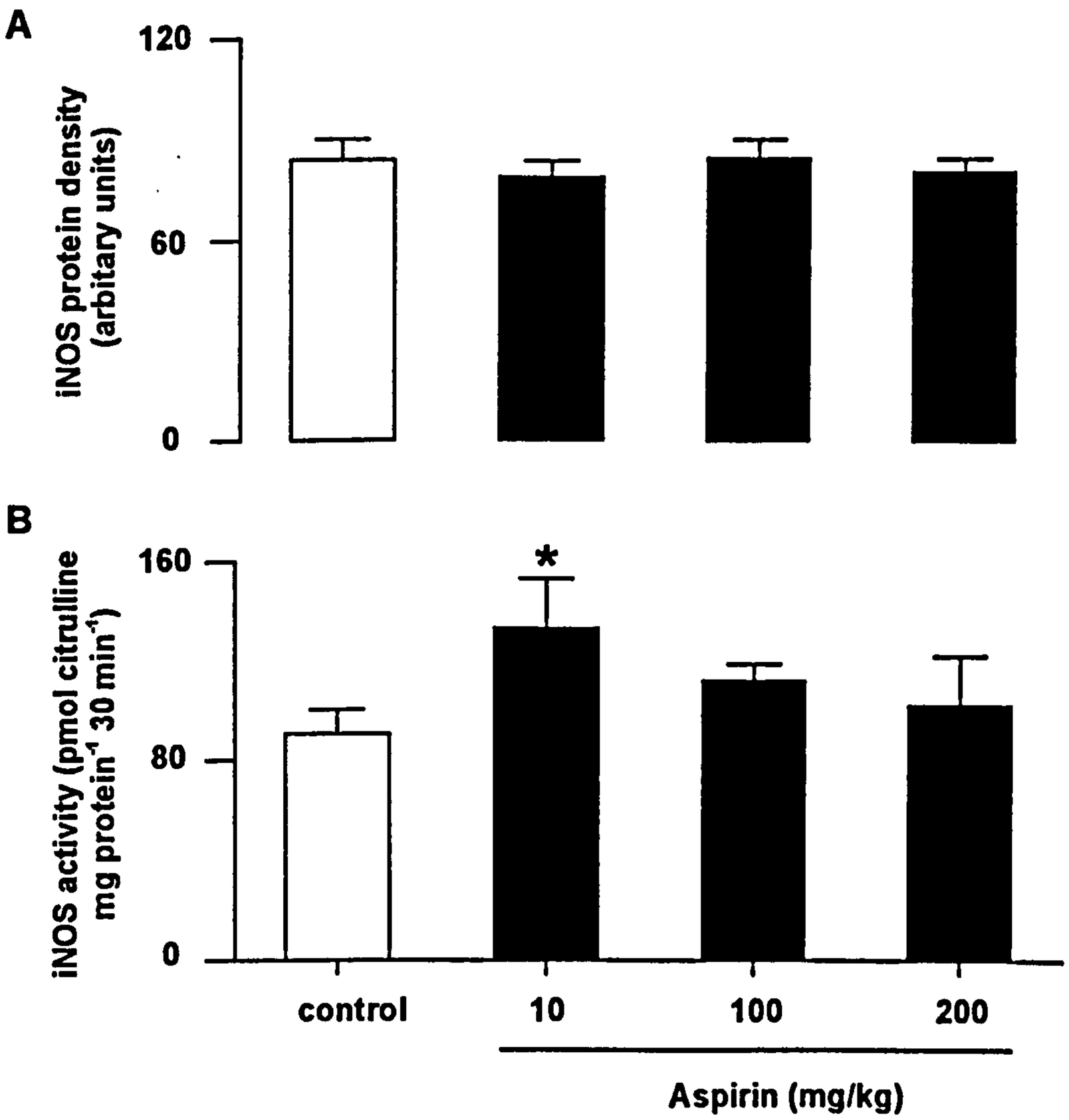

Figure 6.11 Effects of oral administration of aspirin in the murine croton oil-induced chronic granulomatous tissue air pouch at 7 days on the NOS pathway. *Where, (a) is iNOS protein levels measured by densitometry from Western blots and (b) iNOS activity. Data is expressed as mean ± standard error of the mean (n=8 per group). *p≤0.05 in comparison to control values.*

In summary, aspirin significantly increased iNOS enzyme activity in the granuloma at 7 days. Although aspirin had no effect on inflammation at 7 days, a significant reduction in granuloma dry weight was observed at 14 days.

Aspirin (200mg/kg) significantly ($p \geq 0.05$) reduce COX activity as measured by the production of PGE_2 in granulomatous tissue at this time point (Table 6.2).

	dose (mg/kg)	n	COX activity (ng PGE_2/mg protein/30 min)
control	-	22	51 ± 7
aspirin	10	22	25 ± 6 *
	200	22	8 ± 5 *

Table 6.2 Effects of oral administration of aspirin in the murine croton oil-induced chronic granulomatous tissue air pouch at 7 days on COX activity. *Data is expressed as mean ± s.e.m. of n animals per group. * $p \leq 0.05$ in comparison to control mice.*

6.5 Summary of findings

(1) Oral administration of aspirin dose-dependently decreased exudate volume, cell number and PGE_2 levels in the pleural cavity of rats 6h after carrageenin injection. Surprisingly, this resulted in a significant dose-dependent elevation of iNOS enzyme activity and immunoreactivity in recovered inflammatory cells and an increase in nitrite formation in cell-free exudate. The inhibitory effects on inflammation and stimulatory effects on nitrite production of oral administration of aspirin were reversed by local intrapleural injection of the NOS inhibitor AE-ITU.

(2) Stimulation of J774.2 macrophages with LPS caused a significant increase in NO release from these cells and similarly to the carrageenin-induced pleurisy, concomitant administration of aspirin had a stimulatory effects on nitrite release from J774.2 cells into the culture medium.

(3) Stimulation of EA.hy926 endothelial cells with the calcium ionophore A23817 caused a significant time-dependent increase in NO released from these cells, being maximal at 24h. Concomitant administration of aspirin (0.3µg/ml) significantly increased iNOS activity and cNOS activity in the cells and nitrite release into the medium, however no effect was observed on iNOS protein expression. Treatment of these cells with the combination of aspirin and A23817 had no effect on cellular viability.

(4) Oral administration of aspirin (10mg/kg) significantly increased iNOS enzyme activity in conjunction with significantly reducing COX activity. However, aspirin had no effect on granuloma size of iNOS protein expression.

CHAPTER 7

7.1 Discussion

As already discussed at the beginning of this thesis both iNOS protein expression and NO are present in nearly all inflammatory diseases and models of inflammation investigated to date. However, the contribution of NO to the inflammatory environment remains unclear. This investigation aimed to assess the function of NO within a number of different inflammatory processes. Further it was the aim of this thesis to correlate NO production with the expression of other inflammatory mediators such as arginase and cyclooxygenase which may regulate its production or alternatively be regulated by NO. These studies were therfore performed to afford an insight into whether iNOS would be a good therapeutic target for the development of an anti-inflammatory therapy.

7.1.1 NO in the carrageenin-induced pleurisy

Carrageenin is a seaweed extract that causes an acute inflammation through the alternative complement pathway, and has been used for many years in the identification of anti-inflammatory targets and the development of therapeutic agents. In this thesis iNOS protein expression, activity and nitrite formation were mapped throughout the time course of the carrageenin-induced pleurisy followed by modulation using NOS inhibitors. NO, as measured indirectly by nitrite accumulation was generated in the pleural cavity in a time dependent manner with a double peak suggesting that there may be two different sources of NO production in this model. The first peak at 30 min is probably a result of NO production from endothelial cells since the nitrite produced at this early time point was insensitive to dexamethasone inhibition. This was supported by the finding that iNOS protein expression was undetectable in inflammatory cells taken from the pleural cavity at this time point. NO accumulation at 30 min is at a time when other inflammatory mediators such as thromboxane B_2 (Tissot *et al.*, 1984), histamine (Sin *et al.*, 1986) and bradykinin (Tissot *et al.*, 1985) are present. Therefore, it is highly possible that these early mediators, acting via receptor occupancy, could have induced the release of NO from endothelial cells (Fujii *et al.*, 1994). It was found that the injection of NOS inhibitors directly into the site of this acute inflammatory lesion immediately before carrageenin

exacerbated inflammation at 1h, a time prior to the induction of iNOS in influxing inflammatory cells. This was true for all the inhibitors regardless of selectivity between isoforms. However at this time point where NO was probably produced by eNOS, the eNOS partially selective inhibitor L-NIO was more potent at reducing nitrite levels. Possible functions for this early release of NO may be to inhibit platelet aggregation and increase vasodilation in vessels close to the inflammatory site and possibly prevent PMN and monocyte chemotaxis (Kubes *et al.*, 1991; De Caterina *et al.*, 1995).

The second peak in nitrite at 6h coincided with peaks in iNOS protein expression and activity and was most likely from this inducible isoform. The major cell type present in pleural washouts at this time point are PMNs, with monocytes making up the majority of the remainder. Immunolabeling of inflammatory smears at 6h showed that both monocytes and PMNs stained positively for iNOS, with the most intense staining being associated with monocytes. Both cell types have been previously described to produce NO from iNOS (Nathan, 1992; McCall *et al.*, 1989). Interestingly, cNOS was also maximal at this time point, but the total activity detected was far lower than that seen for iNOS. There are two possible explanations of this increase in cNOS activity at this point. PMNs have been documented to contain not only iNOS but also cNOS (Wright *et al.*, 1989; McCall *et al.*, 1989) and therefore a likely source of this activity since no endothelial cells were present in the pleural washouts. This is in agreement with work published by Padgett and Pruett (1995) showing that both rodent and human PMNs were capable of generating nitrite although at considerable lower levels than that produced by rodent macrophages. Inhibition of NO at 6h had the same effects as seen at 1h, with an increase in exudate formation and cellular influx, while nitrite levels were significantly reduced. In additional experiments, AE-ITU was administered into the pleural cavity 2h after carrageenin injection, to investigate the effects of NO inhibition on the second peak of NO formation in the pleural cavity seen at 6h. Again, it was found that while nitrite was significantly reduced, exudate volume and inflammatory cell numbers were significantly increased. Additionally, I have demonstrated that NO inhibition at

both 1 and 6h resulted an increase in inflammatory parameters during the resolution stage (36h) and prolonged the resolution (72h).

In order to elucidate the mechanism by which inhibition of NO generation exacerbates inflammation the levels of a number of candidate pro-inflammatory mediators was measured. As shown by Capasso and colleagues (1975), mast cell-derived histamine peaked in this model between 0.5-1h after carrageenin injection. Given that histamine contributes to oedema formation (Capasso *et al.*, 1975; Giraldelo *et al.*, 1994) and that NO stabilises mast cells, thereby preventing histamine release (Salvemini *et al.*, 1991; Brooks *et al.*, 1999), levels of this acute inflammatory mediator were measured after NOS inhibition. NOS inhibition increased histamine release and correspondingly decreased mast cell numbers in pleural exudates. Further experiments showed that systemic depletion of mast cells with CMP 48/80 (Paton,1951; Feldberg and Talesnik 1953) attenuated the increased plasma exudation observed with NOS inhibitors without altering the increase in inflammatory cells, although both exudate and cell numbers were significantly lower after mast cell degranulation. In support of this observation others have shown that inhibition of NO in mesenteric post capillary venules increased inflammatory cell emigration, plasma extravasation, free radical-mediated tissue damage, mast cell degranulation and histamine release (Gaboury *et al.*, 1996). As well as histamine, levels of the potent rat neutrophil chemoattractant CINC were also determined. CINC, which is induced through a nuclear factor κB (NF-κB) pathway in response to inflammatory stimulation (Blackwell *et al.*, 1994), mediates PMN chemotaxis in the rat (Watanabe *et al.*, 1991) by upregulating PMN CD11/18 expression thus facilitating PMN diapedesis (Frevert *et al.*, 1995). NOS inhibition also increased levels of CINC in cell free exudates, in addition to histamine. This may be a further a contributing factor to the increased inflammatory cell numbers recorded after NOS inhibition.

Since most NOS inhibitors contain a number of highly reactive groups (Peterson *et al.*, 1992) it was essential to check for possible non-specific actions of these

inhibitors on inflammation. Therefore D-NAME, the inactive enantiomer of L-NAME, was injected into the pleural cavity of rats 1h before carrrageenin and the inflammatory response assessed at 1 and 6h. At both doses used (the same molarity as AE-ITU at 3 and 10mg/kg), no effect on inflammation was observed. Therefore, it could be concluded that the effects on inflammation and mediator levels at these time points were a direct result of the inhibition of NO.

Levels of lipid-derived mediators were also measured particularly as inhibition of NO synthesis increases endothelial PGI_2 release (Doni *et al.*, 1988) and that PGE_2, PGI_2 and LTB_4 facilitate oedema formation and inflammatory cell influx. Treatment with NOS inhibitors locally at a time when iNOS protein expression and enzyme activity is maximal had no effect on either PGE_2 or PGI_2 but significantly increased LTB_4. Previous experiments have also shown that NO donors dose-dependently reduce LTB_4 production from activated PMNs (Moilanen *et al.*, 1993). Interestingly, differential cell counts revealed that AE-ITU at 6h caused an increase in the proportion of PMNs, possibly as a result of an increase in CINC and LTB_4. Collectively, these mechanistic studies demonstrate that NO generated at the inflammatory site critically regulates the severity of the inflammatory response by keeping in check levels of pro-inflammatory mediators such as histamine, CINC and LTB_4.

As another mechanism to explain the increase in inflammation after NOS inhibition, cellular and exudate levels of antioxidants were measured by the TAOS and SSA assays. NOS inhibition caused a increase in TAOS and SSA, which suggested that there was an increase in the levels of superoxide and other oxidant species in the absence of NO. Superoxide anion is produced by PMNs and monocytes from the enzyme activity of NADPH oxidase and xanthine oxidase at inflammatory sites. Both enzymes systems contain a heme prosthetic group, which NO can react with to inhibit $O_2^{\cdot}$ release (Fukahori *et al.*, 1994; Wang *et al.*, 1995). Therefore, inhibiting NO removes an inhibitory effect on superoxide production. In support of this notion, others have shown that NO generation reduces superoxide levels while its inhibition increases superoxide

production both *in vitro* and *in vivo* (Gaboury *et al.*, 1993; Guidot *et al.*, 1995; Rodenas *et al.*, 1998). As superoxide has been associated with tissue damage and loss of function during inflammatory episodes (Vega *et al.*, 1998) it is conceivable that yet another contributor to an enhanced inflammatory response, consequent to NOS inhibition, is superoxide generation. Indeed, elevated levels of superoxide increases histamine release from mast cells (Mannaioni *et al.*, 1991), as well as LTB_4 and PMN accumulation in a model of pancreatitis through a PAF-dependent mechanism (Hotter *et al.*, 1997). Finally, NO can decreases NF-kB activation through inhibition of IkB- phosphorylation and degradation (Katsuyama *et al.*, 1998) and can also inhibit directly NF-kB binding to DNA (Park *et al.*, 1997). Therefore, a disturbance in the balance between NO and superoxide production, whereby NO production is inhibited, may lead to an increase in pro-inflammatory mediators and provides a possible mechanism for the exacerbation of inflammation observed in this study.

The increase in superoxide levels seen may underly the three-fold induction of inducible HSP 72 in inflammatory cells at 72h after NOS inhibition. HSP 72 is induced by oxidative and other stresses and helps to refold proteins that have undergone oxidative damage (Ryan and Hightower,1996). This is further evidence that suggests that NO inhibition may exacerbate oxidative stress pathways in this model and prolong pathology.

Finally, NO has been well documented to accelerate the rate of apoptosis both *in vitro* and *in vivo* (Fortenberry *et al.*, 1998; Blaylock *et al.*, 1998; Barthlen *et al.*, 2000). Therefore, it is hypothesised here that inhibition of NO could be increasing the number of inflammatory cells at the site of inflammation by suppressing apoptosis. However, immunohistochemical analysis of DNA fragmentation, using the TUNEL assay, within pleural exudates of rats treated with NOS inhibitors showed no change in the number of positively labelled apoptotic bodies when compared to saline treated animals at 6h. This is not surprising since apoptosis is an active process requiring time for cellular changes to occur. Therefore, a later time point should have been measured.

With hindsight the TUNEL assay also has a number of problems associated with measurement of apoptotic cells. In my experience, there were a large number of false positives making it difficult to assess apoptosis in this model. However at the time these experiments were performed, this was believed to be the best method for measurement of apoptosis. Subsequently, data has shown that neutrophils contain relatively high levels of the enzyme terminal deoxynucleotidyl transferase used for adding DIG to fragmented DNA. Methods that are more appropriate for the determination of apoptosis in this carrageenin-indued pleurisy include caspase measurements, annexin five binding to phosphotidylserine and an acridine orange staining technique. In conclusion, although apoptosis was not affected at 6h one cannot discount the possibility that inhibition of NO may have delayed apoptosis and attributed to the elevation of inflammatory parameters at the later time points.

The vast majority of reports have shown that NOS inhibitors are considered anti-inflammatory in models of both acute and chronic inflammation (Salvemini *et al.*,1996; Weinberg *et al.*, 1994). For instance, in a model of trinitrobenzene sulphonic acid-induced colitis in rats, the non-selective NOS inhibitor L-NAME reduced neutrophil and macrophage influx (Hogaboam *et al.*,1995), while in a carrageenin-induced pleurisy, L-NMMA also significantly reduced exudate formation and cellular influx (Tracey *et al.*, 1995). In these studies, however, NOS inhibitors were administered at high doses away from the site of inflammation i.e. orally or intraperitoneally. Given their lack of selectivity, it is conceivable that systemic administration may also inhibit ecNOS remote from the inflammatory locus resulting in vasoconstriction, reduced blood delivery to the inflamed site and therefore leucocyte margination, hence a reduction in inflammation. Indeed, it was shown that the anti-inflammatory effects of L-arginine analogues given systemically could be reversed by vasodilators (Antunes *et al.*, 1990; Najafipour and Ferrell, 1993; Ridger *et al.*, 1997). In agreement with these studies it was also found that when NOS inhibitors were injected intraperitoneally, immediately prior to intrapleural injection of carrageenin, pleural exudates were significantly reduced. Therefore, in order to

try and avoid the systemic effects of NOS inhibitors, AE-ITU, 1400W and L-NIO were administered locally and found to exert a pro-inflammatory effect, without altering inflammatory cell viability. In support of these findings, others have also reported a protective role for NO. For instance, concomitant administration of NOS inhibitors with lipopolysaccaride (LPS) increased organ damage and mortality following endotoxic shock in rats (Harbrecht *et al.*, 1992; Park *et al.*, 1996). It was suggested that protection was via maintenance of vascular perfusion reducing ischemic damage. In addition, in genetically modified mice, acetic acid-induced colitis in iNOS-deficient mice resulted in increased PMN-associated tissue damage in comparison to wild type animals (McCafferty *et al.*, 1997). A similar inflammatory cell accumulation in hepatic microvasculature was also observed in LPS-treated iNOS knockout mice (Hickey *et al.*, 1997). Finally, this work demonstrated that injection of the slow releasing NOS donor DPTA NoNoate directly into the pleural cavity immediately prior to carrageenin reduced inflammation at 6h, thus reinforcing the hypothesis that these observations were due to NO and that NO was protective in this model. In support of this data Ialenti and colleagues (2000) showed that administration of the NO donor NOC-18 reduced neutrophil accumulation in the rat carrageenin-induced pleurisy. They concluded that the main role of NO produced at the site of inflammation was to reduce inflammatory cell influx. However, from data presented in this thesis it may be concluded that even though at the time these experiments were performed AE-ITU and 1400W were considered to be selective inhibitors for iNOS, there was no difference in their effect compared to the non-selective inhibitor L-NMMA. This leds to the conclusion that the injection of these inhibitors locally at the doses chosen probably inhibited both iNOS and ecNOS, suggesting that NO produced by both sources are important in the control of inflammation in this complement-mediated model, the carrageenin-induced pleurisy. Thus, from studies presented in this thesis and elsewhere using both pharmacological agents and iNOS knockout mice, a protective role for NO may be ascribed regardless of source.

In conclusion, in the rat carrageenin-induced pleurisy, inhibition of NO at the

inflammatory site exacerbates inflammation and prolongs the pathology, suggesting a protective role for NO in this model.

7.1.2 NO in the BSA-induced pleurisy

Injection of BSA into the pleural cavity of rats 12 days after sensitisation results in an immediate type III hypersensitivity reaction (Capasso *et al.*, 1975a). The resulting inflammation is mediated by antigen-antibody interactions and complement fixation. It is worth noting that the sensitisation period of 12 days is required to allow antibody production against the BSA antigen, prior to challenge. The reaction was dominated by PMNs throughout, with a peak in oedema and inflammatory cell influx at 6h, with both parameters being greatly reduced by 24h. Injection of BSA alone into the pleural cavity of unsensitised animal resulted in no recoverable exudate and a considerably lower cell number at 6h than sensitised animals thereby excluding a major contribution to the inflammatory reaction of direct pleural irritation by BSA.

iNOS activity and immunoreactivity were measured in inflammatory cells and nitrite in cell-free exudates obtained from the pleural cavity of challenged animals. iNOS activity was maximal at the earliest time point measured, 2h, and was still high at 6h, but declined after this time point reaching baseline by 48h. This profile was mirrored by iNOS immunoreactivity in the inflammatory cells suggesting that iNOS was the primary source of NO in this model. Nitrite levels were also high at 2 and 6h, but unlike iNOS expression the activity reached baseline at 12h, possible reasons for this discrepancy may be due to the peak expression of arginase at this time point. In this type III immediate hypersensitivity reaction, the activity of arginase was greater than in the carrageenin-induced pleurisy with activity being detected during the resolution stage of this model. This suggests that there might be a competition for L-arginine in the inflammatory cells resulting in a reduction of nitrite levels at 12h. In addition, products from ornithine metabolism, spermine and agmatine aldehyde, are capable of inhibiting NOS activity (Szabo *et al.*, 1994a; Blanz *et al.*, 2000). Therefore, it can be envisaged that during antibody and cell mediated

acute inflammation, arginase could directly modulate NO production by limiting the availability of L-arginine for iNOS and subsequent production of NO. In support of the findings in this thesis it has been shown recently that inhibition of arginase with L-norvaline in LPS stimulated J774.1 macrophages significantly elevated NO production without affecting iNOS enzyme activity (Chang *et al.*, 1998). Additionally, elevation of NO was inversely related to the levels of extracellular L-arginine. A proposed pathway for NOS arginase interactions is shown in Figure 7.1

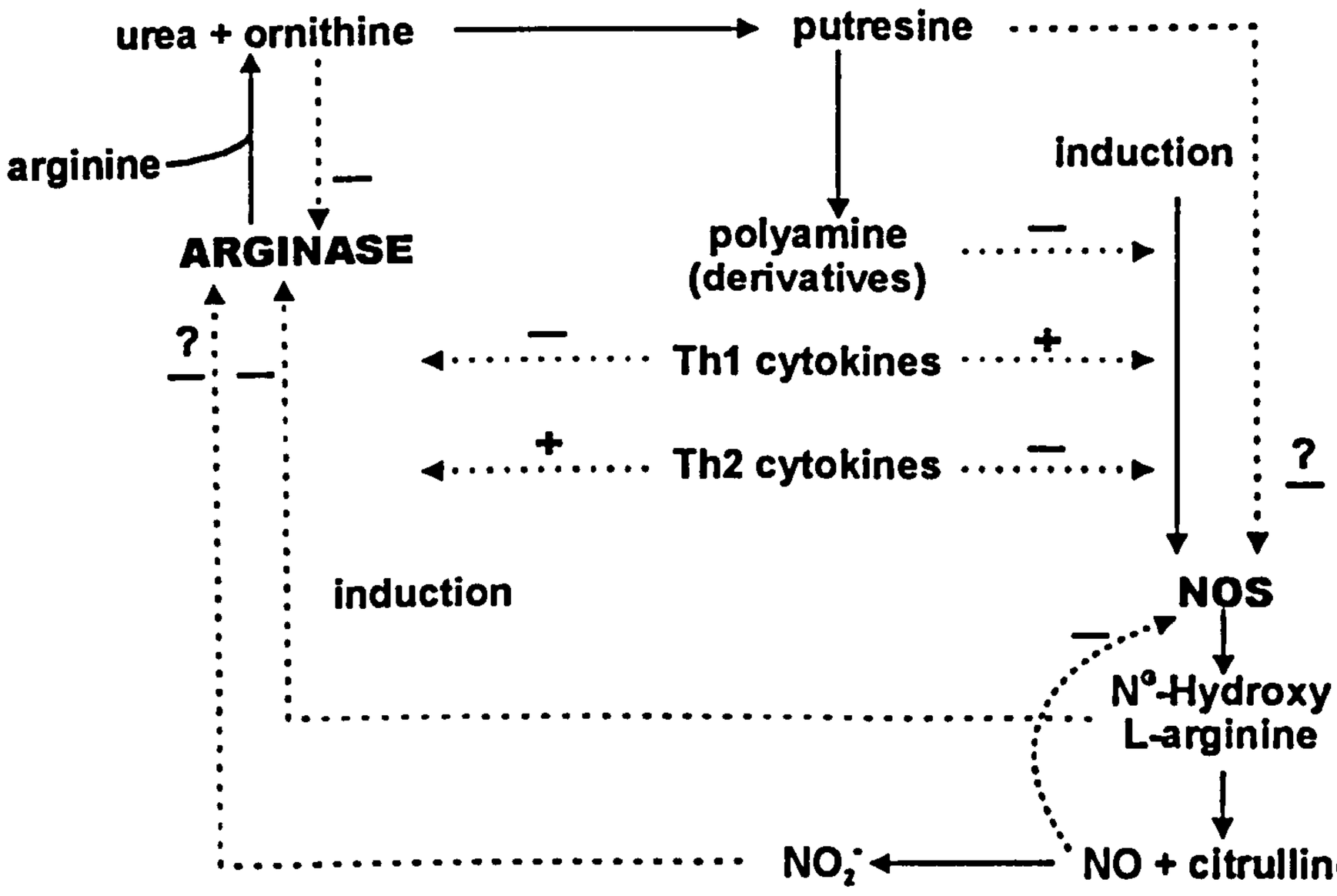

Figure 7.1 Possible regulatory effect in arginine metabolism in monocytes. *Metabolic routes are represented by continuous arrows, regulatory routes by dashed arrows. + and - denote activation and inhibition, respectively. Adapted from Hrabak et al., 1996.*

No immunocytochemistry was performed for iNOS on the inflammatory cells recovered from the pleural cavity, therefore the cellular source of NO can only be supposed. Since this reaction is PMN dominated, this cell type is the most likely source. A possible role for NO may be to down-regulate IL-6 production from macrophages (Deakin *et al.*, 1995). This would reduce the number of antibody-secreting cells, since IL-6 plays a predominant role in promoting differentiation of B-lymphocytes into antibody-secreting cells (Lotz, 1993).

Therefore, IL-6 inhibition by NO would be protective in this, by limiting the humoral response to antigen presentation in this immediate hypersensitivity reaction to BSA.

In this Arthus reaction, PGE_2 levels and COX activity peaked at the resolution stage of this model and the iNOS pathway was maximal at the initial phases of inflammation. Therefore, both pathways were maximal at different times, suggesting that either products from the COX and NOS pathways may modulate the activity of their respective enzymes or there is alternate regulation of these two pathways independent from direct interactions. Cross talk between the NOS and COX enzyme systems has been extensively documented and subject to a number of lengthy reviews (Di Rosa *et al.*, 1996), but investigations have produced conflicting results. A stimulatory role for NO on prostaglandin production can only be proposed in the BSA model due to the temporal expression of these mediators. This is supported by evidence from RAW 264.7 macrophages with a non-functional L-arginine/NO pathway, the nitric oxide donor sodium nitroprusside enhanced PGE_2 production in response to arachidonic acid (Di Rosa *et al.*, 1996). Similarly, sodium nitroprusside increased arachidonic acid-stimulated PGE_2 production by murine recombinant COX-1 and COX-2 (Di Rosa *et al.*, 1996), suggesting that NO stimulates PGE_2 biosynthesis by direct interactions with the COX enzymes, although, direct coupling to the heme group is unlikely (Tsai *et al.*, 1994). It can be hypothesised that the increase in COX expression and prostaglandin synthesis in this model may be a cellular response to further suppress the immune system. Since PGE_2 concentrations similar to those found in inflammatory sites supress lymphocyte function *in vitro* such as responsiveness to mitogens (Goodwin *et al.*, 1978) and cell mediated cytotoxicity (Meerpohl and Bauknecht, 1986). By virtue of the early expression of NO in this model, it can be envisaged that NO plays a regulatory role on PMN trafficking into the inflammatory site by limiting the response to antigen challenge.

7.1.3 NO in the metBSA-induced pleurisy

Injection of methylated BSA into the pleural cavity of rats 12 days after sensitisation results in a DTH-reaction (Lewis *et al.*, 1981). This reaction, unlike that induced by BSA, is cell-mediated, since the reaction in the rat could be passively transferred to naïve animals with lymphocytes (Hambleton and Miller 1988). The resulting inflammatory reaction after challenge was characterised by a biphasic response. Six hours after challenge there was an appreciable increase in exudate volume and inflammatory cell influx which was PMN dominated, this being atypical of a DTH reaction. The reaction observed at this time point was via a direct irritant effect, as methylated BSA injected into the pleural cavity of unsensitised animal resulted in an mild inflammatory reaction with PMNs being the predominant cell type (Moore and Brown, 1996). Post 12h, the reaction developed the characteristics of a typical DTH type inflammation, with mononuclear cells being the major cell type. The inflammation peaked at 24h and then declined thereafter.

iNOS activity and immunoreactivity were measured in inflammatory cells and nitrite in cell-free exudates obtained from the pleural cavity of challenged animals. Both parameters were maximal at 12h and reached baseline by 24h. This profile was mirrored by nitrite levels suggesting that iNOS was the primary source of NO in this model. It seems likely that NO from iNOS may again have a protective role in this model, since the peak of its production was immediately prior to the peak in the inflammatory response. Although anti-inflammatory effects have been observed by administration of NOS inhibitors in cell mediated diseases such as arthritis in MRL-lpr/lpr mice (Weinberg *et al.*, 1994). It is interesting tonote that in this paper NOS inhibitors were given systemically.

There is a more feasible role for NO in this T-cell mediated model. Firstly by the early time of this mediator's expression and secondly from the potent immunoregulatory effects NO exerts. Recent detailed studies have shown that NO can specifically impair T helper 1 (Th1) cells, while Th2 cell function appears largely unaffected (Taylor-Robinson *et al.*, 1994). Therefore, NO can effect

Th1/Th2 balance by favouring Th2 responses such as the up-regulation of IL-4 production (Kallmann *et al.*, 1999). Therefore, there is overwhelming evidence to suggest that NO may possibly have an immunosuppressive effect on Th1 cytokines in this model, favoring the production of anti-inflammatory Th2 derived cytokines.

This work shows that like the BSA-induced pleurisy, arginase activity and PGE_2 production were maximal during the resolution stages of this model. The profiles of arginase enzyme activity and PGE_2 production revealed that exponential elevation of these parameters were greater post the peak of iNOS expression suggeting the arguments for the interaction presented for the BSA-induced pleurisy may also be true in this model.

7.1.4 NO in the croton oil-induced murine chronic granulomatous tissue air pouch

In the murine croton oil-induced chronic granulomatous tissue air pouch model, carmine content was maximal at 5 days and granuloma dry weight peaked at 7 days, with both parameters declining thereafter. iNOS activity and nitrite levels were maximal at day 7, with iNOS protein also maximal at this time point.

Maximal induction of iNOS protein and nitrite levels coincided with the influx of monocytes which are the dominant cell type at this phase of the lesion. It was previously shown by immunohistochemistry that IL-1, TNF-α and bFGF immunoreactivity were present at the earlier time points of granulomatous tissue development (Appleton *et al.*, 1993). iNOS protein expression and nitrite release have been demonstrated to be induced by IL-1β, TNFα, INFγ and bFGF (Suschek *et al.*,1995; Lorsbach *et al.*, 1993; Kunz *et al.*, 1997). These have all been shown to work in synergy to enhance iNOS induction. PMNs, fibroblasts and endothelial cells are also present in this model at 7 days and all are capable of producing nitric oxide (Nathan, 1992). Therefore, this increase in iNOS protein, activity and nitrite production in the murine air pouch between 5 and 7 days may be a result of the effects of pro-inflammatory cytokines on the cell

types present.

iNOS protein and activity were significantly reduced by 14 days. In this model it was previously shown, by immunohistochemical staining, that TGF-β levels gradually increased between day 7 and 10 to reach a maximum from day 14 onwards (Appleton *et al.*, 1993). As TGF-β can down regulate iNOS expression and activity (Vodovortz *et al.*, 1993), this may explain why iNOS activity was significantly reduced at this time point.

This thesis shows that systemic administration of the selective iNOS inhibitor aminoguanidine significantly reduced nitrite levels in cell-free exudates from day 1-7, without an effect on iNOS protein expression or activity. This was expected since aminoguanidine is a competitive enzyme inhibitor (Misko *et al.*, 1993) and has been reported to have no effects on iNOS mRNA (Willis *et al.*, 1994), and hence was unlikely to effect *de novo* protein synthesis. Similarly, the activity assay for iNOS provides excess co-factors and substrate (L-arginine) therefore any inhibitory effects on activity would be nullified by addition of surplus L-arginine. However, cNOS activity was significantly reduced at 5, 7, 14 and 21 days suggesting that aminoguanidine had an inhibitory effect on cNOS enzyme activity. This is supported by findings from Laszlo and colleagues (1995) who showed that aminoguanidine (50mg/kg, s.c) was able to elevate arterial blood pressure over a 1hr period. In the literature it is not clear how aminoguanidine can affect cNOS enzyme activity, however it is possible that aminoguanidine may act as a time dependent irreversible inhibitor of cNOS.

Two other methods for directly inhibiting NO formation by iNOS within the inflammatory site were used. Firstly AE-ITU was injected locally into the air pouch and secondly iNOS gene deleted animals (Wei *et al.*, 1995) were used in this model. Although a protein product was detected using the Santa Cruz anti-iNOS antibody and showed a similar temporal and spacial distribution to the native iNOS protein, this protein was non-functional, since enzyme activity and product (nitrite) were at the lower detection limits of the assays used. It was

essential to check whether or not the sv129 wild type controls reacted in a similar manner to T_o mice. sv129 mice produced a similar profile of inflammation compared with the outbred T_o's, with peaks in granulomatous tissue dry weight and carmine content being beween 5-7 days. Therefore, sv129 mice were deemed suitable for use in this model.

Unlike the carrageenin-induced pleurisy, inhibition of NO with aminoguanidine systemically or by local injection of the iNOS selective inhibitor AE-ITU or iNOS gene deletion resulted in a significant inhibition in granuloma formation in this chronic model when compared to control animals. This was also evident in the general histological appearance of the air pouches, where a reduction in the thickness of the granulomatous tissue was observed. Similar results have been achieved with NOS inhibition in a number of chronic inflammatory models which include, carrageenin-induced granuloma formation (Iuvone *et al.*, 1994), adjuvant arthritis in rats (Oyanagui, 1994) and a wound healing model in rats (Thornton *et al.*, 1998). Therefore, it is highly conceivable that inhibiting NO may have reduced collagen synthesis thereby limiting the size of the resultant granuloma. It has been shown quite clearly that NO can affect collagen deposition, since NO derived from iNOS stimulates collagen deposition in a model of wound healing (Thornton *et al.*, 1998). Additionally, NO donors have been shown to stimulate collagen production in normal dermal fibroblasts (Witte *et al.*, 1996), whilst inhibition of NO by the NOS inhibitor S-methyl-isothiouronium severely impairs collagen deposition in the mouse (Schaffer *et al.*, 1996). Additional mechanisms may be involved, since an increased nitric oxide production in smooth muscle aortic cells inhibited the production of the matrix metalloproteinases 2 and 9, which are essential in the breakdown of basement membrane and extracellular matrix and NO increased the activity of the tissue inhibitor of matrix metalloproteinases 2 (Gurjar *et al.*, 1999). Therefore, inhibition of NO would result in an increase in matrix metalloproteinase activity and a decrease in the tissue resident inhibitors of these enzymes resulting in a more rapid breakdown of extracellular matrix, possibly leading to a reduction in granuloma size. Finally, up-regulation of iNOS in rat fibroblasts increased the onset and progression of

fibrosis in an airways disease model (Romanska *et al.*, 2000). Again an inhibition would likely reduce fibrosis associated with the granuloma and thus its size. Therefore, NO maybe pro-inflammatory in this model by virtue of its ability to increase collagen deposition and inhibit endogenous MMPs. In which case, the reduction of NO in this chronic graulomatous model maybe desirable.

Maximal iNOS expression and nitrite levels coincided with the peak in vascularity and may therefore play a part in the angiogenic response in this model. However, little is known about the involvement of NO in inflammation-driven angiogenesis, but its effects appear to be sensitive to the assay and the concentrations of NO used, with both inhibitory and stimulatory effects ascribed (Seed *et al.*, 1999). All three methods of iNOS inhibition on granulomatous tissue dry weight were similar, however the effects on the vascular component of this model were different. Systemic administration of aminoguanidine caused a significant decreased in neo-vascularisation of the granuloma that was proportional to a decrease in the size of this tissue, whereas local injection of AE-ITU or iNOS gene deletion resulted in an increase in the vascular index (a ratio of vascular volume to granuloma size). The reduction seen with aminoguanidine is probably due to this inhibitors effects on eNOS as well as iNOS, since NO has been shown to promote endothelial cell proliferation and migration both *in vitro* and *in vivo*, whilst NOS inhibition suppresses these events (Ziche *et al.*, 1997a; Morbidelli *et al.*, 1996). In addition, elaboration of urokinase type plasminogen activator, a key protease in the initiation of the angiogenic process, by endothelial cells is also enhanced by incubation with the NO donor sodium nitroprusside (Ziche *et al.*, 1997b). Therefore, inhibiting NO from eNOS would have had an inhibitory effect on the angiogenic response. This in conjunction with a decrease in granuloma dry weight resulted in a net reduction in the vascular index. Local injection of AE-ITU and iNOS gene deletion where used as a more selective way of inhibiting iNOS in this model. iNOS inhibition by these two methods resulted in no change in the vascular content of the granuloma. However, an increase in the vascular index was observed because there was a greater net reduction in the size of the granuloma formed with either

local injection of AE-ITU or iNOS gene deletion. Therefore, in summary NO derived from iNOS did not effect angiogenesis in this model, however, when accompanied by a reduction in eNOS there was an inhibitory effect observed on the angiogenic response.

Arginase activity in the murine croton-oil induced chronic granulomatous tissue air pouch was between 50 and 100 times greater than in the acute models of inflammation. Therefore another functional role for arginase may be predicted in this model. Arginase may participate in the fibrogenic processes via the synthesis of ornithine-derived proline, an essential precursor for the production of collagen. NOS inhibition by oral administration of aminoguanidine was without effect on this enzyme within the granuloma. This is surprising since there have been a number of reports suggesting that inhibition of NO increases arginase activity (Hrabák *et al.*, 1997; Corraliza *et al.*, 1995). However, in contrast abrogation of iNOS activity by gene deletion significantly increased arginase activity within the granuloma, although arginase I expression was only slightly increased. Arginase activity measurements involves both isoforms of arginase (I and II). However, at the time these experiments were conducted, no commercially available antibody for arginase II was available. Although arginase I protein expression was not significantly altered, it is conceivable that the increase in arginase activity may have resulted from increased arginase II expression. Therefore, this increase in arginase activity after iNOS inhibition supports the proposed hypothesis that arginase acts as a rate limiting enzyme in the availability of L-arginine for NO production. This is feasible since the maximal enzyme activity of arginase and iNOS occurs at the same time point. Similar findings have been demonstrated previously, where nitrate was shown to inhibit arginase activity (Hrabak *et al.*, 1996) and conversely, NO inhibition increased arginase formation (Cook *et al.*, 1994).

Inhibition of NO by gene deletion had no significant effect on COX-2 activity in the granuloma, however, like the carrageenin-induced pleurisy there was a trend to an increase. However, this work suggests that inhibition of iNOS derived NO

does not alter COX-2 expression in this chronic model. Although iNOS gene deletion does not affect COX-2 protein, it can't be discounted that inhibition of NO may alter the profile of prostaglandins produced within the granuloma, by a putative effect on down-stream synthases. Therefore this area requires further work.

Surprisingly, iNOS gene deletion did not alter the distribution and expression of HSP 70 and HO-1, since NO inhibition has been shown to modulate both HSP 70 in an acute inflammatory model and HO-1 expression in this chronic model. One possible explanation is that levels of these HSP's in this model are low, therefore any small changes in levels of these proteins in influxing inflammatory cells would be difficult to measure using Western blotting and immunohistochemistry. However, overall it cannot be discounted that specific inhibition of iNOS has no effect on these proteins in this model at the time points measured. However, using an HO-1 activity assay it could be demonstrated that in aminoguanidine treated animals there was an increase in HO-1 activity in the granuloma at 5 days (data not included). This is in line with previously published data from our department that showed in brain homogenates an increase in HO-1 activity after administration of L-NAME. Conversely, the NO donor sodium nitroprusside dose dependently inhibited HO-1 activity in the same tissue (Willis *et al.*, 1995). Although, the exact function of this up-regulation of HO-1 by NO is not clear, it can be postulated that once induced, HO-1 affords protection against oxidative damage by two possible pathways. Firstly, in endothelial cells it was shown that HO-1 is a cGMP sensitive protein and since one of the classical effects of NO is to induce cGMP formation through the activation of guanylate cyclase (Polte *et al.*, 2000), it can be envisaged that NO protects these cells from damage by itself through the same mechanism it uses for its biological action. Although this mechanism seems probable in endothelial cells, it can not be discounted that other cells may utilise different signaling pathways to achieve the same result. In experiments conducted in HeLa cells the stable cGMP analogue 8-bromo-cGMP was unable to produce the same effects seen in endothelial cells. Instead it was concluded that NO activated HO-1 in these cells by the up

regulation of mitogen activated protein kinase ERK and p38 (Chen and Maines, 2000). Regardless of the mechanism by which NO induces HO-1 expression in a variety of cells, there is a consensus within the field that up regulation of this HSP gives cells protection in an inflammatory environment against the massive increase in oxidative stress.

In summary, NO production by iNOS in this model appears to be detrimental to the inflammatory process, since it appears to drive granuloma formation in this model.

7.1.5 Effect of aspirin on iNOS and NO in acute and chronic inflammation

In the rat carrageenin-induced pleurisy oral administration of aspirin dose-dependently reduced both exudate formation and influx of inflammatory cells into the pleural cavity of treated rats. Not surprisingly aspirin caused a significant reduction in PGE_2 levels in cell-free inflammatory exudates. The decrease in inflammation and PGE_2 levels was accompanied by a dose dependent increase in nitrite in cell-free exudates, iNOS protein expression and iNOS enzyme activity in inflammatory cells recovered from the pleural cavity.

In light of the data obtained with NOS inhibitors, a second set of experiments were devised to further dissect the role of this increase in NO after oral administration of aspirin. Injection of AE-ITU into the pleural cavity of rats immediately prior to carrageenin and oral gavage of aspirin attenuated the increase in nitrite and reversed the inhibition of inflammation observed with aspirin alone at 6h. However, the reduction in inflammation at 6h may not be a consequence of an increase in protective NO, but rather a reduction in PGE_2, therfore aspirin was dosed at 4h, a time where levels of PGE_2 are subsiding. This resulted again in a significant suppression of inflammation and an increase in nitrite production in the pleural cavity at 8h. The decrease in inflammation was reversed by prior treatment with AE-ITU, which suggests that aspirin, as well as inhibiting prostaglandin production, also increases iNOS expression in this complement-dependent model of inflammation, and may be an added

mechanism by which aspirin exerts its anti-inflammatory effects. Evidence obtained from the NOS inhibitor studies suggests that both inflammatory cells and endothelial cells participate in the establishment of inflammation induced by carrageenin. Therefore, the stimulatory effects of aspirin on the NOS pathway was investigated in J774 macrophages and Ea.hy926 endothelial cells.

To establish that aspirin can further increase iNOS expression in stimulated cells, a sub-optimal stimulation was used (LPS alone). As was observed *in vivo*, aspirin significantly elevated nitrite production from J774 macrophages. A similar result was obtained from endothelial cells and the murine chronic granulomatous air pouch, where aspirin administration significantly elevated nitrite, iNOS activity and cNOS activity. However, unlike the inflammatory cells removed from the pleural cavity, iNOS protein expression in the endothelial cells and the chronic air pouch model remained unchanged. Therefore, in the chronic model of inflammation the induction of iNOS activity after aspirin treatment may be a consequence of a stimulatory effect of aspirin on endothelial cells, since this cell type is predominant throughout the granuloma.

In hindsight, the increase in NO production by aspirin is not surprising since aspirin has been used for may years as an antiaggregatory compound, a phenomenon that is associated with not only a reduction in thromboxane B_2 but also an increase in NO production (Azuma *et al.*, 1986; Radomski *et al.*, 1987b). Several other reports indicate that aspirin might increase NO levels as presented in this thesis. For example, aspirin was able to antagonise the vasoconstriction induced by the non-selective NOS inhibitor L-NMMA (Rosenblum *et al.*, 1992) and was able to attenuate hypoxia induced contractions in monkey coronary artery strips (Toda *et al.*, 1992). However, little is know about this mechanism of aspirin. There is the potential that aspirin can induce NO production and a number of papers have shown this to be true in the vasculature (Lopez-Farre *et al.*, 1995; Lopez-Farre *et al.*, 1996). The data presented in Chapter 6 indicates that this could also be true under inflammatory conditions.

The data presented on the effects of aspirin are purely pharmacological observation, with no mechanisms dissected. However, the literature provides at least two possible explanations for aspirin's induction of NO. The first centres on the ability of PGE_2 to raise cAMP in a number of cell types. In rat Kupffer cells cAMP has been shown to increase the formation of NO (Gaillard *et al* ., 1991) and in rat aorta smooth muscle cells an elevation of cAMP positively regulates NO production at the level of iNOS mRNA expression (Koide *et al*., 1993). In addition, elevated PGE_2 levels in murine macrophages enhanced cAMP formation and nitrite release, this resulted in an increase in the parasite killing ability of these cells (Mauel *et al*., 1995). Contrary to the above literature, cAMP elevation was also suggested as the mechanism by which PGE_2 could down regulate NO production in murine peritoneal macrophages (Raddassi *et al*., 1993: Milano *et al*., 1995). However, the real effect of cAMP on NO production may be related to the period of cAMP elevation, since it was demonstrated in LPS stimulated J774 macrophages that prolonged elevation of intracellular cAMP by PGE_2 inhibited iNOS expression (Bulut *et al*., 1993). In summary, the mechanism by which intracellular cAMP upregulates iNOS is still unclear, but it has been proposed to increase the stability of iNOS mRNA and/or its transcriptional activation (Koide *et al*., 1993; Imai *et al*., 1994; Muhl *et al*., 1994). cGMP could be involved in the mechanisms by which aspirin elevates NO production, since aspirin treated neutrophils increased cGMP and interfered with the $(Ca^{2+})_i$ signalling pathway in platelets by an L-NMMA-inhibitable mechanism (Lopez-Farre *et al*., 1995). A similar cAMP/cGMP mechanism on calcium flux was demonstrated in endothelial cells (Bolz and Pohl, 1997). It is also known that cGMP is a potent blocker of calcium-related activation in numerous cellular types including platelets (Kroll and Schafer, 1989). This suggests that aspirin could increase NO formation through effects on the secondary messengers cAMP and cGMP.

The second possible mechanism for the induction of iNOS by aspirin was suggested by preliminary observations made by Lopez-Farre's group (1995), who showed that non-cyclooxygenase arachidonic acid metabolites or

arachodonic acid itself may be responsible for the activation of NO by aspirin. Arachidonic acid fulfils several criteria to be considered as a possible mediator, since it can activate NO release from endothelial cells (Furchgott, 1983) and has been proposed as a direct modulator of neutrophil function (Winkler *et al.*, 1993). Indeed, it was suggested that aspirin inhibition of COX caused a shunting of arahidonic acid down the 12-LO pathway, leading to the production of 12-hydroxy-(5Z, 8Z, 10E, 14Z) eicosatetraenoic acid (12-HETE) in vascular smooth muscle cells, since the non-selective LO inhibitor NDGA attenuated salicylate induced NO production, whereas the selective 5-LO inhibitor caffeic acid was without effect. Furthermore, nitrite production in IL-1β stimulated vascular smooth muscle cells was enhanced by 12-HETE, but not 15-HETE (Shimpo *et al.*, 2000). A direct relationship between NO and 12-lipoxygenase products have also been shown in other cell types that include pancreatic islets (Hotter *et al.*, 1996; Ma *et al.*, 1996) and rabbit platelets (Fujimoto *et al.*, 1998).

Elevation of NO in these cells and inflammatory models may decrease the number of leucocytes that would traffic into the inflammatory site, therefore adding to the already described anti-inflammatory effects of aspirin. The hypothesis presented here for the mechanisms of aspirin in inflammation are plausible, however, they remain unproven. Therefore further work is required to substantiate these mechanisms *in vivo*.

7.1.6 Concluding remarks

Data presented in this thesis supports the conclusion that NO is an important mediator in the processes involved in both the acute and chronic inflammation. However, the effect that NOS inhibition has on the inflammatory process differs depending on the type of inflammation examined. Therefore, both advantageous and deleterious effects can be attributed to NO production. Local NOS inhibition in the acute model of inflammation resulted in a significant elevation in chemotactic mediators for leucocytes, elevated mast cell reactivity and an increase in oxidative stress resulting in a prolonging of this acute pathology. This suggest a protective role for NO in this model, by keeping the inflammatory

response in check. This is not surprising since NO is extensively documented to inhibit neutrophil trafficking in acute inflammatory models. In addition, the likelihood of extensive NO mediated damage is limited by the fact that high levels of this mediator, in the carrageenin-induced pleurisy, are restricted to quite a short time period (~6h). Therefore, it can be envisaged that in acute inflammation the beneficial effects of NO probably out-weigh its destructive potential. In contrast, NOS inhibition in a chronic inflammation resulted in a significant reduction in granulomatous tissue size. This probably reflects the complex nature of this inflammatory process, with the model being more reliant on additional processes that include tissue formation and remodelling. Therefore, simply inhibiting a degree of neutrophil trafficking by increasing NO has a minimal effect on granuloma size compared to the stimulatory effects NO has on collagen formation. This is supported by the findings in a number of chronic pathologies where inhibition of NO by either gene deletion or pharmacological interventions in the main has beneficial effects by reducing the severity of the ensuing pathology. In conclusion, although NO may down regulate the immune system and inhibit neutrophil chemotaxis, the damage caused to the DNA and energy metabolism of host cells by high levels of NO over a number of weeks outbalances its benefits.

The interactions that NO has with the heat shock family of proteins in inflammation is also reflective of the type of model used. HSP 72 expression was significantly increased after NOS inhibition in the carrageenin-induced pleurisy with no effect of HO-1 protein expression. However, in the chronic model the opposite was true after NO inhibition with aminoguanidine. Similarly, with arginase activity, no interaction was observed in the acute non-immunological model whereas in chronic inflammation suppression of NO resulted in increased arginase activity. Therefore the interaction of these pathways may require concomitant expression of their products in close proximity to each other.

Aspirin increased NO production in all the models and cell lines tested. This suggests that either COX products have inhibitory effects on NO production

and/or that the effects of aspirin on NO were independent of its inhibitory effect on COX. However, regardless of either a direct or indirect effect of aspirin on NO formation, this increase in NO production may contribute to aspirins potent anti-inflammatory profile.

It may be concluded from work presented in this thesis that inhibition of NO as a short term therapy during flares in chronic pathologies such as rheumatoid arthritis may be of benefit, by limiting the degree of the inflammatory response. However, in chronic lesions where excessive granuloma formation occurs it may be advantageous to inhibit NO derived from iNOS thereby limiting excessive matrix deposition. Therefore, the benefits of NO as a therapeutic target in inflammation may be reliant on the type of inflammation, the time and length of treatment and the development of non-toxic specific inhibitors.